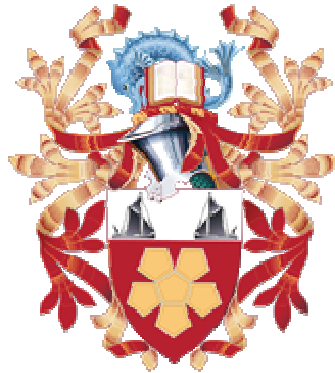# A study on the effects of lime on the mechanical properties and behaviour of London clay

A thesis submitted in partial fulfilment

of the requirements for the

Degree of Doctor of Philosophy

By

ZOHEIR KICHOU

Department of Urban Engineering

School of Built Environment and Architecture

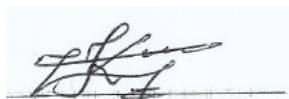**London South Bank University**

December, 2015

This work is dedicated to my wife Assia, my daughter Sarah and my son Sami

DECLARATION

I hereby declare that the work reported in this thesis has not been previously submitted elsewhere for any degree. All material in this thesis is original except where indicated by reference to other work.

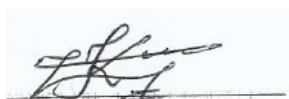Signed   (Candidate)

Date: 12th April, 2016

STATEMENT OF COPYRIGHT

The copyright of this thesis belongs to the author under the terms of the United Kingdom Copyright Acts. Due acknowledgement must always be made of the use of any material contained in, or derived from this thesis.

Signed   (Candidate)

Date: 12th April, 2016

Abstract

Lime is commonly used as a stabiliser to improve the engineering properties of soils in particular for roads and pavement foundation. Despite the popularity of the technique, only a limited amount of existing experimental data for lime treated soils from advanced testing is available, in part due to the length of the tests. As lime stabilisation is increasingly used for other engineering applications (e.g. embankments, railway layers, canal linings, earth dams, buildings...etc), advanced testing to describe the mechanical behaviour of the treated soils is required.

In this research a comprehensive experimental program was carried out to investigate the engineering properties and behaviour of a lime treated high plasticity clay (London Clay). A number of Unconsolidated Undrained (UU), Consolidated Drained (CD) and Consolidated Undrained (CU) triaxial tests were performed to identify the effect of lime dosage, compaction water content and curing time on the shear strength parameters, stress-strain behaviour, volumetric response and dilation of the treated soil. Moreover the study focused on understanding the mineralogical and physicochemical transformations occurring during the curing stage. Based on a number of additional tests (XRD analysis, pH measurement and other chemical testing) they provided a useful reference for the interpretation of the triaxial test results; in order to support hypotheses made on the evolution of the chemical reactions and the development of cementation bonds.

Results from CD tests showed that yield, peak, and ultimate strength were greatly improved by an increase in lime content. London Clay samples treated with lime showed a considerable increase in peak stress ratio $\left(q/p'\right)_{peak}$, particularly at lime addition beyond the initial consumption of lime (ICL). An increase in the angle of shearing resistance and cohesion intercept with increasing lime content was observed consistently. The stress–strain behaviour of treated London Clay was observed to be nonlinear with a contractive–dilative response. This response is found to be strongly influenced by lime content and the curing period. An increase in dilation with lime amount as well as a progressive suppression in the dilation by the effective stress increase was also observed. A Critical State Soil Mechanics (CSSM) framework was used to interpret the results. Lime addition, curing time and compaction water content were observed to have an impact on the critical

state parameters in the compression plane $(v - p')$. However, the overall critical state line (CSL) in the stress space $(q - p')$ of lime treated London Clay appears to be almost parallel to untreated London Clay CSL at the same M value, but lying above the untreated CSL with a cohesion intercept. Moreover, the domain where the untreated soil subsists was observed to expand with lime addition and further enlarge with an increase in the lime content. These features can be further explored by deriving a suitable constitutive model for predicting the mechanical behaviour of lime treated soils.

ACKNOWLEDGEMENTS

thesis. I extend my thanks to the London South Bank University research committee for providing an adequate environment that a PhD student would have wished for.

Finally, big thank you to all my friends who were my most fervent supporters. I would also like to express my deepest gratitude to my parents, brothers and sisters, my wife Assia, my daughter Sarah, and my son Sami for their patience, encouragement and continuous support throughout the completion of my thesis.

List of publications

1. **Kichou, Z**., Mavroulidou, M., & Gunn, M. J. **(2015)** Triaxial testing of saturated lime-treated high plasticity clay. *XVI European conference on Soil Mechanics & Geotechnical Engineering, "Geotechnical engineering for infrastructure and development"* 13-17 Sep. 2015, Edinburgh, Scotland, UK.

2. Mavroulidou, M., Zhang, X., **Kichou, Z.,** & Gunn, M. J. **(2015)** A study of the water retention curve of lime-treated high plasticity clay. *XVI European conference on Soil Mechanics & Geotechnical Engineering, "Geotechnical engineering for infrastructure and development"* 13-17 Sep. 2015, Edinburgh, Scotland, UK.

3. Mavroulidou, M., Zhang, X., **Kichou, Z.,** & Gunn, M. J. **(2013)** Hydro-mechanical properties of lime-treated London Clay. *Proceeding of the 18th international conference on soil mechanics and geotechnical engineering,* Paris, Sep. 11-16, 2013

4. Zhang, X., Mavroulidou, M., Gunn, M. J., Sutton, J., Cabarkapa, Z., & **Kichou, Z. (2013)** Application of a novel laser sensor volume measurement system to the triaxial testing of unsaturated lime-treated soil. *Acta Geotechnica*, 9 (6), pp. 945-957

Table of contents

SYMBOLS AND ABBREVIATIONS

CAH	Calcium Aluminate Hydrates
CASH	Calcium Aluminate Sulphate Hydrates
CBR	California Bearing Ratio
CD	Consolidation Drained
CEC	Cation Exchange Capacity
CF	Calibration Factor
CRSP	Constant Rate Strain Pump
CSH	Calcium Silicate Hydrates
CSL	Critical State Line
CSSM	Critical State Soil Mechanics
CU	Consolidated Undrained
CWC	Constant Water Content
D	Dilatancy
DTA	Differential Thermal Analysis
DPT	Differential Pressure Transducer
ESP	Effective Stress Path
FT-IR	Fourier Transform Infrared (spectroscopy)
IC	Imperial College
ICL	Initial Consumption Lime
IR	Infrared (spectroscopy)
LC	London Clay
LFP	Lime Fixation Point
LL	Liquid Limit
LVDT	Linear Variable Differential Transformer
MCC	Modified Cam Clay
MIP	Mercury Intrusion Porosimetry
NCL	Normal Compressive Line
NMR	Nuclear Magnetic Resonance (spectroscopy)
OCR	Over Consolidation Ratio
OWC	Optimum Water Content
PL	Plastic Limit
PI	Plasticity Index

PSD	Particle Size Distribution
PSL	Peak State Line
PWP	Pore Water Pressure
SEM	Scanning Electron Microscopy
SSBS	Stable State Boundary Surface
SWRC	Soil Water Retention Curve
UCS	Unconfined Compressive Strength
USL	Ultimate State Line
UU	Undrained Unconsolidated
WF	Wykeham Farrance
XRD	X-Ray Diffraction
d	Specimen's diameter
e	Void ratio
e_i	Initial void ratio
e_0	Post-curing void ratio
e_s	Void ratio at saturated state
e_c	Void ratio at consolidated state
$e_{e/s}$	Void ratio at the end of shearing state
e_{cs}	Void ratio at critical state
E	Young's modulus of elasticity
G_s	Specific gravity
I_B	Brittleness index
I_{sr}	Strength index
l	Specimen's length
M	Slope of the critical state line
n	porosity
N	Intercept of isotropic normal compression line
p	Mean stress
p'	Effective mean stress
p'_y	Effective mean stress at initial yielding
p'_{cs}	Effective mean stress at critical state

p_0	Reference size of yield locus
p'_{peak}	Mean effective stress at failure
$p'_{(min)}$	Minimum mean effective stress
$p'_{(max)}$	Maximum mean effective stress
p'_c	Pre-consolidation pressure (yield stress)
p'_e	Equivalent consolidation pressure
q	Deviator stress
q_u	Unconfined compressive strength deviator stress
q_{UU}	Undrained unconsolidated deviator stress
q_{CD}	Consolidated drained deviator stress
q_{peak}	Deviator stress at failure
q_y	Deviator stress at initial yielding
q_{ult}	Deviator stress at ultimate state
q_{cs}	Deviator stress at critical state
$\bar{q}$	Bearing capacity
$\bar{q}_u$	Ultimate bearing capacity
S_r	Degree of saturation
V	Volume
$v=1+e$	Specific volume
w_c	Gravimetric water content
w_{dry}	Water content (dry of optimum)
w_{wet}	Water content (wet of optimum)
σ	Total normal stress
σ'	Effective normal stress
σ_a	Axial stress
σ_r	Radial stress (cell pressure)
σ_1	Maximum principal stress
σ_3	Minimum principal stress
σ'_1	Effective axial stress

σ'_3	Effective radial stress
τ	Shear strength
δ	Small increment
Δ	Small variation
c'	Effective cohesion intercept
ϕ'	Effective friction angle
ϕ'_{peak}	Effective friction angle at failure state
ϕ'_{cs}	Effective friction angle at critical state
λ_{iso}	Slope parameter of isotropic normal compression line
λ_{cs}	Critical state slope parameter in the compression plane
η	Stress ratio q/p'
Γ	Intercept of the CSL in the compression plane
κ	Slope of the elastic line
ε_a	Axial strain
ε_s	Shear strain
ε_r	Radial strain
ε_v	Volumetric strain
ε_v^e	Elastic volumetric strain
ε_v^p	Plastic volumetric strain
γ_d	Dry unit weight
γ_{sat}	Saturated dry unit weight
$\rho_{d(max)}$	Maximum dry density
u	Pore pressure
u_i	Initial pore pressure
u_b	Back pressure
u_t	Pore pressure at time t
u_w	Pore water pressure
ψ	Dilatancy angle
ψ_{max}	Maximum dilatancy angle

LIST OF TABLES

LIST OF FIGURES

Chapter 2

Chapter 3

Chapter 6

Chapter 1

1. General Introduction

1.1. Background

During the construction of large infrastructure projects, it is usual to encounter soils with inadequate engineering properties. These may include soft soils (clays or organic soils) that are meant to be used as foundation soils for infrastructure projects, highly plastic shrinking/swelling clays, collapsible, liquefiable or contaminated soils. Such soils would have been excavated and disposed of into landfills and historically replaced by more suitable imported aggregates. An increase in environmental awareness has however resulted in the growing demand for alternative techniques, aiming at the improvement of the originally unsuitable in-situ soil instead of its disposal and replacement. In addition, modern sustainability concerns also encourage the possibility of using dredged and waste soils or other materials in infrastructure projects. To achieve this, several ground improvement methods have emerged in recent years and are increasingly used in infrastructure development (Cecconi & Russo, 2012).

Improvement of unsuitable soils for construction is a broad field which may involve different chemical agents and techniques. These include conventional binders (Portland cement, hydrated lime, pulverised fuel ash and blast furnace slug) or novel binders (zeolite, cement kiln dust, compost and silica fume / microsilica and MgO cement). Other non-traditional stabilisers include – e.g. sulfonated oils, potassium compounds, ammonium compounds and polymers (Petry and Little, 2002). Depending on the needs of the project, the process may include the mixing (shallow or deep) or injection of commercially available additives aiming at altering the nature of the soil (gradation, texture and/or plasticity) and/or act as cementing agents to improve the mechanical properties (stiffness, shear strength) and hydraulic characteristics (hydraulic conductivity and water retention) of the soil. For the case of contaminated soils, solidification / stabilisation of the contaminants is also necessary (e.g. Locat et al., 1996; Singh et al., 2008; Cecconi & Russo, 2012; Al-kiki et al., 2012). Among the various stabilising agents investigated by numerous

researchers, the most prominent is lime, followed by Portland cement (Bhattacharja et al., 2003).

Soil-cement or soil-lime was initially developed mostly as a technique for the improvement of the mechanical behaviour of base materials in road or airfield pavements, leading to a reduction in the total thickness of sub-base layers (Noble & Plaster, 1970; Mitchell, 1986). Better knowledge and control of ground improvement techniques resulted in the development of further methods of implementing lime in a wider range of applications including slope protection for embankment dams, canals, river banks, spillways, and highway and railway embankments (e.g. Cardoso & Maranha das Neves, 2012; Dahale et al, 2012). Lime treatment can be used in these engineering applications to enhance the strength of the soil and increase its capability to resist deformation. Scientific studies of the mechanical properties of lime treated soil only started in the 1950's; this has since become an important topic for both researchers and practical engineers (e.g. Bell, 1996; Locat et al., 1996; Narasimha Rao & Rajasekaran, 1996; Porbaha et al., 2000). A large amount of laboratory and site investigation of the behaviour of soils treated with lime is available in the literature, however, there are few systematic and theoretical studies of the mechanical properties of lime treated soils that can be applied to practical problems (e.g. Locat et al., 1996; Bordman et al., 2001; Bhattacharja et al., 2003; Consoli et al., 2008; Liu et al., 2010).

Many investigations have previously focused on the hydro-mechanical behaviour of natural soils under both, saturated and unsaturated state conditions. A number of these studies investigated the significant contribution of cementation bonds in controlling the behaviour of soils (e.g. Sangrey, 1972 and Burland, 1990). A lot of research was devoted in understanding the behaviour of naturally cemented soils by broadly using artificial cementation in laboratory testing. However, much of the research on artificially cemented soils has focused on studying the behaviour in which aspects such as grading, initial void ratio and degree of bonding could be controlled (e.g. Clough et al., 1981; Coop & Atkinson, 1993 and Huang & Airey, 1998). However, for lime treatment, additional complications are linked to the behaviour of the treated soils. This is because in a lime-treated soil continuous chemical reactions occur up to potentially very long times after treatment (e.g. some researchers as Brandl, 1981 observe changes in the lime treated soil up to seven years after treatment). These reactions linked to the slow diffusion of lime

within clay particles, can affect both the mineralogy and fabric of the soil, in addition to creating bonding effects. These chemical reactions are affected by percentage of lime and available water. The behaviour of lime treated soil in time as a function of these factors has rarely been investigated through triaxial testing. This is true even for most state of the art work, e.g. Zhang (2011) at LSBU, carrying out EPSRC funded research which investigated the behaviour of partially saturated lime-treated clays. Due to the length of the suction controlled testing, Zhang's (2011) research on the mechanical behaviour of lime treated clays was based on one type of specimen only, i.e. treated with one specific lime percentage compacted at one specific dry density and water content and cured for seven days. The effect of these important factors (lime percentage, compaction characteristics and curing time) on the mechanical behaviour of the lime-treated soil was not studied and was recommended as the focus of further work. The investigation described in this thesis is presented as a continuation of this work investigating the effect of a number of factors such as the variation of lime amount, curing time and compaction water content.

1.2. Aims and objectives

The research is aimed at determining the mechanisms of the cemented soil behaviour resulting from lime addition, by investigating the effects of lime treatment on the engineering properties of the material and comparing these with those of compacted untreated London Clay. The particular objectives of this study were to:

- Assess the influence of lime amount, curing time and the compaction water content on strength gain and clarify the role of newly formed cementation bonds (bonding).

- Study the yielding response at shear (gradual bond degradation) of the lime treated London Clay.

- Investigate the state of the material at failure (complete bond destruction) and its dilatancy behaviour.

- Determine volumetric and shear strength parameters, as these are fundamental to develop practical constitutive models for geotechnical analysis and design related to lime treated soils.

- Analyse the results within the critical state soil mechanics framework (CSSM). Results are intended to supply new reliable data, and establish the mechanisms and effects of lime addition to the behaviour of London Clay. Thus the potential impact of this research will be significant to the construction industry in terms of the economy and safety of many major projects.

1.3. Layout of the thesis

The thesis is composed of seven chapters. A review of research findings relevant to the present investigation is presented in chapter 2. This focuses on the available literature concerning soil stabilisation, particularly lime treated soil properties and behaviour from a mechanical point of view. A review of constitutive models for cemented soils is also presented.

The description of sample preparation and experimental procedures adopted in laboratory testing are reported in Chapter 3. The same chapter provides a detailed description of the triaxial systems used in this study, including instrumentation calibrations and performance. The physicochemical tests performed on lime treated and untreated London Clay along with the obtained results are presented in Chapter 4.

The triaxial testing experimental results are presented in Chapter 5 (isotropic triaxial compression tests). First a series of UU testing results are presented investigating the effects of lime percentage, curing time and compaction water content. These are followed by CD testing results which are interpreted and discussed using plots such as (q, ε_a), $(\varepsilon_v, \varepsilon_a)$ and (ε_v, p') curves, particularly the effective stress plane (q, p') and the compressive plane (v, p'). The comparative shear behaviour of all specimens is discussed. The analysis outcome is clarified in terms of the newly formed cementation bonds and the different characteristics of the tested materials. The compression behaviour of lime treated

London Clay specimens is compared to that of the original soil. The effect of bonding due to the addition of lime to London Clay is interpreted on the graphs $\left(q_y, p'_y\right)$ in which a yield curve at shear has an increased size. The influence of cementation bonds on the strength and failure pattern behaviour is also discussed.

Chapter 6 is dedicated to the analysis and interpretation of the obtained data based on the critical state concepts. Stress paths and stable state boundary surfaces (SSBS) are discussed.

The final Chapter 7 contains a summary of the main findings and draws the main conclusions from this study. The chapter finishes with a number of recommendations and suggestions for future work.

Chapter 2

2. Literature review

2.1. Introduction

This chapter presents previous studies related to the use of lime for geotechnical engineering purposes with particular reference to lime-clay interactions and their effects on the soil properties. The effect of cementation bonds resulting from the lime treatment of the clay soils are explored adopting a structured soil approach. The review of previous research consists of four sections. The first section presents the concepts of structure, fabric and bonding used to describe naturally or artificially cemented soils. The following section presents basics of clay mineralogy which help understand the mechanisms involved in the clay improvement by lime. These are presented later in the same section (lime-clay interaction reactions). The third section reviews previous work on lime-treated clays and the effects of lime on salient geotechnical properties. The fourth section presents a brief review of recent developments in the constitutive modelling of cemented soils, and discussion on the proposed models to simulate artificially cemented soil behaviour, particularly the yielding and pre-failure behaviour.

2.2. Soils

Soils are described as multi-phase materials consisting of a solid, a liquid and a gaseous phase. The solid phase consists of a mineral fraction (usually silicates but also carbonates and metal oxides or hydroxides) and possibly some organic fraction. The resulting solid particles constitute the soil skeleton. Voids around the particles can be filled with water and / or air.

During their geological history, natural soils acquire a certain structure, a term encompassing the arrangement of the particles and other features at both macroscopic and microscopic levels, as well as any bonding agents between particles. Cotecchia & Chandler (2000) proposed a simple classification of structure for natural soils, whereby 'sedimentation structure' refers to the elements of structure developed during

sedimentation and consolidation, whereas 'post-sedimentation structure' refers to the elements of structure developed after sedimentation and burial. The geological processes that lead to the development of natural structure can be mechanical unloading (over-consolidation), a change in physical or chemical composition (diagenesis), and cementation. Several investigations on clay soils have highlighted the differences between the behaviour of natural and reconstituted clays as a consequence of the effects of structure [e.g. Vallericca Clay, (Rampello & Silvestri, 1993); Pappadai Clay, (Cotecchia & Chandler, 1997); London Clay, (Gasparre et al., 2007)]. Structure is thus recognised as one of the most important features of a natural soil from the engineering behaviour point of view (Mitchell, 1976). At a microscopic scale, 'structure' refers to the combination of both inter-particle forces (*Bonding*) and the soil particle arrangements (*Fabric*) (Mitchell and Soga, 2005).

Fabric is generally defined as the geometric or spatial arrangement of individual soil particles or particle groups and voids / pore spaces in soil. Figure 2.1 shows different types of fabrics of natural soils.
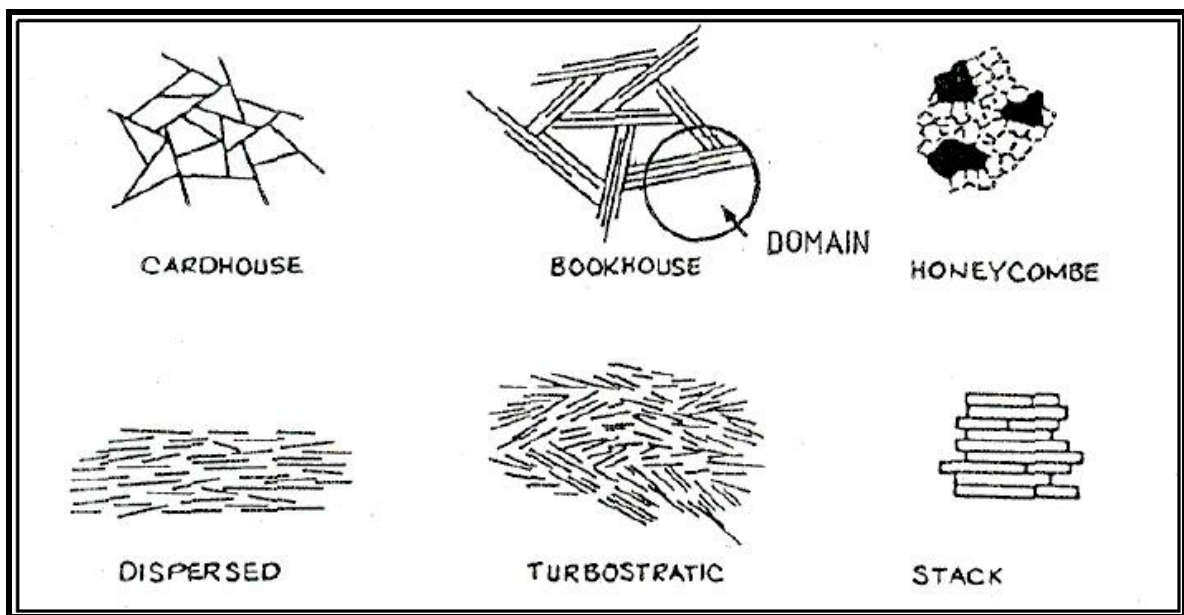
Figure 2.1: Classification of types of fabric (Gasparre, 2005).

A number of factors can be responsible for creating some form of bonding between particles to one degree or another. These include inter-particle attractive forces between clayey soils, suction effects, cold-welding at inter-particle contacts under high pressures or

the presence of various 'cementing' agents, such as deposition of carbonates or silica between particles, hydroxides and organic matter from solution etc. (Leroueil and Vaughan, 1990). A review of the literature illustrates that cementation bonding created in the process of diagenesis and subsequent geological history, is more common than previously anticipated and can occur in a large range of materials such as clays, sand, residual soils and soft rocks. Cementation can build up onto particle surfaces by material precipitation at inter-particle connections (e.g. carbonates or silica as explained earlier), but also inside the pores, affecting the fabric of the soil. The strength of the bonds holding the solid particles together determines the stability of soil structure and its potential to withstand the effects of external forces. It has thus been recognised to have important effects on the geotechnical properties (strength and stiffness) and the stability of geomaterials (Sorensen et al., 2007)

Chemical treatment can affect clay structure in terms of both fabric changes and bonding (by the creation of artificially caused 'cementation' bonds between particles). Cementation is the main aim of the process referred to as 'soil stabilisation' (see later, section 2.4.2), used in practical geotechnical applications to improve the properties of the soil in terms of strength, stiffness and hydraulic behaviour. The following sections discuss in detail why lime can cause these effects in clay soils.

2.3. Clay minerals

Clay soils result from the chemical weathering of rocks due to the action of water (especially if this is slightly acidic or alkaline), oxygen and carbon dioxide. This leads to the formation of crystalline particles of colloidal size (<0.002 mm). The basic structural units of clay minerals are the silica tetrahedron and alumina octahedron (see Fig. 2.2) although isomorphous substitution may take place and silicon and aluminium may be then replaced by other elements (for instance Si^{4+} can be replaced by Al^{3+} or Al^{3+} can be replaced by Mg^{3+} or Fe^{3+} or Fe^{2+}). Such substitutions can result in positive charge deficits which are compensated by interlayer cations (hydrated or otherwise) which are exchangeable.

(a)   **(b)**
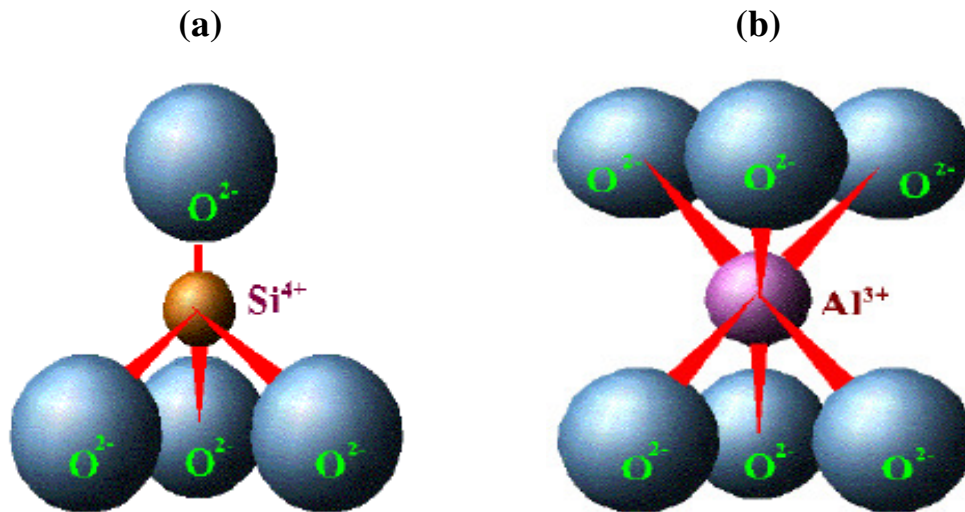
Figure 2.2: Representative drawing of (a) Silica tetrahedron and (b) Alumina octahedron
(Lasledj, 2009)

These basic tetrahedral and octahedral structures are then joined together in sheets. The different clay minerals result from the different arrangements of the above units in sheets of 1:1 or 2:1 lattice and the different types of bonding between these. For instance, the mineral kaolinite has a 1: 1 structure, i.e. it consists of one tetrahedral and one octahedral layer held tightly by hydrogen bonding, preventing interlayer hydration (Fig 2.3a). This results in very low shrinkage / swelling characteristics and little isomorphic substitution inside the lattice; only cations on the external surfaces can be exchanged. Accordingly, the Cation Exchange Capacity (CEC) of this clay is very low 5-10 Meq/100g (Cabane, 2004).
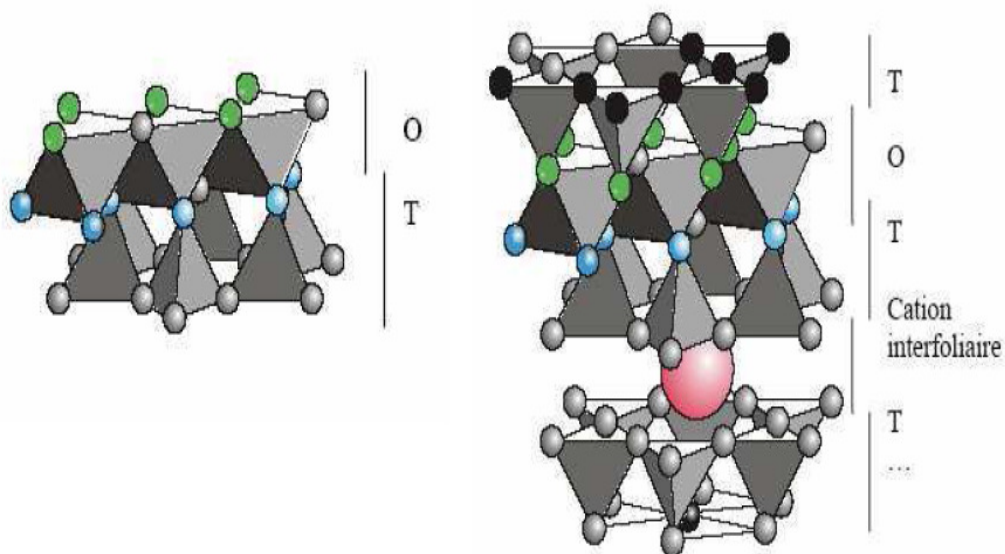
2.3 (a) Group 1:1 structure sheet: **2.3 (b) Group 2:1** structure sheet: two Tetrahedron

Tetrahedron layer S_iO_4 (T) overlayed S_iO_4 (T) layers surrounding an Octahedron Al_2O_6

by Octahedron layer Al_2O_6 (O)   (O) layer, two consecutive layers held by potassium cation

Figure 2.3: Clay minerals structure: T-O & T-O-T (Lasledj, 2009)

Minerals of the 2:1 group contain one octahedral unit surrounded by two tetrahedral units; atoms from the oxygen and hydroxide layers bond and the atoms common to both become oxygen rather than hydroxide ions. This arrangement is less stable and subject to ionic substitution in both the tetrahedral and octahedral units. This leads to different minerals of the 2:1 group depending on the nature of the atoms involved in the substitution. In addition the weaker bonding between sheets and the presence of interlayer cations susbtantially increases their CEC as well as their propensity to attract water molecules. For instance in the mineral montmorillonite (a 2:1 mineral), there is partial substitution of aluminium by magnesium in the octahedral unit, but no substitution in the tetrahedral unit. The bonding between sheets is weak and this allows water molecules to enter between the layers and separate them, making montmorillonite very susceptible to swelling. Montmorillonite has a very high CEC, typically in the order of 100 Meq/100g. On the other hand, illite minerals are of a similar 2:1 structure, but here there is partial substitution of aluminium by magnesium and iron in the octahedral unit and partial substitution of silicon by aluminium in the tetrahedral unit (Fig 2.3b). In addition, the

layers are held together by relatively weak potassium bonds; however, the potassium cations fit in the hexagonal holes formed when the tetraherda are combined into sheets. This hinders the mobility of these cations, and hence their replacement by other cations. Illites thus show a CEC of 20-50 Meq/100g. (Cabane, 2004)

As mentioned earlier, the substitution of different cations in the octahedral sheet (which leads to different clay minerals) results in charge imbalance and a surface charge of the clay particles. This leads to several interactions between the components of clay. The most important interaction is the formation of adsorbed ion layers on the clay surfaces. The negatively charged clay surface attracts the cations present in the pore water to the particle surfaces, while the like charged anions are repelled. At the same time, the cations tend to move away from each other because of their same charges and physical size when hydrated. The net effect is that the cations form a dispersed layer adjacent to the clay particle, known as "diffuse double layer" or simply "double layer" (see Fig. 2.4). The thickness of the double layer determines the plasticity of the clay (Bhattacharje et al., 2003). In a smectite, this layer can be several times thicker than the clay particle. The cation concentration decreases with distance from the clay surface until the concentration becomes equal to that of the free water in the void space (Schmitz, 2006).
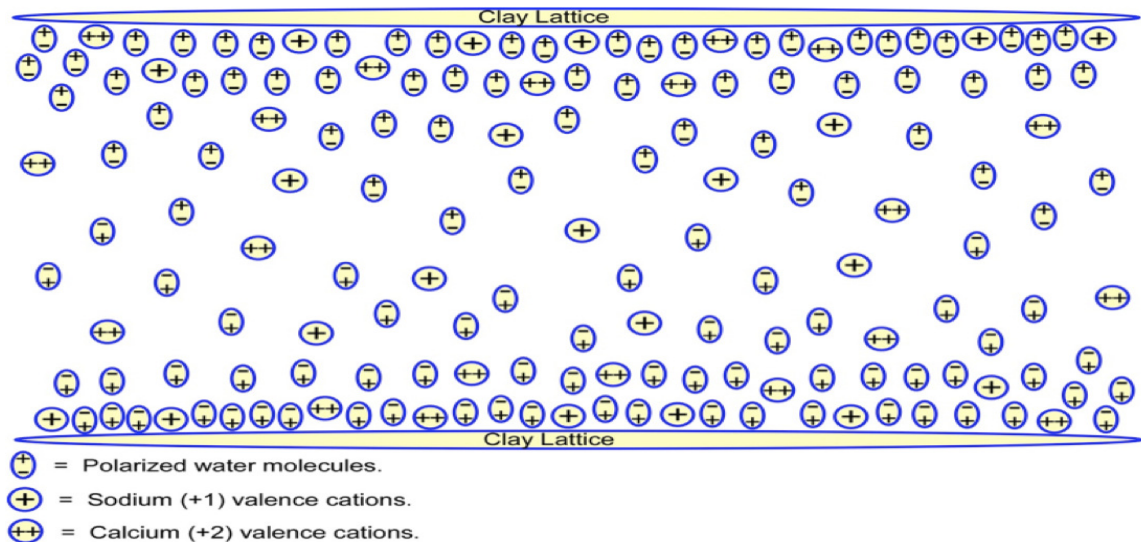
Figure 2.4: Distribution of ions adjacent to a clay surface according to the concept of the diffuse double layer (Advanced Geotechnical soil stabilisation [AGSS], 2014)

The above brief background on clays can explain why chemical, and in particular lime-treatment has been succesful in atlering the clay properties, as detailed in the following sections.

2.4. Lime-clay interactions

Lime is a common name used for $CaCO_3$, $Ca(OH)_2$ and CaO. These are commonly known as limestone, hydrated/slaked lime, and quicklime respectively. The former type of lime is of interest in agricultural applications and is not used in this form for civil engineering ground improvement applications. For these, the latter two lime types are used instead, and in particular CaO; carbonation of the CaO or $Ca(OH)_2$ while used in-situ can of course occur in the presence of CO_2, which is actually believed to be undesirable in the context of engineering ground improvement, as explained later.

When lime is added to a soil, the following processes occur: (a) cation exchange and flocculation of the clay (these are short-term reactions commonly called 'modification' reactions); (b) depending on the lime content used, pozzolanic reactions may develop (these are long-term reactions commonly called 'stabilisation' reactions); (c) finally, carbonation can also occur in the presence of carbon dioxide.

(a) Modification reactions

If hydrated lime is used, first, dissolution of $Ca(OH)_2$ will release calcium ions and hydroxyles in solution (the latter are responsible for the rise in pH noted when treating the soil with lime):

$$C_a(OH)_2 \rightarrow C_a^{2+} + 2OH^-$$
Eqn 1

Cation exhange occurs when the divalent calcium (Ca^{2+}) cations saturate the solution and become adsorbed at the clay surface or in-between sheets in preference to cations originally present, according to their position in the Lyotropic series but also due to ion concentration differences. An agglomeration of the clay particles is observed at this stage (flocculation). This is a result of the reduction in the thickness of the double-layer (due to

cation exchanges and the increased quantity of calcium ions adsorbed on the clay surface), causing the particles to become closer and hence attract each other. This short-term reaction takes place within hours after the addition of lime (Locat et al., 1990). In practical terms this is manifested as a change in the nature of the soil (texture/grain size and an immediate modification in the plasticity characteristics of the soil) and consequently a change in the swelling potential of the soil (if this was of a swelling nature) as well as its compaction characteristics (Bell, 1996, Osula, 1996). Note that other authors (Eades and Grim, 1960 or Diamond and Kinter, 1965) argued that this flocculation could also be due to the early formation of small quantities of calcium silicate or calcium aluminate hydrates, which could create some bridging between particles and consequently flocculation. A small short-term increase in the strength of the soil often reported may also be due to these mechanisms.

Note that if CaO is used instead (on a wet soil), first an exothermic hydration reaction is produced according to which $Ca(OH)_2$ is formed as:

$CaO+H_2O => Ca(OH)_2 + 15.5$ KJ/mol

The practical implication of this reaction is an immediate reduction in the water content of the soil. Note that Boynton (1980) reported a certain volume expansion of the soil upon CaO hydration. As in natural soils, a decrease in water content is followed by a certain increase in strength and bearing capacity of the soil. However the improvement of these properties upon lime treatment is mostly the result of the other phenomena (ionic exchanges and pozzolanic reactions) described in this section.

After this reaction, the dissolution of $Ca(OH)_2$ occurs as described in Eqn 1 and the ensuing phenomena disscussed above follow.

(b) Stabilisation reactions

Depending on the amount of lime used, long-term 'pozzolanic' reactions may follow. A pozzolana is a material that is capable of reacting with calcium in the presence of water to produce cementitious compounds. In this case, the clay is a natural pozzolana as it contains silica and alumina. Due to the high alkaline environment induced by the lime, silica and

alumina from the clay are dissolved (especially at plate edges). This leads to the formation of calcium-silicate-hydrate (CSH) and calcium-aluminate-hydrate (CAH) gels. These gels have the ability to bind the clay together, and possibly also block off the soil pores. Over time, the gel gradually crystallises into compounds also found in ordinary Portland cement (see e.g. Fig. 2.5). This leads to artificial cementation of the lime treated soil. For this reason in this thesis these reactions will be preferentially called 'cementation' rather than 'stabilisation' reactions. Note that it was recently shown that lime-treated soils have high concentrations of calcium throughout the lime stabilised clay aggregates, chemically altering the clay, as opposed to cement stabilised clay where the cement forms a protective coating around the clay aggregates and very little calcium actually diffuses into the clay (Harris and Scullion, 2009).

For pozzolanic reactions to occur, lime in excess of the complete saturation in calcium of the treated clayey soil must have been supplied. After complete saturation in calcium of the clay, with full completion of cationic exchange reactions, any excess calcium will then be available for pozzolanic reactions and the creation of cementitious products (e.g. Sivapullaiah, 2000; de Brito Galvao et al., 2004; Al-Mukhtar et al., 2010 and Okyay and Dias, 2010). A practical test performed to determine the lime percentage threshold beyond which such reactions can occur (variable for each soil) was suggested by Eades and Grim (1966). This is a pH monitoring test called the Initial Consumption of Lime (ICL) test, specifying that cationic exchange has been completed when the pH of the soil at 25 °C has been raised to 12.4 which correspond to that of a calcium-saturated solution. Lime beyond the percentage which achieved this pH, would then be available for pozzolanic reactions as stated earlier. Note that the validity of the test was questioned by Rogers and Glendinning, (2000) who suggested that it should be used as an indicator of the necessary amount of lime accompanied by evidence of change in their mechanical properties. An alternative method to identify the minimum necessary lime percentage is the identification of the lime fixation point (LFP) through plasticity testing. LFP is the lime percentage giving a maximum increase in the plastic limit value. Additional lime would then result in soil stabilisation reactions.

The pozzolanic reactions are lengthy as the available lime has to diffuse through both the soil structure and initial cementitious products to the reaction site, and since clays are materials of a very low permeability, the lime movement is identified to be very slow.

This slow diffusion and the gel crystallisation process is commonly presented as the reason why reaction between lime and clay is time-dependent (referred to as 'curing' in the same fashion as when referring to the increase in the strength of concrete with time). The pozzolanic reactions will thus continue over time as long as there is sufficient calcium in the lime-water system to react with the silica and alumina, the pH is high enough to maintain solubility of the silica and alumina, and also provided that sufficient water and silica are available (e.g. Asghari et al., 2003; Al-Mukhtar et al., 2010). Note that temperature during curing was reported as having a beneficial effect on chemical soil improvement (i.e. the effects are enhanced upon elevated temperatures and anihilated below 4°C). Temperature dependence was attributed to the fact that when clay minerals are subjected to significantly elevated temperatures at about 500 °C they may collapse while others transform into other minerals (Rao & Shivananda, 2005b; Al-Rawas et al., 2005), consequently the soil nature changes. Note that for in-situ lime treatment, usually carried out with quick lime, heat is generated during the hydration process, which in turn affects the rate of the chemical reactions taking place.
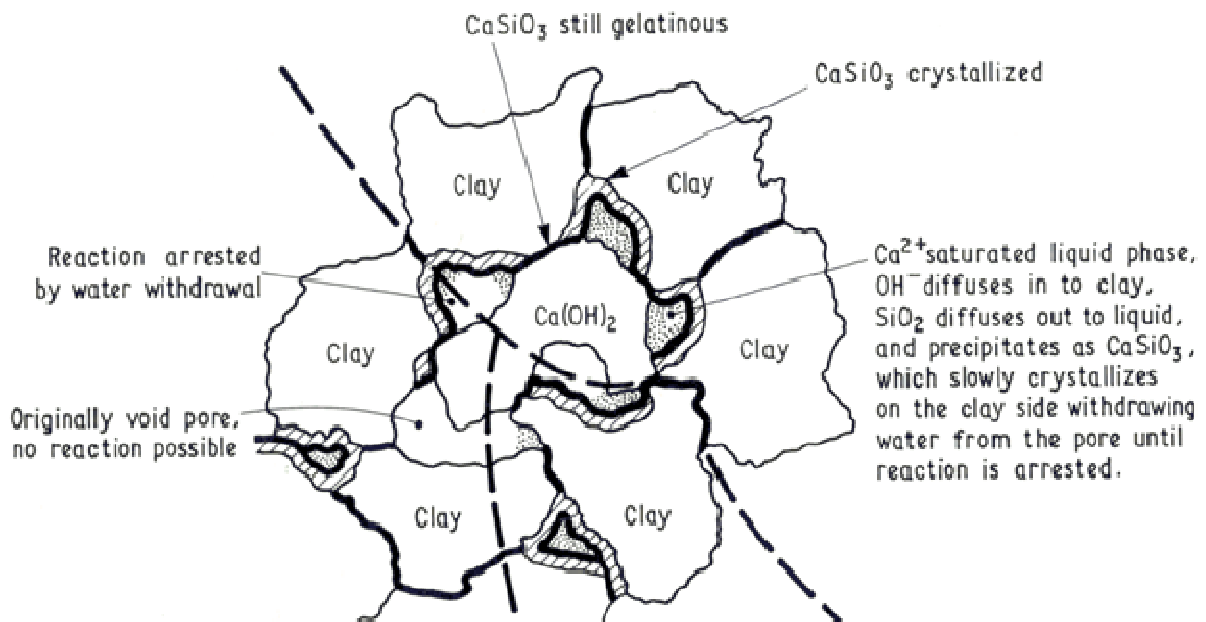
Figure 2.5: Mechanism of lime stabilisation (Ingles & Metcalf 1972)

In practical geotechnical applications one can see the manifestation of the complex pozzolanic reactions as a considerable increase in the strength of the soil, associated to the

different cementitious products developed and the resulting cementation bonds. These are of diverse nature for different soils; different products also take different times to form. For instance, in lime treated kaolinite, Goldberg and Klein (1952) reported the formation of C_3AH_6, Glenn and Handy (1963) identified CSH and CAH, Bell (1996) also recognized CSH (tobermorite) and C_4AH_{13}, CAH_{11}, CAH_{10}. In lime treated montmorillonite, Hilt and Davidson (1960) identified C_4AH_{13} and Bell (1996) reported the formation of CAH and CSH gels. Rajasekaran and Narasimha Rao (1997) noted the formation of CAH, CSH and $CSAH$ in marine clays treated with lime.

Ahnberg (1996) claimed that it was possible to calculate the approximate amount of reaction products that would potentially form cementitious bonds in the soil upon the addition of different binders including lime, assuming complete hydration and that sufficient alumina and silica are present in the soil during the stabilisation process. These products are reported in Figure 2.6, where the blue, or pale shaded, bars represent the more rapid cement reactions (modification) and the yellow or non-shaded bars represent the more long-term pozzolanic reactions (stabilisation / cementation) with the soil. The red, or darker shaded, bars, for a mixture of cement and fly ash, characterise the pozzolanic reactions that may take place with the fly ash itself, since silica and alumina are normally more readily available in the fly ash than in the soil.
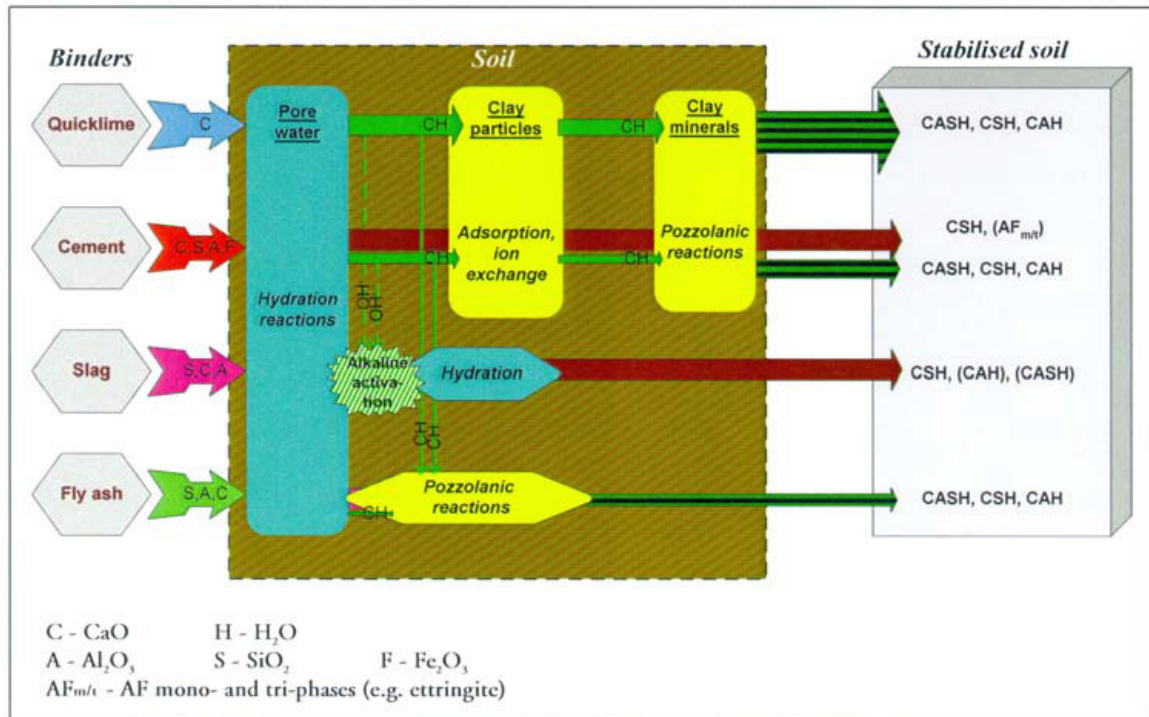
Figure 2.6: Rough outline of the principal chemical reactions and reaction products formed by different types of binders in a soil. (Ahnberg, 1996).

(c) carbonation reactions

These occur as a result of lime reacting with CO_2 in the air. When the CO_2 is dissolved in the pore water soil, it reacts with the hydroxyl ions, forming carbonate ions, which subsequently reacts with the calcium ions. This results in the formation of calcium carbonate $CaCO_3$, a weak cement whose formation is undesirable (unless a relatively high amount of lime is used), as this reaction consumes lime which would have otherwise been used in pozzolanic reactions for the formation of strong cementitious bonds. Another undesirable effect of carbonation is the fact that it delays penetration of ions on the surface of the clay and increases the time for these to reach the reaction sites (Barker, 2002).

The carbonation reactions can be described as follows:

$$CO_2 + 2HO^- \Rightarrow CO_3^{2-} + H_2O$$

$$CO_3^{2-} + Ca^{2+} \Rightarrow CaCO_3$$
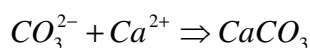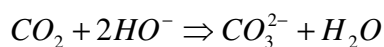
2.5. Detection of the progress of the lime-clay reactions

As explained in the previous section, the progress of lime modification and pozzolanic reactions with time can be monitored by measuring changes in the Atterberg limits and strength (usually in terms of unconfined compression strength) (Hilt and Davidson 1960; Holtz 1969; Bell 1988; Holt and Freer-Hewish 1996; Rogers and Glendinning 1996; Rogers et al., 1997; Boardman et al., 2001). However researchers can further support the findings in terms of effects of lime on soil properties by methodically investigating the development of reactions using microscopic analyses, mineralogical studies, as well as by performing physico-chemical testing (e.g. pH changes, electrical conductivity changes, calcium concentration and soluble ion concentration measurements etc.). Thus, scanning electron microscopy (SEM) and / or mercury intrusion porosimetry (MIP) performed in parallel with hydro-mechanical testing of lime treated soils have been extensively used for examining the changes in the micro-fabric and to confirm (by direct inspection or indirectly, in terms of effects on the porosity) the development of different cementation products (e.g. Choquette et al., 1987; Delage et al., 1996; Locat et al., 1996; Ninjgarav et al., 2007; Koliji et al., 2010). Mineralogical studies are also commonly performed by X-Ray Diffraction Analysis (XRD). These are used to follow the evolution of the clay-lime reaction by identifying and potentially quantifying the mineralogical changes in the soil as well as any new chemical reaction products formed in time (i.e., CSH, CAH, CSAH, $CaCO_3$ etc) if new reflection intensities appear on the spectrum of the results (e.g. Lambe & Whitman 1959; Eades & Grim 1960; Mitchell, 1976; Arabi & Wild, 1989; Bell, 1996; Al-Mukhtar et al., 2010; and Metelkova et al., 2012). For instance, Lambe and Whitman (1959) and Eades and Grim (1960) found that upon lime addition, new reflections were visible at d-spacings of 3.87, 3.67, 3.035, 1.619, and 1.582 Å (1 Å = 0.1 nm), which appeared to be indicative of calcite, feldspars, kaolinite, and chlorite, respectively. Another example of XRD results that can be used to identify the evolution of pozzolanic reactions is shown in Figure 2.7 (after Al-Mukhtar et al., 2010). The figure shows CAH products clearly identified in the lime-treated soil through the XRD results (not present in the untreated soil), and that their characteristic reflections intensities increased with curing time.
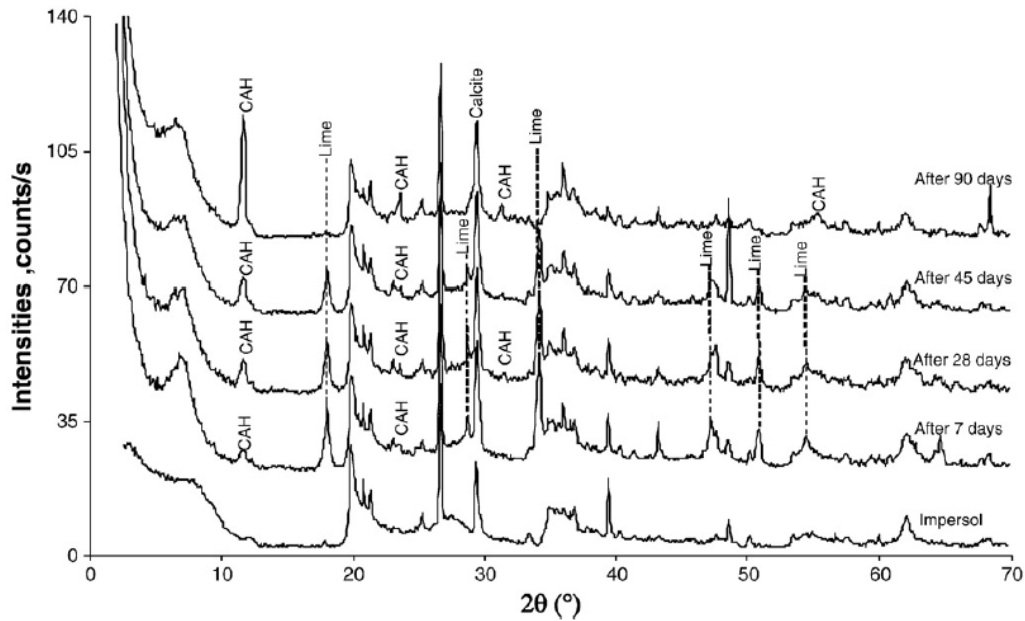
Figure 2.7: X-Ray diffraction of 20 % lime treated and untreated bentonite with curing time (Al-Mukhtar et al., 2010)

Other techniques used for clay mineralogy studies (e.g. Differential Thermal Analysis (DTA), various spectroscopic methods such as infrared spectroscopy (IR), nuclear magnetic resonance spectroscopy (NMR) etc) can be applied to detect mineralogy changes in the soil due to lime treatment. Examples of such studies include Maubec (2010) using XRD and NMR to detect the effect of lime on Polwhite kaolinite and calcium bentonite or Eisazadeh et al. (2012) who used Fourier transform infrared (FT-IR) spectroscopy and solid state nuclear magnetic resonance (SS-NMR) to detect the time-dependent changes in the structure of lime stabilized montmorillonitic and kaolinitic clays.

Moreover, the progress of pozzolanic reactions can be monitored by pH measurements. An initially high pH is observed due to the presence of the Ca^{2+} and hydroxyls in solution. This would be expected to remain constant as long as lime modification reactions have been completed. Instead, a pH reduction is observed in the longer term which can be linked to the consumption of the necessary Ca^{2+} and OH^- for pozzolanic reactions, thus confirming that such reactions are developing (Broadman et al., 2001; Rao and Shivananda, 2005b; Al-Mukhtar et al., 2010). Note that the maximum pH that the soil can reach is that of a saturated solution in $Ca(OH)_2$. This varies with temperature and is 12.64 at 20˚ C (Maubec, 2010).

Another indicator can be the changes in the electric conductivity of suspensions of the materials in water. These follow the same pattern as the pH changes, i.e. an initial rise in conductivity, followed by a period of constant conductivity indicating (according to the literature) that pozzolanic reactions are not yet happening, and then a continuous drop in the conductivity which is believed to be concurrent with the consumption of Ca^{2+} and OH^- for pozzolanic reactions (Broadman et al., 2001; Rao and Shivananda, 2005b).

2.6. Practical implications: Reported geotechnical properties of lime-treated clays

The previous section mentioned the implications of lime treatment in qualitative terms for the respective stages of modification and stabilisation/cementation, linking these to the chemical reaction mechanisms. This section provides examples of reported geotechnical parameters / soil properties which are of practical relevance to the geotechnical engineer, giving an appreciation of the expected changes in the geotechnical properties in quantitative terms. Of course as noted earlier, the exact results of the treatment would be variable and would depend on a number of factors identified above, namely: the soil type / mineralogy, the lime amount, curing method, curing time and conditions during curing (e.g. temperature, humidity etc.), and the possible presence of deleterious substances for lime treatment (gypsum, organic content etc.) amongst other.

Most studies in the literature are based on simple tests, and refer to changes in basic characteristics or indices such as Atterberg limits, Proctor characteristics, CBR or unconfined compressive strength (UCS). For these a vast literature exists and only some selected indicative examples will be shown. Conversely much fewer and recent studies refer to more advanced testing (e.g. triaxial testing) and could thus provide parameters that could be used for constitutive modelling. These studies will be reported in more detail.

2.6.1. Plasticity characteristics

It was mentioned that lime has an immediate effect on reducing the plasticity of the soil. Several authors report a substantial reduction in plasticity index (PI) for clay soils when mixed with lime (Sherwood, 1993). However the change in the plastic and liquid limit individually (which usually is reported to happen to some extent for both limits) (see e.g. Brandl, 1981; Sivapullaiah et al., 2000; Dash & Hussain, 2012) differ depending on the

type of soil as they do not always go in the same direction, so that the eventual effect on the plasticity index is also variable. For instance Ola (1978) reported an increase in both the liquid limit and the plastic limit with the lime amount increase, resulting in plasticity index decrease which is due to faster increase in plastic limit. Conversely Osula (1991), studying a problematic lateritic soil from Nigeria stabilised with lime, found a reduction in liquid limit and a slight increase in plastic limit with lime content increase. The differences, due to the different soil type, can be seen clearly on collective graphs of researchers studying more than one soil. For instance Figure 2.8 below from de Brito Galvao et al., (2004) represents the effects of lime on the Atterberg limit of two Brazilian soils of different origin (a brown saprolitic soil noted (1) and a red lateritic soil noted (2)). The figure shows no substantial change in the plasticity index of soil 1 (although the liquid limit and plastic limit both increased slightly) as opposed to a clear decrease in the plasticity index of Soil 2 for up to 6% lime addition. The latter effect was due to the decrease in the liquid limit (for 2 – 4% lime addition), while the changes in the plastic limit were far too small to be considered of significance.
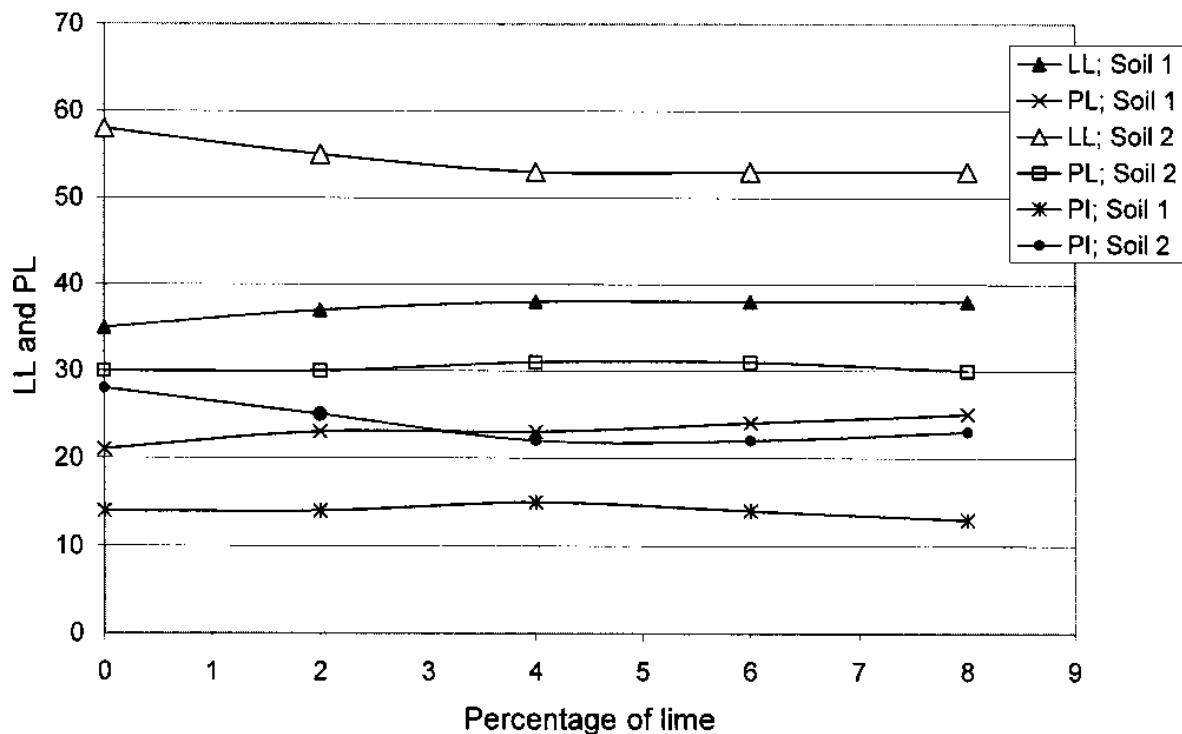
Figure 2.8: Variation of liquid limit and plastic limit with lime content of soil

(de Brito Galvao et al., 2004)

The differences were even more pronounced in the study by Dash & Hussain, (2012) on a montmorillonite-rich expansive soil (ES) and a silica-rich non-expansive residual soil (RS) (see Fig 2.9 & 2.10). The liquid limit of the former soil was clearly shown to decrease. Conversely the residual soil (other than for some non-monotonic changes with lime percentage immediately after treatment) showed generally a clear increase in the liquid limit, which became more pronounced with curing time. The authors attributed this behaviour to the production of increased quantity of water holding gelatinous products during pozzolanic reactions, and suggested that this is the typical behaviour of soils rich in silica treated with lime. As for the plastic limit this generally increased for both soils (except for some non-monotonic changes with lime percentage immediately after treatment observed for the ES soil). In particular for the silica-rich soil RS, the plastic limit was shown to increase dramatically with curing times, and this was again attributed to the water holding CSH gel formation.

The former were but examples of variations in the plasticity characteristics reported in the literature. Due to the differences in the findings depending on the soil subjected to treatment, the studies on lime treatment always start by reporting the effects on the plasticity characteristics of each particular soil, often for varying lime amounts added to the soil until the specified plasticity requirements for construction are met.
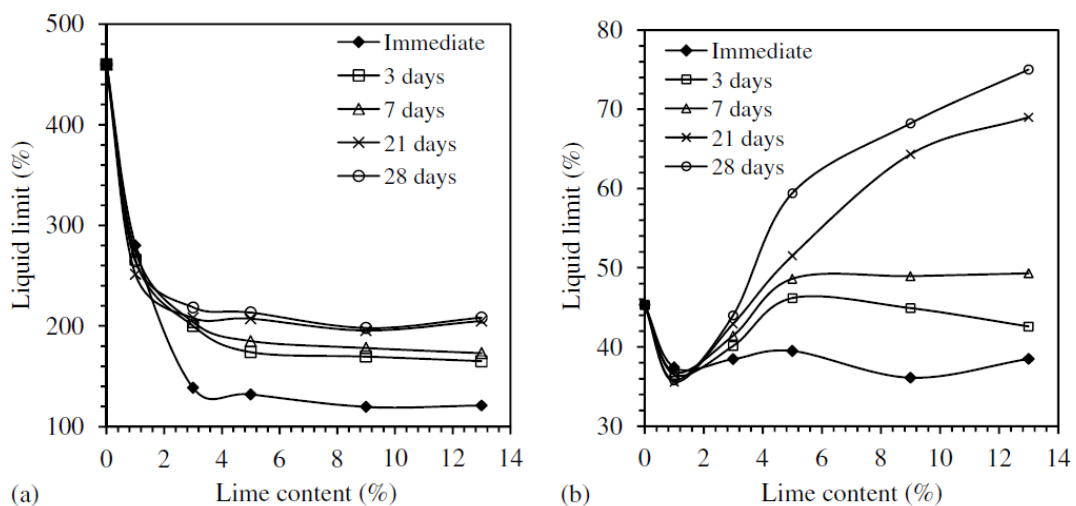
Figure 2.9: Variation in liquid limit with lime content: (a) expansive soil and (b) residual soil (Dash & Hussain, 2012)
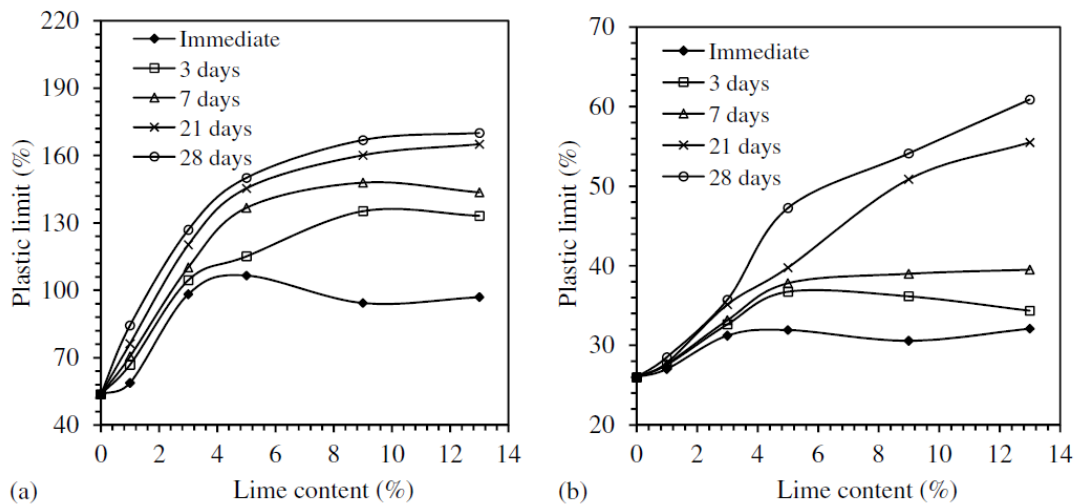
Figure 2.10: Variation in plastic limit with lime content for (a) expansive soil and (b) residual soil (Dash & Hussain, 2012)

2.6.2. Swelling and shrinkage

A substantial amount of work was carried out to assess the effect of lime on the swelling/shrinking behaviour of soils. In fact the treatment of non-sulphate bearing swelling soils with lime has been one of the most common engineering applications of lime treatment. The beneficial effect of lime on the swelling potential /deformation of shrinking swelling of non-sulphate bearing soils (consistent with the change in the nature of the soil and its plasticity characteristics) was thus the main focus of a large number of studies. Examples include (amongst many others):

- Brandl (1981) who observed that different lime-treated soils all absorbed less water than the respective untreated soils but also dried in the air much slower than the untreated soils. The swelling potential of montmorillonitic soils was also improved. Overall 1-3 % lime was found to be sufficient for improving the shrinking/swelling characteristics of the soils beyond which no further improvement was noted.
- Bell (1996) who found that linear shrinkage of Upper Boulder Clay and Tees Laminated Clay treated with various amounts of lime reduced drastically compared to the untreated soils (beyond 8% lime however no further changes were observed).

- Al-Rawas *et al.* (2005) who investigated the effect of cement, lime and Sarooj (an artificial pozzolan) for expansive soils from Oman and found that lime performed best of all other stabilisers (or their combination) in improving the swelling characteristics of the soil; namely with the addition of 6% lime, both the swell percent and swell pressure were reduced to zero.

- Nalbantoglu and Tuncer (2001) who tested expansive marine clays of the Degirmenlik flysch, in Northern Cyprus and found almost 0% swelling potential for lime percentages higher than 3% and curing times of seven days or more.

- Rao & Thyagaraj (2003) treating an expansive Indian black cotton soil with lime slurry columns and noticing a 30% reduction in the swelling potential of the soil.

It is interesting to note however that Rao et al. (2001) claimed that the beneficial effect of the lime treatment on the volumetric stability of expansive soils would be at least partly reversible upon cycles of wetting/drying, based on studies of Indian Black Cotton Soils.

2.6.3. Strength and shearing behaviour characteristics

In common practical applications the strength of the chemically stabilised soils is usually assessed in terms of the unconfined compressive strength (UCS), q_u. In fact the UCS of the lime-stabilised soil is one of the criteria used for the selection of appropriate lime percentages[1] in addition to plasticity testing and/or ICL testing. The literature concerning the effects of lime on the UCS of different soils is therefore vast and only the salient features together with recent papers will be reviewed. The main findings are that the UCS is affected by a number of factors mentioned above on which the success of lime treatment and the development of pozzolanic reactions depend; thus empirical correlations were also suggested to address its dependence of such factors. Examples of such correlations follow in this section. Very few papers investigated the shear strength characteristic and behaviour based on advanced triaxial testing. These will be reviewed in detail as they are of particular relevance to the present study.

---

[1] For common highway engineering applications the CBR of the soil can also be used to support the selection of an appropriate lime percentage

As explained above, the pozzolanic reaction development and hence the acquired strength generally depends on the quantity of lime consumed and the resulting amount of cementitious gel produced. Thus the added lime should be beyond a certain threshold (indicated as the LFP or ICL of the soil), to enable pozzolanic reactions. In general increasing amount of lime is reported to increase the strength; for instance in recent testing of a highly expansive soil treated with varying lime percentages (0 - 20%), Al-Mukhtar et al. (2010), showed that for all percentages used, the q_u increased in time with high lime percentages (see Fig 2.11). As the tests were accompanied by XRD analyses, the authors were in position to prove their findings in terms of pozzolanic reaction products. It was thus found that at low lime percentage addition (2 and 4%), strength kept developing up to 28 days curing. In terms of the modification reactions (believed to be completed within a few days), this would appear to be a rather long term evolution; however there was no evidence of any pozzolanic products forming based on the XRD results. The authors thus concluded that no pozzolanic reaction products were created in the treated soil for these lime amounts, even if there was some strength increase also for lower percentages of lime. Pozzolanic products were detected for lime quantities $\geq 6\%$ which showed a sustained increase in the UCS with curing time, so that the q_u of the specimens treated with 6% lime was found to be 5 times higher after 28 days curing and 6 times after 90 days curing compared to the q_u of the untreated specimen. With 20% lime addition, q_u increased by 8 times for 28 days curing and 17 times after 90 days curing compared to the q_u of the untreated specimen. Note the very high percentages of lime used for this soil, which contradicts statements that usually 1%-3% by soil weight would be enough for soil treatment when using quicklime (e.g. Bell, 1996), and 2 to 8% of hydrated lime are used for soil stabilisation (e.g. Basma & Tuncer, 1991) but shows the strong dependence of the necessary lime percentage on the type of soil.
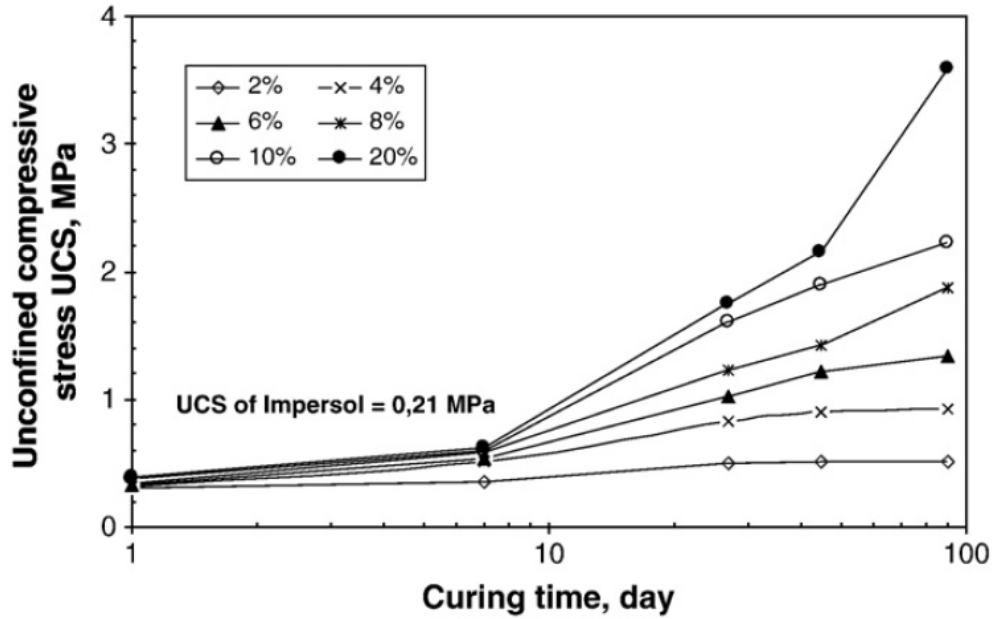
Figure 2.11: Unconfined compressive strength (UCS) of bentonite soil with curing time for various amount of lime (Al-Mukhtar et al. 2010).

Consoli et al. (2009) investigated the influence of the amount of cementitious agent, the porosity and the moisture content on the strength of a sandy lean clay material from Southern Brazil, treated with two different chemical additives, i.e. lime and cement (only lime will be reviewed here). The UCS tests showed a linear relationship between lime percentage and unconfined compressive strength (q_u), for different compaction dry densities. The authors also investigated the effect of the water/cementitious material ratio and found that this did not appear to be a useful parameter in the analysis of the strength development of the studied lime-treated soil. Similarly, varying the moisture content while keeping the dry unit weight unchanged was not found to affect considerably the q_u of the soil. However they suggested the existence of a unique, linear relationship to describe the increase in q_u with the ratio of porosity/ lime content (see Fig 2.12) and concluded that this ratio plays a fundamental role in the target strength determination. This finding would be useful for practical applications, as the required lime percentage could be adjusted for specific target strength. For their particular soil, they expressed this relationship as:

$$q_u = -49.5 \left(\frac{n}{L_{iv}^{0.06}} \right) + 2110$$

n, is the porosity and L_{iv}, is the volumetric lime content

The figure shows a scatter plot with x-axis labeled $\eta/(L_{iv})^{0.06}$ ranging from 26 to 42, and y-axis labeled q_u: kPa ranging from 0 to 1000. Legend:
- $L = 3\%$
- $L = 5\%$
- $L = 7\%$
- $L = 9\%$
- $L = 11\%$
- $q_u = -49.5[\eta/(L_{iv})^{0.06}] + 2110.1$
- $R^2 = 0.98$
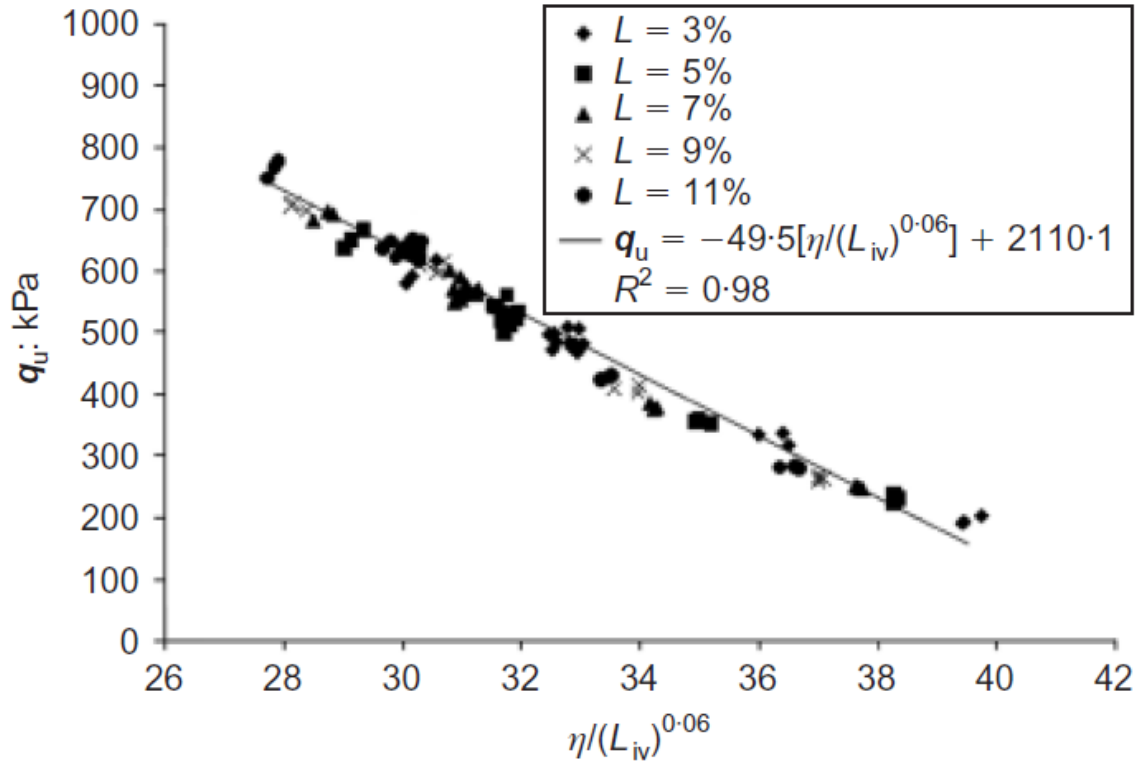
Figure 2.12: Variation of unconfined compressive strength with adjusted porosity/volumetric lime content (Consoli et al. 2009)

Of course, for the possible generalisation of these findings to other soils, further studies on more soils would be required.

In other studies it was however shown that strength does not increase linearly with lime content and that it may in fact decrease upon excessive lime addition. Thus it has been observed that the q_u would first increase with the addition of lime; then, after reaching a maximum, it would start declining upon further lime addition (Brandl, 1981; Bell, 1996; Dash & Hussain, 2012). The latter authors suggest that some soils, predominantly silica-rich soils that form silica gel, when treated with lime percentage higher than just the LFP can lose strength after a prolonged curing period (see Fig. 2.13). To understand this, it should be kept in mind that cementation is limited by the available amount of silica; when all silica in the clay is used up, further lime addition would not result in the formation of

any new cementation products (Hausmann, 1990). One would then expect the strength to remain constant rather than to decrease. Dash & Hussain (2012) attributed the observed strength reduction to the fact that with increasing lime amount, the soil structure tends to become increasingly porous (due to the excess formation of the high-porosity silica gel), thus counteracting the strength gained through cementation. The explanation put forward by Bell (1996) is that the lime does not have a suitable friction or cohesion, and that the excessive lime amount serves as lubricant to the soil particles, which decreases the strength of the soil. Brandl (1981) specifically states that the particles 'swim' without touching each other within the gel, which thus acts as lubricant. He also notes however that the maximum strength indicates "the point of saturation which shifts towards higher dosage with curing time". He claims that the reaction products gradually grow into "crumbs" (which is probably consistent with the observation of Dash & Hussain, 2012 that the cementitious products are more 'porous') and he also points at the possible carbonation, which can be of importance regarding its effects on strength.
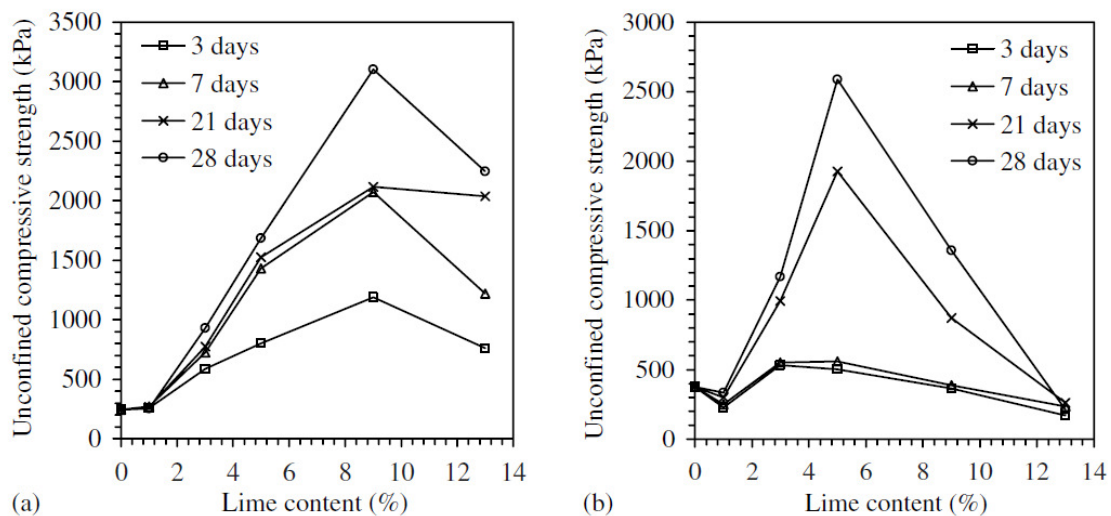
Figure 2.13: Variation in unconfined compressive strength with lime content:

(a) expansive soil and (b) residual soil (Dash & Hussain, 2012)

The above discussion again shows the high dependence of the findings on the nature of the soil and can lead to the conclusion that complementary testing (mineralogy, chemistry, pH, microstructural analysis with ESEM etc) is necessary to support any assumptions in terms of mechanisms affecting the strength change of a particular soil.

Regarding the effect of curing time in particular, Figures 2.11 & 2.13 presented above (from Al-Mukhtar et al. 2010 and Dash & Hussain, 2012 respectively) show that in general q_u would increase with curing time until it reaches a maximum after which very little further evolution happens. The evolution of curing was reported to be linked to the type of soil and it was shown to be dependent on the percentage of lime used (Sherwood, 1993). Some authors reported rather early times where further strength development may stop (e.g. Zhang, 2011) but others, like Brandl (1981) observed an evolution of q_u with curing times of up to seven years after which no further evolution in strength was apparent (even for highly active clays, which show strength change over long curing periods). Brandl stated that the q_u evolution with the log of the curing time would be approximately linear after 7 days of curing and suggested the following relationship:

$$q_{u,t} = \tan \alpha \log \left(t/7 \right) + q_{u,7}$$

Where

$q_{u,t}$, Is compressive strength at time t

$q_{u,7}$, Is compressive strength after 7 days

t, Is the period of curing (days)

$\tan \alpha$ is the gradient of the straight line of cementation

Another study that addressed the expected rate and degree of strength increase in time was that by Ahnberg (1996). Figure 2.14 which is based on this study, shows the strengths measured for the three tested soils treated with different binders (including lime) together with the amount of reaction products (their approximate calculation as suggested by Ahnberg (1996) was reported in section 2.4 (b) above). The average strength values of specimens tested after 28 days curing were moderately proportional to the theoretical amount of short-term reaction products formed, unlike results obtained from specimens tested after one year curing (these showed a considerably higher strength in a number of cases). The variation in strength for different soils was found to be greater for binders such as lime that are likely to react mainly with minerals in the soil. However Ahnberg pointed out that the rate of strength gain may also be influenced by other factors, such as chemical

constituents initially contained in a particular soil, which may hinder or accelerate its strength increase.
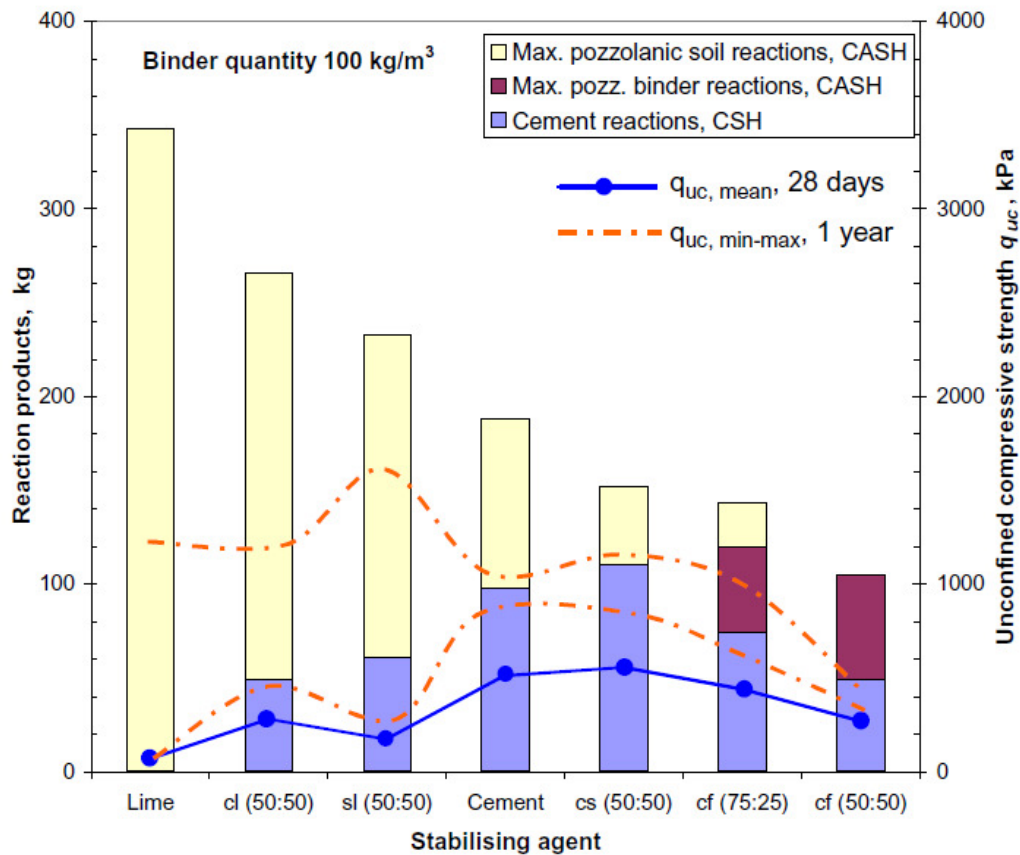
Figure 2.14: Estimates of the amount of reaction products contributing to the strength of stabilised soils (bars) together with measured strength in three soils one month and the range one year after mixing. [c = cement, l = lime, s = slag, f = fly ash]. (Ahnberg, 1996.)

Finally, the q_u was found to be dependent on the compaction delays (i.e. what is called in the literature the 'mellowing' time, as opposed to 'curing' time, which refers to times after compaction). The (up to three hours) strength characteristics of lateritic soil treated with a maximum of 8% lime (by dry weight) were introduced by Osinubi (1998a). These indicated that the compaction and strength properties of lime treated soil declined with an increase in mellowing time (Figure 2.15). Note that the studied compaction delay (mellowing) times in Osinubi (1998a) are indeed quite short – the British Standards specify for a minimum of 12 hours for untreated London Clay samples and between 24 and 48 hours duration for lime treated samples to allow for mellowing (BS.1924 – 1: 1990)
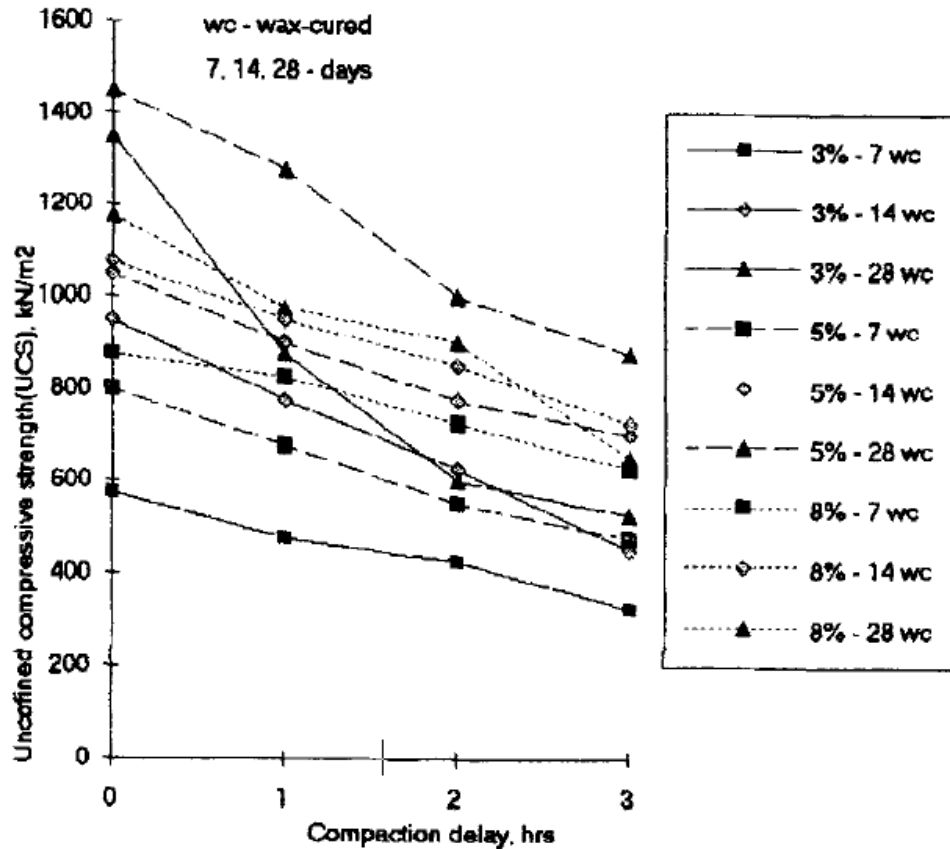
Figure 2.15: Variation of UCS of lime-stabilised lateritic soil with compaction delays / Standards proctor (Osinubi, 1998a)

Some papers discussed the stress-strain behaviour of the soils tested in UCS. Figure 2.16 describes strains at failure decreasing with increasing unconfined compressive strength (Ahnberg et al., 2003). The somewhat apparent change from a higher to a lower (almost constant) failure strain, reflects the transition from contractive to dilative behaviour as the strength of the stabilised soils increases. This was attributed to the formation of higher amount of cementation bonds between soil particles within a short curing time. A more ductile behaviour with larger strains at failure can be observed for soils with lime contents higher than the LFP, when tested at high confining pressures (1 MPa and beyond).
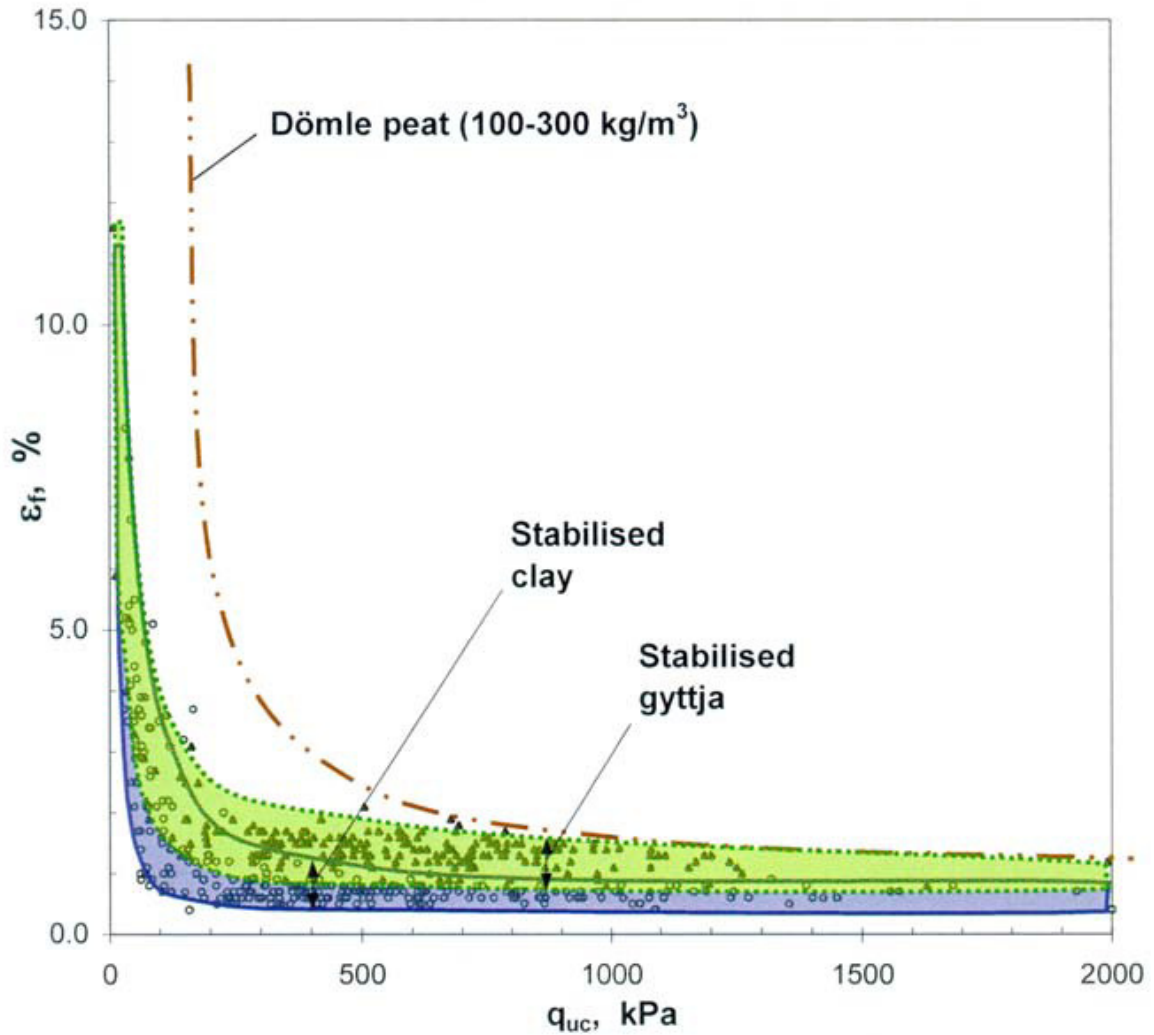
Figure 2.16: Changes in strain at failure with increase in unconfined compressive strength. (Ahnberg et al., 2003)

As opposed to the abundant literature on the UCS of lime treated soils, there is a paucity of information on the shear strength and shear strength characteristics, as well as the overall behaviour of lime-treated soils based on triaxial testing. Some rare studies include those by Oh et al. (2008); Ahnberg (2007) and Zhang (2011). The first of these papers presented a large number of conventional consolidated undrained triaxial tests on a saturated clay soil. The results in terms of peak strengths plotted far above the Critical State of the untreated material. However upon breakage of the cementation bonds the strength of the soil reduced to the critical state strength of the untreated soil, consistently with findings on natural cemented soils when compared to remoulded soils (e.g. Coop and Atkinson, 1993). The shear strength of the treated soil therefore lied between the tensile strength envelope, which constitutes its upper limit, and the Critical State of the untreated soil. An increase was also

noted in the yield point with increasing lime content and curing time (represented in terms of (q,ε_s) , (u,ε_s) as well as (q, p') plots).

Ahnberg (2007) presented the results of an extensive programme of saturated soil triaxial testing, based on two different high plasticity clay soils from Sweden, stabilised with three different stabilisers (cement, lime and slag) and also binary combinations of these three binders. The aim of the study was to investigate the effects of the quasi-pre-consolidation pressures (i.e. yield stresses due to cementation forming rather than the effect of the previous loading history) on the strength behaviour of the stabilised soil. In addition, the effect of curing under different stresses was to assess the implications for deep soil mixing purposes. The tests included triaxial extension and compression under drained and undrained conditions. Oedometer tests were also performed in parallel to enable comparisons based on the quasi-pre-consolidation pressures obtained from these tests. As expected from the literature review, a large variation in the strength of the soils was found, depending on the type of clay, type and amount of binder, curing time but also due to the curing stress and testing conditions. In particular it was found the strength and quasi-pre-consolidation stress of stabilised samples subjected to confining stresses during curing were higher than those of samples cured at zero confining stress. On the other hand, it was found that the soils would behave as overconsolidated materials if the consolidation stress during triaxial testing was higher than the quasi-preconsolidation pressure and as normally consolidated soils otherwise (note that the results of the cement stabilised soils manifested a more brittle behaviour than the lime-treated ones). This led to the recommendation to apply the construction load (e.g. from an embankment) as soon as possible to produce a certain compression of the material shortly after treatment. It was also concluded that for deep mixing (i.e. at high confining stresses) the strength of the untreated and treated soils (especially the lime treated ones) were mobilised at similar strain levels especially in undrained loading. Mobilisation of shear strength was observed within low strain levels in drained shearing at low confining stresses, with a subsequent abrupt loss in strength linked to brittle behaviour. This was particularly the case for cement treated samples compared to lime treated samples and in both instances this occurred much earlier than in the untreated soil. A yielding model proposed by Larsson (1977) for natural clays (similar to the model by Leroueil and Barbosa (2000) suggested for unsaturated clays and clays of varying microstructure) was found to be applicable to describe the strength behaviour of the stabilised soils.

To the Writer's knowledge, Ahnberg's (2007) paper is perhaps the most comprehensive study published in English on triaxial testing results for saturated lime-treated clay soils.

Finally, a recent PhD work conducted at London South Bank University (Zhang, 2011) investigated the mechanical properties of lime-treated London Clay through triaxial testing, focussing in particular on suction-controlled testing. Limited saturated soil triaxial tests were performed to complement the results and address the effect of suction. These results also showed the beneficial effect of the lime on the shear strength within ranges of strain relevant to engineering design (despite the observed strain softening behaviour). The results also indicated that although the properties of the soil have obviously changed upon lime treatment, the behaviour of the unsaturated lime treated soil presented behaviour trends consistent with the reported behaviour of uncemented unsaturated soils regarding the effect of suction or mean net stress on the shear stress and shearing behaviour of the soil. The research supplied valuable quality data of suction controlled testing of lime-treated soils and addressed the behaviour of the lime-treated soil, within an unsaturated soil mechanics framework. However, due to the length of the constant suction triaxial testing undertaken, it was not possible to consider different lime percentages and compaction conditions. These are likely to affect the properties of the lime-treated soil in terms of the resulting differences in the soil fabric as well as cementation bonding. Indeed, for natural bonded soils it was demonstrated that both fabric and degree of cementation affect the shear strength and shearing behaviour of the geomaterials in terms of position and shape of the yield surface (e.g. Maccarini, 1987; Vaughan, 1988; Bressani, 1990), stiffness, peak strength magnitude or mobilisation strain range and brittleness or ductility (Cuccovilo and Coop, 1993)

2.6.4. Permeability

Although not as well researched as the UCS and plasticity characteristics, permeability of lime-treated soils was investigated in a number of studies. Permeability is an important property, as it can directly affect the pore water pressure response at loading and, depending on the rate of loading, influence the extent to which undrained or drained conditions govern the strength behaviour (Ahnberg, 2006). Moreover, during the stabilisation course, permeability will affect the rate of consolidation after construction and

the possible impact on the environment from the leaching of stabilisers (in addition to losing part of the stabiliser meant to be necessary for stabilisation purposes).

The findings of previous studies on lime-stabilised soil permeability appear to be inconclusive, in that many studies report in some instances an increase in permeability (which is generally attributed to particle aggregation e.g. Brandl, 1981; Nalbantoglu and Tuncer, 2001; Rajasekaran & Narasimha Rao, 2002) but in other instances a decrease in permeability with respect to that of the untreated soil or both an initial increase and subsequent decrease depending on the lime amount used, the curing period, the stress conditions and the macro-structure of the stabilised soils (e.g. Locat et al., 1996).

For instance, Nalbatoglu and Tuncer (2001) testing an expansive marine clay from Northern Cyprus, found an increase in permeability compared to that of the untreated soil, regardless of the amount of lime used or curing time (see Fig 2.17 below). Brandl (1981) showed an increase in permeability of "over one or two decimal exponents". He suggested that the more 'cohesive' and reactive the untreated soil is, the higher the increase in permeability due to initial flocculation. de Brito Galvao et al. (2004) investigated the effect of lime on the permeability of two Brazilian soils of a different origin, namely brown saprolitic soil (1) and red lateritic soil (2). Results obtained from the test indicate that the coefficient of permeability for soil 1 increased about five times with only 2% lime addition, presumably due to flocculation-aggregation, then decreased on further lime addition (without reaching the low permeability recorded for the untreated soil) which was attributed to the formation of cementation products, filling the voids within the aggregates. The permeability then continued to drop with lime addition but at a lower rate. On the other hand soil 2 (the lateritic soil) experienced a continuous decrease in the coefficient of permeability with lime addition, which was also attributed to the cementation product formation.
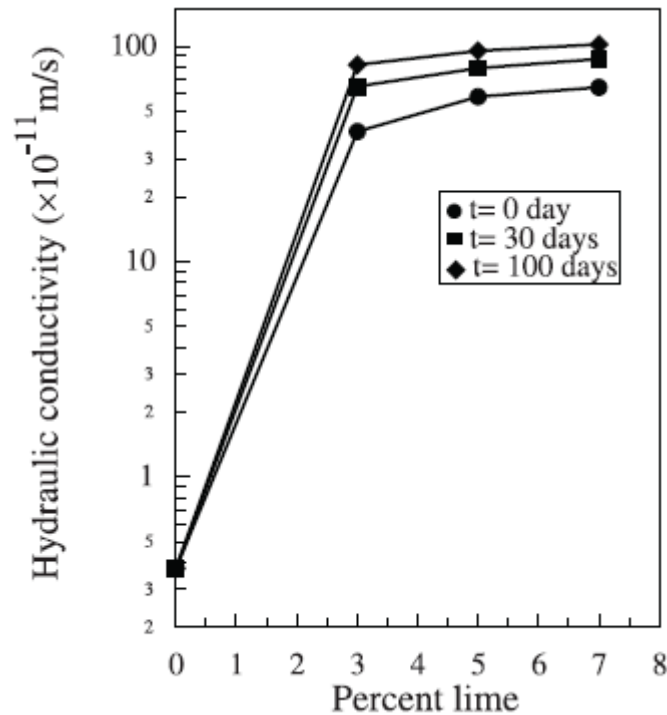
Figure 2.17: Lime content effect on hydraulic conductivity at different curing time
(Nalbantoglu & Tuncer, 2001)

Locat et al. (1996) tested soft organic clay and found that the cementitious material produced during the process of artificial cementation filled the pore spaces, so that 3.5-10% lime content addition resulted in a reduction of hydraulic conductivity with curing time by up to one order of magnitude compared to that of the untreated soil for different initial soil void ratios (Figure 2.18). The authors correlated the permeability decrease with the consumption of lime during curing (see Fig. 2.18b). Lower lime percentages however appeared to have increased the permeability of the soil.
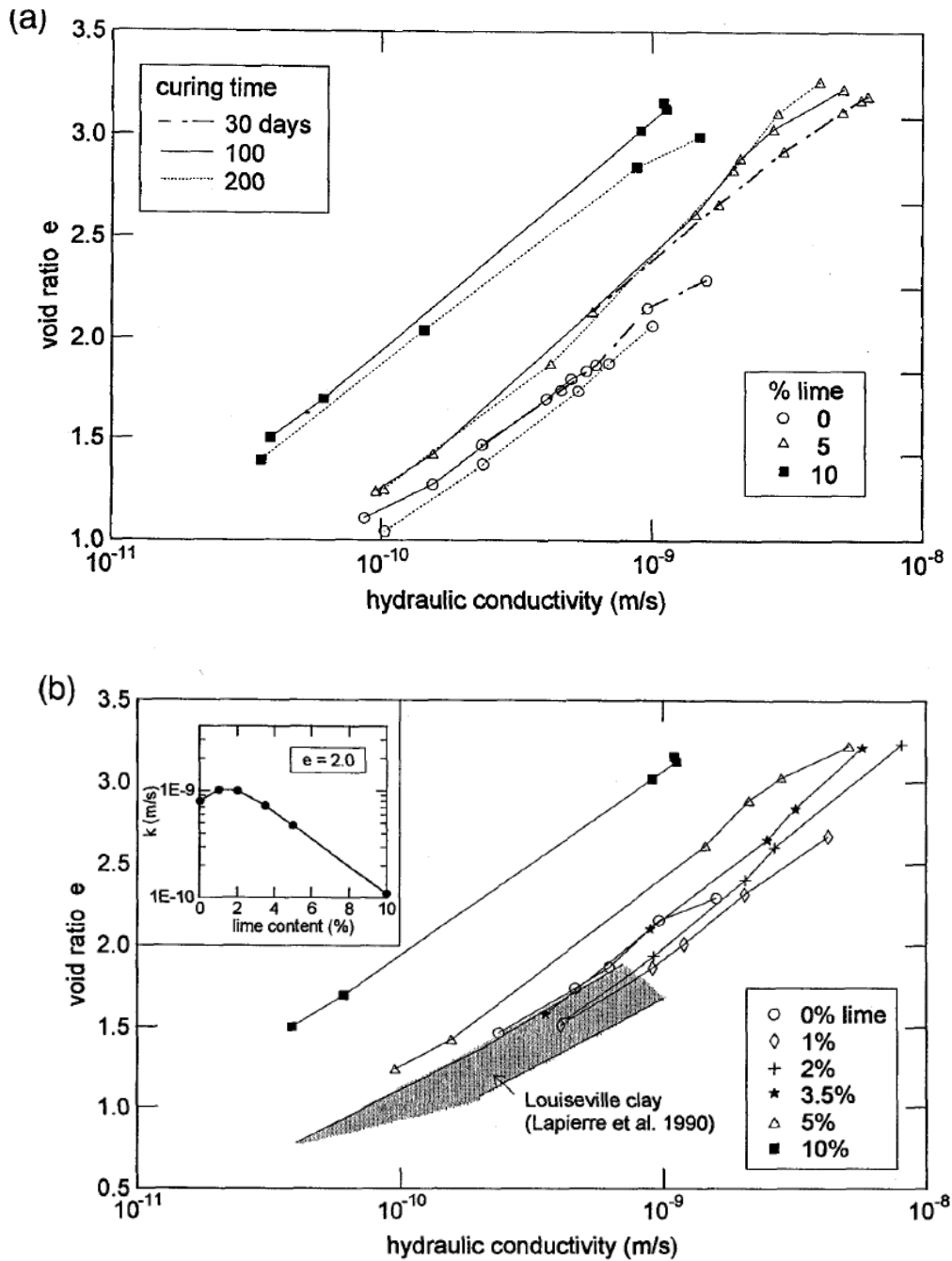
Figure 2.18: Permeability curves Vs Void ratio: a) Time effect at 30, 100 and 200 days curing, b) lime content effect at 30 days of curing (hydraulic conductivity Vs lime content at e = 2.0) (Locat et al., 1996)

Osinubi (1998b) followed the changes in permeability of specimens treated with varying percentages of lime, compacted at different conditions and cured for different time periods. Non cured specimens were also tested immediately after treatment. The effects on the permeability were observed to be variable, with overall an initial increase for up to 14 days of curing and a subsequent decrease (with one exception only where permeability was

almost constant -slightly lower- then increased to subsequently decrease again slightly). The interpretation of the findings was that an initial flocculation and other structural changes instantly transformed the permeability after stabilisation. Osinubi (1998b) suggested that as a rule, a permeability increase would be expected during the stabilisation process, although the addition of a large quantity of cementing agents to highly organic soils, combined with pre-determined compaction energy, could instead cause an initial decrease in permeability. Permeability would then decrease with time, due to the different cementitious products forming (see Fig 2.19). The author attributed the observed variations in the complexity of the lime-soil reaction mechanisms, which are very dependent on the amount and type of clay mineral present in the soil. The interpretation is consistent to that of Metelková et al. (2012) suggesting that the initial change in permeability (during the formation of primary reaction products) is associated with a change in the void ratio, and can also be approximately related to the moisture content change after mixing and possible compaction and that the cementation process leads to about the same relative decrease in permeability as to the increase in strength associated with pozzolanic reactions. This appears to be a fair conclusion on the effects of the lime on the permeability of soils, consistent with the review of other papers in the literature.
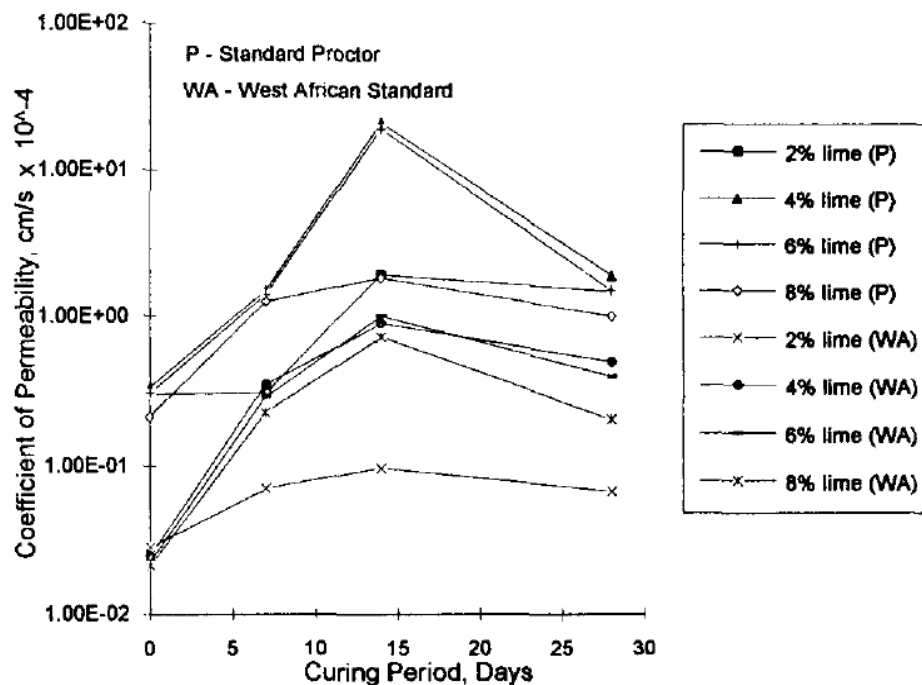
Figure 2.19: Variation of coefficient of permeability of treated Lateritic soil with curing period (Osinubi, 1998b)

2.6.5. Compressibility

Whereas plasticity, shrinkage and swelling, UCS and CBR of lime treated soils have been extensively investigated, relatively fewer studies investigated the effect of lime treatment on the compression behaviour of the soil, mostly through oedometer testing.

Examples include Nalbatoglu and Tuncer (2001) and Rao and Shivananda (2005a) who studied respectively the K_0 compression behaviour of expansive soils from Northern Cyprus and India, or de Brito Galvao et al. (2004) who investigated the effect of lime stabilisation on the compressibility of two Brazilian soils of different origin, namely a brown saprolitic soil, and a red lateritic soil. These have all demonstrated the beneficial effect of lime leading to a sharp reduction in the compressibility of the lime-treated soil compared to the respective untreated soil. This is manifested both by the increase in the vertical effective yield stress p'_c (apparent pre-consolidation pressure), as well as the post-yield stiffness of the soil. An example is shown in Fig 2.20 (a) & (b) based on the results by de Brito Galvao et al. (2004). The increase of the yield stress of the lime-treated soil compared to that of the untreated saturated soil is consistent with the behaviour of cemented geomaterials. Nalbantoglu and Tuncer (2001) argued that for lime-treated soils it is due to a chemically-induced pre-consolidation effect, caused by the cation-exchange reaction, as well as cementation bonds (the latter is the reason most other authors invoke for the decrease in the compressibility of the soil, e.g. Ingles and Metcalf (1972) and de Brito Galvao et al. (2004)). According to Nalbantoglu and Tuncer, both aggregation formations of the clay treated with lime as well as cementation effects on soil particles result in stronger aggregates and give higher resistance to compression which results in an increase in yield stress and stiffness. Various ways of estimating different compression parameters of stabilised soils have been suggested including the vertical yield stress as related to the void ratio (Tremblay et al., 2001; Rotta et al., 2003). For instance, Tremblay et al. (2001) experimentally investigated the one-dimensional compression behaviour of a number of clays from eastern Canada treated with lime or cement. Based on the experimental data, they developed a general compressibility model, estimating the compressibility reduction for a given soil treated with a particular additive, by defining relationships between initial void ratio, additive content, and vertical effective yield stress. Rotta et al. (2003) highlighted the importance of the void ratio during the formation of

cementitious bonds. The authors demonstrated that the yielding stress variation with void ratio and cement content is dependent of curing stress.

(a)

(b)
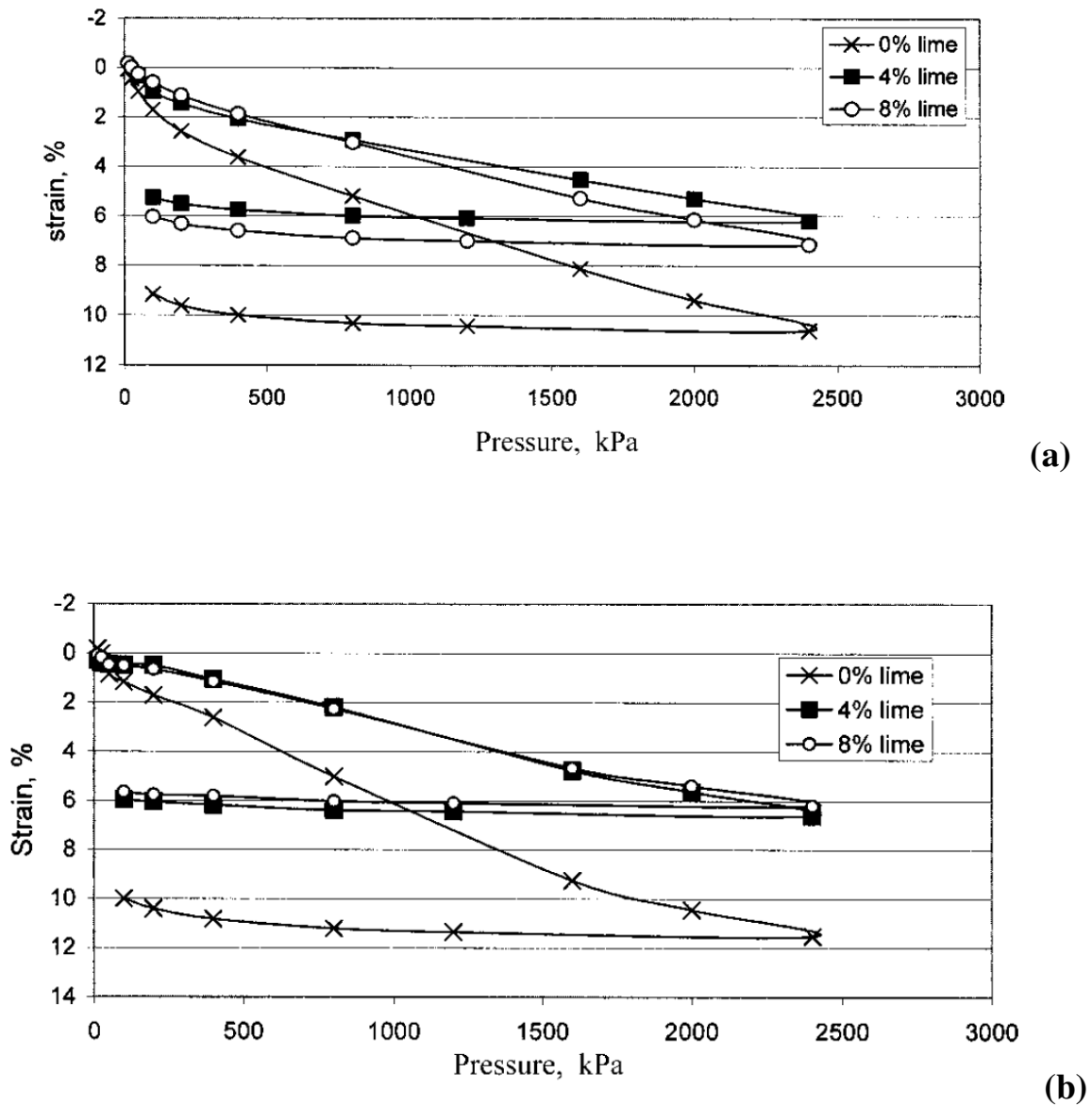
Figure 2.20: Strain Vs Pressure for (a) brown saprolitic soil and (b) red lateritic soil, treated with lime. (de Brito Galvao et al., 2004)

It is interesting to note that in the above Figures by de Brito Galvao et al. (2004), the results on the compressibility lines of the lime-treated soil did not eventually converge to that of the untreated soil; this would be the expected behaviour based on the well-documented broader literature on naturally cemented geomaterials when subjected to destructuration (e.g. Lagioia & Nova, 1995; Callisto & Calabresi, 1998; Coop, 1999). The

expected behaviour is shown qualitatively in Åhnberg's (1996) thesis, who presented a schematic variation of the oedometric compression modulus with increasing confining stress, expressed in accordance with the model normally used for calculations of settlements of natural soft soils in Sweden (e.g. Larsson et al., 1997) (see Fig. 2.21). According to Åhnberg after passing a yield stress, the modulus reaches a minimum value. Thereafter, it increases with further increase in stress and, as an effect of the breakdown of the cementation forces with increasing stress level, is then governed by a modulus number M' of the same magnitude as that of the unstabilised soil.
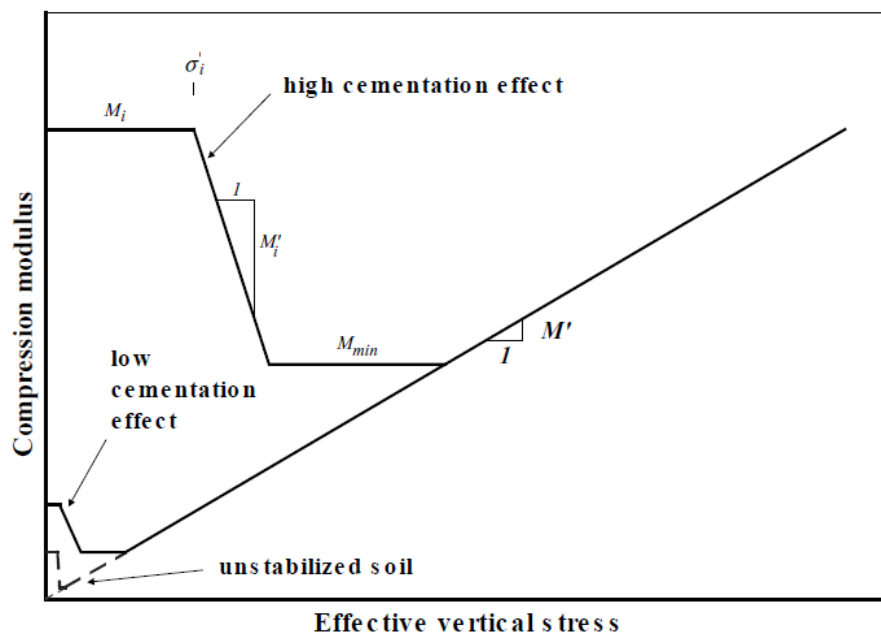
Figure 2.21: Schematic variation in compression modulus to oedometer tests
(Åhnberg 1996)

Of all papers mentioned above on lime-treated soil compressibility, only Rao and Shivananda (2005a) demonstrated the effect of full destructuration by performing one dimensional compression load tests, applying a maximum load up to 12.8 MPa. Thus the authors noted an initial yield linked to the start of the cementation bonding destructuration at lower load application but the full breakage of cementation bonds, which brought together the compression curves of the treated soil, only occurred in the range of 3.9 and 5.2 MPa (see Fig. 2.22 &2.23). However, so high load stresses are not relevant for common geotechnical applications of lime-treated soils especially when used in shallow mixing.
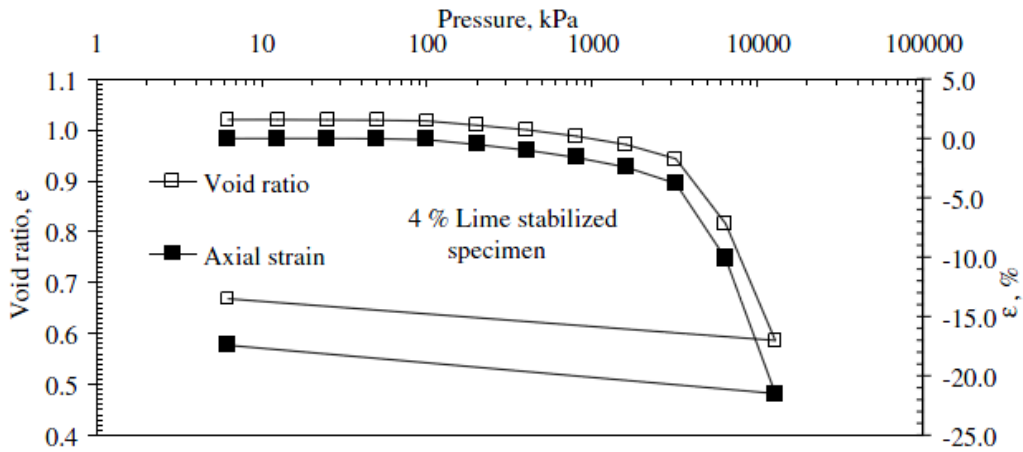
Figure 2.22: Compression curves of 4% lime-stabilized specimen
(Rao & Shivananda, 2005a)
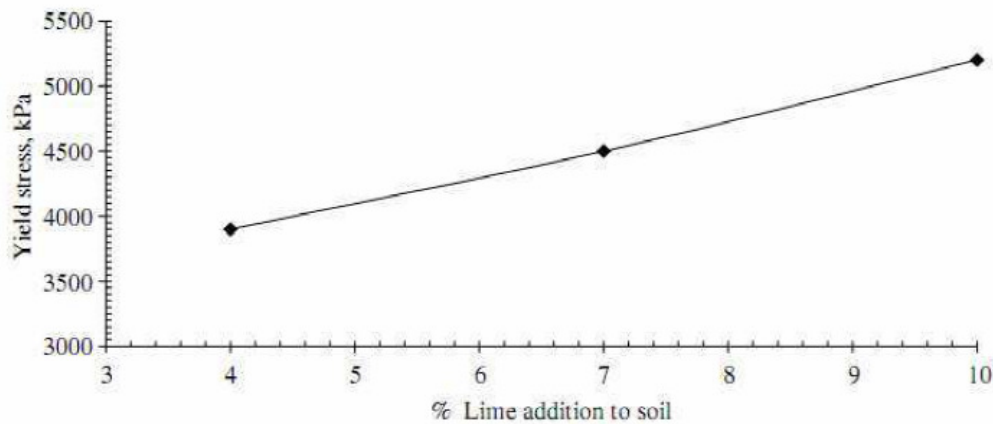
Figure: 2.23: Variation of yield stress with soil-lime content (Rao & Shivananda, 2005a)

Based on the latter paper the compressibility of the lime-treated soils can be considered as consisting of an elastic zone, plastic zone and post failure zone (same as for natural structured soils). Hong et al. (2012) suggested that it consists of the following three zones:

i)   The pre-yield zone characterised by small compressibility, with soil structure resisting the deformation up to pre-consolidation yield stress.

ii)   The transitional zone characterised by the start of structure resistance gradual loss between the initial yielding point up to maximum pre-consolidation yielding stress a natural clay can withstand.

iii) The post transitional zone, when the effective stress is higher than the transitional stress.

2.7. Constitutive modelling

Traditional geotechnical engineering has focussed on parameters describing ultimate limit state conditions linked to simple failure criteria, such as the Mohr-Coulomb criterion. The criterion has been used to express failure of both naturally and artificially cemented soils but a curved failure envelope has been reported for low confining stress levels of cemented soils (Muhunthan and Sariosseiri, 2008). In addition, as due to cementation the treated soil acquires properties and behaviour similar to a soft rock, common failure criteria such as Griffith's crack theory (e.g. Mitchell 1976; Muhunthan and Sariosseiri, 2008) or Hoek-Brown's failure criterion (e.g. Karaoulanis and Chatzigogos, 2011) used in rock mechanics to describe failure due to cracking, have also been used in their originally expressed or modified form to express the failure of cemented soils.

On the other hand, for the analysis design of problems in which displacements and stresses under working load well below failure linked to serviceability limits control design, some more detailed description of the behaviour of the material is necessary, especially when numerical modelling is involved. This can only be achieved with constitutive modelling also capturing the behaviour of the material from the pre-yield region to yielding in addition to post-yield and failure. Such models can be complex and involve a large number of parameters that need to be identified based on sophisticated testing. However as the previous review showed, most previous research results and design for practical applications of lime-treatment have been based on simple testing and found to be insufficient to provide these parameters, as opposed to more advanced testing (in particular triaxial testing) which is only rarely found in the literature of lime-treated soils. Consequently, constitutive models describing the behaviour of lime-treated soils in particular, are lacking from the international literature. Conversely a large number of quality triaxial data have been obtained for naturally cemented soils or more generally natural soils with structure over several decades (Sangrey, 1972; Clough et al., 1981; Maccarini, 1987; Bressani, 1990; Coop and Atkinson, 1993; Cuccovilo & Coop, 1993 to name a few) as well as cement treated soils for stabilisation purposes , often produced as analogue for the laboratory study of naturally cemented soils (e.g. Huang & Airey, 1993;

Uddin et al., 1997; Horpibulsuk et al., 2004; Kamruzzaman et al., 2009). Based on the substantial amount of experimental evidence, a large number of models have been developed for naturally cemented or structured soils and some models were also proposed for soils stabilised with cement (e.g. Horpibulsuk et al., 2010). Such models were not proven for lime-treated soils in particular and differences in the structure as well as property values of lime-treated clays compared to other cemented clays (or soils) can be expected. However as a key reference by Leroueil and Vaughan (1990) has shown (followed by further experimental evidence on this in subsequent years) cemented /bonded or in general structured soils of different nature and of cementation/bonds/structure arising from different factors (soft rocks, weak and weathered; stiff clays or aged sands; residual soils) show some common behaviour characteristics. Thus, it can be expected that models suggested for natural or cement treated soils could possibly be used to describe the behaviour of a lime treated soil potentially with some adaptation to better reflect this type of soil.

The observations regarding the common characteristics of bonded/structured soils can be summarised as (Leroueil and Vaughan, 1990; Gens and Nova, 1993; Tamagnini et al., 2011):

- Experimental results showed that in naturally bonded or structured soils, geological history produces a diagenetic microstructure, causing the elastic domain of natural soils to be substantially increased. Similar effects can be obtained by artificial cementation of the soil.

- The geomaterial exhibits tensile strength and true cohesion due to bonding.

- These effects are however subject to degradation upon mechanical or chemical disturbance, when the cemented bonds may be destroyed, leading to a loss of stiffness, strength (often brittle failure) and softening.

- The general behaviour of this type of material (bonded/cemented) is a stiff response in loading, followed by yield. It was pointed out by Leroueil and Vaughan, (1990), that a similar effect is observed as a consequence of over-consolidation (despite the fact that this is a distinct phenomenon).

- In general, yield phenomena are very marked with clear yield loci evident during testing. These can be determined for different modes of yield, i.e., upon compression, shear or unloading. An initial yield is often also observed with the stress path still inside the main yield locus.

- Following yield, bonds degrade gradually until full debonding / destructuration. In the case of compression/consolidation (whether isotropic or under K_0 conditions), the consolidation curves after a distinct yield point, tend to converge towards the consolidation curves of the unstructured / unbonded material, as discussed earlier.

- Similar to the behaviour of rocks (on a different scale) these materials would show a brittle/dilating behaviour when shearing under low confining stresses which is gradually becoming more ductile/compressive at higher confining stresses.

- Similarly, stiffness and deviator stress at yield may decrease when confining stresses increase.

These observations have been supported by experimental evidence on either naturally or artificially lightly cemented soils (the latter were created in the laboratory for the purposes of studying the naturally cemented soils). Overall, the two main features of the generalised framework proposed by Leroueil and Vaughan (1990) were (a) the need to consider the structured soil behaviour in comparison to that of the unstructured / unbonded soil and (b) the fundamental role of yielding phenomena in the description of the behaviour of the bonded/structured geomaterial. Based on these pertinent observations on the similarities between these geomaterial types, a number of constitutive models were formulated to address these features, using as a starting point the mathematical structure of common constitutive models suggested for unbonded soils (i.e. models capable of describing the behaviour of the reconstituted soil as a reference state). Such models include the critical state soil mechanics (CSSM) framework and Cam-Clay type models, with some modifications/extensions, to accommodate the particularities of the bonded/structured geomaterials.

A key reference in the constitutive modelling of cemented soils is the framework suggested in a series of publications by Nova and co-workers with various extensions/modifications (e.g. di Prisco et al., 1992; Gens & Nova, 1993; Lagioia & Nova, 1995), based originally on data from calcarenite. In this non-associative elasto-plastic model, shapes for both yield surface and plastic potential are described using the expression given by Lagioia et al. (1996). Elastic behaviour is described by a four-parameter hyper-elastic formulation (Borja et al., 1997). In total the model contains thirteen parameters. Apart from stress (or elastic strain) any material state is described using two independent internal scalar variables with stress dimensions, which control the size of the current yield surface as well as of an inner reference surface corresponding to a fully destructed material. The first variable is linked to stress memory of the material i.e., similar to the usual pre-consolidation pressure and hence either increasing or decreasing, depending on the state of stress and history of the material; the second is related to the effects of bonding /structure and can only decrease with plastic strains (in further developments, e.g. Nova et al. (2003) this variable is also dependent on weathering and/or chemical degradation). Consequently, either softening or hardening can take place, depending on the relative amount of the rate of change of the internal variables. Note that the concept of using an independent hardening/softening variable was subsequently used in other, more complex, elasto-plastic models of bonded or structured soil behaviour, e.g., enhanced to include amongst other anisotropic behaviour (Rouainia & Wood, 2000)[2] or stiffness nonlinearity in the model of Baudet & Stallebrass (2004). The latter model was suggested for structured clays. It incorporates a sensitivity parameter "s" to characterise the expanded yield surface due to structure ("the sensitivity surface"). This surface starts from the axes origin in the p–q space, and is s times larger than the intrinsic yield surface for fully remoulded states. Natural soil structure is assumed to be composed of meta-stable and stable elements, i.e. not degrading with straining. They defined a damage strain as a function of plastic volumetric and shear strains so that, upon destructuration the surface shrinks gradually as sensitivity decreases exponentially with the damage strain. Ultimate states (i.e. the fully disturbed state) are not made to converge to a unique critical state surface in the p–q–e space. Note that this model does not consider the development of tensile strength that is produced by inter-grain bonds.

---

[2] Note that artificially cemented materials with cement or lime-treated can reasonably be considered to be isotropic due to remoulding while mixing

Yu et al. (2007) developed an isotropic hardening model but considering the effects of true cohesion and the development of tensile strength due to bonding between soil particles. To achieve this, they introduced two bond-related parameters to define the size and location of the yield surface as shown in Fig 2.24. The evolution laws of the pre-consolidation stress parameter $p_c{}'$ and cohesion c can then simulate the progressive degradation of the bonds. The model is not, however, intended to simulate the brittle mode of failure that is linked to an abrupt destruction of the true cohesion.
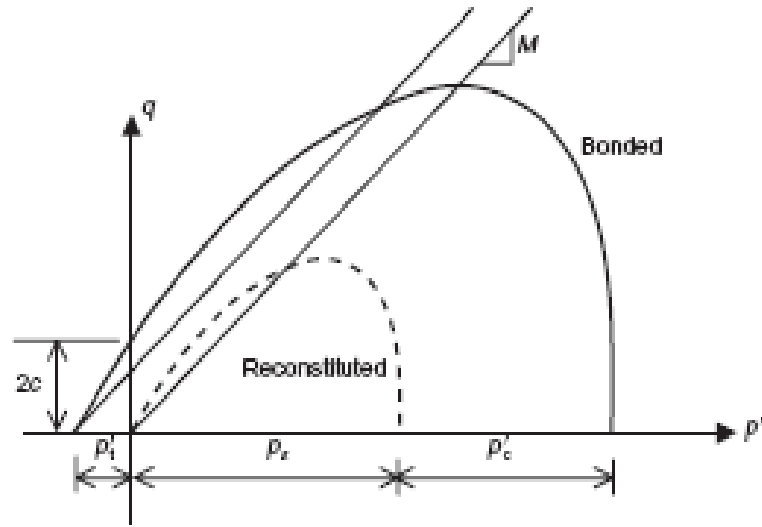
Figure 2.24: Yield surfaces for reconstituted and bonded materials (Yu et al. 2007)

Vatsala et al. (2001) modelled the behaviour of the cemented soil as the coupled response of the soil skeleton represented by the modified Cam Clay and that of cementation bonding component for which a new elasto-plastic model was formulated. The stresses attributed to each of these separate components were thus calculated for each strain level and added to generate the overall response of the cemented soil. The proposed model was successfully applied to a number of naturally cemented soils (both clays and non-clayey material) to simulate their compression behaviour. However according to this model the microstructure of the material is not considered to have changed due to cementation. This may therefore not be a good representation of the lime-treated soil for which microstructure is expected to change according to the previous literature review.

A model to simulate the compression behaviour of the structured soil was also suggested by Liu and Carter (1999). To describe the virgin compression of the structured soil the effects of structure are directly introduced explicitly through a mathematical relation

between additional void ratio of structured soil compared to that of the reconstituted soil. The model thus begins in the oedometric (or isotropic) compression plane where the initial yield limit and excess void ratio of structured soil compared to the reconstituted soil at this yield limit are considered as parameters of structured soil. An equation for the virgin compression curve of structured soil dependent on these parameters is formulated and the 'de-structuring index' is used to represent the rate of structure degradation corresponding to a non-linear decrease of the void ratio of the structured soils as a function of the ratio of current pressure over the initial yield limit. The model was then extended (Liu and Carter, 2002) to also simulate structure degradation due to deviatoric effects using a strain hardening rule as in modified Cam-Clay model. The model contains a formulation to find the additional void ratio based on the mean yield effective stress and a "b" parameter called the destructuration index, which should be obtained for a specific soil based on experimental data. The model was later adopted with modifications by other authors e.g. Horpibulsuk et al. (2010) to model the constitutive behaviour of artificially cemented clays; the concept to express critical state behaviour used a yield surface was shifted to the left in the $p'-q$ plan, so that its intercept with the q axis was not zero. The model was found to reasonably predict the shearing behaviour of a number of artificially cemented soils.

Note that although the above models have often been used in the literature to describe both naturally and artificially cemented clays, Sasanian (2011) pointed out that there appears to be significant differences in the behaviour of the natural and artificial structure, which are not fully understood and addressed. Therefore, the author studied the mechanical response of artificial and natural "Ottawa clay" specimens subjected to complex stress path tests, in order to compare the behaviour of the two types of structure (natural and artificial). Important distinctions were observed between the behaviour of naturally structured and artificially bonded material. For instance, the undisturbed Ottawa clay showed a more sudden structural collapse compared to the artificially cemented specimens which undergo a gradual destruction. In addition, the yield locus of the artificially cemented soil was found to be more elongated than the naturally structured soil. As a result, Sasanian proposed a new framework to define the yield locus of the artificially cemented material. This consists of a combination of two elliptical models, the elliptical cap (Chen & Mizuno, 1990) for $M_e \leq \eta \leq M_c$ and the modified cam clay model (Muir Wood, 1990) for $M_e \leq \eta \leq \eta_c$ and $\eta_e \leq \eta \leq M_e$. This requires three parameters (the isotropic yield

stress $\left(p'_0\right)$, the mean effective stress $\left(l\right)$ corresponding to CS and the gradient $\left(M\right)$ of the CSL). The newly proposed framework successfully estimates the experimental data in compression, while some difficulties were encountered by the author to produce a yield loci which best estimates the experimental data in extension.

Other authors attempted to recover the constitutive models for cemented soils starting from thermodynamics principles. Thus, Tamagnini et al. (2010), Tamagnini et al. (2011) and Yan and Li (2011) derived thermodynamically consistent Cam-Clay type models with associative flow rules (as opposed to most other common approaches) modified to account for the effect of cementation. To do this, they used the concept of frozen (or locked) energy accumulated in the bonds/soil structure which upon destructuration is then gradually released so that the soil gradually approaches more stable states (remoulded states). The yield surface in the model of the former authors is based on the Modified Cam-Clay formulation whereas the latter model modifies the shape of the yield surface to a teardrop shape surface by using an additional parameter as suggested in Collins and Kelly (2002). An additional internal variable is then introduced; in the former model this represents the amount of bonding created due to cementation; in the latter model this represents the bonding evolution. Both models are validated against experimental data for various types of bonded geomaterials.

A simple model for cement-treated clays was suggested by Arroyo et al. (2011). The model also incorporates a bonding variable "b", so that the yield surface grows with an increasing amount of bonding in the soil. The model only required unconfined compressive strength data, and measurements of porosity as well as of the cement amount in the mixture. With this information the main state variable of the bonded soil elastoplastic model were identified. The model successfully simulated laboratory testing data for cement-treated Bangkok clay.

While most models suggested for the behaviour of bonded geomaterials were within the frameworks of hardening elasto-plasticity and critical state soil mechanics, other frameworks were also used for bonded / cemented materials, for instance visco-plastic formulations. Thus, in a conference on hard soils and soft rocks, Oka et al. (2011) used a Perzyna - type elasto-viscoplastic formulation to model the triaxial behaviour of soft porous rocks (tuffs). The effect of the cementation on the yielding surface was

incorporated via the quasi-overconsolidation. In the same conference, another visco-plastic formulation (Duvaut-Lions) was also introduced by Karaoulanis & Chatzigogos (2011) together with Hoek-Brown's failure criterion, to model the time-dependent behaviour of soft rocks.

2.8. Conclusion

The literature review covered previous work on lime treatment of clay soils. The review highlighted the complexity of the phenomena and the strong dependence of the processes on the particular soil. From this literature review findings, it was clearly concluded that to interpret the changes in the hydro-mechanical properties of the soil, accompanying testing is necessary (e.g. XRD, ESEM, electric conductivity testing, analytical testing etc.) to investigate the mineralogy changes and the evolution of the reactions based on the new products formed. This will therefore be the methodology followed in this study to interpret the findings of the geotechnical testing. Moreover, it was found that hydro-mechanical properties have mostly been related to simple tests, mainly adopted for road construction applications such as (CBR, UCS, and plasticity testing), which would be insufficient to provide parameters for advanced constitutive modelling as those required in the reviewed models for structured/bonded soils. The need for further advanced testing, in particular triaxial testing was therefore highlighted and this will be the main focus of the research described in the following sections.

Chapter 3

3. Material description and laboratory testing procedures

3.1. Introduction

This chapter describes the material used during the experimental programme. It also highlights the selected chemical agent for the material treatment.

The methods developed for specimen preparation are also presented. Finally the chapter describes the equipment used, the instrumentation calibration, the experimental procedures and the testing programme of this research, which aimed at investigating the effects of lime percentage, compaction characteristics and curing time on the mechanical properties and behaviour of the lime-treated soil, through a series of extensive triaxial tests.

3.2. Materials

3.2.1 London Clay

In this study bulk London Clay samples from a deep excavation at Westminster Bridge in London were obtained from a depth of approximately 26-30 m below ground level. The London Clay Formation is a well-developed marine geological formation found in the London Basin and Hampshire Basin, UK, reaching an average thickness of 130 m. It is therefore a soil extensively encountered in construction in the London area and the South Eastern England, including pavement construction, airports (e.g. Heathrow Terminal 5), underground railway (an example of recent engineering works being the Crossrail project), embankment and building foundation construction. In its natural state London Clay is a stiff over-consolidated clay, as in most parts of the London Basin, substantial erosion has taken place in the late Tertiary and Pleistocene times, removing the upper parts of the London Clay, and any other overlying Tertiary (King, 1981).

- **London Clay main characteristics**

A number of comprehensive studies were carried out on the characteristics of London Clay. These include works by Bishop et al. (1965); Ward et al. (1959 & 1965); Webb (1964) and Skempton et al. (1969), for soil coming from the London area, such as Ashford common, Prospect Park and Wraysbury reservoir. The data was re-analysed by Wroth (1972), and reviewed by Burland (1990). Later, Hight and Jardine (1993) investigated the characteristics on London Clay related to its geology by considering samples from different sites in Central London. More recent studies include those by Gasparre (2005) and Hight et al. (2007) who added the newest comprehensive information on the London Clay based on tests performed on the new Heathrow terminal 5. Standing and Burland (2006) highlighted the effects of the geological characteristics on engineering applications, while Pantoulidou and Simpson (2007) emphasised the geotechnical variation of London clay across central London.

The unit weight of the excavated London Clay was found to be about $19.5-20 kN/m^3$, and the in situ natural moisture content of the natural London Clay material range between 25 and 30%, which is consistent with the findings of Standing and Burland (2006), for samples from St James Park, a region close to Westminster Bridge.

Particle size distribution analysis carried out by Zhang (2011) on two duplicate London Clay samples has identified from the same sources the material as approximately 53% clay and 45% silt (see Figure 3.1).
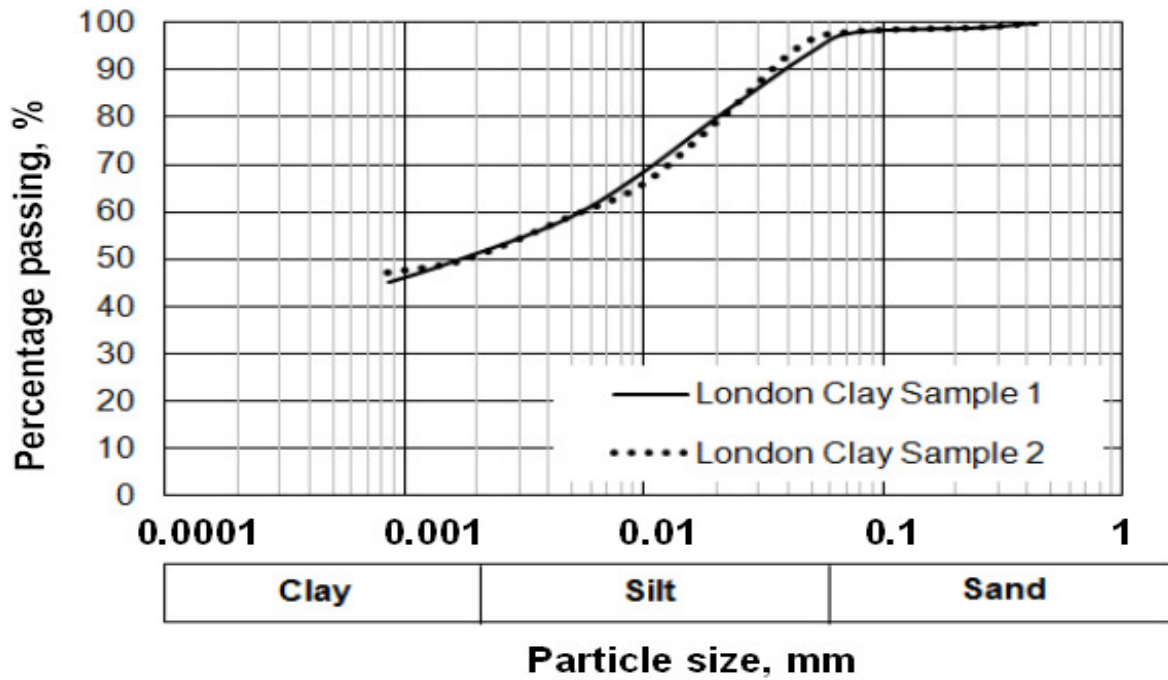
Figure 3.1: Particle size distribution curves of London Clay (Zhang, 2011)

3.2.2. Lime

Lime is a broad term which is used to describe calcium oxide CaO as quicklime, calcium hydroxide $Ca(OH)_2$ as slaked or hydrated lime and calcium carbonate $CaCO_3$ as carbonate of lime. Lime is used as chemical stabiliser for soils, particularly expansive clays. Lime is considered as low cost material, making it a popular choice among many other effective stabilisers. Nowadays, lime treatment for soil improvement is extensively employed within the civil engineering industry, such as embankment, road construction, foundation slabs and piling applications. Adding lime to clayey soils in the presence of water, a number of reactions take place, resulting in soil engineering properties enhancement.

The use of quicklime CaO is generally preferred to hydrated lime $Ca(OH)_2$, this is attributable to the availability of high amount of calcium cation content, per unit mass, which is crucial for the development of the reactions. Moreover, the highly exothermic slaking reaction speeds up the development of pozzolanic bonds among the grains (Greaves, 1996). However, due to its greater vulnerability in exposing the user to skin and eye burns, the type of lime used during this study for London Clay treatment is chosen to

be hydrated lime, it comes in the form of fine dry powder. Chemical analysis carried out on two separate lime samples illustrated that its calcium hydroxide content ranges between 95% and 97%.

3.3. Specimen preparation

Specimens have been prepared following the same procedure as the previous research carried out by Zhang (2011) on lime treated London Clay to ensure consistency and a compatible link between the two research studies. However, it is possible that the London Clay samples used in this study may not have always come from exactly the same depths as in Zhang (2011) (depths of collected samples varied from 26-53 m).

In order to obtain quality results during the laboratory testing, a certain expertise on specimen preparation was developed. The specimen preparation process consisted of the following main phases (see Figure 3.2), namely:

- Air drying
- Grinding
- Sieving
- Clay-lime dry mixing
- Adding water and mellowing
- Static compaction.
- Curing period.

Air drying

Grinding

Sieving

Soil-lime dry mixing

Mellowing

Compaction

Compacted sample

Curing samples
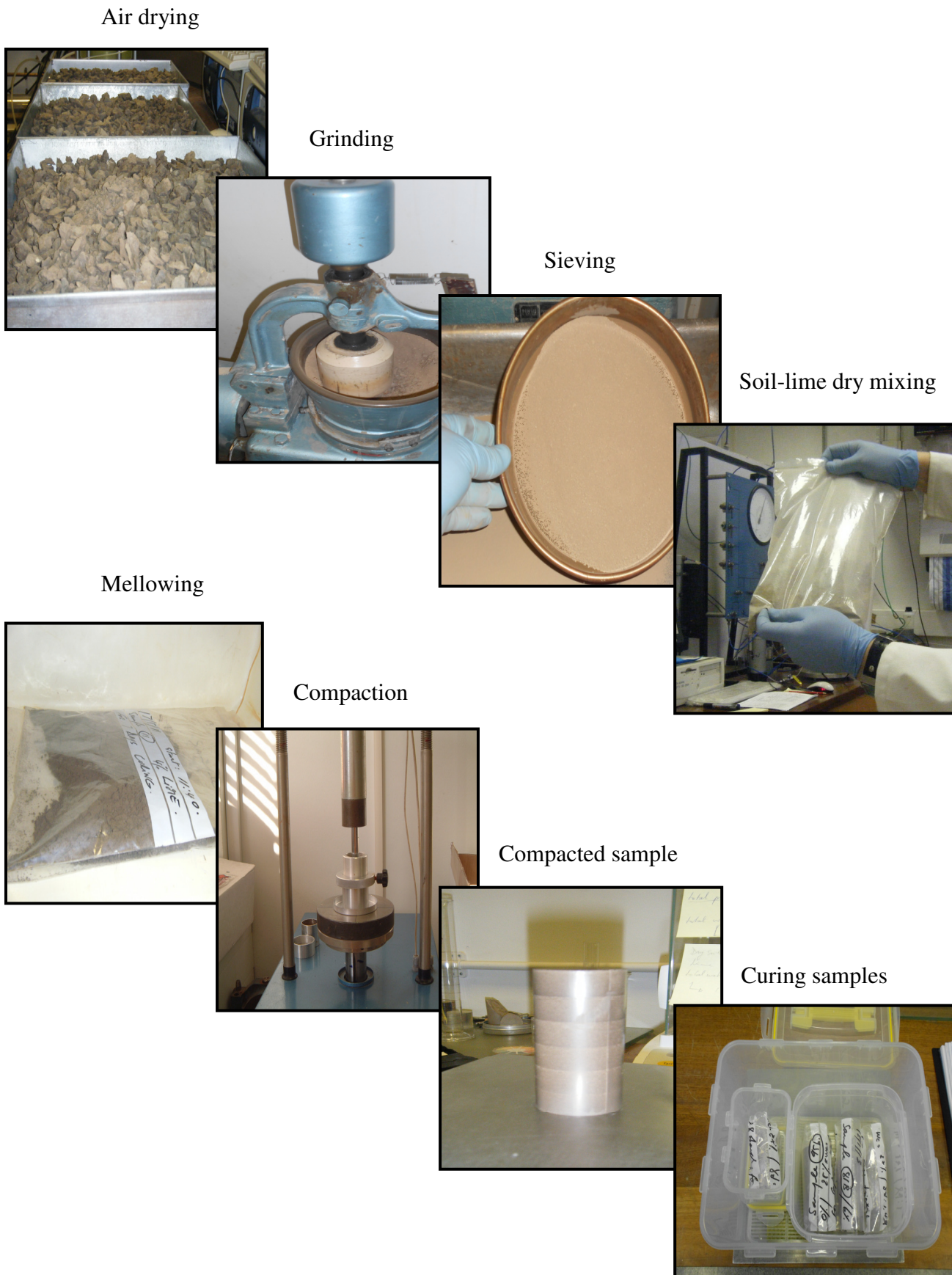
Figure 3.2: Specimen preparation stages

(a) Air drying and grinding

Part of the soil obtained from the excavation was broken into small lumps using a rubber pestle, exposed to an open air in metallic trays at controlled room temperature for approximately one month (air drying). During the drying process, soil lumps were turned upside down on a regular basis to avoid local drying. Next was the grinding in a mechanical grinder at Imperial College to fine particles passing the $425\mu m$ sieve (No. BS 410). The process generated clay powder, which was inserted in sealable plastic bags and stored for future use.

(b) Clay-lime dry mixing

Each soil sample was individually prepared using the same basic soil. A standard procedure was followed to accomplish consistent results in the main tests.

In order to obtain a homogeneous clay-lime mixture, the clay powder was first mixed with lime in a dry state for an approximate duration of 5 minutes inside a sealed polyethylene bag, until the colour of the mixture became uniform. An extra 0.5 to 1g of clay powder was added to compensate for the loss of particles during the mixing.

(c) Adding water and mellowing

Adding water was the next stage, lime treated and untreated London Clay samples all had water added using distilled water. This was de-aired by the use of water de-airing (ELE) system device, which removes air bubbles contained from a liquid. The wetting procedure was carried out within a reasonable time in accordance to BS 1377 – 4: 1990, lasting an average of 20 minutes to ensure that lime was not exposed to the air for too long.

De-aired water was added by increments of 2 to 4% alternating with mixing. Once the desired moisture target was reached, and an homogenous material was obtained, the wet mixture was immediately inserted in a separate sealed polyethylene bag to preserve the obtained moisture content target by preventing water evaporation. Without delay the sealed wet mixture was stored in a room with a controlled temperature of $20°\pm1°C$ for a minimum of 12 hours for untreated London Clay samples and 24 hours duration for lime

treated samples to allow for mellowing, before proceeding the following day with subsequent static compaction. These arrangements guaranteed the homogeneity of water content within the specimen by uniformly distributing the water. A small portion of the prepared wet mixture was also oven dried overnight to determine / confirm the water content of the specimen.

Note that both the required lime and the water amounts per dry soil weight to be added during dry mixing and water addition respectively were calculated taking in consideration the residual water content of the London Clay which was found to be between 4 and 5%.

(d) Static compaction

Research has shown that more consistent, uniform clay specimens are obtained by static compaction (compression) compared to dynamic compaction (Sivakumar, 1993; and Tabani, 1999). The literature identifies two different types of static compaction, depending on whether the compaction effort or the target dry density is controlled during the compaction process. Venkatarama Reddy and Jagadish (1993) named these two methods as the "Constant peak stress – Variable stroke compaction" and the "Variable peak stress – Constant stroke compaction" respectively. In the former method the applied stress is gradually increased at a defined rate until a specific peak stress is reached. The thickness of the compacted specimen and the required compacting energy are dependent on the water content of the soil. In the latter method, which was used in this study, compaction is carried out by controlling the target dry density of the soil (i.e. the static force is applied at a constant rate, until a specific final specimen thickness is achieved).

In this study the cylindrical specimens were statically compacted in a custom built brass mould of 38 mm in diameter and 76 mm in height, by a gradually applying a monotonic force on to the soil, triggered by the vertical movement of a piston at a rate of 1 mm/min, until this was achieved. A compression frame (ELE) with a compressive capacity of $28kN$ was used. The compacting effort was measured via an attached (separately calibrated) proving ring with a calibration constant of $26N$ per division (see Figure 3.3).
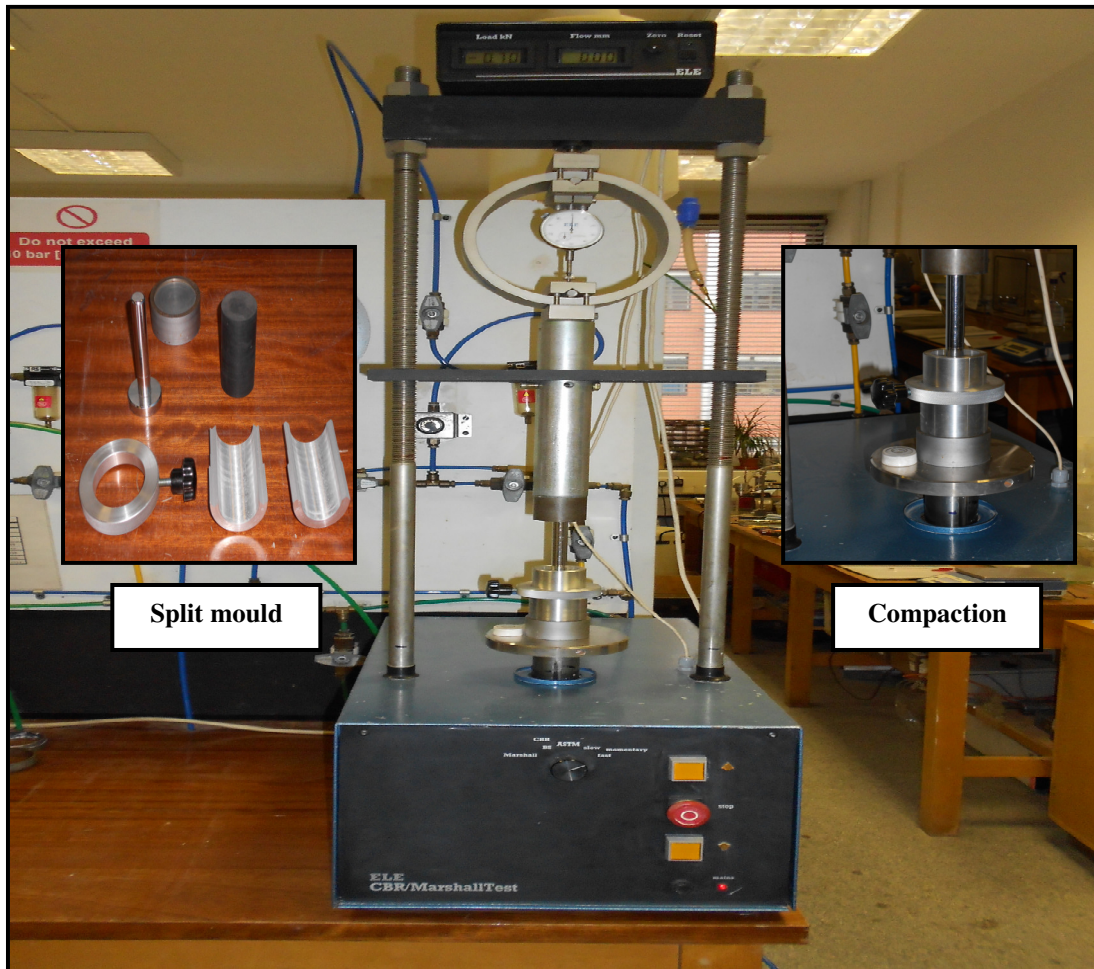
Figure 3.3: Split mould and ELE compacting device

All specimens were consistently compacted in six equal layers, using the same amount of mass per layer, and scarified before a further layer was added. Once the sixth layer was compacted, the cylindrical specimen was kept under the compacting load for a duration of 5 minutes in order to reduce rebound up on load removal (Jotisankasa, 2005). The compacted specimen was then carefully extracted from the mould, followed by acquiring the specimens' mass, average height and diameter, which were separately noted for future use. In order to facilitate the specimen's extraction, silicon oil had been lightly wiped around the inside of the brass mould surface before the compaction, as recommended by BS 1377 – 1:1990 / part 4 (BSI, 1990).

It should be noted that before adopting the above mentioned compaction procedure, an investigation of possible variations was carried out. In particular, research at Imperial College, London (e.g. as described in Jotisankasa, 2005) followed a static compaction

procedure by compressing specimens in several layers, except that the mass was checked for every compacted layer, and the varying soil mass to add was determined for each compacted layer in order to compensate for any loss of mass. The author believes that this procedure is time consuming and results in more mass loss, since the mass reduction is mainly due to water evaporation, which may become more pronounced if the compaction procedure lasts longer, due to the mass checks mentioned above. Replacement by wet mixture containing both soil and water does not represent the real loss and may lead to the specimen being over-compacted due to extra soil added during the use of this procedure. Layers should be of approximately similar mass, to have a uniform density for the specimen throughout their height; Whitman et al. (1960) as well as Booth (1975) proved that if the same soil mass was used for each layer, statically compacted specimens showed no density variation with height, when the sample's diameter to height ratio is 1:2, as in the case of these specimens.

This was verified by the author by performing mass and volume measurements from different heights of trial compacted specimens, for which the standard compaction procedure using layers of equal mass was used.

For this reason, in this study, an equal mass (1/6 of the total required mass) of the wet mixture was added for each layer; mass checks were only performed after the completion of the fifth layer, to verify the exact amount of wet mixture needed to complete the last layer. Consequently, the possibility of ending up with extra dry soil mass in the specimen was reduced by up to five times, minimising the likely error margin on the dry density target.

All specimens selected for Triaxial testing were assessed to be within $38 \pm 0.5mm$ diameter and $76 \pm 1mm$ height at the time of the extrusion from the brass mould. Specimens outside these required ranges were discarded. It was also verified that they were within $\pm 1\%$ of the dry unit weight of the target value, as well as within $\pm 0.5\%$ of the required water content target value.

Repeatability was verified on randomly selected specimens, oven-dried to determine the dry mass and the initial water content. It was generally found to be consistent within an acceptable margin variation $\pm 0.35\%$ for water content and $\pm 0.75\%$ for the dry unit

weight, establishing the good reproducibility of the compacted specimens.

(e) Curing

With the intention of preventing moisture loss, after the extrusion, the specimen was immediately wrapped in several cling film layers, inserted in a sealable polyethylene bag, and finally stored in an hermetic container, and left in a controlled room temperature of $20 \pm 1^\circ C$ for the desired curing duration.

Each specimen measurements (length and diameter) were taken twice before being subjected to triaxial testing (as compacted measurements and as cured measurements). Slightly higher values were observed after the curing period essentially due to the inevitable rebound.

3.4. Experimental apparatus

3.4.1. Triaxial testing systems used in this study

In this study the following two triaxial testing systems were used:

- A stand-alone Wykeham Farrance unit (WF) without stress path control, which was only used for simple testing such as unconsolidated undrained (UU) tests.

- One stress path apparatus referred to as the Imperial College (IC) cell was used for shearing specimens under stress path control in saturated state.

The systems are described in more detail in the following sections.

(a) Wykeham Farrance Triaxial system (WF)

The WF 1020 loading frame is of a rigid chromed steel twin column construction. For rigidity at large loads the loading platen is made of stainless steel and can impose displacements at rates between 0.0006 and 1.140 mm / minute. It is accompanied by 70 mm diameter triaxial cell, which can house a specimen of 38 mm in diameter. The main

body of the cell consists of two parts; namely the circular base plate of the cell, which lies on the moving base plate of the frame, and the cell with the loading piston. Both the base plate and the ram are made of stainless steel in order to reduce the weight and increase their resistance to pressure and rust. The cell chamber, made of Plexiglas, reinforced by three plastic strips, is designed to resist an operating pressure up to 1500 kPa (Figure 3.4). As the WF was used for UU tests only no internal instrumentation was necessary.
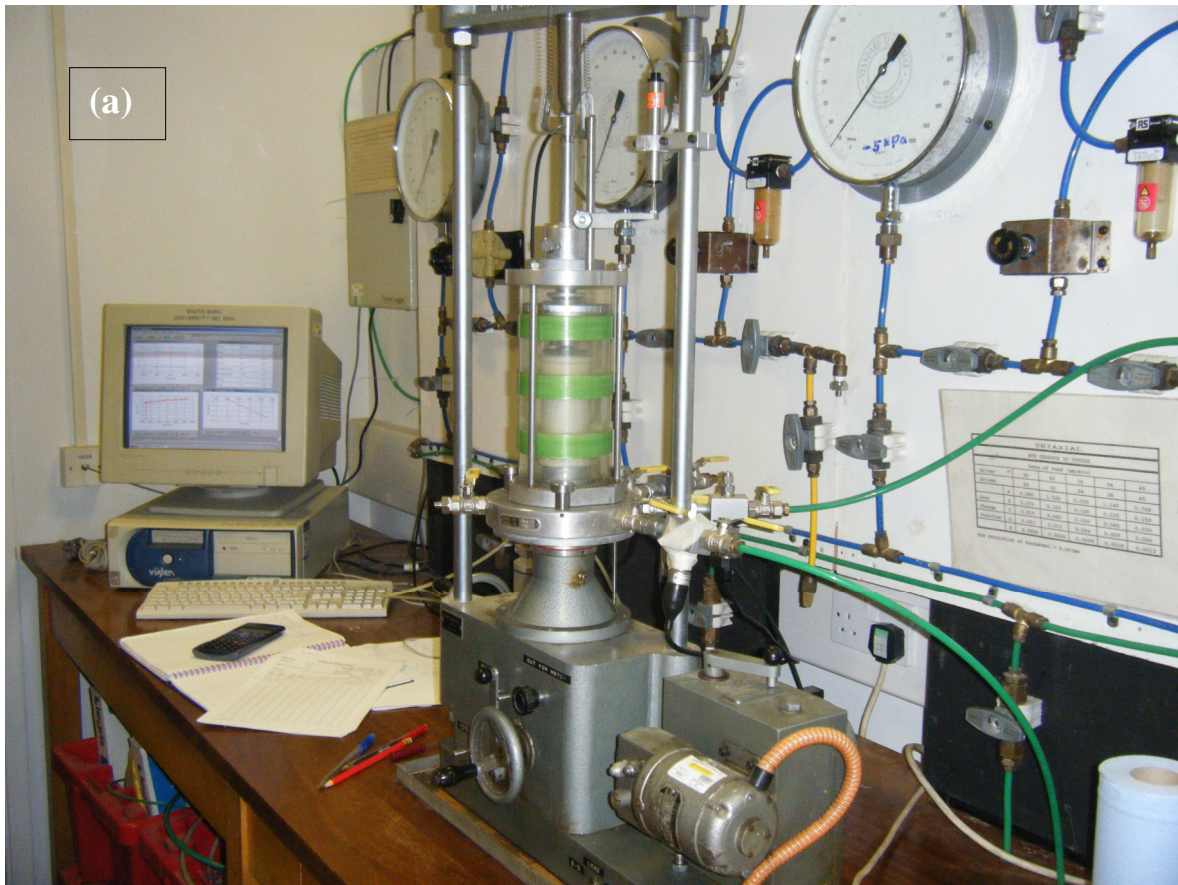
Figure 3.4 (a): Wykeham Farrance body frame
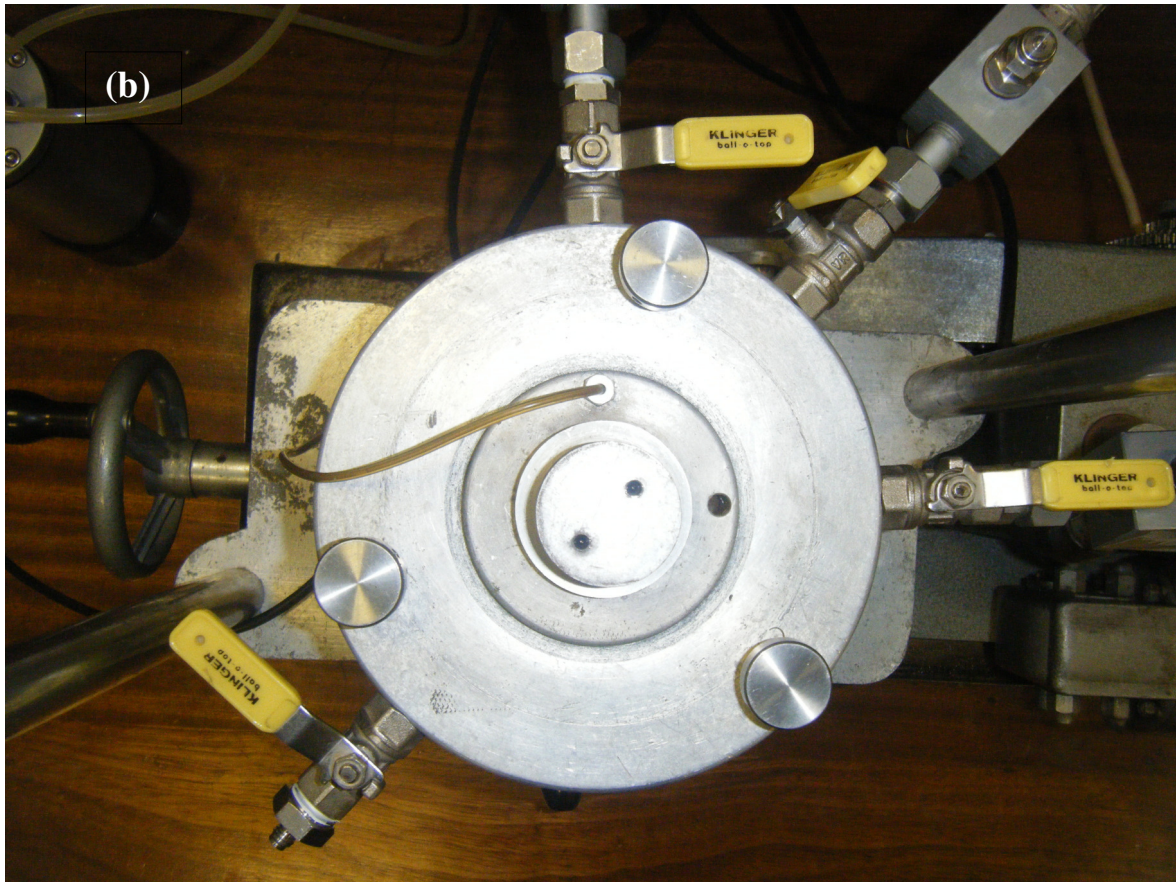
Figure 3.4 (b): Wykeham Farrance base plate

(b) Imperial College Triaxial system (IC)

IC system consists of a Bishop and Wesley type cell (Bishop and Wesley, 1975). The system accommodates cylindrical specimens 38 mm in diameter and 76 mm in height. It can be used for stress path controlled Triaxial tests, under either saturated or unsaturated state conditions; for the latter a simple modification to the system should be introduced to accommodate the axis translation technique (Hilf, 1956). However, during this research study, tests on the IC Triaxial system were only performed on saturated specimens under drained and undrained conditions.

The top plate is designed to accommodate an internal submersible load cell with a mechanism to maintain it in a fixed position by means of an adjustable rod passing through the top plate and threaded mechanism, allowing the internal load cell to be lowered or raised according to the specimen height. The air pressure supplied to the system is adjusted by a servo-control electric pneumatic valve / pressure converter. The pressure applied to

the pressure lines, namely the back pressure and the cell pressure, is generated by an air compressor at a maximum capacity supply of $700kPa$ through separate pipe lines to reach the air water interface (Figure 3.6) before being transformed into hydraulic pressure. The existing constant rate strain pump (CRSP) within the system is guided by a stepper motor and a gearbox, operated by a frequency pulse box.

Unlike the WF system, the IC system is controlled by a computer via an encoded input / output interface for the connected PC. Tests are controlled and data recorded using TRIAX software developed by Toll (2002). Figure 3.5 shows the IC system, connected to Datascan 7200 modules for data logging.
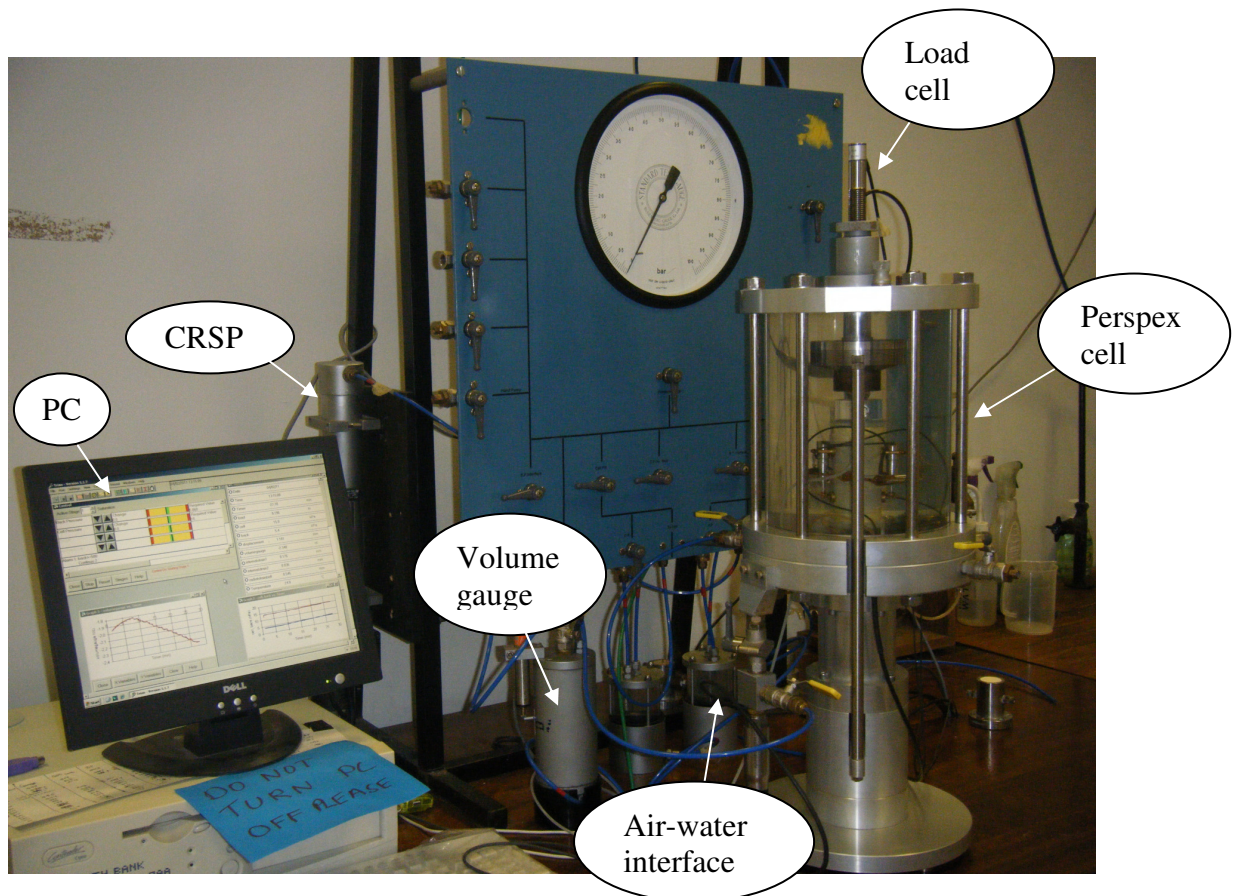
Figure 3.5: Imperial College Triaxial cell body
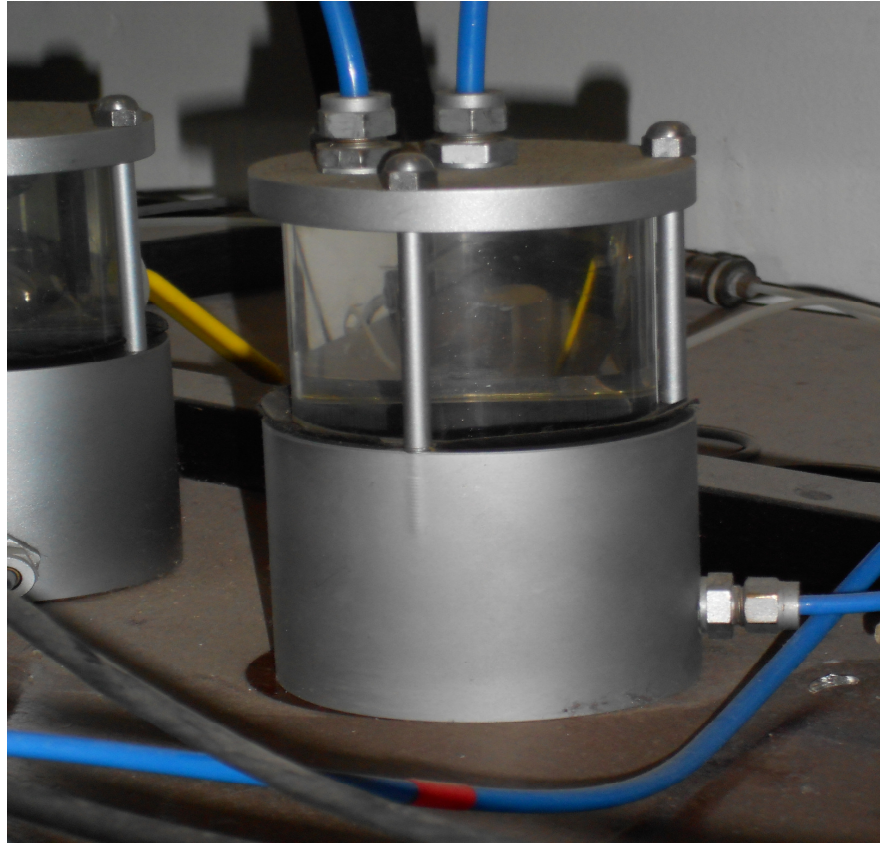
Figure 3.6: Air water interface

The following instrumentation is used in the IC system for volume change measurements:

i)   *A linear variable differential transformer (LVDT)* with a maximum range of 25 mm is attached outside to the top of the cell to measure the movement of the cross head in order to determine external axial strain.

ii) *Miniature submersible RDP D5 / 200W LVDT transducers*, consisting of two axial and one radial transducer. They are placed on the outer membrane surrounding the specimen for local measurements of the axial and radial strains, and hence the determination of the volumetric strain of the specimen. Two identical secondary coils are placed on a common bobbin and a moveable armature. The armature movement from its initial position produces an output proportional to the armature displacement. The combined output from the local LVDT represents the difference in the voltage induced into the secondary coils (Cuccovillo and Coop, 1997). Each transducer's armature is supported by a lower mount, and the body is mobilised by tightening the

large-headed screw on the upper mount to hold the transducer's upper part (Figure 3.7). The mounts were specially designed to allow the barrelling or the development of shear plane for the tested specimens without causing the armature to jam (Gasparre, 2005). Great care is required during the installation of the internal transducers to ensure perfect alignment.
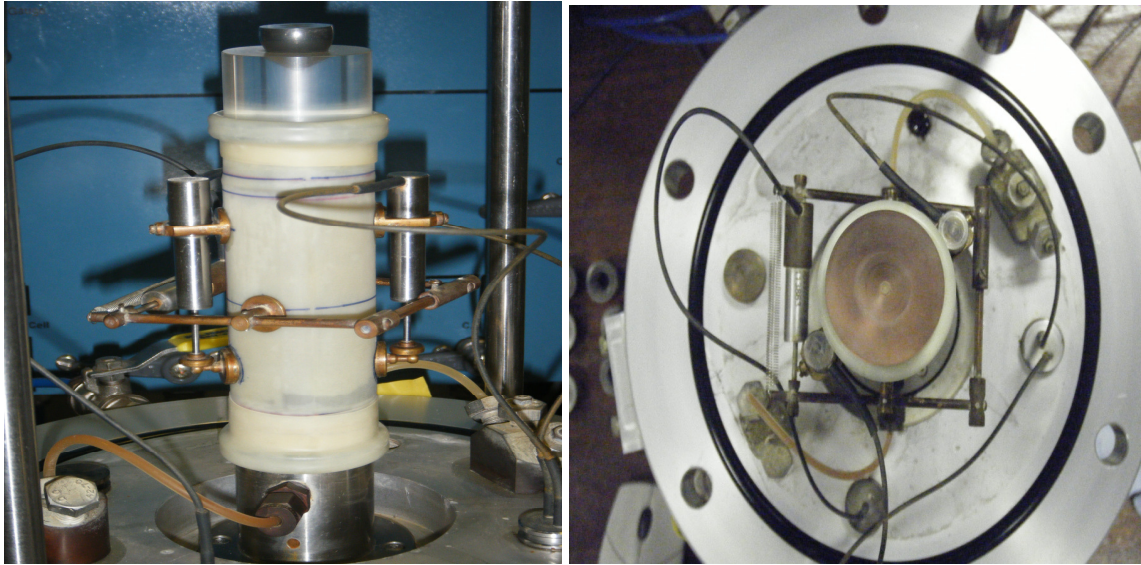
Figure 3.7: Local axial & radial LVDTs mounted on London Clay specimen

iii) ***A 50 cc Imperial College volume change gauge*** connected through the back pressure line to the IC Triaxial cell to measure the water volume change. The volume gauge is essentially a semi-rigid air-water interface, which measures the water flowing in and out of the specimen by the piston movement (Figure 3.8) via an LVDT attached onto the volume gauge. The obtained value is corrected for dimensional changes of the Perspex chamber caused by the pressure applied during the test stages; corrections for deformation due to pressure and creep are also applied. Air pressure supplied by an electro-pneumatic controller, is converted in the gauge to a desired water pressure, which is then applied to the tested specimen (Nishimura, 2005).

Figure 3.8: IC Volume change gauge

3.5. Instrumentation calibrations

The following section explains the general procedures followed for the calibration of different types of instrumentation involved in the testing. These consist of fully submersible load cells installed in all triaxial cells, pressure transducers for cell, pore pressure measurements (used in the Triaxial cells for the pressure control/measurement function), and LVDTs for external or local strain measurements. In addition, calibrations of the IC volume gauge are shown.

Sample calibration for transducer type is shown, whereas indicative data calibration is included in Appendix A. The calibration factors are determined and summarised in Table 3.1.

3.5.1. Load cell calibration

In the lack of a large dead weight device the calibrations of all load cells were performed based on the readings of a proving ring containing a reading dial gauge, fitted in the WF compression frame. A brass cylinder of 38 mm and 76 mm height and a top cap were used during the calibration process (see Figure 3.9). After initialisation of the dial gauge, the calibration begun by inputting and recording the actual readings using TRIAX software for each applied load, up to the maximum achievable point. A similar repeated procedure was followed during the load decrease input and record. The maximum hysteresis and non-linearity were found to be $\pm 0.5\%$ in full scale. An example of calibration curve generated using this procedure is shown in Figure 3.10

Figure 3.9: Load cell calibration using (WF) body frame and a proving ring
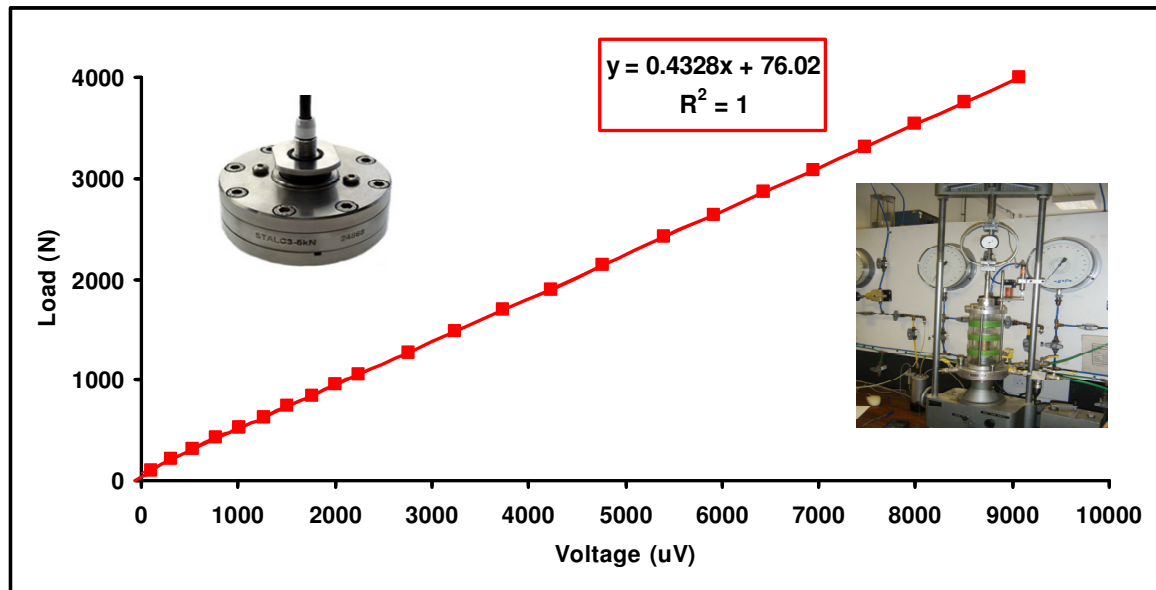
Figure 3.10: Submersible load cell calibration curve

3.5.2. Pressure transducer calibration

Pressure transducers were all calibrated using a hydraulically operated dead weight calibration unit manufactured by Budenburg Ltd (Figure 3.11). The procedure consisted of placing precise loads on the hydraulic piston cylinder, while the pressure transducer was connected to the second cylinder of the device. The fluid pressure in the reservoir was increased by turning the handle until a large enough force was obtained to just lift the piston-weight combination. As the piston floated, the pressure applied to the transducer was measured. The wiring connection of the pressure transducer (consisting of a shield from cable wires ending to a 5 pin socket plug) was directly connected to the data logger box from which, using the software interface, the raw output of the transducer (in terms of voltage) corresponding to the applied pressure was recorded. The procedure was repeated until several calibration points were obtained. In order to identify any hysteresis, calibrations of pressure transducers were performed over a range between 0 and 600 kPa using the pressure system under loading and unloading conditions.

Regression analyses were then performed, using the software (TRIAX) to show the relationship between voltage and pressure. These were saved in the computer program allowing real time plotting and recording of the transducer outputs. An indicative calibration curve for a pressure transducer (in this case the pore water transducer) is shown

in Fig 3.12. A 100 % linearity can be seen for the recorded pressure range. The rest of the pressure transducer calibrations performed in the same fashion is presented in Appendix A1.

Figure 3.11: Budenburg dead weight calibration unit
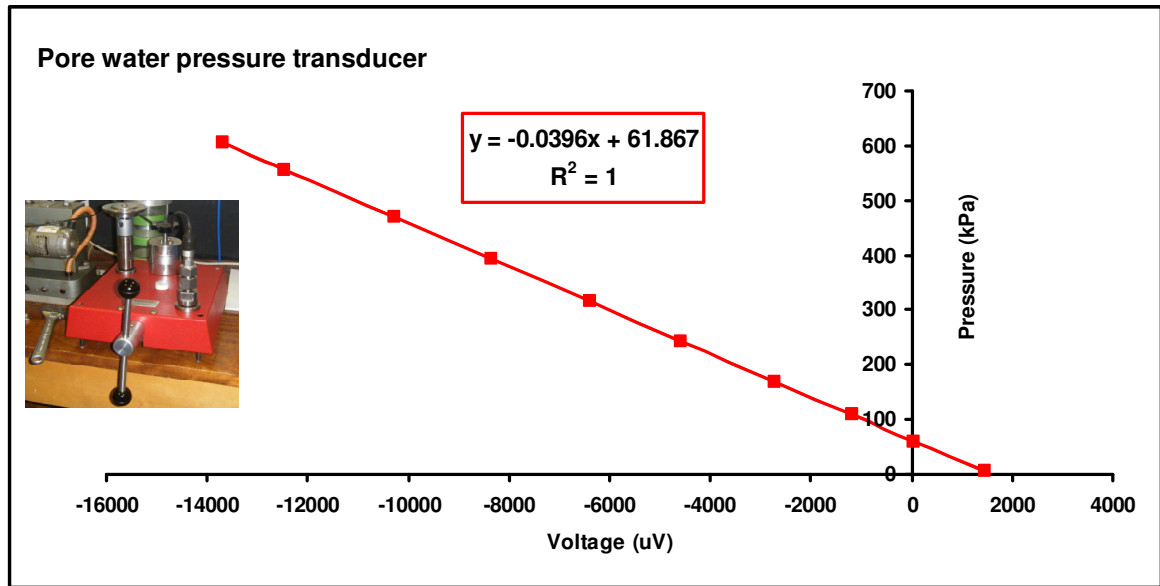
Figure 3.12: Indicative pressure transducer calibration curve

3.5.3. Internal and external LVDT calibration

LVDTs are all calibrated in similar procedure as detailed by Dineen (1997) and Kuano (1999), using a specially designed depth micrometer (Figures 3.13a & 3.13b) with 0.01 precision achieving a linearity of 100% (Figures 3.14, 3.15a & 3.15b). Calibration is done after the imposition of wanted amounts of applied displacement by means of micrometric slides. The calibration of the radial strain belt transducer was also carried out using a micrometer rig as shown in Figure 3.15b with a linear range of $50 \pm 1mm$ between the two pads.
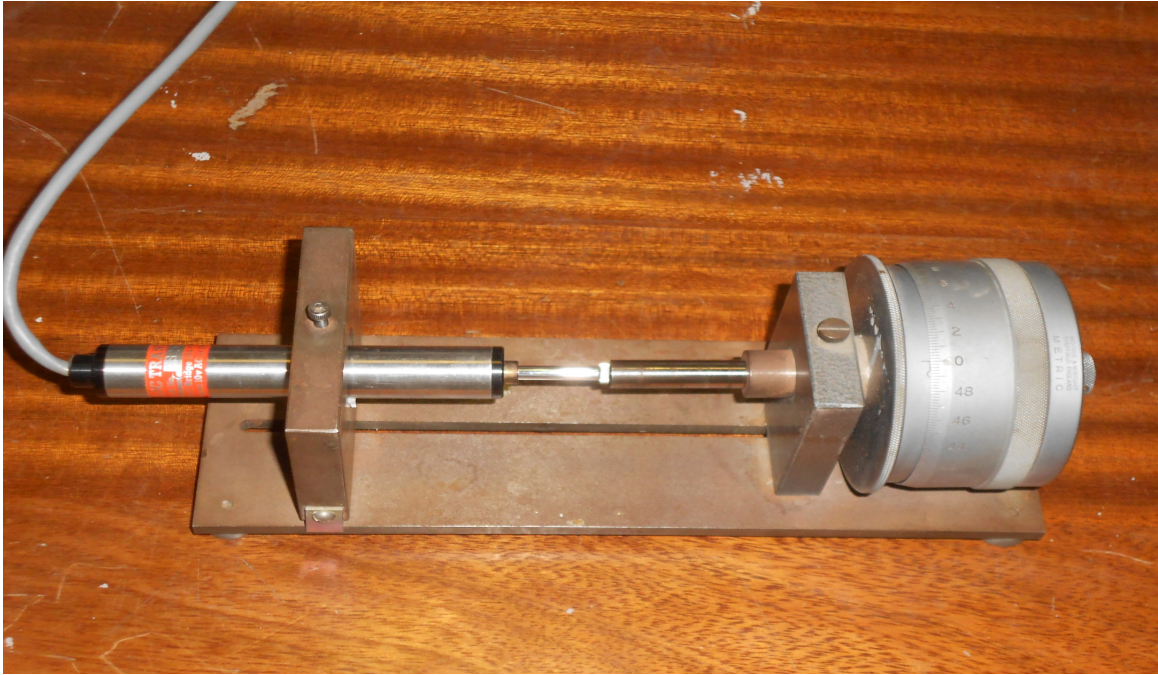
Figure 3.13 (a): calibration of an external LVDT by means of depth micrometer rig
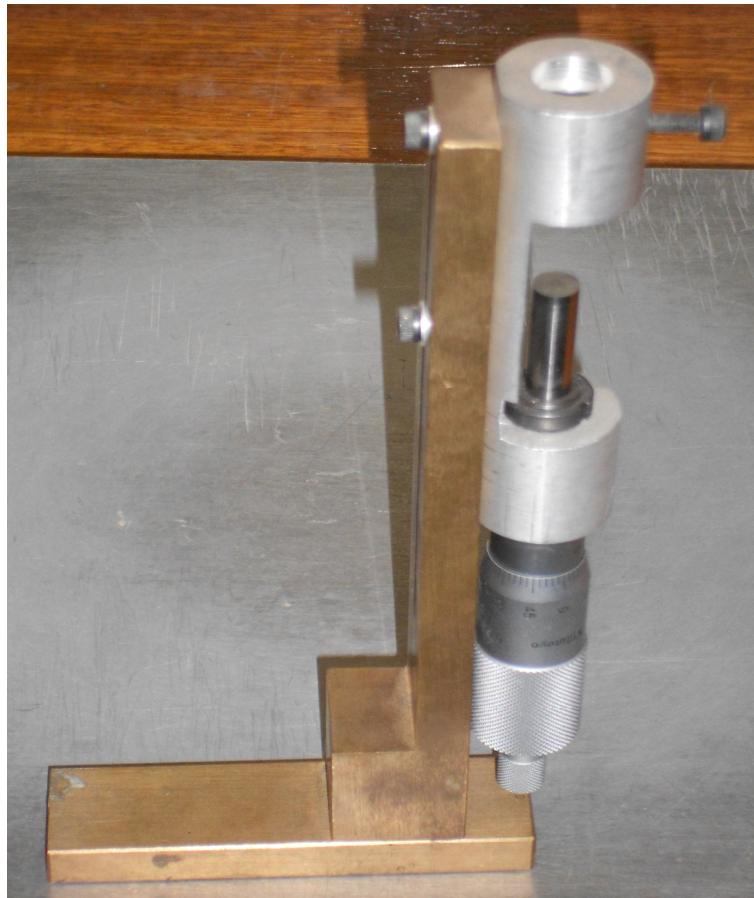
Figure 3.13 (b): Micrometer rig used for local RDP and DPT
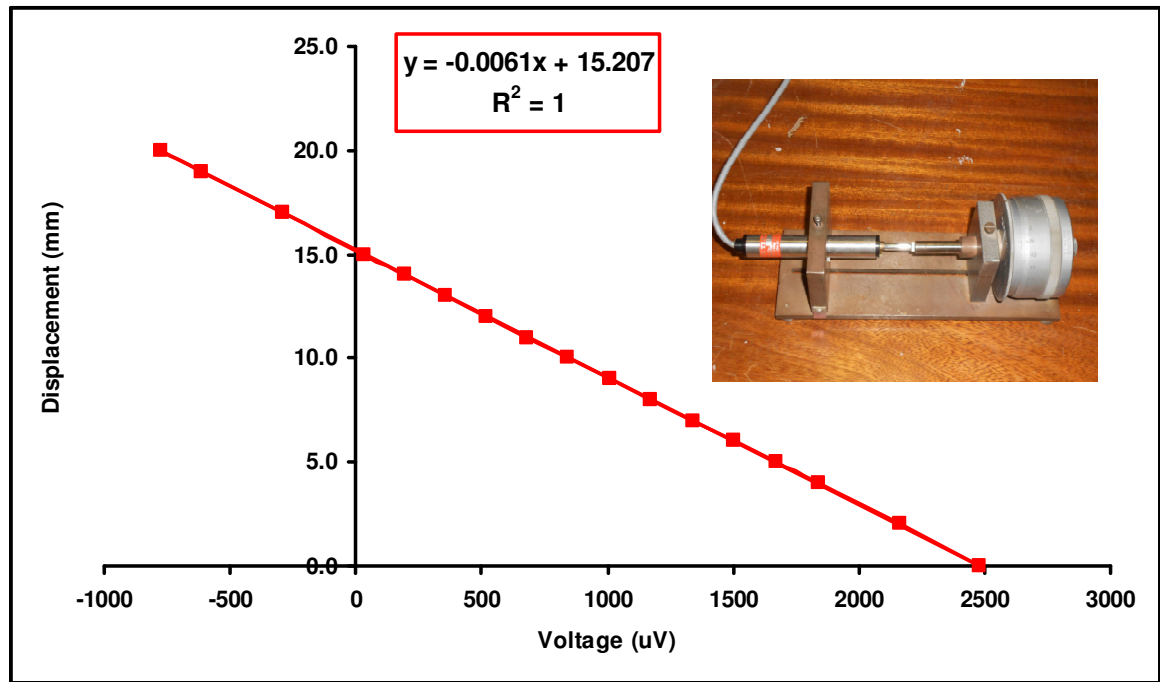
Figure 3.14: External axial displacement transducer calibration curve
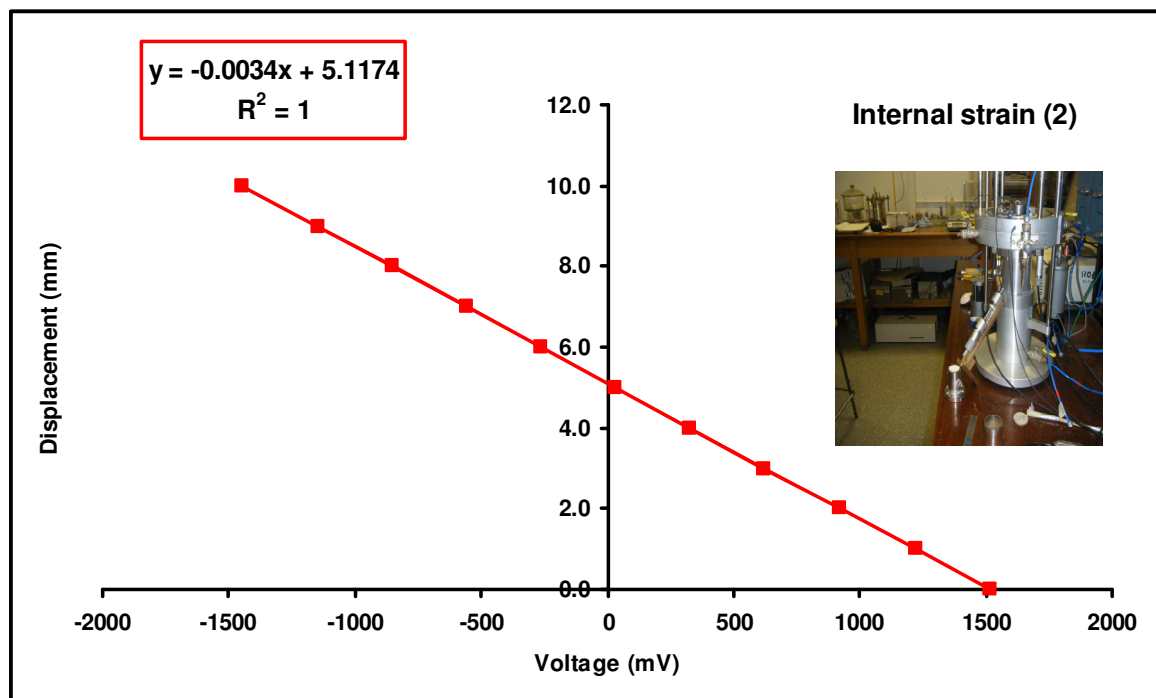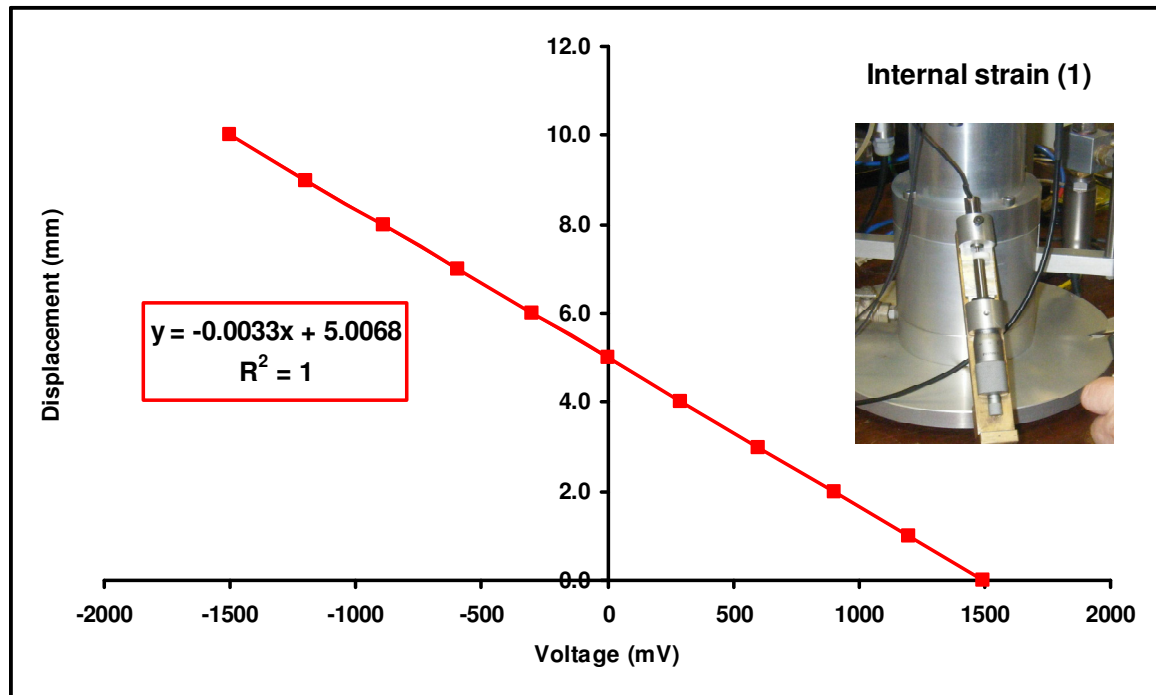
Figure 3.15 (a): Calibration of the RDP (1) & (2) for axial strain measurements
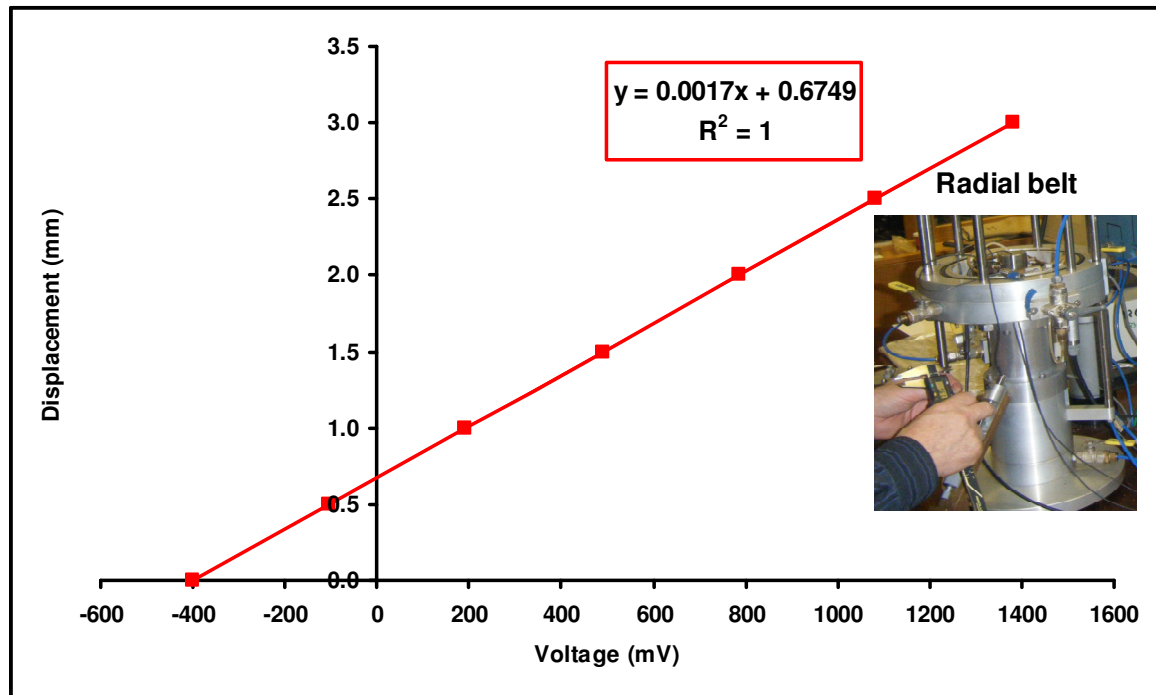
Figure 3.15 (b): Calibration of the DPT for radial strain measurements

3.5.4. IC Volume change gauge calibration

The IC volume change gauge was calibrated following the method described in Zhang (2011) using a GDS controller. An empty volume gauge is connected to water filled digital controller through the top, and linked to the air water interface via the bottom, which in turn is connected to a pressure gauge panel (Figure 3.16). Water contained in the controller's cylinder was allowed to gradually flow into the volume gauge, with a measured volume accuracy of $\pm 1\%$. The LVDT readings were recorded in terms of raw voltage using the TRIAX software calibration module for every 1cc, until 10cc; then every 5cc thereafter, and up to 20cc. This procedure was carried out under a back pressure of 20 kPa, which is the pressure value used during the saturation stage. The calibration was also performed in the reverse way allowing water to flow from the volume gauge to the GDS controller, and recording voltage for every 5cc taken into GDS controller (Figure 3.17). It is noteworthy that although generally during the triaxial testing, the range for the volume gauge varied between 0 and 10cc, the calibration was extended to 20cc as a precaution.

To determine the apparent volume change in the volume gauge originated from the compressibility of the water, the back pressure was gradually raised stepwise at $50kPa$

steps up to a pressure of $400kPa$ (the highest back pressure value used during triaxial testing in view of the available air pressure in the laboratory), and kept at this pressure level for 24 hours. The pressure was then decreased to $100kPa$ (Figure 3.18). The maximum volume change caused by pressure increase, as well as the internal gauge rolling diaphragm deformation was approximately $15 \times 10^{-3} cc$ for the gauge used in the IC system. The measured effect was considered during the volume change determination, and adjustments were made to all tests carried out in the IC system as explained in Appendix B.
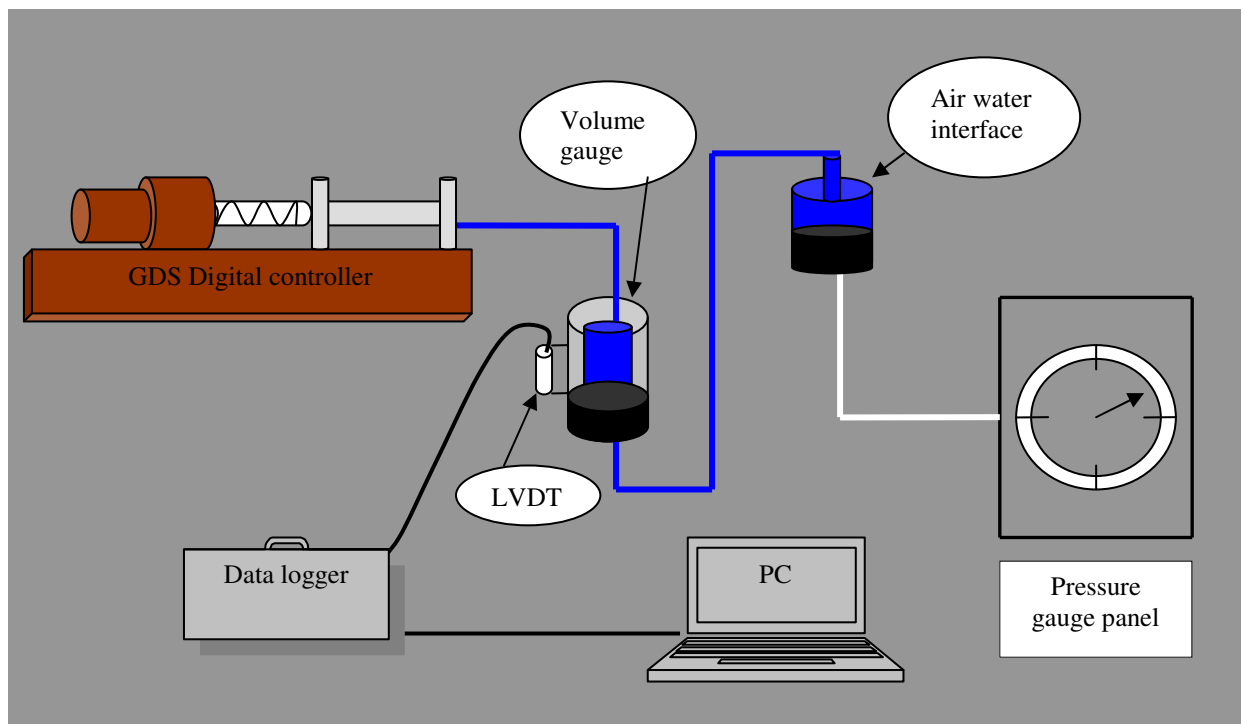
Figure 3.16: Layout of the IC volume gauge calibration
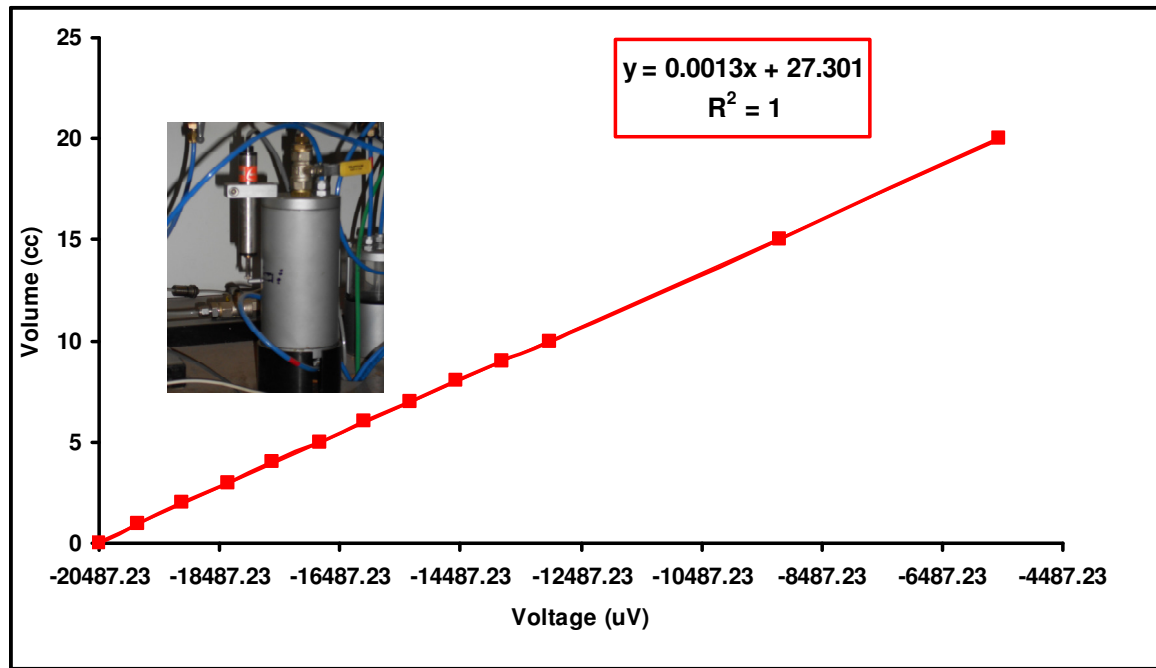
Figure 3.17: IC Volume gauge calibration curve
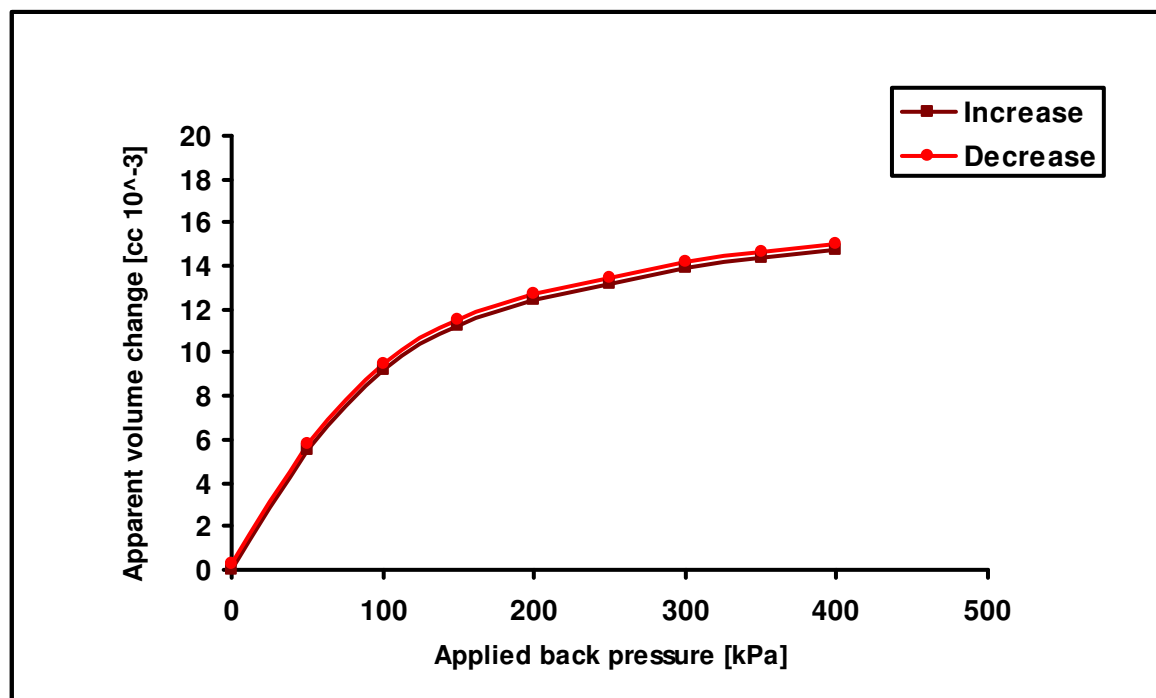
Figure 3.18: IC Gauge volume variation with respect to the back pressure

3.5.5. Calibration constants

Following the calibration of all necessary instruments, resulting in the best calibration curves, it was discovered that devices were not all linear within the full calibration range. For instance this is particularly noticeable at high stress level for both external and local LVDTs as well as the IC volume gauge. Therefore for these devices, calibrations were conducted so they can operate accurately over the central part of their travel (Richardson, 1988). This almost eliminated the non-linearity as it was shown on the calibration curves.

A calibration constant was then selected for each device, ordering the system to assume devices as linear. The offset magnitude is not great, but still needs to be assessed to determine the error margin.

For the axial load cell used for the determination of deviator stress in conventional triaxial compression tests, the force will typically range from zero to the final positive compressive value, and non linearity will be covered. Generally errors due to non-linearity are significant only when working at low stress level. During this investigation, tests were conducted at sufficiently moderate stress level; therefore the errors due to non linearity would be negligible.

Table 3.1 shows the calibration constants for each device and the respective accuracy.

Table 3.1: Characteristics of instruments used in the experimental study

System	Transducer type	S/N	Working Range	Voltage output	Calibration factor	Accuracy
WF	Load cell	1080	5 KN	30mv	0.4328	0.1%
	LVDT	6441	50 mm	5000mv	0.0007	0.1%
	PWP	6100A	1000 kPa	100mv	0.0396	0.1%
	CP	4-306	1000 kPa	100mv	0.0495	0.1%
IC	Load cell	1081	4.5 kN	30mv	0.0778	0.1%
	LVDT	2624	50 mm	5000mv	0.0061	0.1%
	IC V_{CG}	6442	50 cc	5000mv	0.0014	0.1%
	CP	2710	700 kPa	100mv	0.0203	0.1%
	PWP (BP)	191494	1000 kPa	100mv	0.0201	0.1%
	PAP	191474	1000 kPa	100mv	0.0203	0.1%
	RDP L1	113869	10 mm	1000mv	0.0033	0.1%
	RDP L2	113857	10 mm	1000mv	0.0034	0.1%
	RDP LR	113863	5 mm	1000mv	0.0017	0.1%
	Temp.	002	0-50° C	1000mv	0.0223	0.2%

3.6. Triaxial testing programme

In this study, three types of triaxial compression tests were performed on a series of lime treated and untreated London Clay specimens. The tests were carried out at London South Bank University geotechnical research laboratory and comprised (a) Unconsolidated Undrained tests (UU) on as compacted specimens, (b) Consolidated Drained (CD) and Consolidated Undrained (CU) tests on saturated specimens.

The UU tests were used as a quick and simple way to investigate the effect on a number of parameters on the undrained shear strength of the treated soil, namely:

- The effect of the lime percentage on specimens compacted at the same dry density and water contents for two lime percentages (4% and 6%) compared to the untreated specimen, the former percentage having been identified as the minimum necessary amount to induce the complete development of both cationic exchange and pozzolanic reaction (more details are provided in chapter 4).

- The effect of the compaction characteristics, such as water content (using characteristics both below and above the Proctor optima).

- The effect of the curing time (i.e. the time period between end of compaction and beginning of testing), using six different curing times ranging from one day to 250 days for both lime percentages (the selected curing times and respective strength values are shown in Chapter 5). From this investigation, appropriate curing times for the specimens were then identified, beyond which curing would not be expected to greatly affect the properties of the soil. This was very important for consistent comparisons between tests in view of the length of the triaxial testing, during which the specimen continues to cure in the water.

Undrained shearing for all previously mentioned tests was performed at a confining cell pressure equal to 200 kPa for all specimens and compacted to a similar dry density $\rho_d = 1.43 g/cm^3$.

The rest of the triaxial tests (CD and CU), which were more sophisticated and lengthy, they have been performed to investigate the effect of the same parameters on the mechanical behaviour of the specimens in more detail. However due to the length of each test, a control lime-treated mix was selected to be studied thoroughly, whereas parametric studies varied each of the other parameters (namely compaction water content – both dry and wet of Proctor optimum, as well as lime percentage) for a limited number of tests. The control mix was 6% lime-treated soil cured for 28 days and compacted at the same dry density and water content values as in Zhang (2011) (who tested saturated water-cured 4%

lime-treated London Clay specimens and saturated untreated London Clay specimens). These were respectively $\rho_{d(\max)} = 1.43 g / cm^3$ and $w = 27\%$ (i.e. dry of the standard Proctor optimum of the lime-treated soil). As these did not correspond to the standard Proctor optimum of the 6% lime treated London Clay (which were respectively $\rho_{d(\max)} = 1.38 g / cm^3$ and $w_{opt} = 29.5\%$) a higher compacting effort was required to achieve the 1.43 g/cm³ dry density for 6% lime treated London Clay specimens compared to 4% lime-treated specimens.

The identification of tested specimens follows the general nomenclature:

$$UU_n(x-y)_m, \ CD_n(x-y)_m \ \text{and} \ CU_n(x-y)_m$$

Where

UU , unconsolidated undrained

CD , consolidated drained

CU , consolidated undrained

n , number of the test

m , the applied stress (σ_3) for UU tests and the effective stress (σ_3') for CD and CU tests

x and y , are the lime amount and the curing period respectively

The triaxial testing plan is summarised in Tables 3.2 for UU tests. Whereas the CD & CU testing program are outlined in table 3.3. All triaxial test results and analysis are presented in Chapter 5.

Table 3.2: Performed UU triaxial tests on lime treated and untreated London Clay

Specimen ID	Lime (%)	Curing time (Days)	Confining stress σ_3, (kPa)	Water content w_c (%)	Dry density $\rho_d \left(g/cm^3 \right)$
$UU_1(0-0)_{200}$	0	N/A	200	25	1.43
$UU_1(4-1)_{200}$	4	1	200	27	1.43
$UU_2(4-7)_{200}$	4	7	200	27	1.43
$UU_3(4-28)_{200}$	4	28	200	27	1.43
$UU_4(4-60)_{200}$	4	60	200	27	1.43
$UU_5(4-120)_{200}$	4	120	200	27	1.43
$UU_6(4-250)_{200}$	4	250	200	27	1.43
$UU_1(6-1)_{200}$	6	1	200	27	1.43
$UU_2(6-7)_{200}$	6	7	200	27	1.43
$UU_3(6-28)_{200}$	6	28	200	27	1.43
$UU_4(6-60)_{200}$	6	60	200	27	1.43
$UU_5(6-120)_{200}$	6	120	200	27	1.43
$UU_6(6-250)_{200}$	6	250	200	27	1.43
$UU_7(6-1)_{200}$	6	1	200	32	1.43
$UU_8(6-7)_{200}$	6	7	200	32	1.43
$UU_9(6-28)_{200}$	6	28	200	32	1.43
$UU_{10}(6-60)_{200}$	6	60	200	32	1.43
$UU_{11}(6-120)_{200}$	6	120	200	32	1.43

Table 3.3: Summary of CD & CU Triaxial tests on lime treated and untreated London Clay

Saturated CD Triaxial compression tests					
Specimen ID	*Lime* $(\%)$	*Curing time* $(Days)$	*Effective stress* $\sigma_3{}'\ (kPa)$	*Water content* $w_c\,(\%)$	*Dry density* $\rho_d\left(g\,/\,cm^3\right)$
$CD_1(0-0)_{100}$		N/A	100		1.43
$CD_2(0-0)_{200}$	0	N/A	200	w_{opt}	1.43
$CD_3(0-0)_{300}$		N/A	300		1.43
$CD_1(4-7)_{100}$			100		1.43
$CD_2(4-7)_{200}$	4	7	200	w_{opt}	1.43
$CD_3(4-7)_{300}$			300		1.43
$CD_1(6-7)_{100}$			100		1.43
$CD_2(6-7)_{150}$		7	150		1.43
$CD_3(6-7)_{200}$			200	w_{dry}	1.43
$CD_4(6-7)_{300}$			300		1.43
$CD_5(6-28)_{100}$			100		1.43
$CD_6(6-28)_{200}$	6		200	w_{dry}	1.43
$CD_7(6-28)_{300}$		28	300		1.43
$CD_8(6-28)_{100}$			100		1.43
$CD_9(6-28)_{200}$			200	w_{wet}	1.43
$CD_{10}(6-28)_{300}$			300		1.43

Saturated CU Triaxial compression tests					
Specimen ID	*Lime*	*Curing time*	*Effective stress*	*Water content*	*Dry density*
	$(\%)$	$(Days)$	$\sigma_3', (kPa)$	$w_c(\%)$	$\rho_d(g/cm^3)$
$CU_1(6-28)_{158}$	6	28	158	w_{dry}	1.43
$CU_2(6-28)_{250}$		28	250	w_{dry}	1.43

The following section describes in detail the triaxial testing procedures followed in this study, including apparatus setting up prior to testing.

3.7. Testing procedures

3.7.1. Triaxial testing of saturated specimens

3.7.1.1. Pre-test checks

Checks prior to triaxial testing are essential procedures and must not be overlooked. It is important to ensure that all pipe lines are air free and leak free, as the slightest leak must not be tolerated. Consequently, the back pressure and cell pressure lines were pressurised to a maximum working pressure equal to $700kPa$ (according to the capacity of the laboratory system air-pressure) and left overnight in order to identify any existing leaks and eliminate all traces of trapped air within the pipe lines. Moreover, it is necessary to flush the system and recharge it with freshly de-aired water before the start of each triaxial test.

3.7.1.2. Testing procedure

(a) Setting up

All pressure line valves were closed prior to specimen setting up. A pre-saturated porous disc was first placed on the pedestal without trapping any air, then a filter paper cut to size, and finally the compacted specimen was placed. A second filter paper and a second pre-

saturated porous disc (with excess surface water removed) were positioned on the top end of the specimen; the top cap was then placed with a half steel bearing ball on it. In order to prevent any water ingress from the cell chamber to the specimen during the long lasting test, two rubber membranes were used, separated by coated silicon grease. When the first membrane was inserted on the specimen, an upwards stroking with the fingers was applied to remove as much air as possible between the specimen and the membrane. Without disturbing the specimen, two tight fitting "O" rings are slipped over to seal the membranes at each end. This operation was made easier by using the split steel stretcher. The internal strain transducers (RDP D5/200W) were then carefully mounted on the specimen with a minimum disruption. The two axial strain transducers were rigorously mounted on opposite sides of the specimen by gluing the purpose built mounts on the outer rubber membrane surrounding the specimen. Adjustments were made to the armature resting on the lower mount, through the upper mount screw; this should be near-perfect in vertical position, subsequently followed by the radial strain transducer mounting using a similar procedure. The Perspex cell chamber was then installed with great care, ensuring the load cell piston was vertically aligned on the same central axis as the half steel bearing ball placed on the top cap without making direct contact. A minimum gap of 3 to 5 mm was left between the load cell and the half steel ball, to allow the specimen to freely move upwards during the saturation process without restrain. The cell chamber was then filled with freshly de-aired water. At the end of this stage, the pressure line valves were opened, followed by the initialisation of all the necessary variables on the TRIAX software before commencing the triaxial test.

In addition to the above steps, several necessary measures were taken before the start of each test to prevent incorrect volume measurements from the IC water volume gauge. These were as follows:

i) The system was flushed several times with fresh de-aired water to eliminate any existing air bubbles within the inner gauge;

ii) The back pressure line connected to the gauge was pressurised to the maximum available pressure $(700kPa)$, and left overnight in order to dissolve any trapped air bubbles.

iii) Triaxial tests were performed in temperature controlled environment in order to minimise the temperature's effect on volume gauge.

Note that the volume gauge expansion and contraction may be considerable during the tests due to back pressure variation. However, in this study, compression for each tested specimen was performed at a constant back pressure, therefore this effect was considered negligible. Despite the above precautions, the volume gauge did exhibit measurable pressure change compliance, and required correction of its measured value as previously explained.

(b) Saturation phase

Saturation was performed by applying increments of back pressure, automatically also incrementing the cell pressure accordingly, to ensure that the effective stress in the specimen remained constant during saturation. This was achieved by the use of air pressure regulator valves controlling the cell pressure and the back pressure systems simultaneously with a variable speed electric motor drive. Initially, the system was set to seek a cell pressure equal to $30kPa$, followed by a target back pressure equal to $10kPa$, and hence an effective stress of $20kPa$ in the specimen, which was maintained during the saturation stage. Once the equilibrium was established (after approximately two hours) the automated system would slowly introduce de-aired water to the specimen through the drainage system.

In order to avoid a sudden pore water pressure increase resulting in a hasty swelling, an incremental saturation rate of no more than $1.5kPa$ per hour was deemed to be suitable. Thus the triaxial saturation stage for each specimen, lasted an average of 14 days. Note that previous work by Schnaid et al., (2001) and Consoli et al., (2001) on triaxial response of cemented soils have shown that B-values of about 0.90 or higher result in negligible suctions, if any. In this study, a Skempton parameter B value check was performed at the end of saturation phase; values above 99% and between 91 and 98% were obtained for the untreated and lime-treated specimens respectively, depending on lime amount, initial water content and the curing time (see Fig. 3.19). When a satisfactory B value was acquired, the specimen was left under the same pressure conditions until stable reading of pore water pressure was achieved or the pore pressure was relatively equal to the back pressure.
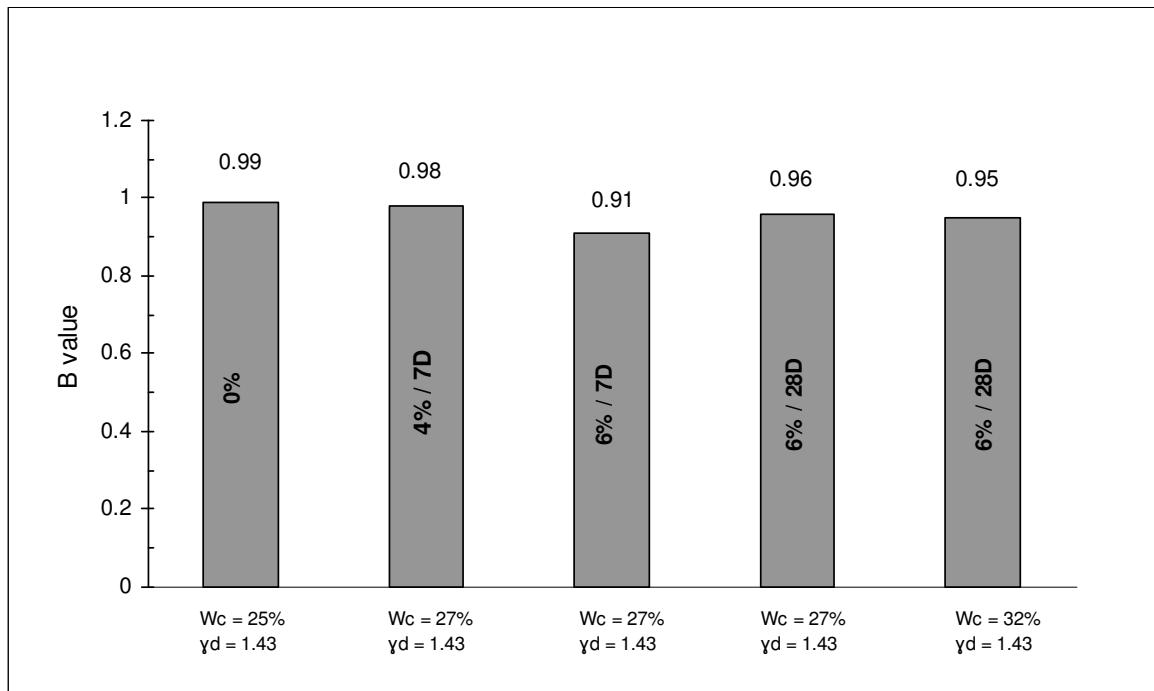
Fig. 3.19: Average B-value for lime treated and untreated London Clay

It should be emphasised that the saturation volume measurement in the IC system is considered to correspond to the amount of water transferred from the volume gauge to the specimen, occupying the air void space inside the specimen by dissolving the existing air into water. The initial air volume was therefore determined for each specimen and was subtracted from the water volume absorbed by the specimen during the saturation. Table A2.1 in appendix A indicates the steps followed for a selected specimen to determine the volume of the initial air void. Other corrections applied to the IC volume change measurements to obtain the true specimen's volume change are also shown in Appendix B.

(c) Isotropic consolidation phase

Once the B value check is confirmed to be appropriate, the loading stage can be set to the desired effective stress (ranging 100 - 300 kPa), either by raising the cell pressure at the rate specified below to reach the desired value, or by reducing the back pressure (the latter technique is acceptable providing the back pressure is not reduced below $400kPa$ for lime treated specimens as recommended by Head (1986) for compacted samples), or by the combination of both, then allowing the tested specimen to consolidate.

In this study, each tested specimen was consolidated by applying an isotropic load

increment, this is performed by means of an automatic cell pressure increase at a loading rate equal to $1.2kPa/h$, while the back pressure is kept constant. The aforementioned rate was determined based on the method suggested by Head (1986). Once the effective stress target is reached, and in order to achieve equalisation, a waiting time period is observed by keeping the specimen under the same loading pressure until the rate of change in volumetric strain fell below $0.05\%/day$ as recommended by Sivakumar (1993). Consolidation is considered to be achieved once the pore water pressure dissipation is greater than or equal to 97%. This consists of applying a calculating method to determine the amount of pore pressure dissipated at time (t) using the following equation:

$$u\big(\%\big)=\frac{u_i-u_t}{u_i-u_b}\times100\%$$

Where u_i is the initial pore pressure, u_t is the pore pressure at time t, and u_b is the back pressure.

(d) Shearing Phase

Axial load was gradually increased while the confining pressure remains unchanged until failure occurs. In this study, the shearing stage was performed beyond failure point in order to reach the critical state. The specimen was sheared either under drained or undrained conditions, up to a maximum axial strain varying between 20 and 23%, under controlled and sufficiently low shearing rate equal to $0.1\%/h$ as recommended by Consoli et al., (2001), which is approximately equivalent to $1.2\mu m/\min$. For the drained tests, compression was applied slowly enough to allow pore pressure changes to equalise throughout the whole specimen while the volume change measurement is recorded. For the undrained tests, shearing was fast and the generated excess pore water pressure was continuously monitored using pressure transducers. Constant rate strain pump (CRSP) was used to keep the strain rate constant during the shearing stage. Relevant data was collected using the computer logging system supported by TRIAX software, set to scan every 20 minutes switching to 5 minutes scan during the shearing stage.

At the end of each triaxial test, the specimen was immediately removed from the base

pedestal to prevent any swelling. The water content was determined by weighting and oven drying the specimen. Any soil which may have adhered to the porous disc or drains was included in the measurement of the water content.

3.7.1.3. Applied corrections and used formulae

Stress-strain and volume change measurements are vital parameters in triaxial testing. In order to better understand the data analysed in this chapter, a brief explanation of the applied corrections to the measurements is given in Appendix B. In addition, the main formulae's used in the analysis are also included.

Chapter 4

4. Physicochemical property testing

4.1. Introduction

Several basic properties of the soil were determined from preliminary tests. These include specific gravity test, Proctor test, plastic and liquid limit tests, free swell test, pH testing, chemical tests (calcium and sulphate content tests) and X-Ray diffraction testing.

Moreover, the aim of the study presented in this Chapter is to observe the changes in the soil with time due to short term (cationic exchange) and long term (pozzolanic) reactions during the curing time at a moderate temperature ($20 \pm 1°C$). These are evidenced by the changes in pH and calcium level with curing time as well as changes in the mineralogy based on X-Ray diffraction testing.

4.2. Suitability assessment of London Clay lime treatment

In order to proceed with lime treatment, it was necessary to identify the suitability of the soil for lime treatment by performing a sulphate content test. It is widely known that in the presence of excess water, sulphates can be highly damaging to the lime stabilisation process due to the potential reactions with the calcium (from the lime) and the dissolved silica and alumina (from the soil). The reaction products namely ettringite or thaumasite are expansive in nature and thus occupy a greater volume than the combined volume of the reactants (Sherwood, 1993). This in turn causes heave and then damage of light weight structures (Mitchell & Dermatas, 1992; Puppala et al., 2005; Yong & Ouhadi, 2007 and Little et al., 2010). For this reason, the total sulphate content of the soil was determined by the gravimetric method using the acid extract according to BS: 1377 – 3:1990 / part 5.

Figure 4.1: Determination of sulphate content on prepared solution – Gravimetric method

The acid soluble sulphate (hydrochloride acid) content of soil was first prepared. This solution was prepared at 10% (v/v) by diluting 100 ml of concentrated hydrochloride acid (relative density 1.8) in 1000 ml distilled water. Good practice in chemical testing requires that duplicate specimens should be tested. Two small containers with a quantity of fine grained soil (passing the $425\mu m$) were weighed and inserted in the oven overnight for a set temperature (70 - 80°C). The following day, the soil quantity was weighted again and each of the soil's dry mass (m_1 : Initial mass of the soil to use in the test) was determined.

The dry soil was put in a 500 ml beaker; then a small amount of distilled water was added by washing the container to clean it from any remaining soil particles, 150 ml of diluted hydrochloride acid is added to the beaker where the soil is contained then put on the hot plate. Once the solution is brought to the boiling point, a 10 ml Barium chloride solution was added by small drops. The precipitate was transferred to a suitable filter paper type (N° 42) in the glass funnel and filtered, connected to a 300 ml conic beaker which was linked to vacuum source. The total sulphate present in London Clay soil was extracted, precipitated as barium sulphate, and then ignited (see Fig. 4.1).

An ignition of about 15 minutes at red heat was sufficient. The crucible was cooled to room temperature in a desiccator and weighted to the nearest 0.001g. The next step was to calculate the mass of ignited precipitate (m_2).

The sulphate content is expressed in terms of SO_3, the % of total sulphates as SO_3 in the fraction of the soil sample was determined using the following equation (Head, 2006). Where the mass of SO_3 is equal to (radical mass/molecular mass) = 80/233 = 0.343

$$SO_3 = 100\% \times 0.343 \times \frac{m_2}{m_1} (\%)$$

The average from the two results was taken and found to be less than 0.1%; hence lime stabilisation should not cause problems due to the formation of expansive crystals.

4.3. Lime percentage

To determine the necessary lime quantity for the soil used in this study both the "Initial Consumption of Lime" (ICL) method and "Lime fixation point" (LFP) method were used (Eades and Grim, 1966). The latter method estimates the necessary amount of lime based on plasticity change whereas the former method defines the minimum amount of lime as the percentage of lime per dry soil mass, causing the pH value of the soil-lime mix to rise up to 12.4.

4.3.1. Initial consumption of lime (ICL)

The minimum required lime percentage was determined through the Initial Consumption of Lime (ICL) test. The ICL test was performed according to BS 1924 – Part 2 (BSI, 1990). A duration time between 8 and 24 hours was allowed for the prepared solution contained in tightly stoppered bottle, before being subjected to pH measurements by means of digital pH meter. The pH meter was calibrated using two buffer solutions pH = 4.01 and pH = 7. The error was estimated to be between 2 and 2.5%.

According to pH measurement results (see Figure 4.2), 3.45% is the least required lime addition to London Clay in order to reach the minimum essential pH level of 12.4. The pH then stabilises between 12.4 and 12.5 for a variation of lime portions between 4 and 14%. The ICL of the soil is therefore 3.45%.
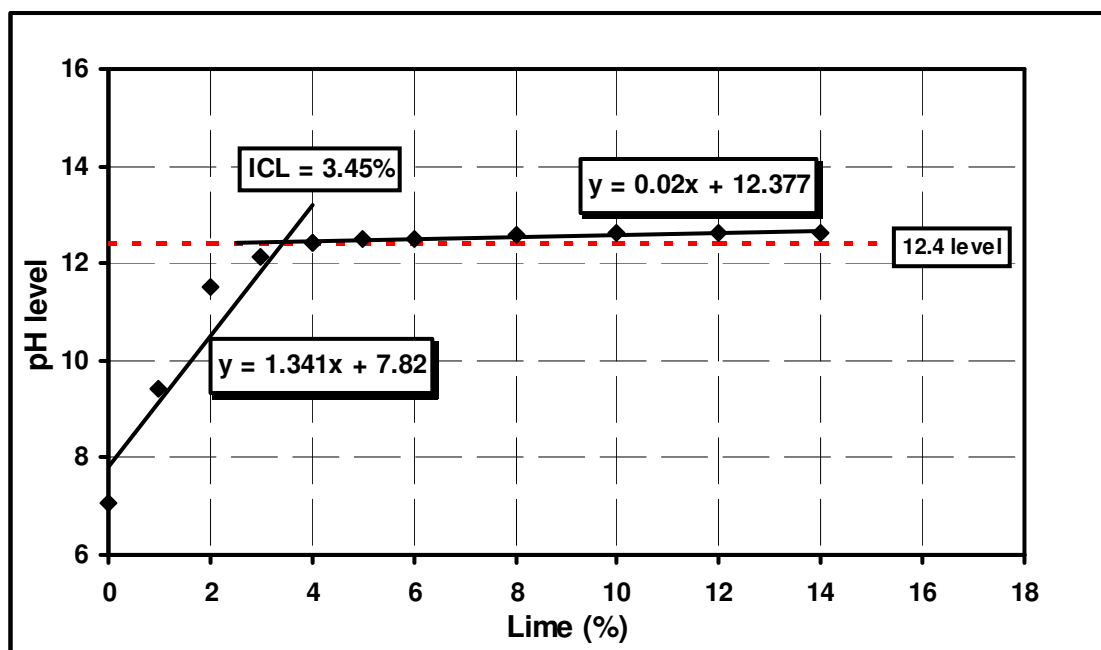
Figure 4.2: pH variation of lime treated London Clay

4.3.2. Lime fixation point (LFP)

The lime fixation point (LFP) is the other method based on plasticity tests of several London Clay samples treated with different lime percentages. Figure 4.3 indicates the plasticity evolution for several lime amounts. A plasticity increase is observed in conjunction with the lime fractions, up to a value slightly below 4%; it then stabilises for higher percentages. The exact LFP value is found to be equal to 3.47%, which is very consistent with the ICL value of 3.45%. It is interesting to note that this contradicts claims by Rogers & Glendinning (1996) that the ICL overestimates the necessary lime percentage.
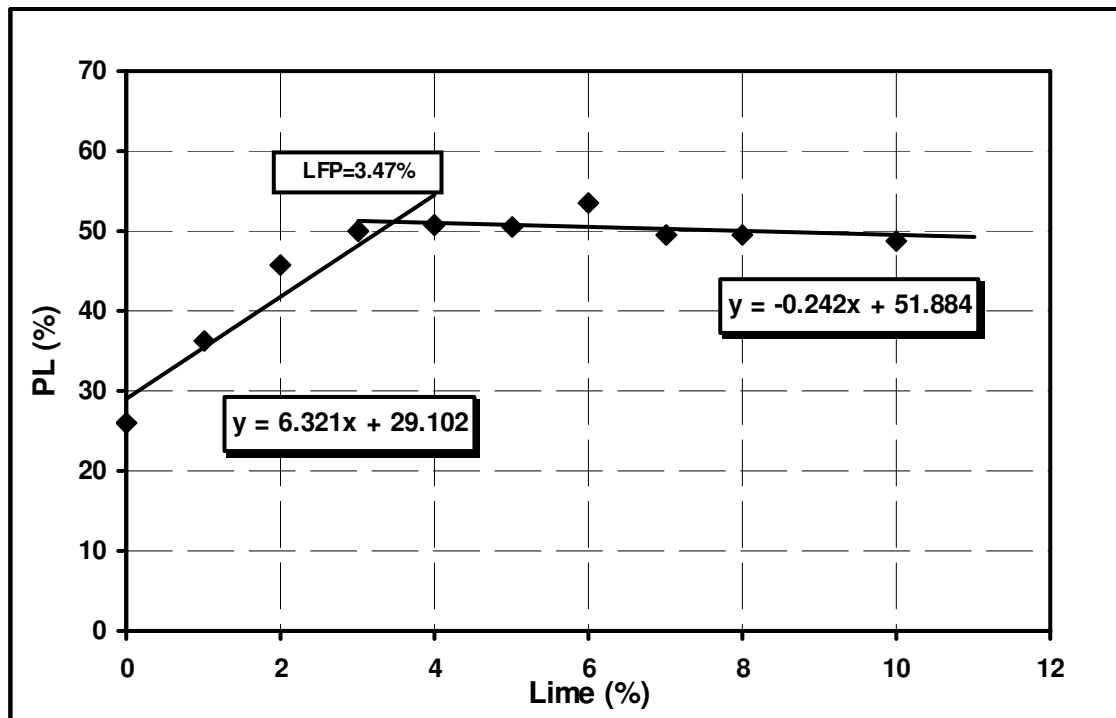
Figure 4.3: Plasticity tests on lime treated London Clay

Based on the findings of the above two methods, an amount of 4% lime per dry soil mass is considered to be sufficient for triggering both cationic exchange and to some extent pozzolanic reactions for London Clay. This amount of lime was consistent with previous assessments made by Tembo (2005) and Clark (2007) in different projects carried out at London South Bank University. However, in this study, two lime percentages 4 and 6% were used, above the minimum required percentage (according to the above mentioned tests).

4.4. Identification tests

A series of identification tests have been performed on both lime treated (4 and 6%) and untreated London Clay, in particular the determination of Atterberg limits and the specific gravity measurement. The grain size distribution test was performed by Zhang (2011).

4.4.1. Atterberg Limits

In order to understand the plasticity characteristics of the soil, the Atterberg's limits corresponding (0, 4 and 6%) lime content were determined after 24 hours of lime addition as commonly done for lime treated soil. Table 4.1 gives the values of the liquid limit, plastic limit and plasticity index of the lime treated and untreated soil.

Lime treatment increase the liquid limit to 86.2 and nearly 90% for 4 and 6% lime addition respectively. This is consistent with the change in the mineralogy of the soil due to immediate modification reactions. In addition, the lime treatment increases the plastic limit from 26.1 to almost 54% at the highest added lime amount (6%). The observed increase in the plastic limit indicates the decrease of the adsorbed layer (Rogers and Glendinning, 1997).
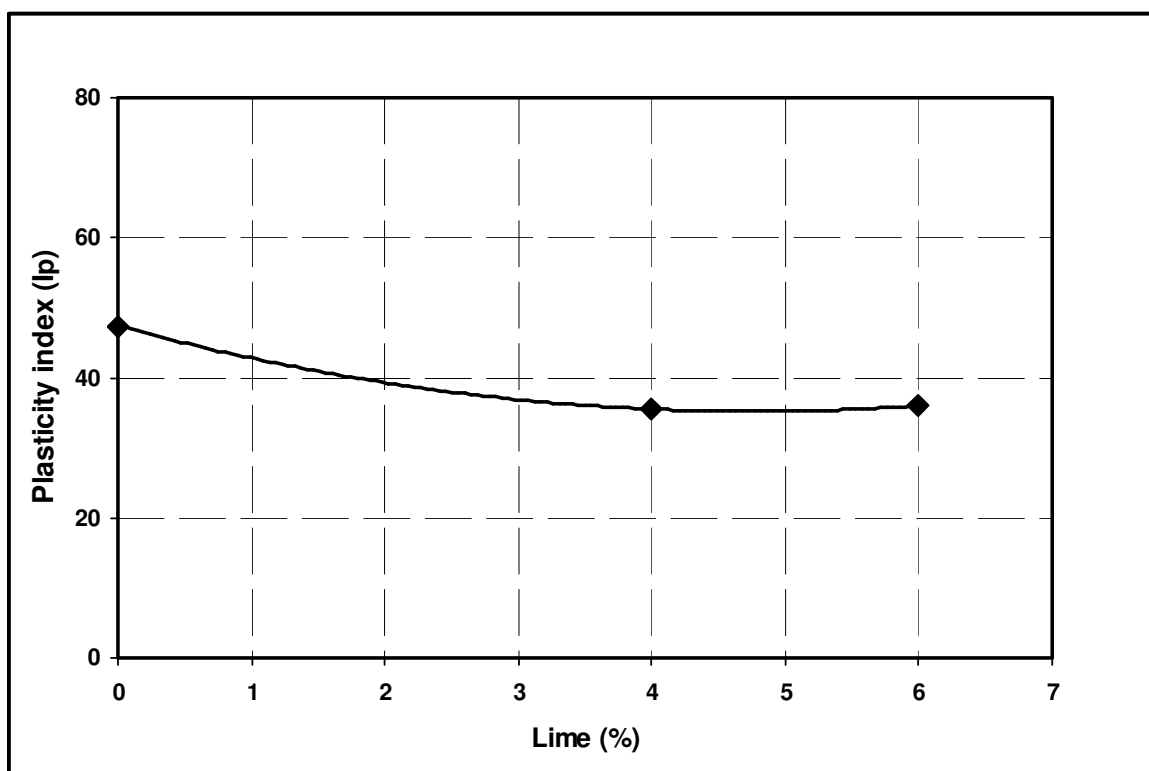
Figure 4.4: Plasticity index $\left(I_p \right)$ variation with lime percentage

Fig. 4.4 shows that the plasticity index $\left(I_p \right)$ decreases with the lime content. There is an average of 10% reduction compared to the untreated soil. The plasticity reduction could be attributed to the flocculation taking place due to Ca^{++} and OH^{-} presence. The lower

plasticity index implies that the treated soil, when subject to water content changes will be less susceptible to volume change and soil strength reduction. The drop in plasticity index due to lime addition which leads into more workable material is useful for excavation, loading, discharging and levelling. In this study, the plastic limit and liquid limit were both observed to increase with lime addition for up to 6% (see Table 4.1), but the decrease in plasticity index was mainly due to faster increase in plastic limit. Similar plasticity index decrease was reported by Ola (1978) caused by an increase in both the liquid limit and plastic limit with lime increase. Whereas the plasticity index decrease observed by de Brito Galvao et al. (2004) for red lateritic soil (up to 6% lime addition), was attributed to the liquid limit decrease, while changes in plastic limit were too small to be considered.

4.4.2. Specific gravity

London Clay and lime treated London Clay specific gravities were determined through the small pycnometer method, according to BS 1377 – 2: 1990. The specific particle density for lime on its own could not be accurately achieved due to high solubility of lime in distilled water. Hence, the specific gravity of each lime treated London Clay soil (4% and 6% lime respectively) was determined. The results are presented in table 4.1. These are each an average of three readings having a scatter of about ± 0.005.

4.5. Standard Proctor compaction characteristics

Standard Proctor compaction was carried out on the three types of the studied mixtures (0%, 4% and 6% lime), according to BS 1377 – 4: 1990. In order to obtain a uniform water content within the prepared samples, a minimum mellowing time of 12 hours was used for untreated London Clay samples, and 24 hours for lime treated samples. Three layers of each tested specimen were remoulded inside $104.84mm$ diameter metallic mould; each layer was compacted by the free falling of $2.5Kg$ rammer for 27 blows from $302mm$ height. The same procedure was applied to all three soil types. All the dry densities and water contents of each compacted mixture (0, 4 & 6% lime) are determined and plotted in Figure 4.5.

Lime treatment flattened the compaction curve; it increased the optimum water content and decreased the maximum dry unit weight of the soil. This behaviour was reported for both

lime and cement treated soils (e.g. Bell, (1988) and Sariosseri & Muhunthan, (2009) respectively). The maximum dry density $\rho_{d(\max)}$ and the optimum water content $w_{(opt)}$ for each mixture are presented in Table 4.1.
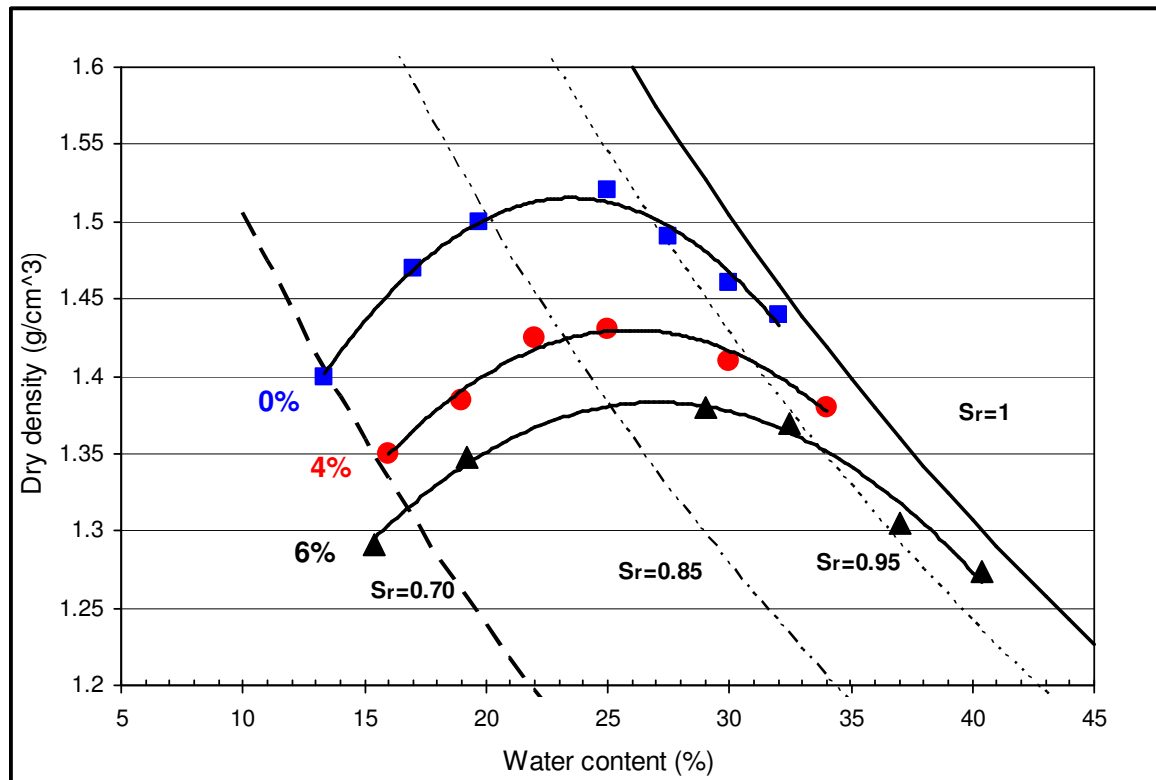
Figure 4.5: Standard Proctor compaction test on lime treated & untreated London Clay

Table 4.1 presents the variation of the main physicochemical characteristics of lime treated and unthread London Clay.

Table 4.1: Lime treated and untreated London Clay main characteristics

Soil type	W_L	W_p	I_p	G_s	$w_{(opt)}$	$\rho_{d(\max)}$
	(%)	(%)	–	–	(%)	(g/cm^3)
London Clay	73.5	26.1	47.4	2.76	25	1.52
+ 4% lime	86.2	50.7	35.5	2.74	27	1.43
+ 6% lime	89.6	53.6	36	2.74	29.5	1.38

4.6. Free swell test

Free swell tests performed as per BS 1377 – 2: 1990 on several lime fractions added to London Clay. Free swell is defined as the increase in volume of soil from loose dry powder form when it is poured into water, expressed as a percentage of the original volume. Soils with free swell values less than 50% are not likely to show expansive properties (Head, 2006). Free swell test on untreated London Clay produced an 80% volume increase, whereas several lime frictions added to London Clay showed a free swelling of approximately 69% and 48% for 4 and 6% lime addition respectively (see Figure 4.6). Therefore, 6% lime addition is considered as sufficient to reduce the swelling capacity of London Clay since it does not exceed the maximum tolerable swelling percentage of 50%.
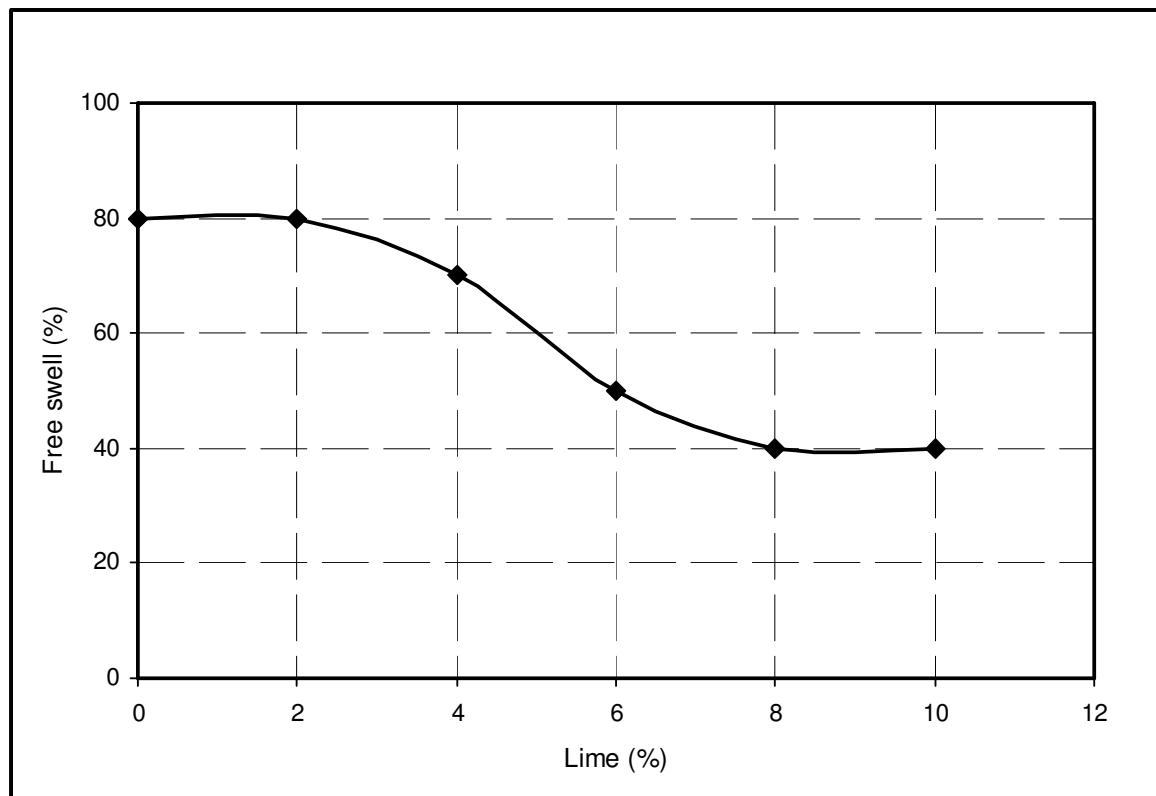
Figure 4.6: Free swell test on lime treated London Clay

The free swell reduction is attributed to the reduction of water absorption capacity of the material used. The lime amount which showed the minimum free swell is 8%. Adding extra lime beyond this percentage did not produce any further swelling reduction.

4.7. Calcium concentration measurements

The free lime which was not consumed during London Clay lime treatment was measured by means of calcium concentration measurements, using a spectrometer (Hitachi Z-8100). The preparation of soil-lime solutions was carried out using 0.5g of dry London Clay mixed with two lime percentages (4 & 6%) by dry soil weight, scattered in 40cc distilled water. The solution was then poured in a glass tube, hermetically sealed to avoid lime carbonation, and finally mechanically rattled. After 1, 7, 28 and 60 days of curing at $20 \pm 1°C$, the solutions were extracted and calcium content was measured. The calcium concentration was converted into lime percentage based on a chart of calcium concentration for pure lime; the absorbed lime during the imposed curing periods for 4 and 6% lime addition is indicated in Table 4.2.

Table 4.2: Consumed lime during the curing period in days

Lime (%)	Curing periods (Days)			
	1	**7**	**28**	**60**
	Consumed lime content (%) / **Represented percentage from total lime**			
0	N/A	N/A	N/A	N/A
4	3.1 / **(77.5%)**	3.3 / **(82.5%)**	3.4 / **(85%)**	3.5 / **(87.5%)**
6	4.7 / **(78.5%)**	5.1 / **(85%)**	5.3 / **(88.5%)**	5.4 / **(90%)**

The consumed lime content after one day curing for 4% lime addition is shown to be 3.1%. Additional lime was then consumed but at a much slower rate. The higher the lime addition, the bigger the difference in lime consumption is observed. After 28 days the consumption reached 3.4% for an addition of 4% lime, which represents 85% of the total lime amount. For 6% lime the consumption was 5.3% (88.5% of the total lime content) during 28 days curing. However, a very small further amount of lime was consumed between 28 and 60 days. Fig. 4.7 shows a similarity in lime consumption rate increase from 1 to 60 days curing; an almost identical trend for both 4 and 6% lime addition is observed.
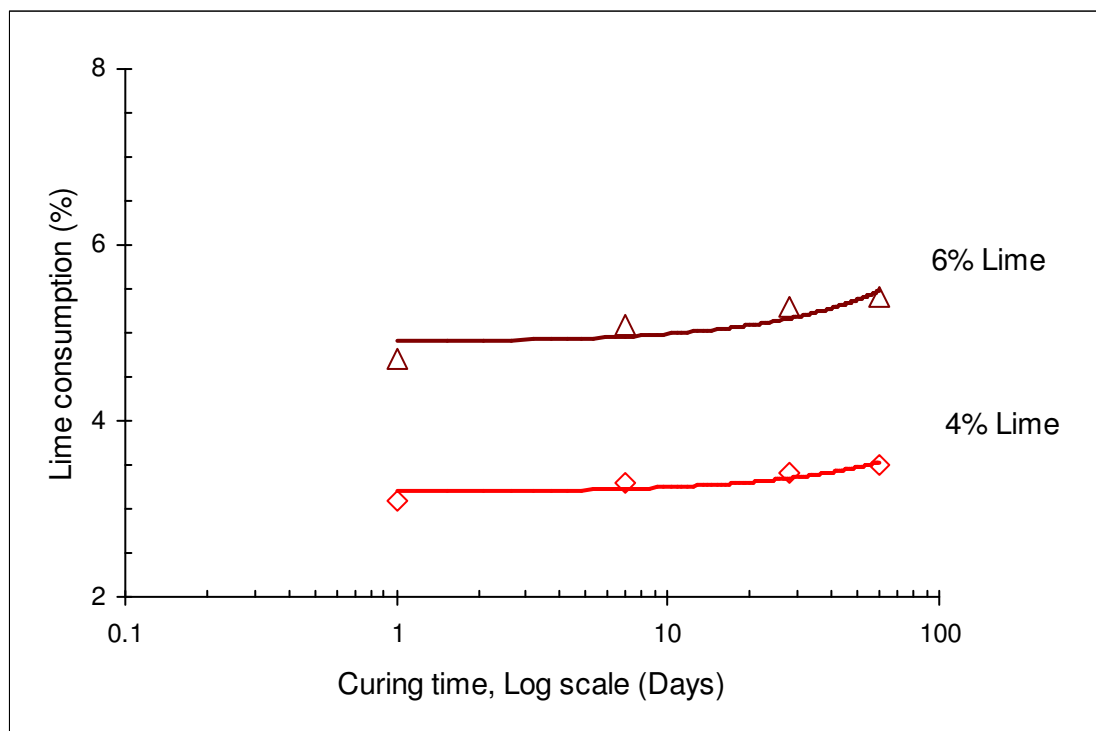
Figure 4.7: Evolution of lime consumption with curing time

4.8.   pH evolution in lime treated London Clay with curing time

The dissolution of clay minerals is highly dependent on pH level. Figure 4.8 shows the pH values of lime treated London Clay decreasing with curing time. Up on lime addition the pH values increased to 12.4 for 4% lime and 12.5 for 6% lime as observed during the ICL test (see Fig. 4.2); subsequently they started decreasing with curing time. A fast pH decrease to reach a value equal to 12 is observed between 1 and 7 days of curing for 4% lime treated sample. In later times the 4% lime treated sample maintained a sufficiently high pH level (>10) but lower than the 6% lime treated specimen which had a pH value just below 12.4 after 28 days curing. This is still a very high pH value ensuring the successful production of pozzolanic reactions, further strengthening the choice of 28 days as the minimum required curing time for 6 % lime treated London Clay samples.

Figure 4.9 shows the trend for the remaining lime and pH value with curing time up to 60 days for both 4 and 6% lime addition, they appear to follow similar decreasing rate. A decrease in the available lime reflects a pH decrease with curing time as it would be expected due to the use of calcium in chemical reactions.
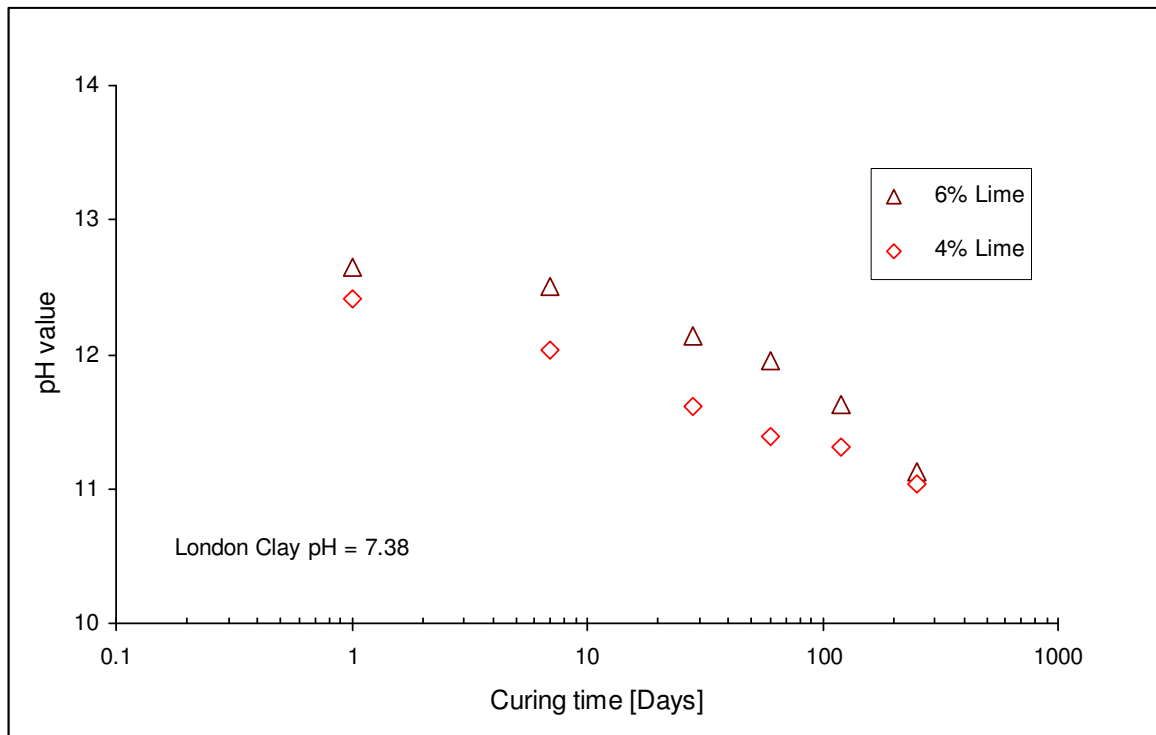
Figure 4.8: pH evolution with curing time of compacted lime treated London Clay
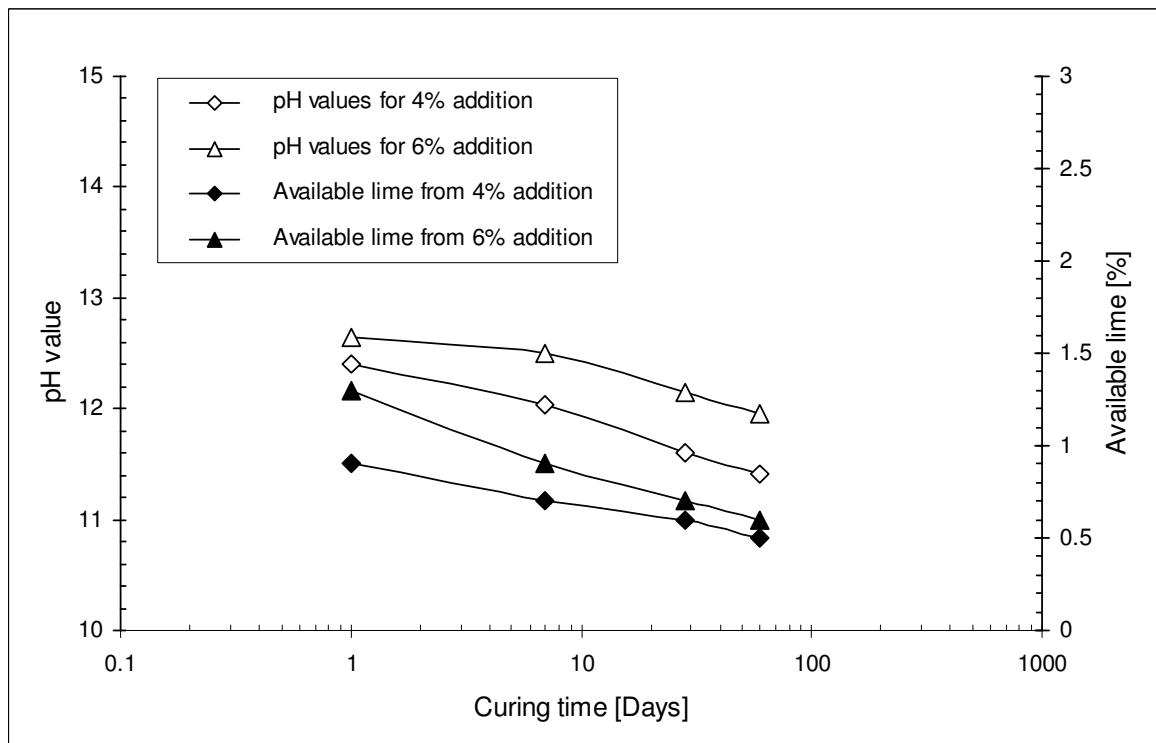
Figure 4.9: pH evolution and the available lime variation with curing time of compacted lime treated London Clay

4.9. X-Ray Diffraction test (XRD)

In order to identify the phase compositions and mineralogy modifications related to the effect of lime addition to London Clay, X-Ray diffraction (XRD) was performed on selected specimens using a Bruker D2 Phaser diffractometer (Figure 4.10). The method is based on the principle that for a given X-Ray emitted source with a wavelength $\lambda = 1.5406 \text{Å}$, the scanning along an angle (θ) between 10 and 60° allows the identification of all spacing (d) of the material (d-spacing is a fixed perpendicular separation between each plane, also called interplanar spacing). Data were analysed using $Bruc\,\text{ker}\ DIFFRAC^{plus}\ EVA$ software.
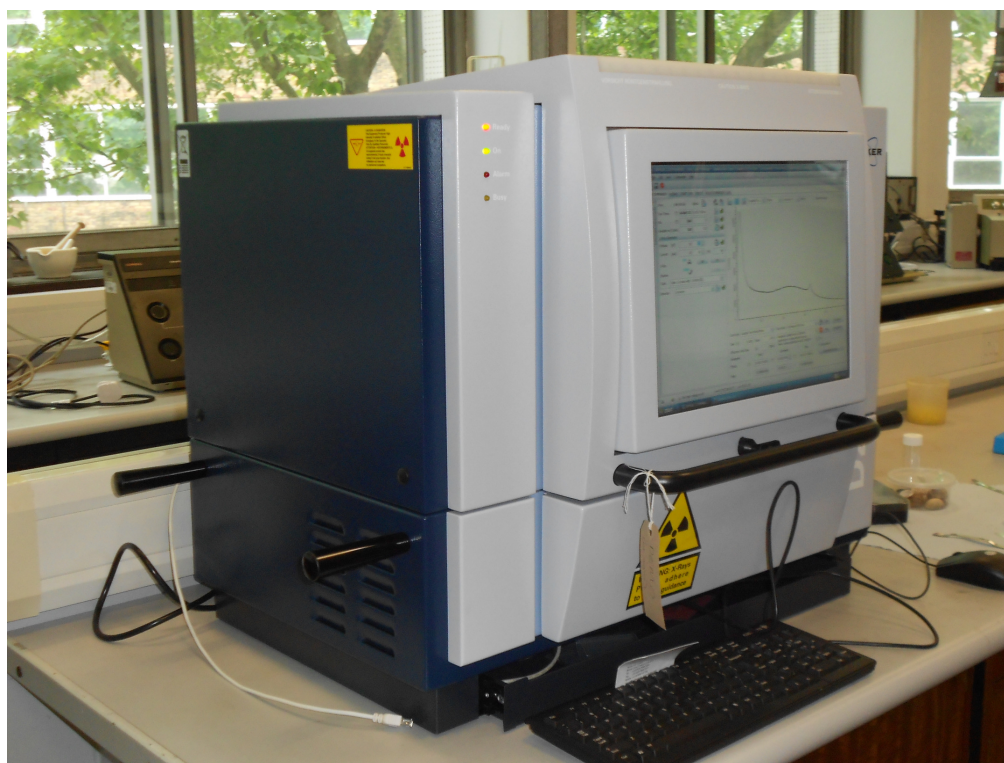
Figure 4.10: X-Ray diffractometer (Bruker D2 Phaser)

The study was carried out on pulverised untreated & lime treated London Clay samples. Two lime percentages (4 & 6%) and different curing periods (1, 7, 28 and 60 days) at a moderate temperature (20 - 22 °C) were used. The choice of different curing times allows the study of the mineralogy evolution affected by lime treatment. 60 days being the highest period here was identified as reasonable curing time where sufficient pozzolanic reaction

development has occurred (see Chapter 5 / section 5.2.1). All powder samples were prepared by manual grinding of the cured specimen (after air drying) in a porcelain mortar using a pestle.

4.9.1. Mineralogy evolution of lime treated London Clay

Figure 4.11 presents the untreated London Clay diffraction, indicating the clay mineral peaks such as Illite (I) at an angle (2θ=19.7; 24,9; 34.8 and 45.7°) and Kaolinite (K) at (2θ=12.3 and 54.7°), as well as non clay minerals such as goethite (g) at (2θ=36.5°), feldspar (F) at (2θ=27.4 and 42.3°) and quartz (Q) at (2θ=20.7; 26.5; 39.4 and 50°). In addition, the presence of gypsum (G) is identified at an angle 2θ= 11.56° and d spacing equal to 7.68Å. The base line intensity of London Clay is used as a reference to compare the different diffractions obtained during the XRD tests performed on lime treated London Clay samples.

Figures 4.12 & 4.13 present all the diffractions of lime treated London Clay at different curing periods. The investigation of lime-clay reaction evolution is easily identified on the highest lime percentage (6%) by the changes observed with the curing periods (new phases appearing, and potential clay minerals destruction). The diffractions show diminishing reflexions at 2θ=37.05° indicating that lime is consumed with curing time increase. Similar decreasing peak reflexion is observed at 2θ= 54.03° but at lower intensity. In addition, the gypsum initially identified in London Clay sample is observed to gradually disappear from the first day of curing period as shown for 4% lime treated London Clay (Figure 4.12) as well as for 6% lime treated samples (Figure 4.13) at a similar curing time. A peak at an angle 2θ= 15.7° in the lime treated London Clay is identified as Ettringite. The presence of this peak while the gypsum disappeared illustrates that it has been rapidly consumed at early age to form the new mineral, but the XRD patterns shown in Figures 4.12 & 4.13 do not indicate a large amount of ettringite formed (hence sulphate induced risk would be low), probably due to low gypsum content identified in London Clay sample (1.2%). This is consistent with the sulphate content test presented earlier on London Clay which indicated a negligible amount of soluble sulphate.

The pozzolanic reactions between lime and clay minerals occur and progress gradually with curing time as indicated in the XRD analysis, producing some calcium silicate hydrate

(CSH) in the form of $Ca_3HO_9Si_3$. This hydrate crystallises with time (one reflexion is observed in 4% lime treatment at 7 day curing, progressing to two as from 28 days curing). In addition, a Calcium Aluminate Hydrate (CAH) in the form of $Al_2Ca_3H_{12}O_{12}$ is shown to start forming as early as the 7th day of curing at $2\theta = 32.1°$ at a low intensity increase with curing time.

For a higher lime addition (6%), the diffraction pattern shows some clearer CSH peaks, and a higher reflexion number (4 reflexions observed) at higher intensity than the ones observed in 4% lime treatment. This new compound rapidly formed in the presence of higher lime amount (more calcium as indicated in section 4.7). It started appearing as from 7th day of curing period. Although not at significant intensity, these reflexions appear to increase with curing time indicating that a higher number of cementation bonds formed at higher curing periods. In addition, a CAH phase also formed for 6% lime treatment, at an angle $2\theta = 32.08°$, but detected at an earlier age (7 days) compared to the 4% lime treated sample. Another reaction was detected at a longer curing period (60 days). This reaction resulted in the formation of Calcium Silico-Alumina Hydrate (CSAH) which appeared at an angle of $2\theta = 13.44°$ in the form of $Al_{2.11}Ca_2H_{18}O_{16.25}Si_{1.11}$.
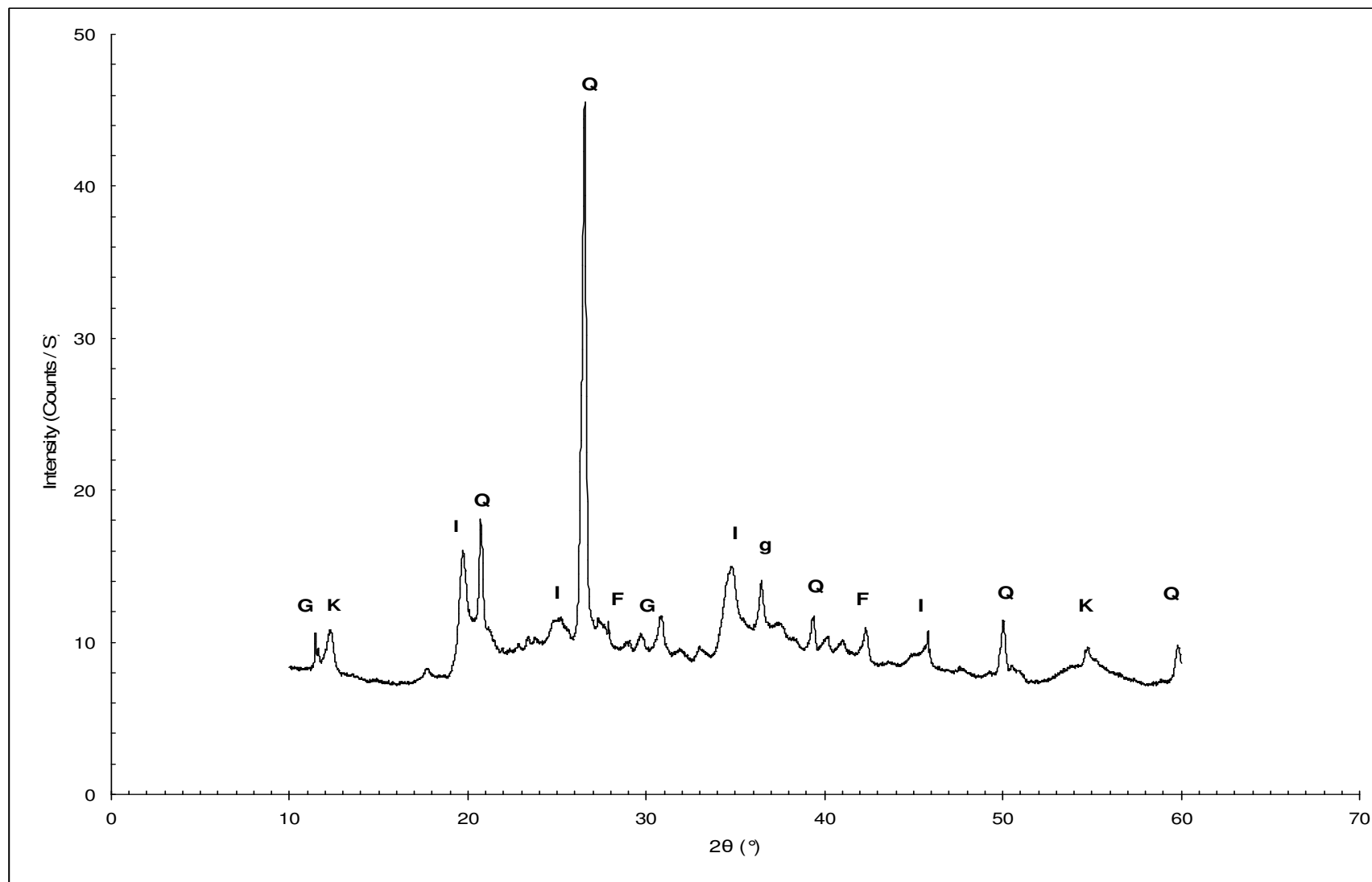
Figure 4.11: X-Ray diffraction of untreated London Clay / Illite (I), Kaolinite (K), goethite (g), Feldspar (F), Quartz (Q) and Gypsum (G)
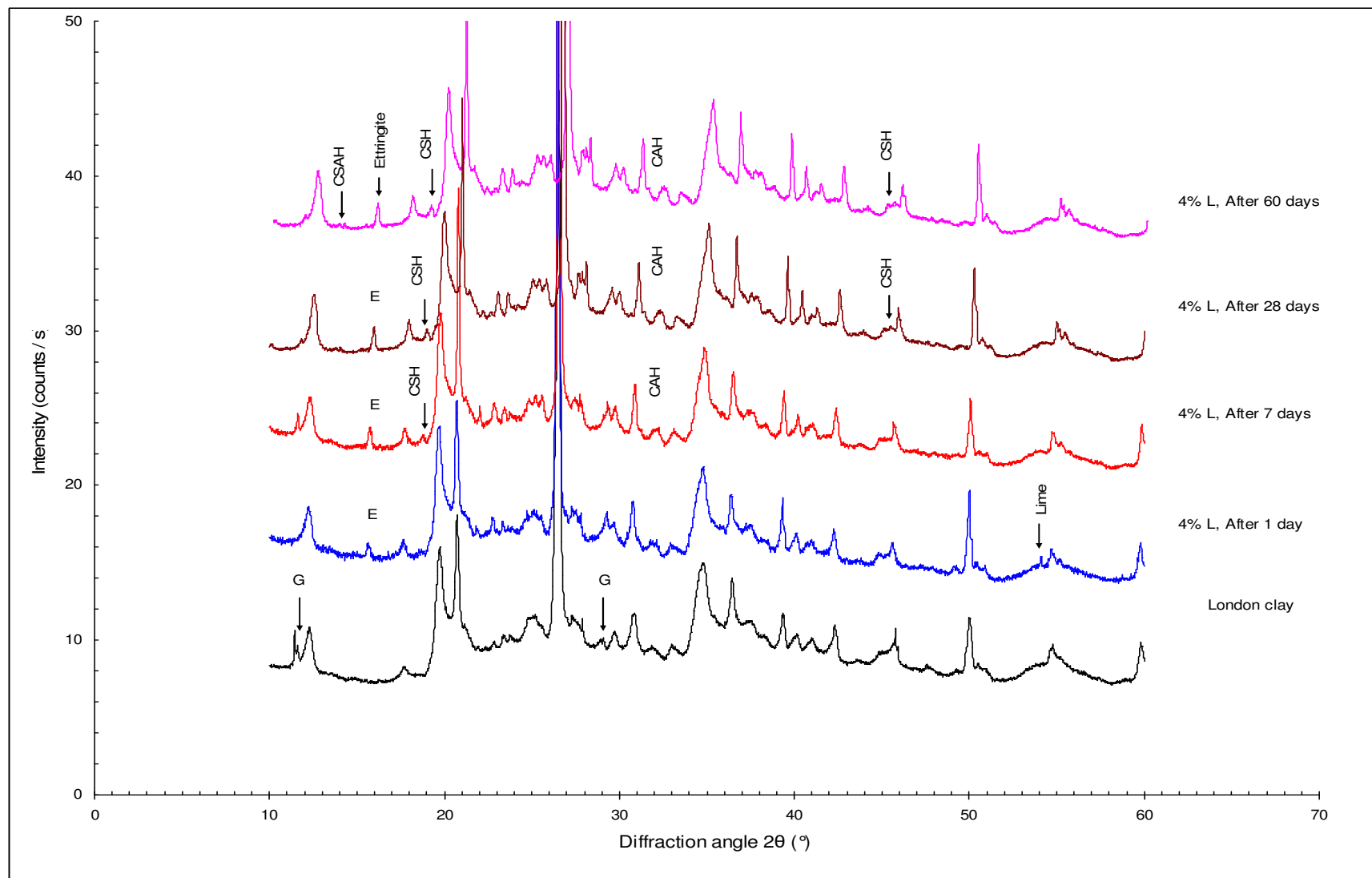
Figure 4.12: X-Ray diffraction on 4 % lime treated London Clay
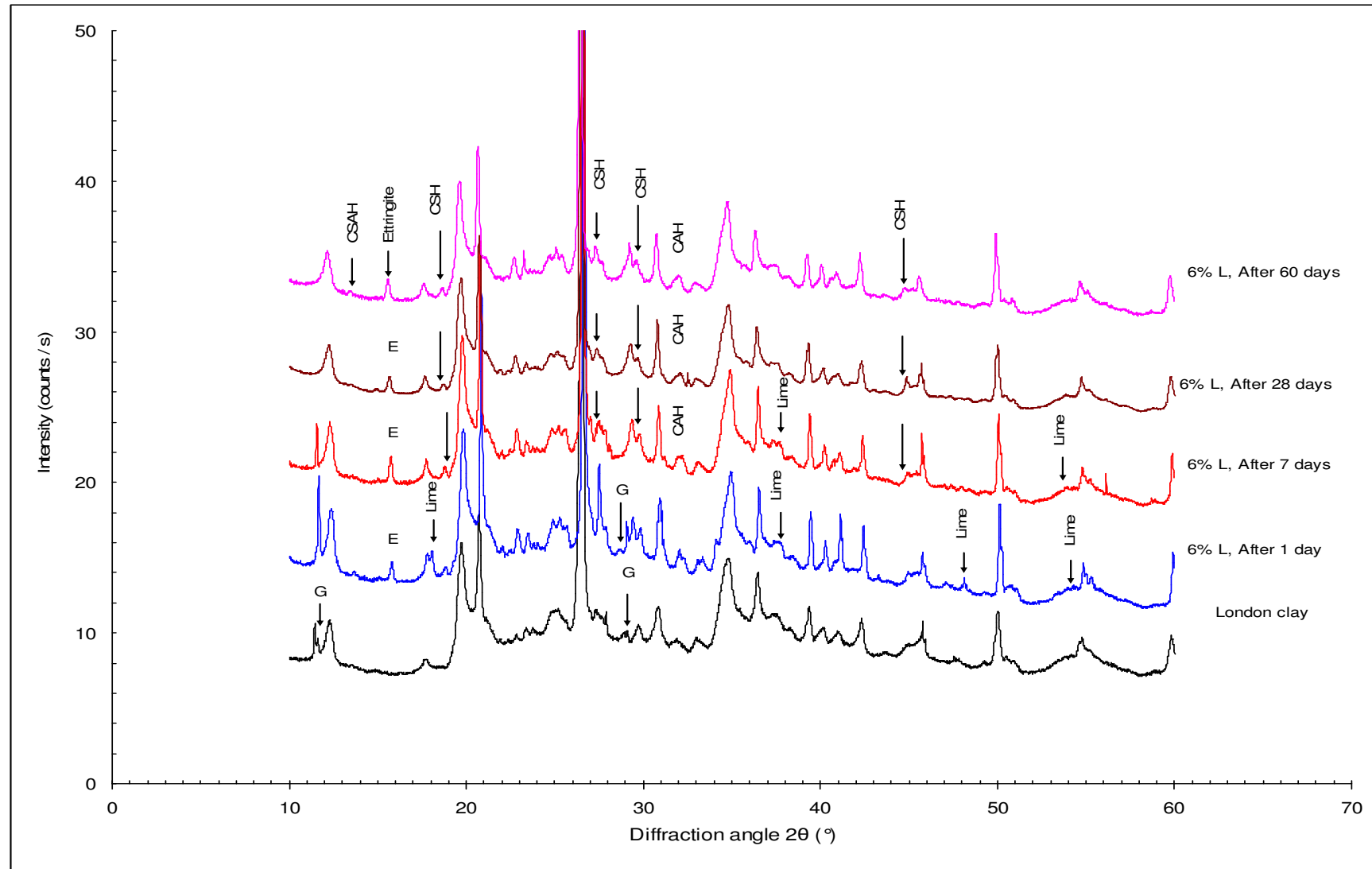
Figure 4.13: X-Ray diffraction on 6 % lime treated London Clay

From the above observations of the XRD patterns it can be concluded that already at early curing times (7 days), the effect of a higher lime amount on the quantity of hydrates is visible. The intensity of these hydrates is also observed to increase with curing period at slightly faster rate for 6% compared to that of the 4% lime addition. Although the peaks are small due to the quantity of free lime available, it is observed that lime consumption increases with the amount of lime added and the curing time increase, which is in agreement with the lime consumption reported in section 4.7. Similar findings were reported by a number of other researchers (Eades & Grim, 1960; Clara & Handy, 1963; Ormnsby & Kinter, 1973; Cabrera & Nwakenma, 1979; Arabi & Wild, 1986; Wild et al., 1986; Locat et al., 1990; Locat et al., 1996; Bell, 1996; Rajasekaran & Narasimha Rao, 1997; Khattab, 2002).

For the 4% lime, the limited lime amount available was mostly consumed at early curing times by cation exchange during the short term reactions. This is in agreement with the results of calcium concentration percentage indicated in section 4.7. Thus a limited amount of pozzolanic reactions occur, generating a low hydrates production. The newly formed reflexions are of a low intensity and are in some cases not easily detectable by the XRD diffractometer.

Chapter 5

5. Triaxial test results, presentation and discussion

5.1. Introduction

The chapter presents in detail the results of Undrained Unconsolidated (UU), Consolidated Drained (CD) and Consolidated Undrained (CU) Triaxial tests performed on lime treated and untreated London Clay samples. The effects of lime addition, curing time and the initial water content on London Clay yielding behaviour and shear strength are comprehensively studied. An attempt to explain the formation and the breakage of the cementation bonds phenomena is also made.

Presentation and discussion of the triaxial compression tests results under saturated conditions, is based on stress-strain $(q - \varepsilon_a)$, volumetric strain-axial strain $(\varepsilon_v - \varepsilon_a)$, pore water pressure and effective stress paths plots. The mechanical behaviour of lime treated and untreated London Clay are compared. The dilation of the lime treated specimens is also examined and discussed. This considers the effect of effective confining pressure, lime amount, curing time and the initial water content on the stress-dilatancy behaviour of the soil.

5.2. Unconsolidated undrained (UU) Triaxial tests

5.2.1. Stress-strain response and strength development

Initially, the strength of lime treated and untreated London Clay samples was assessed by means of series of Unconsolidated Undrained (UU) triaxial compression tests at as compacted conditions. In these series of experiments, two lime dosages and a variation of curing times are considered. Curing time is defined as the duration elapsed from the end of static compaction to the beginning of the testing. These tests are principally significant for control purposes and as an indicator of strength evolution. Figures 5.1 (a & b) show the stress strain curves from the UU triaxial tests performed at a 200 kPa confining pressure.

The lime treated London Clay samples were cured for periods of 1 to 250 days and labelled accordingly as 1D, 7D, 28D etc (1D being 1-day curing, 7D for 7 days curing etc) on the figures. In these figures, the deviator stress - axial strain relationship shows the strength evolution with curing time.

From the figures it can be seen that the axial strain at peak deviator stress (q_{uu}) ranged from 1.5 to 4%. Most lime treated London Clay specimens failed by single slip line, while others failed by displaying multiple surfaces in different directions as shown in Figure 5.2. The untreated London Clay presented a ductile behaviour with a deviator stress levelling at high strains. At earlier curing times 4% lime treated London Clay specimen manifested a similar ductile behaviour, with the post-peak stress gradually decreasing to reach a constant low deviator stress at a value close to the one produced by the untreated London Clay specimen. At a higher lime content (6%), the treated specimen shearing behaviour (except for the 1 day cured sample) became much more brittle with an abrupt loss in strength in the post-peak stress zone. This is similar to the behaviour of heavily over-consolidated or highly structured natural soils (Leroueil & Vaughan, 1990). The brittleness and the sudden stress drop in the post peak region is also observed to be more pronounced for longer curing periods as indicated in Figure 5.1 (a & b).

Although results of this part of the study are associated with UU tests rather than the Unconfined Compressive Strength (UCS) tests usually reported in the literature, the observed undrained strength behaviour is consistent with the UCS testing results of many other researchers' work on lime treated clay soils (e.g. Bell, 1989 & 1996; Osinubi, 1998a & 1998b; Arabani et al., 2005; Al-Mukhtar et al., 2010).
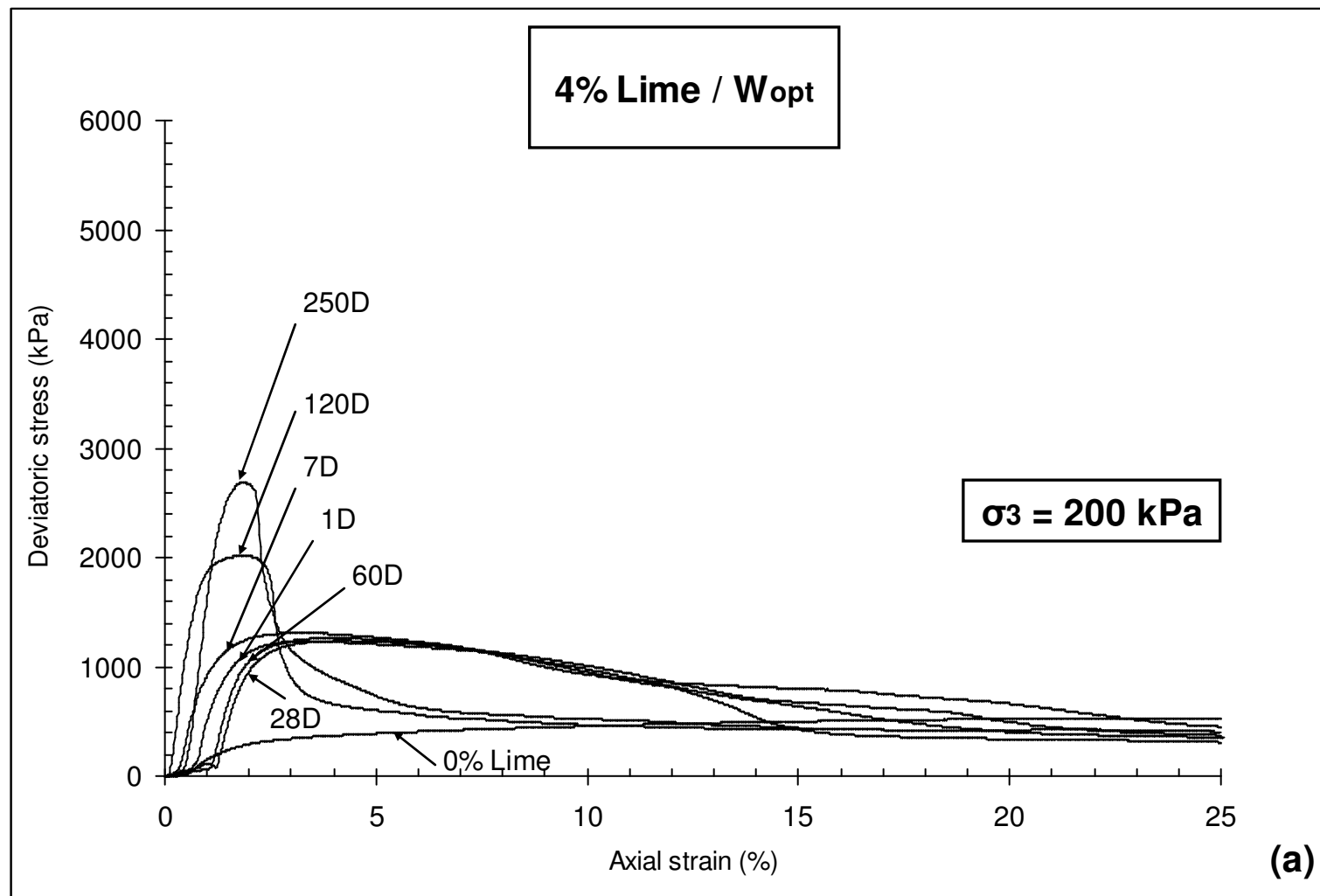
Figure 5.1 (a): UU Triaxial compression tests on 4% lime treated London Clay (200 kPa confining pressure).
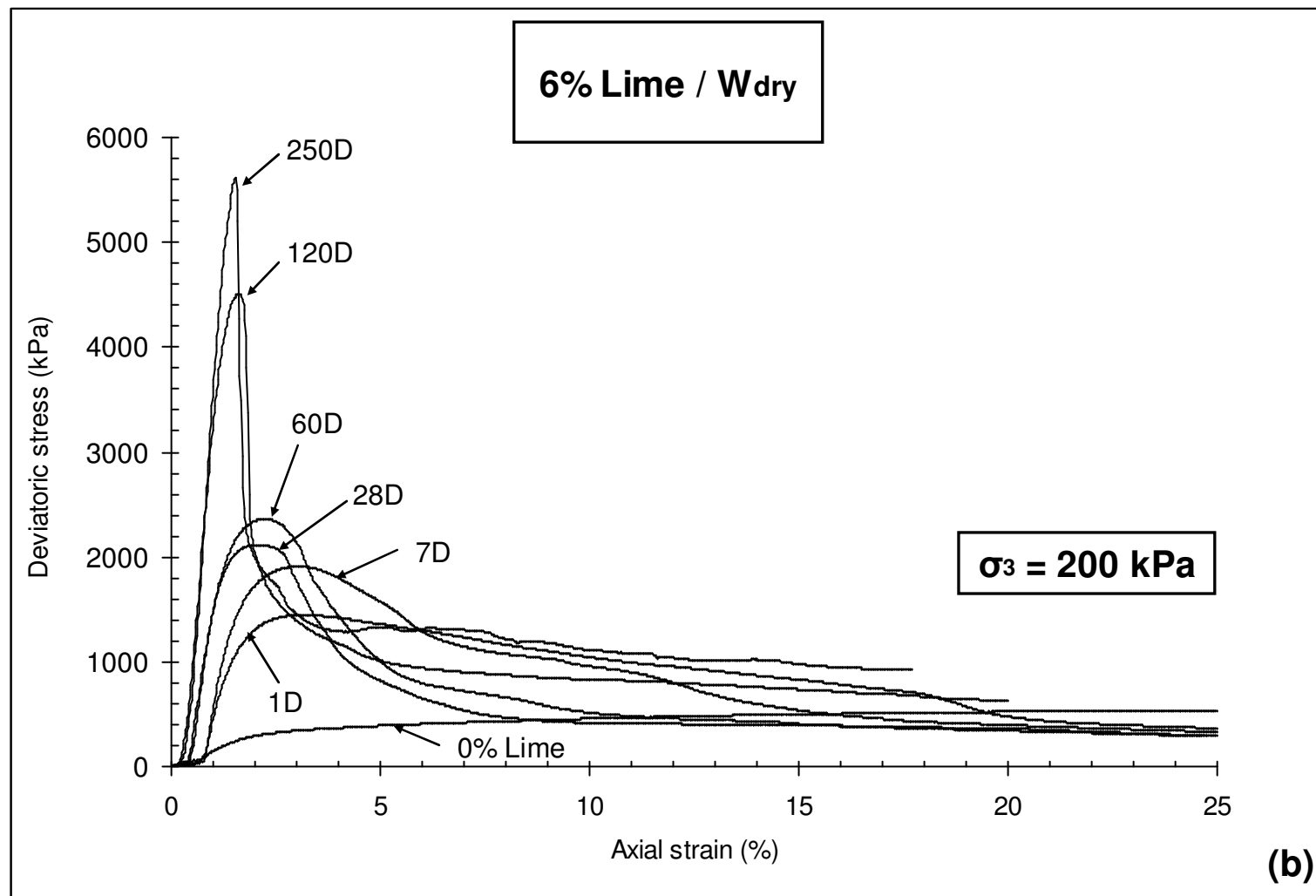
Figure 5.1 (b): UU Triaxial compression tests on 6% lime treated London Clay (200 kPa confining pressure).

The shear behaviour of lime treated London Clay up to the peak state, depends largely on the cementation products formed during the curing time (this is better explained through XRD tests in Chapter 4).

Figure 5.2: Failure type of untreated and lime treated London Clay samples in UU Triaxial tests (Sheared as cured)

To better illustrate the effect of different factors considered, Fig. 5.3 presents peak deviator stress evolution with curing time for 4 & 6% lime treated and untreated London Clay samples. No clear pattern of change that relates to curing time or the initial water content for 6% lime treatment is observed. However, the results obtained show some variability

with respect to strength development, and suggest that higher lime addition induces a higher strength gain. This is in agreement with findings reported by a number of other researchers (e.g. Bell, 1996; Rajasekaran & Narasimha Rao, 1997; Al- Mukhtar et al., 2010). In addition, the curing time evolution is found to be consistent with the work presented by Dumbleton, (1962) on 10% lime treated London Clay; his UCS test results showed a similar trend of strength evolution with curing time as the present work. Similar trends of strength increase with curing time were also observed in other studies. (e.g. Ahnberg & Johanson, 2005; Al-Mukhtar et al., 2010; Dash & Hussain, 2012) performed on different soils.

Moreover, Figure 5.3 indicates that varying the initial water content while keeping the same dry density has a minor influence on lime treated London Clay strength (up to 28 days curing) similar findings were reported by Consoli et al. (2009). However, at later curing times, the 6% lime treated specimens' compacted to wet of optimum $\left(w_{wet}\right)$ display a higher strength than similar specimens prepared to dry of optimum $\left(w_{dry}\right)$.
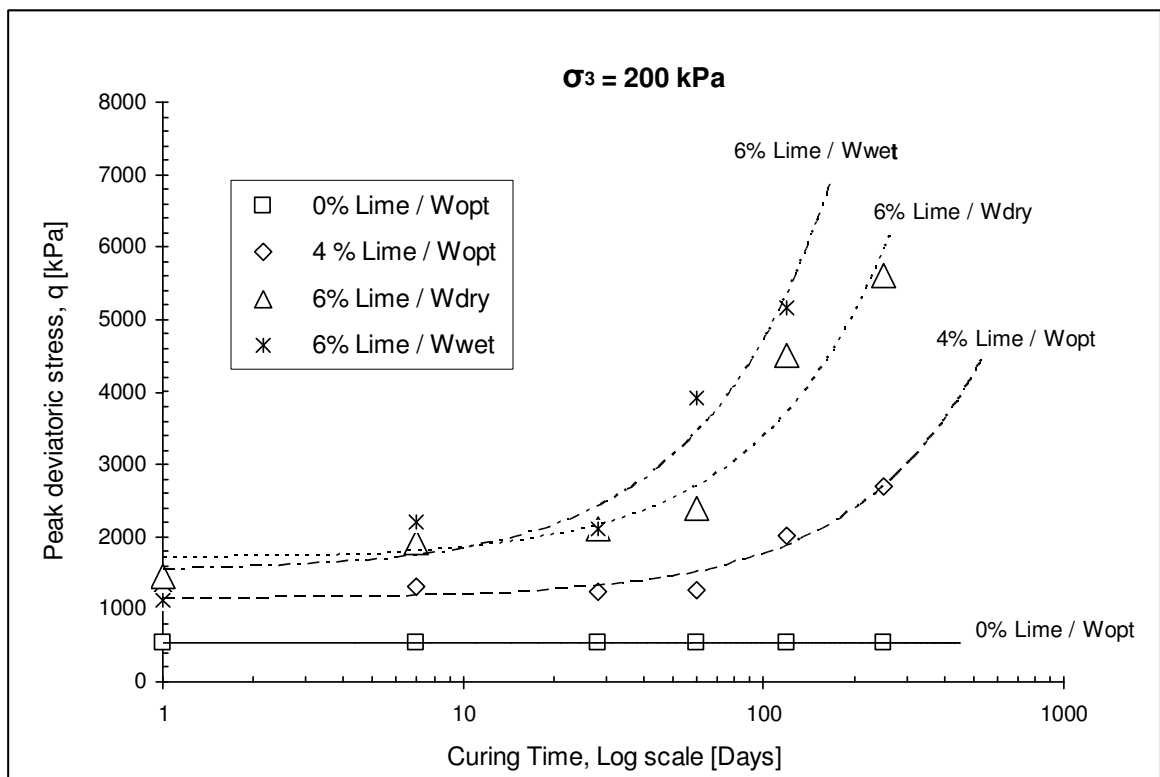
Figure 5.3: Curing time & initial water content effect on lime treated London clay strength

In the literature, no boundaries are clearly defined between strength gain due to "Modification" and that due to "Stabilisation". While no figures are available, Sherwood (1993) suggests that "Modification" is associated with at least a three-fold increase in strength improvement. Therefore to acquire a clearer picture of the strength evolution with curing time and its likely causes, the results of Figure 5.3 are plotted again in two separate graphs (Fig. 5.4(a) and (b) for the 4% and 6% lime-treated soils respectively), with the strength gain marked. From Figure 5.4(a) it can be seen that for the 4% lime-treated, cured for 7 days there is a 145% strength increase compared to that of the untreated soil (2.45 times). This is approximately half of the three-fold strength gain, which Sherwood (1993) attributes to modification rather than stabilisation reactions. It can then be noted that there is no further strength gain up and to 60 days curing. This is consistent with the XRD results which show no considerable differences in the treated soil spectra between 7 and 60 days. Any reaction products appear to have been produced within the first 7 days of treatment which is consistent with the usual short-term timelines suggested for modification reactions in the literature. A further supporting evidence is provided from the evolution of the calcium consumption of the 4% lime-treated soil which shows very little evolution after 1 day. All these results would consistently converge towards the conclusion that 4% lime was not sufficient to produce long-term pozzolanic reactions. It is however, surprising to see that in much later curing times there is a remarkable increase in strength. As there are no XRD (or lime consumption) results for these curing periods it is not possible to attribute this delayed strength gain on the possible formation of potential pozzolanic reaction products. However, it should be noted that the pH of the soil showed considerable decrease between 60-120 days of curing, which potentially implies some further reactions. Although there is not enough evidence to interpret the sharp increase in strength at later curing times, it should be pointed out that similar results were shown in Sherwood (1993) for London Clay treated with 10% lime (see Fig. 5.5). The strength magnitudes shown in Sherwood (1993) were different to the ones presented here (possibly due to sample preparation and testing procedures) but the trends were similar.
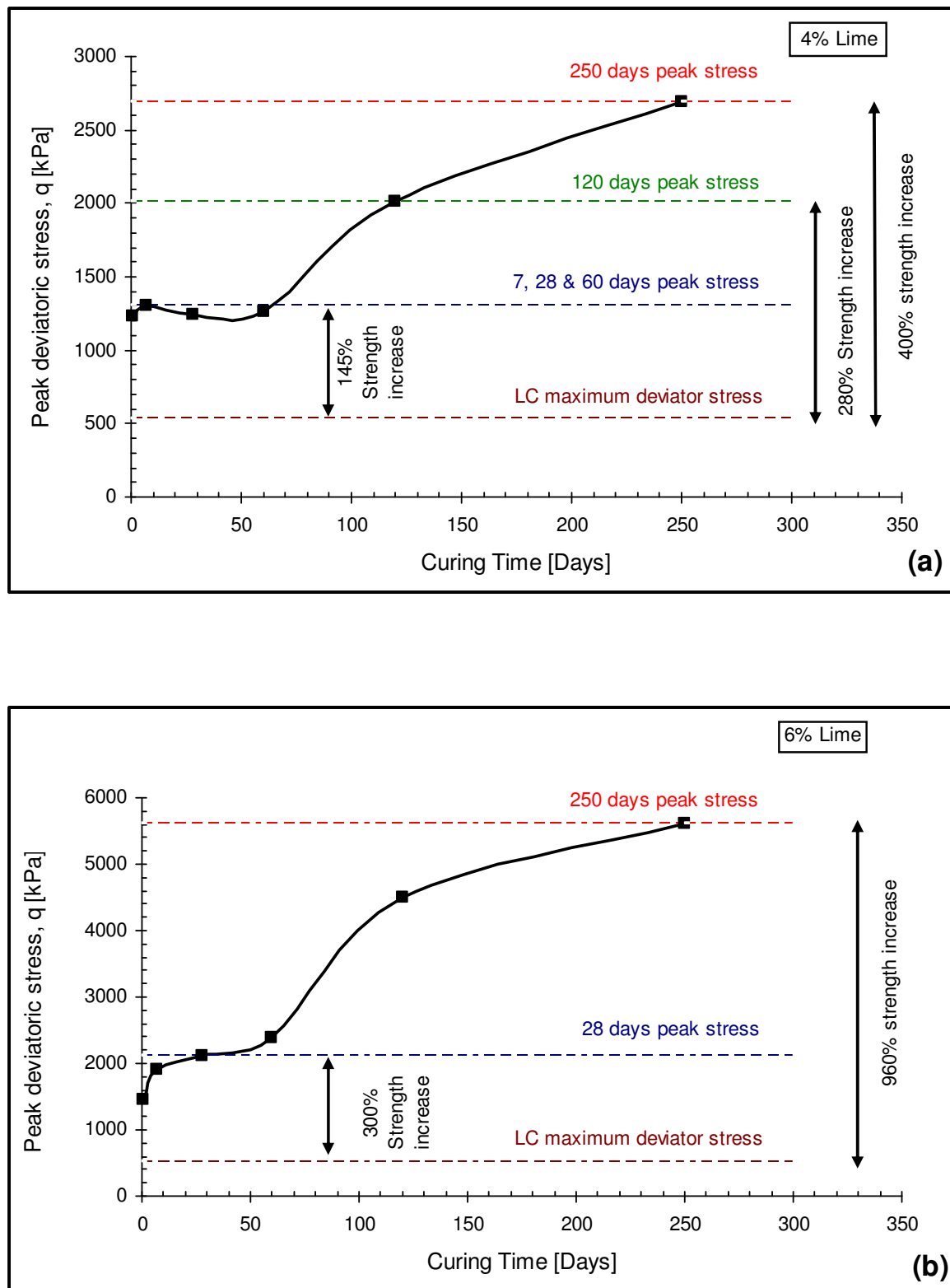
Figure 5.4: Strength evolution of lime-treated London Clay with curing time. (a) 4% lime, (b) 6% lime.
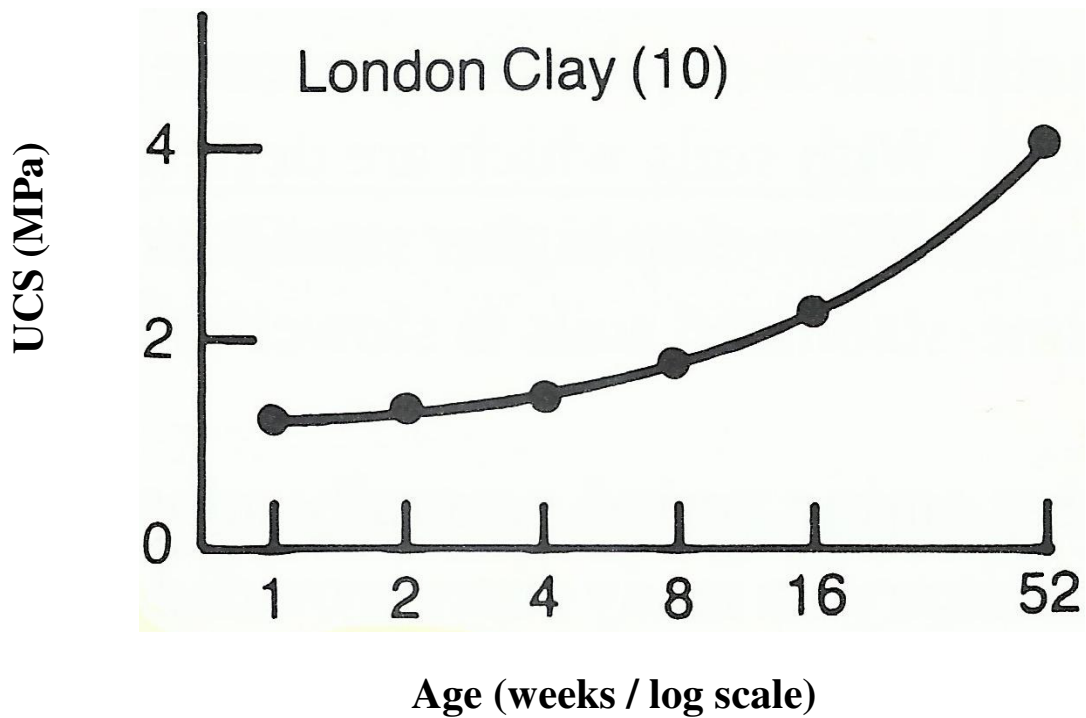
Figure 5.5: Relationship between unconfined compressive strength and curing time
(Sherwood, 1993)

Comparing Figure 5.4(a) to Figure 5.4(b) it can be seen that all 6% lime-treated specimens (irrespective of moisture content) showed much higher strength than those achieved by the 4% lime treated one, and a continuous strength gain in time, after the beginning of curing. Within 28 days of curing this amounted to 300% strength gain, approximately, compared to that of the untreated soil; the strength gain continued with time and showed again a sharp increase as did the strength of the 4% lime-treated soil after 60 days of curing, to reach a strength gain of about 960% compared to that of the untreated soil, after 250 days curing. The higher and continuous strength gain of the 6% lime cured soil compared to that of the 4% lime treated soil (which showed a lower and almost constant strength between 7 and 60 days of curing) is consistent with the XRD results reported in Chapter 4 which showed clear peaks corresponding to CAH and CSH already after 7 days of curing (these were also noted for 4% lime treated soil) and the formation of additional cementitious products (CSAH) after 60 days of curing. There is also more available lime for reactions and its consumption was shown to continue at a higher rate compared to the 4% lime-treated soil (see Fig. 5.6). Beyond 60 days of curing there is again no further evidence from XRD or calcium concentration measurements to support the interpretation of strength increase. It is however reasonable to assume that due to the higher amount of available

lime, pozzolanic reactions in the 6% lime-treated soil continued for longer curing times as evidenced by many authors (Brandl, 1981; Sherwood, 1993; Rogers & Glendenning, 2000; Boardman et al., 2001; Rao & Shivananda, 2005(a) and Al-Mukhtar et al., 2010) which resulted in the observed strength gains. This interpretation is also consistent with the pH measurements shown in Figure 4.8 (Chapter 4).
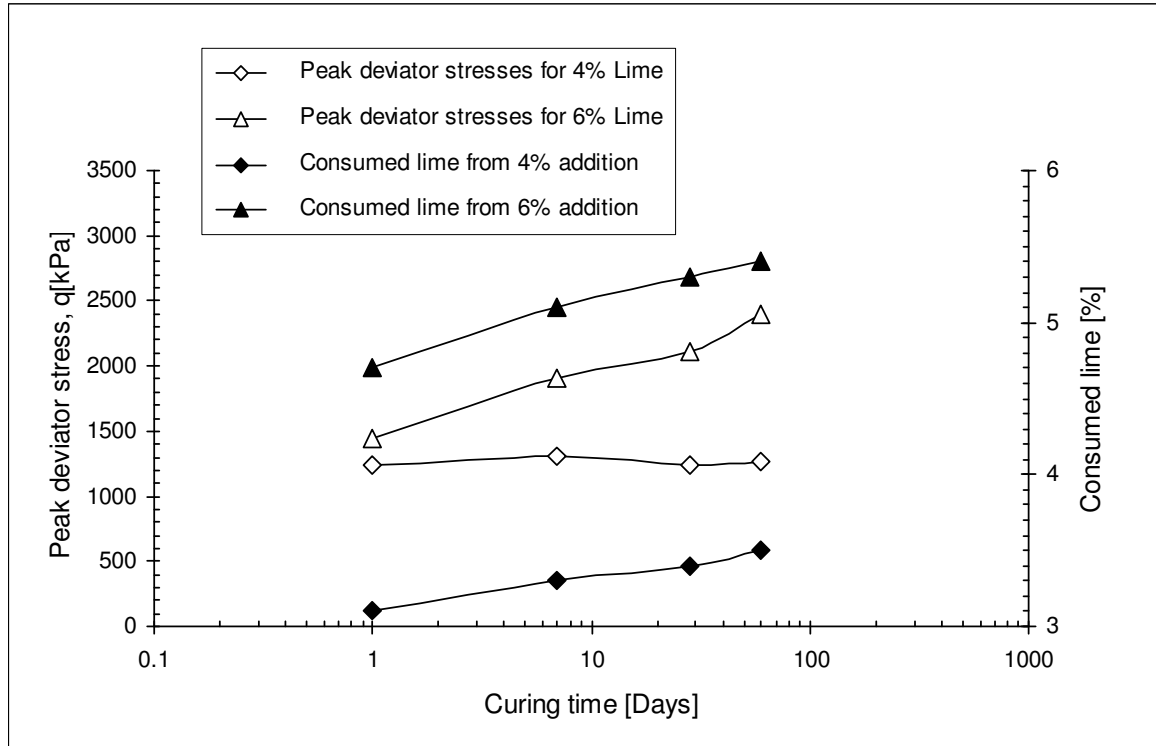
Figure 5.6: Correlation between mechanical performances and lime consumption at different curing time.

Thus, it was decided that the majority of subsequent tests would use 6% lime at 28 days curing to ensure adequate pozzolanic activity based on the results of XRD analysis that had indicated commencement of pozzolanic activity after 7 days curing. Nevertheless, for comparison purposes, samples prepared with 4% lime cured for 7 days were also included in the triaxial testing programme.

5.3. Isotropic compression (IC) triaxial tests

5.3.1. Introduction

The safety of the structure is influenced by the soil compressibility as much as by the shear strength. However, only few studies have been performed to investigate the impact of lime treatment on the compressibility behaviour of clay soils (Rao and Shivananda, 2005a). For this reason, isotropic compression tests on 4% lime treated (cured for 7 days) and untreated London Clay samples were performed in the IC system. However, due to the lack of multiple available triaxial testing equipment and the limitations of the apparatus the 6% lime treated soils were not performed. The isotropic compression behaviour of saturated lime treated and untreated soil is presented from a range of initial specific volumes (v).

5.3.2. Isotropic compression response of saturated lime treated London Clay

Untreated London Clay samples were compacted to an equivalent degree of saturation $s_r = 0.80$, and an initial void ratio $e_i = 0.936$, whereas for 4% lime treated London Clay samples, they were compacted to an approximate degree of saturation $s_r = 0.74$, and a void ratio equal to $e_i = 0.916$. Although, lime treated and untreated specimens were compacted to similar dry density, their corresponding void ratio is different due to the difference in specific gravity of 2.74 and 2.76 for treated and untreated soil respectively. Prior to performing the isotropic consolidation tests, lime treated and untreated London Clay specimens were saturated under a similar mean effective stress equal to $20kPa$. The saturation process for lime treated specimen results in a volume increase varying between 8 and 12% of the initial (as cured) volume. This is due to the amount of water absorbed by the treated sample. This observed volume increase may have an impact on the bonding particles, consequently affecting the compression response, depending on lime amount and the curing period.

The isotropic compression curves are summarised in the semi logarithmic compression plane $(v - p')$ (Figure 5.7). However, due to the limitation of the equipment in terms of achievable pressures, it was difficult to obtain data for the compression behaviour of the lime treated soil. Some data based on a limited range of pressures are presented in Figure

5.7. These show that the lime treated soil achieve states far beyond the NCL of the untreated soil, which was the expected behaviour of a cemented soil. There is some indication of the start of yield for the 4% lime treated specimen at approximately $153kPa$. However, as shown in Rao and Shivananda (2005a) (see Chapter 2) this point would most likely not correspond to the yield stress where complete breakage of bonds occur and probably the actual parameter λ_{iso} may not be obtainable within the range of the presented results. The value of λ_{iso} shown in Table 5.1 for the 4% lime treated soil is thus given with some reservation as it may correspond to an early stage of cementation bonding breakage, beyond which the slope of the graph could change further until the post yield zone is clearly identified. It is however possible that the extend of the zone of progressive bond breakage and hence the changes in the compressibility parameter may be small for the 4% lime treated soil due to the limited amount cementitious products observed. Either way no firm conclusion can be given.

Values of compressibility parameters λ_{iso}, and N obtained from the post-yielding linear lines (for 0 and 4% lime), and values of the elastic swelling parameter κ obtained in the pre-yielding range for lime treated and untreated London Clay, as well as the identified pre-consolidation pressure at which the specimen starts yielding are presented in Table 5.1. These parameters are fundamental for the development of constitutive models. Note that the gradient of the line λ_{iso}, and the intercept of the NCL " N " at $p'=1kPa$ are obtained through the regression analysis performed on the saturated normal compression lines. Similar regression analysis on the elastic pre-yielding line (0 and 4% lime) provides the swelling parameter κ representing the slope of the elastic line.
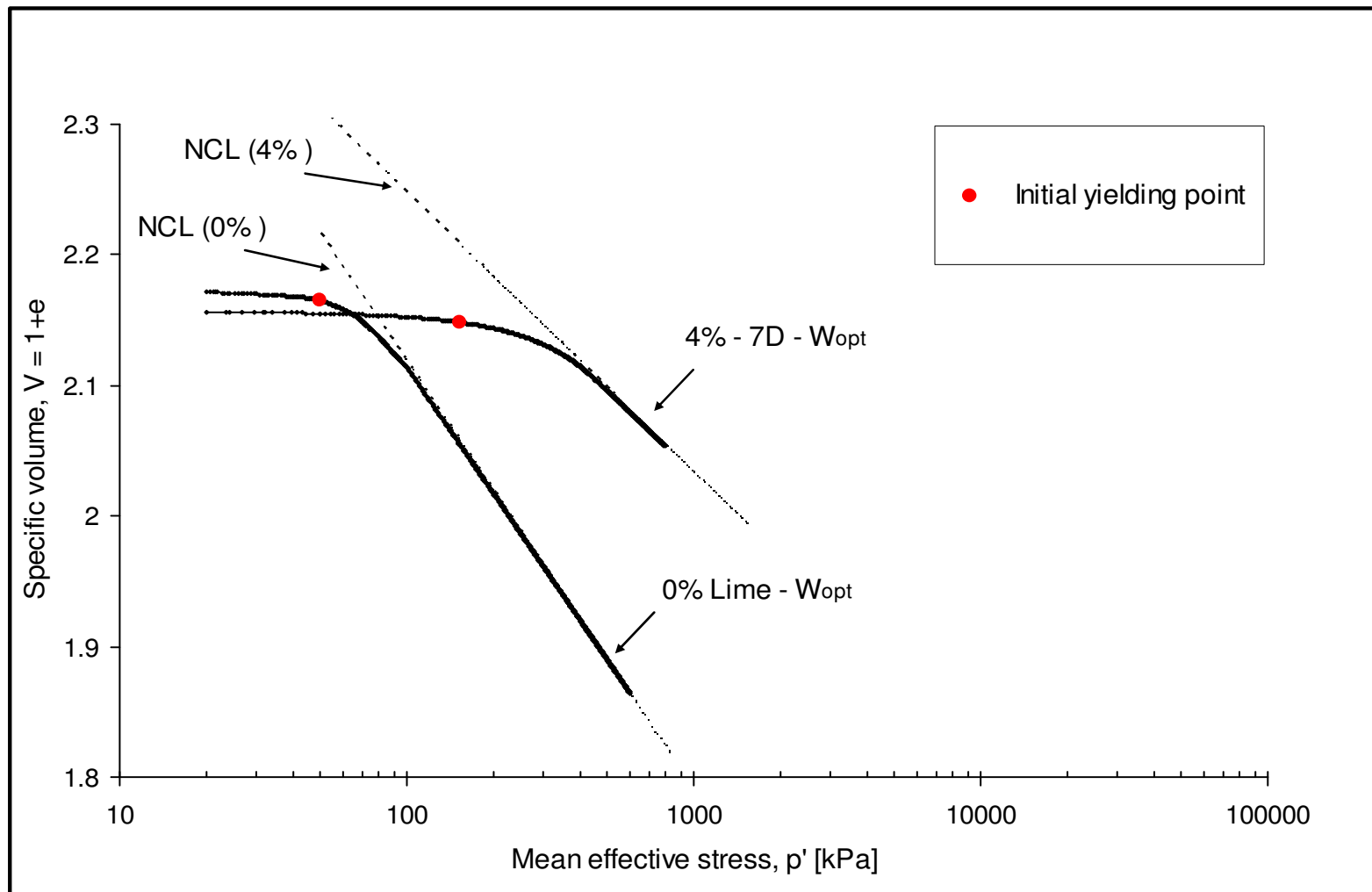
Figure 5.7: Isotropic compression curves for 4% lime treated & untreated London Clay

Table 5.1: Compression parameters for lime treated and untreated London Clay

Lime	Initial water content	Curing time	λ_{iso}	κ	N	$p_c{}'$
(%)	(%)	(Days)	-	-	-	(kPa)
0	w_{opt}	N/A	0.142	0.0062	2.772	49.9
4	w_{opt}	7	0.093	0.0049	2.676	152.7

5.4. Consolidated drained (CD) Triaxial tests

This section presents results from saturated consolidated drained (CD) triaxial tests, which have been performed at different effective stresses (100, 200 & 300kPa), the presentation of the results is organised as follows: a) First the stress-strain behaviour of the soils is shown; b) Yielding behaviour during shearing compression tests of lime treated soil is recorded; c) the void ratio changes for each mixture is then presented; d) shear strength indices are obtained and the shear strength parameters of the soil according to Mohr-Coulomb's failure criterion are then determined; e) finally the dilatancy behaviour of lime treated soil is investigated. The yielding, peak and dilatancy positions are marked on the $(q - p')$, $(\varepsilon_v - \varepsilon_a)$ curves and discussed accordingly. Note that in the following section "failure" will denote the peak state of the material.

5.4.1. Stress-strain and volumetric response of lime treated London Clay

The $(q - \varepsilon_a)$ graphs have been plotted to identify the strength increase associated with lime treatment, as well as strength degradation due to bond breakage. The stress-strain curves of untreated London Clay specimens, display a continuous deformation until a steady stress state is reached (Figure 5.8a). The $\varepsilon_v - \varepsilon_a$ plot (where ε_v is the volumetric strain and ε_a the axial strain) of untreated London Clay samples showed a compressive response until failure at a constant volume change. Bulging was observed at approximately 10% axial strain (ductile failure / see Fig. 5.10a).

Figure 5.8b indicates the deviatoric stress (q) versus Axial strain (ε_a) for 4% lime treated London Clay. A clear linear part of the stress-strain curve before the plastic zone can be seen. A plateau is reached where peak deviator stress is maintained constant; a moderate brittle failure due to slip line was observed (see Fig. 5.10b). This is followed by a gradual decrease in deviator stress with increasing axial strain. The volumetric response of 4% lime treated samples shows an initial compression, followed by dilation after rupture of the specimen. This is consistent with the expected behaviour for lightly over-consolidated specimens except that dilation occurs after the peak strength. As expected, the axial strain at the failure state is observed to increase with increasing effective confining stress. Moreover, it can be seen that the stiffness increases with an increase in the effective confining stress. However, the effect of effective stress is less pronounced for the 4% lime treated specimen compared to the untreated specimen.

The results of the 6% lime treated London Clay specimens were plotted into separate graphs (Fig. 5.9 a, b & c) for better clarity, in view of the number of curves presented. It can be seen that all 6% specimens had higher peak strengths than the 4% lime specimens and exhibited an even more pronounced brittle behaviour with a significant loss of strength after rupture. It is important that this sudden strength reduction be carefully modelled to better understand the lime treated ground behaviour beyond the peak conditions under large strains. The peak / failure strength occurred at lower axial strains, ranging between 1 and 4%, accompanied by the formation of the shear bands at an angle of 60-70°; 7-day cured specimens showed a vertical multi-fissure splitting type (see Fig. 5.10c). Further deformation led to rupture along localised zones and an abrupt loss in strength; the strength continued to decrease towards a constant value (see Fig. 5.8b). The volumetric strain curves of the 6% lime-treated specimens were similar to those of the 4% lime-treated specimens, showing an initial small volumetric compression followed by dilation; dilation was more pronounced in the case of the 6% lime-treated specimens compared to 4% lime-treated specimens. Again (as for the 4% lime-treated soil) the behaviour pattern $\varepsilon_v - \varepsilon_a$ is similar to that of heavily over-consolidated clayey soils as indicated by Leroueil & Vaughan (1990) with the difference that the maximum rate of dilation occurs after the peak strength. A possible interpretation of the volumetric behaviour of the lime treated soil is that the newly created chemical compounds occupy some of the pore space by cementing the particles, consequently creating a denser material similar to a heavily over-consolidated

material. At higher strain the dilation rate approached zero. This ultimate condition can be considered to be close to the critical condition. This is also consistent with the constant stress of the soil recorded in this strain range. The dilative behaviour of the lime treated soil is further discussed in section 5.4.4.

The more pronounced strength and brittleness of the 6% lime-treated soil can be attributed to the formation of the cementitious bonds as a result of the pozzolanic reactions (supported by the detection of cementing compounds during the XRD analysis), and their subsequent breakage.

A measure of the brittleness of the specimens that can be used to support the above observations on the specimen mode of failure, is the brittleness index (I_B) defined by Bishop (1971) as follow:

$$I_B = \left(\frac{q_{peak}}{q_{ult}} \right) - 1 \qquad\qquad (5.1)$$

Where q_{peak}, is the deviator stress at peak, and q_{ult}, is the deviator stress at the ultimate state

Fig. 5.11 shows the variation of brittleness index versus the effective stress for untreated, 4% and 6% lime treated London Clay. As would be expected, the brittleness increased significantly with increasing lime percentage (implying increased cementation) and decreased with an increase in the effective confining pressure for specimens treated with 6% lime. It can be observed that brittleness indices for untreated and 4% lime treated soil are relatively constant while for 6% lime treated specimens brittleness index decreased initially and appears to stabilise at higher effective stress. 6% lime treated soil cured for 7 days exhibited a higher brittleness index, while no major effect of the compaction water content was observed at 28 days curing.

For a clearer picture of the effect of lime percentage, curing time and compaction water content on the strength of the soil, the peak and ultimate state deviator stresses are plotted in Figure 5.12 and summarised in Table 5.2. From this figure it can be seen that the higher the lime content, the higher the location of the respective peak stress envelop. Thus peak

stress envelops of all lime-treated specimens are located above the CSL of the untreated soil but not parallel to it, highlighting the cementation effect which is characterised by an intercept. The intercept of the lime treated soil can be justified by the expected bonding brought about by the lime addition. Considering the slope of the envelopes it can be implied that the addition of lime increased the peak friction angle. The effect of lime on the shear strength parameters is quantified based on Mohr-Coulomb's in section 5.4.5.

Concerning curing time, the 28 day cured specimen showed a lower strength than the corresponding 7 day cured specimen. Figure 5.12 shows that London Clay samples prepared with 6% lime addition, cured for 7 days, tested under saturated conditions, resulted in slightly higher peak / failure envelope than similarly prepared samples cured to 28 days. This was not the expected behaviour and it is difficult to explain as cementation reactions would normally lead to increased strength development (which was observed in UU results but not the CD results), one reason could be the lower saturation achieved for the 7 day cured specimen (see Chapter 3 / Fig. 3.19). This result is also believed to be partly related to the initial change in structure of the newly formed material during the curing period. Although the cementation process to produce the bonds is assumed to have developed in the same way for 6% lime treated specimens, cured for both 7 and 28 days, since they have been prepared in similar way, but it is believed that once the sample is in contact with abundant water during saturation stage, the cementing gel which formed during 28 days curing period developed a higher plasticity within the material (softened / degraded quicker).

Finally, from Figure 5.12 the effect of compaction water content can be assessed; specimen prepared at wet of optimum $w_{wet} = 32\%$, cured for 28 days resulted in higher strength compared to specimens prepared at dry of optimum $w_{dry} = 27\%$. This can be due to the better conditions for cementation bond development in the presence of a higher amount of water during the curing period, which is in line with the findings presented by Locat et al. (1990). According to the authors, a higher humidity environment leads to better particle dispersion, facilitating the movement of calcium ions, which favours the development of pozzolanic reactions and the development of a stronger and longer lasting cementation bonds. Overall (with the exception of the curing time effect), the results are consistent with other studies and published data for cemented soils, showing that the peak/failure

envelopes of cemented samples lie above those of the corresponding reconstituted samples and have an intercept on the q axis (e.g. Kasama et al., 2000; Consoli et al., 2001; and Asghari et al., 2003).

Table 5.2: Peak / failure state parameters

Specimen ID	σ'_3	*Peak void ratio* e_p	q_{peak}	p'_{peak}	$(q/p')_{peak}$	ϕ_{peak}
	(kPa)	-	(kPa)	(kPa)	-	(Deg)
$CD_1(0-0)_{100}$	100	0.988	133.83	144.61	0.93	23.63
$CD_2(0-0)_{200}$	200	0.899	256.97	283.73	0.89	22.69
$CD_3(0-0)_{300}$	300	0.840	361.34	420.45	0.86	22.08
$CD_1(4-7)_{100}$	100	1.122	314.94	204.98	1.54	37.79
$CD_2(4-7)_{200}$	200	1.082	507.45	369.15	1.38	34.12
$CD_3(4-7)_{300}$	300	1.059	745.40	548.47	1.36	33.67
$CD_1(6-7)_{100}$	100	1.126	1243.02	514.34	2.42	59.57
$CD_2(6-7)_{150}$	150	1.129	1330.22	593.41	2.24	54.64
$CD_3(6-7)_{200}$	200	1.126	1558.92	719.64	2.17	52.83
$CD_4(6-7)_{300}$	300	1.119	1945.38	948.46	2.05	49.82
$CD_5(6-28)_{100}$	100	1.099	952.03	417.34	2.28	55.70
$CD_6(6-28)_{200}$	200	1.080	1231.68	610.56	2.02	49.08
$CD_7(6-28)_{300}$	300	1.068	1636.96	845.65	1.94	47.14
$CD_8(6-28)_{100}$	100	1.030	1068.77	456.26	2.34	57.32
$CD_9(6-28)_{200}$	200	1.022	1324.70	641.57	2.06	50.06
$CD_{10}(6-28)_{300}$	300	1.014	1716.26	872.09	1.97	47.86

(a)
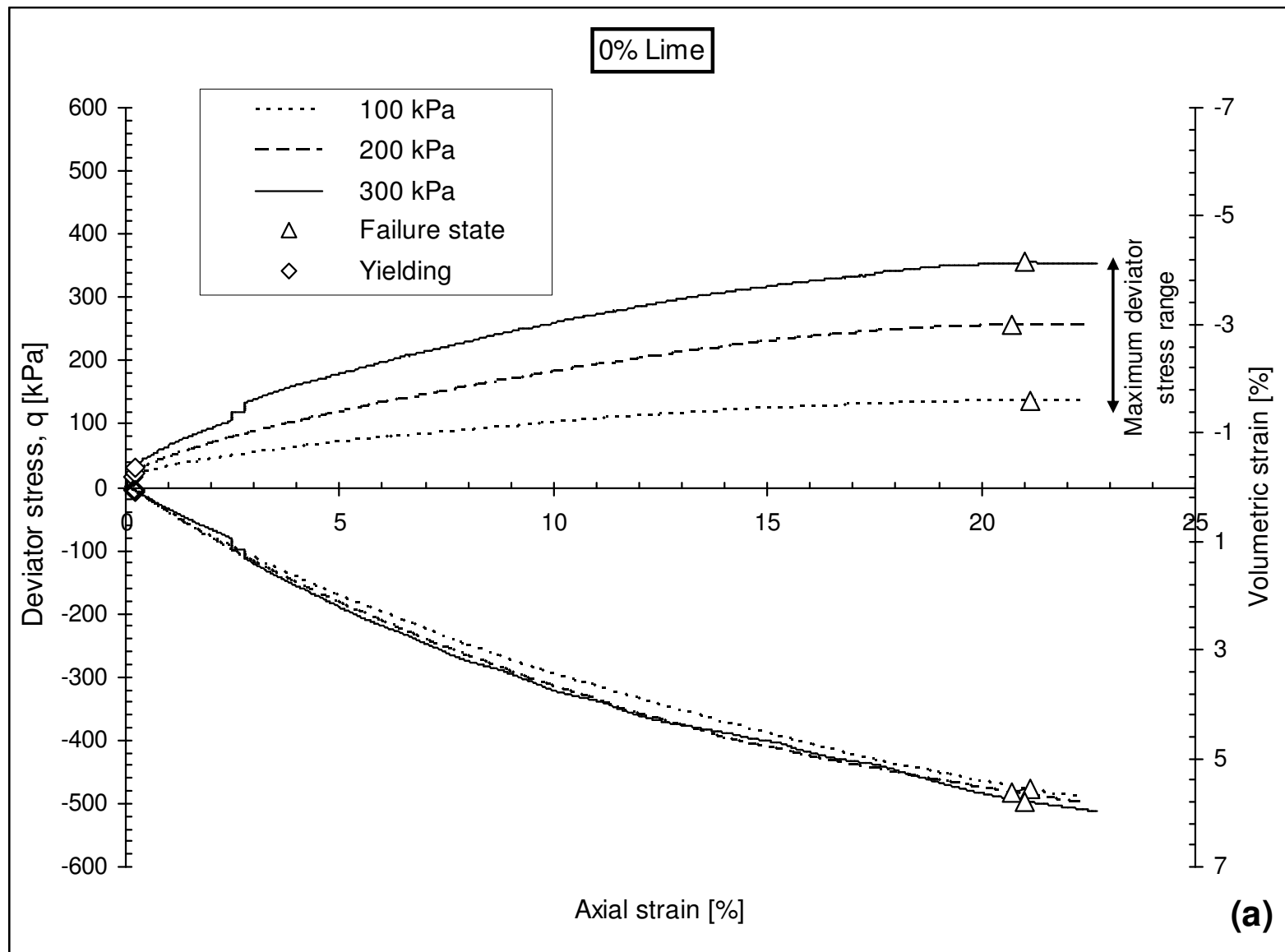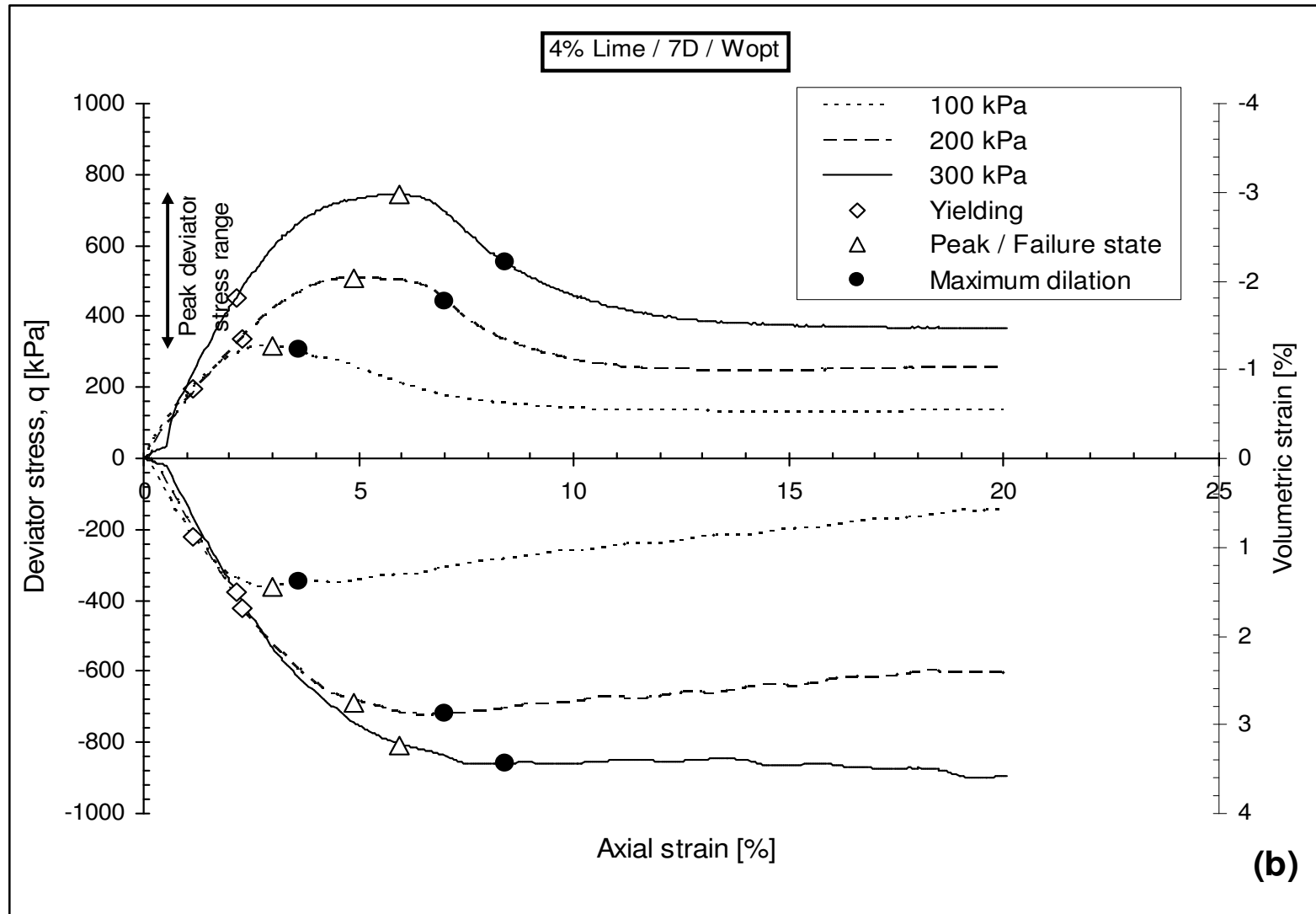
Figure 5.8: Drained triaxial tests for **(a)**: London Clay, **(b)**: 4% lime treated London Clay, $(q - \varepsilon_a)$ & $(\varepsilon_v - \varepsilon_a)$

(a)
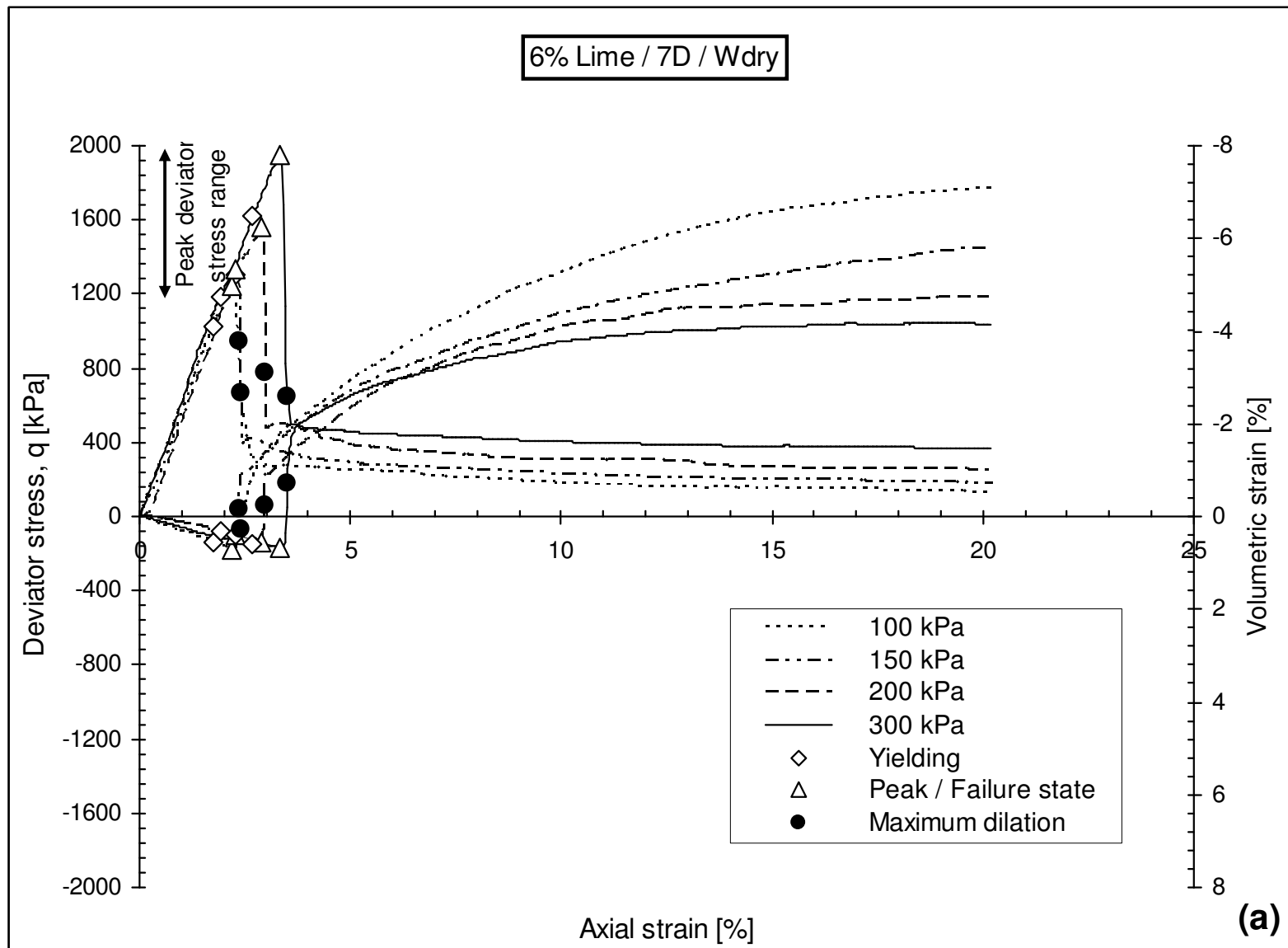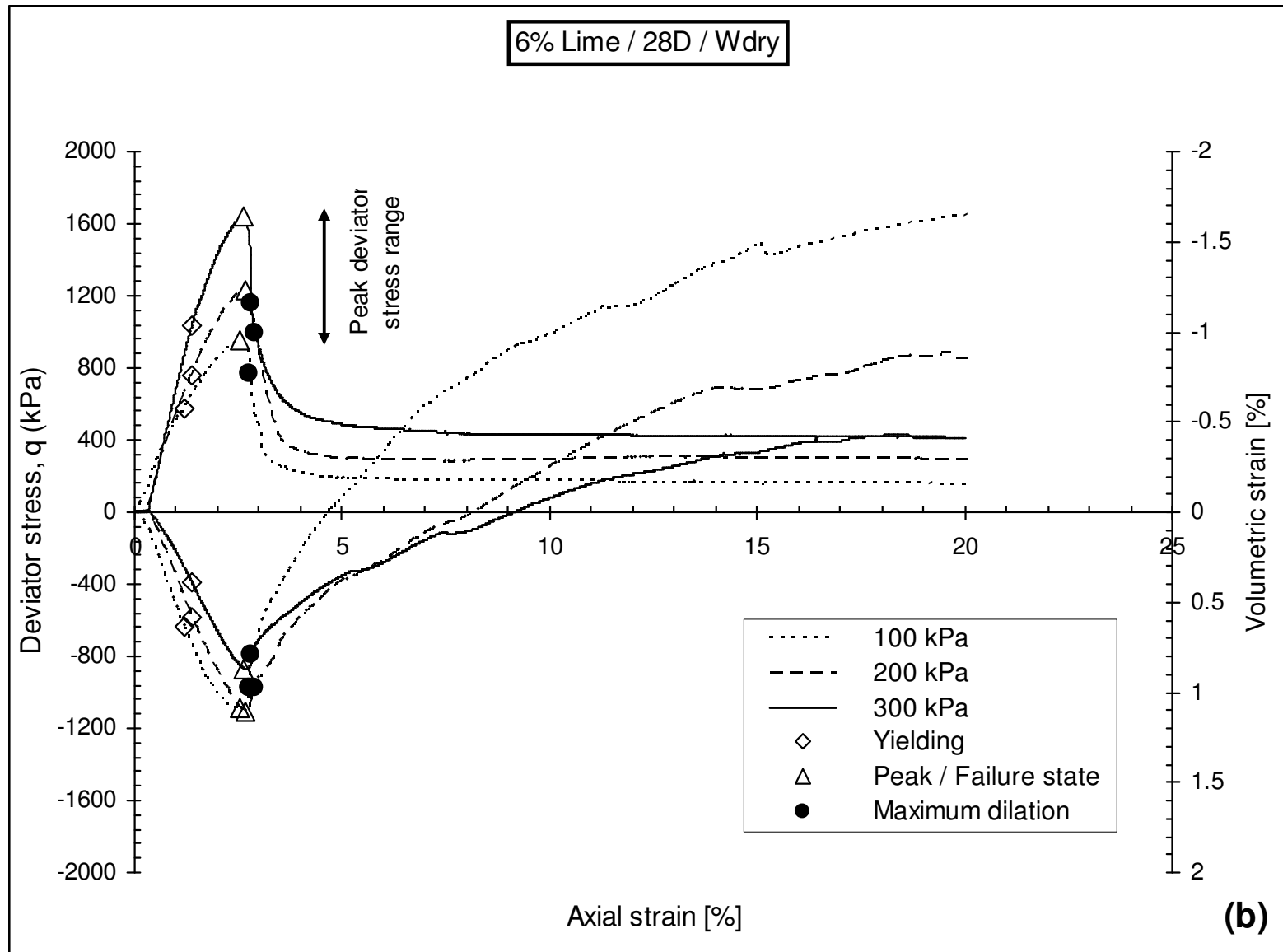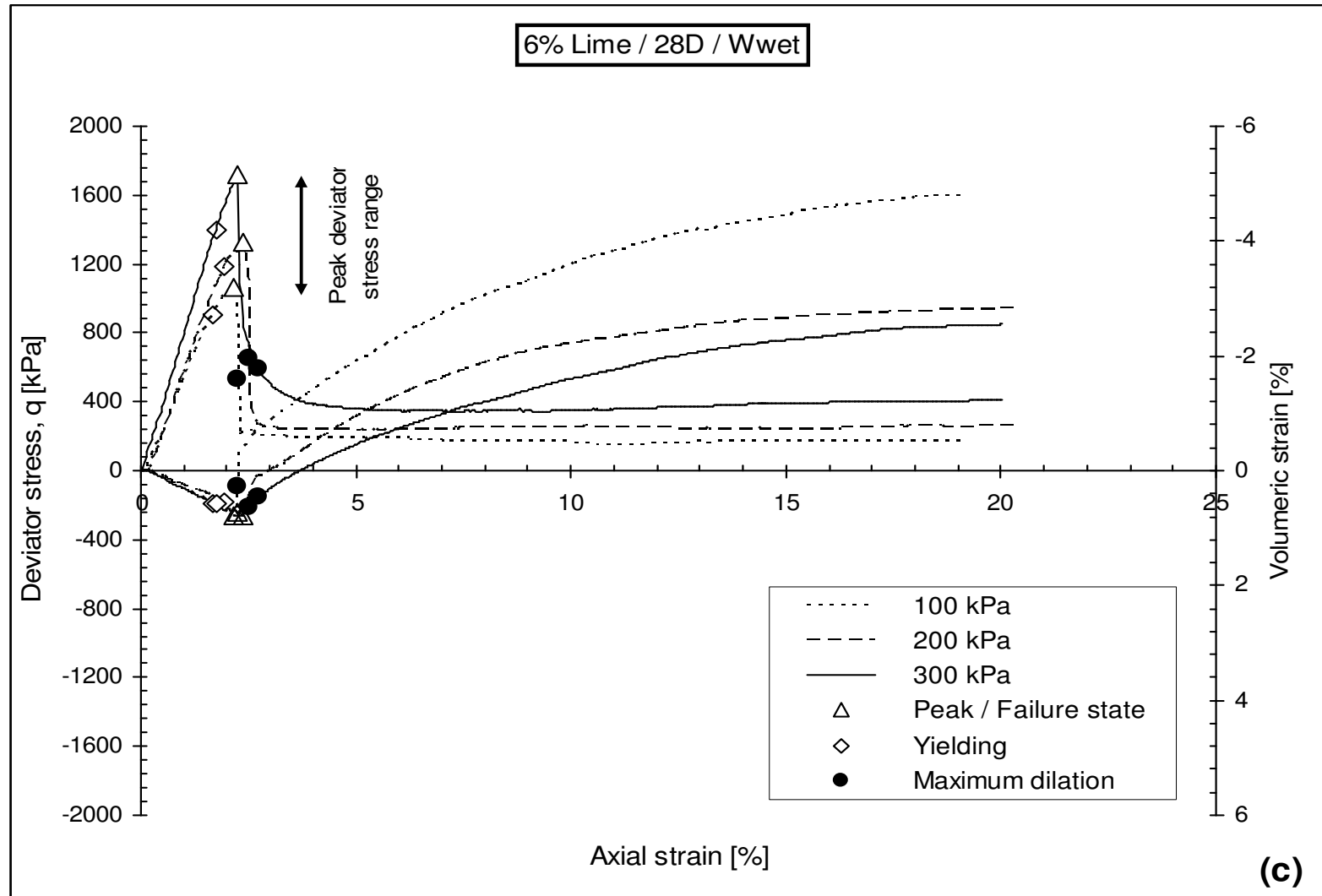
Figure 5.9: Drained triaxial tests for 6% lime treated London Clay, ($q - \varepsilon_a$) & ($\varepsilon_v - \varepsilon_a$), **(a)**: 7D - w_{dry}, **(b)**: 28D - w_{dry} and **(c)**: 28D - w_{wet}
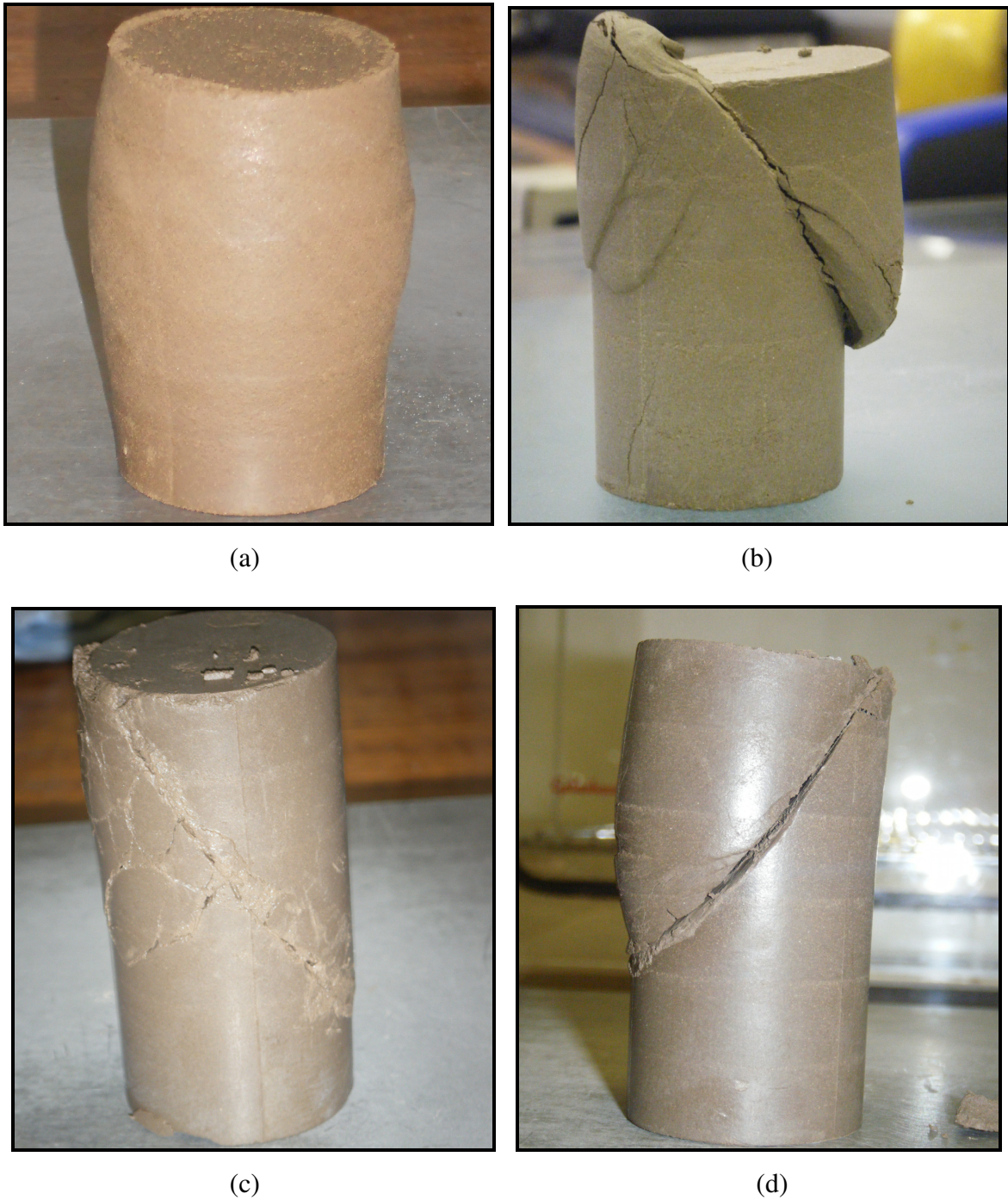
Figure 5.10: Mode of failures of treated and untreated LC under saturated state

(a): 0% Lime / Barrelling (b): 4% L – 7D / slip line. (c): 6% L – 7D /

Multiple fissures. (d): 6% L – 28D / Slip line
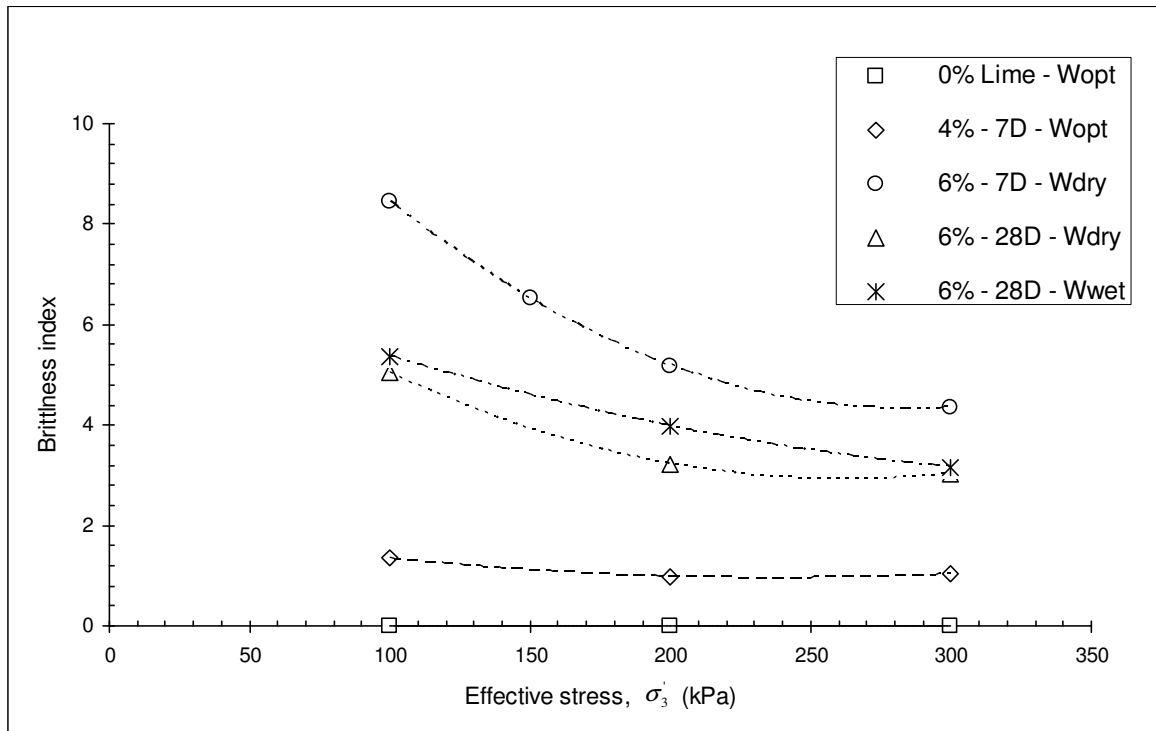
Figure 5.11: Variation of brittleness index Vs effective stress for lime treated London Clay
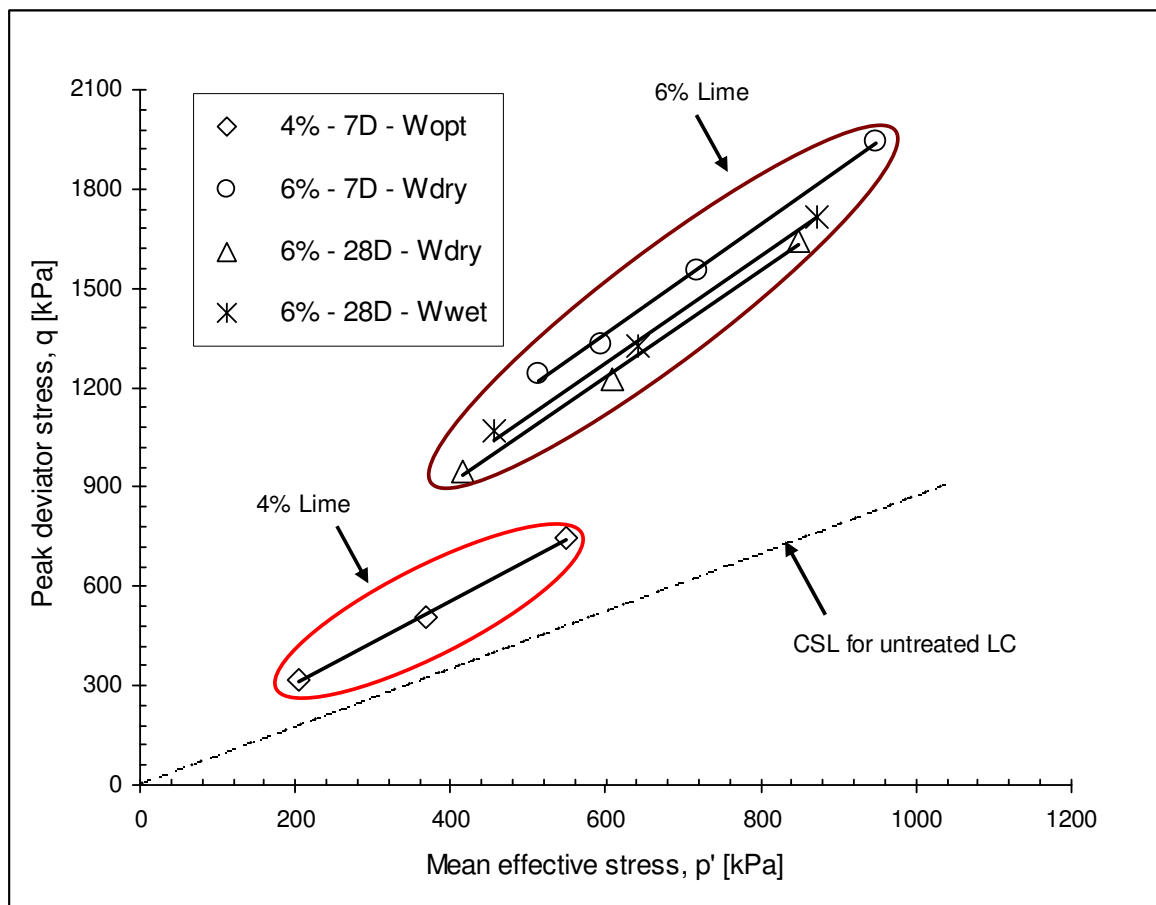
Figure 5.12: Peak / failure state envelopes for lime treated London Clay

A number of detailed observations on the yielding and dilatancy behaviour will now follow. These will be based on the results presented in Figures 5.8 and 5.9. In addition the void ratio evolution during the CD testing will be presented, as this information will be used in Chapter 6. Finally, the shear strength parameters and other strength indices of the soil, based on the presented CD and UU triaxial testing results will be quantified.

5.4.2. Yielding behaviour in shear of lime treated London Clay

Yielding in a material is considered to occur during the transition from elastic to plastic behaviour, directly associated with the development of sharp curvature in stress-strain relationship that had been linear during the elastic deformation. Hence, irrecoverable strains develop in the pre-yield zone, and some of the deformation will be permanent and non-reversible which is identified as plastic deformation.

The difficulties in identifying the yield points of cemented soils have been reported by several researchers (Barksdale & Blight, 1997; Smith et. al, 1992 and Cecconi et al., 1998). Yield is best recognised from stress-strain curve when plotted on a linear or log-log scale (Leroueil & Vaughan, 1990). The soil grading as well as the micro features of the cementitious agent (e.g. Ismail et al., 2002b) can add considerable difficulties in determining the yield points for artificially cemented soils. Rotta et al., (2003) indicated the gradual onset of the breakage of the cementation bonds in artificially cemented soils. They suggested the point where the stress-strain curve deviates from its initial linear trend as the primary yielding point in the isotropic compression space. A similar method can be applied to identify the yielding point in the shearing compression space at which breakage of cementation bonds first commences (Cuccovillo & Coop, 1997). This is how the initial yield point was determined in this research.

Initial yielding points for CD triaxial tests performed on lime treated and untreated London Clay are plotted in $q - p'$ stress spaces (Figure 5.13). Based on this figure it can be seen that the yield points do not increase linearly with mean effective stress p', instead they form a curved envelop with convex shape.

The results are also plotted in terms of initial deviator yield stress q_y versus the applied

confining effective stress (see Fig. 5.14). In this case a linear increase of the yield stress with effective confining stress is noted, which is the expected behaviour.
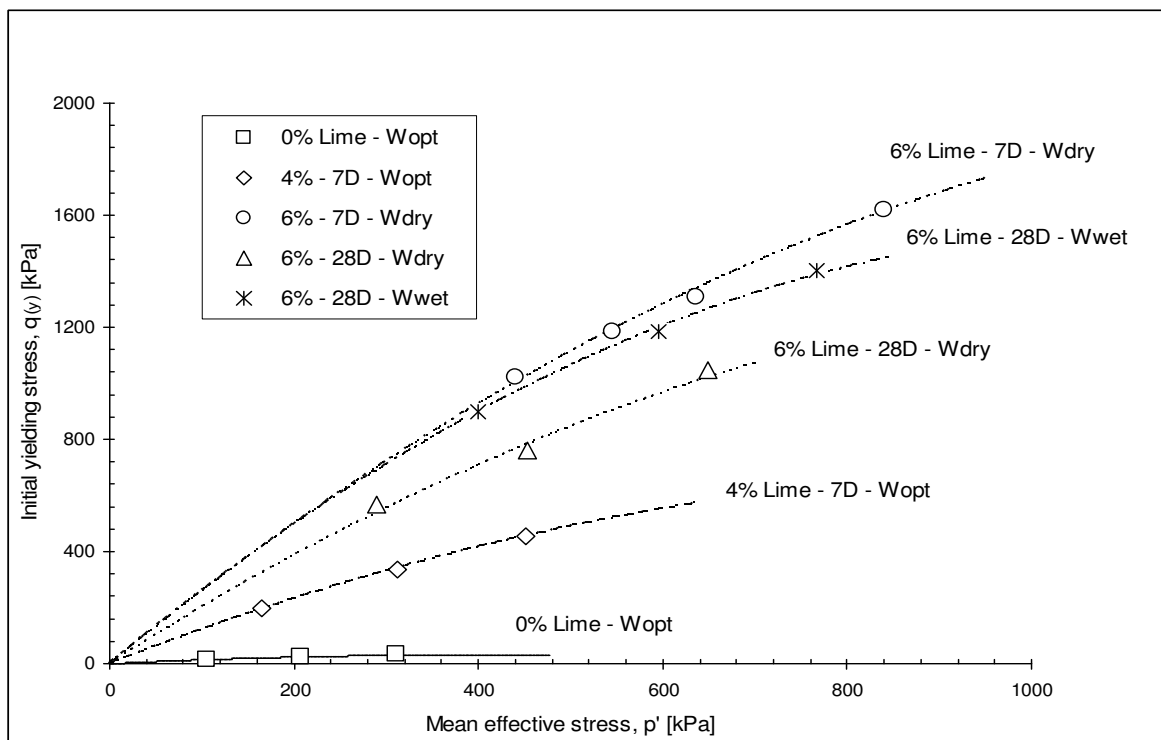
Figure 5.13: Yield curves in shear for untreated and lime treated London Clay
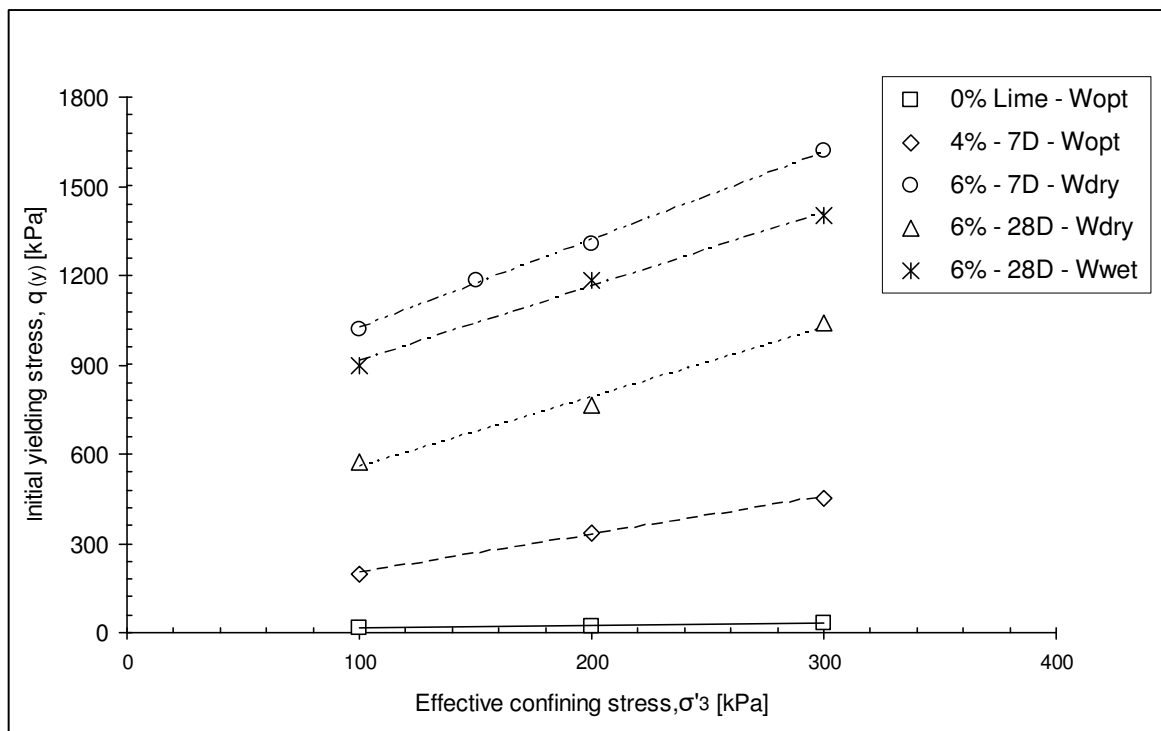
Figure 5.14: Effect of effective confining pressure on yield stress

134

Table 5.3 summarises the yielding point values obtained during the CD triaxial testing of lime treated and untreated London Clay specimens under saturated conditions.

Based on Table 5.3 & Fig. 5.13 the following observations can be made regarding the effect of lime dosage, curing time and compaction water content:

a) Effect of lime dosage on yielding response

London Clay specimens treated with 4% lime addition showed an expanded yield curve compared to the untreated London Clay. This suggests that lime addition influences the size of the yield curve, by shifting it higher than the untreated London Clay yield curve. Figure 5.13 also shows that a lime amount increase from 4 to 6% shifted the yielding curve even higher, indicating that the new material developed a higher stiffness with increasing lime amount during shearing compression. This can be attributed to the higher number of cementation bonds formed due to the higher lime content.

b) Effect of curing time on yielding response

The yield point envelop of the 6% lime treated specimens cured for 7 days plotted above all other envelops (highest yielding surface) when compared to similarly prepared specimens at 28 days curing. The experiments on 28 days cured samples revealed a smoother transition from elastic to plastic behaviour. Conversely, the yielding response observed for 6% lime treated specimens, cured for 7 days is not shown to be strictly elasto-plastic and exhibit a less apparent yielding behaviour (almost elastic pre-yield response). It can be observed that peak strength / rupture occurs soon after yielding commences (Figure 5.9a), which could be attributable to stronger cementation bonds created by lime addition. This was not what was initially expected. It is probable that the difference in the initial void ratio due to volume expansion during the curing period, and the timing of the saturation (saturation after 7 days curing compared to 28 days) may have had an effect on these results (consistent with strength results). In addition, the difference in the average B value achieved during saturation stage for each mixture (see Chapter 3 / section 3.7.1.2) could have had an impact on this obtained result.

c) Effect of compaction water content on yielding response

The compaction water content increase from dry of optimum $\left(w_{dry} = 27\%\right)$ to wet of optimum$\left(w_{wet} = 32\%\right)$ had a clear impact on 6% lime treated London Clay initial yielding stress; the yielding curve envelop for specimens prepared at wet of optimum cured for 28 days plotted higher than the yield curve generated from specimens prepared at dry of optimum, cured for 28 days (see Fig. 5.13 & 5.14). This can be attributed to the favourable effect of the additional water during the curing period for specimens prepared at wet of optimum.

Table 5.3: Summary of yield points

Specimen ID	σ'_3	Yielding void ratio e_y	P_y'	q_y
	(kPa)	-	(kPa)	(kPa)
$CD_1(0-0)_{100}$	100	1.104	105.62	16.86
$CD_2(0-0)_{200}$	200	1.012	207.77	23.30
$CD_3(0-0)_{300}$	300	0.952	311.20	33.60
$CD_1(4-7)_{100}$	100	1.134	165.61	196.82
$CD_2(4-7)_{200}$	200	1.105	312.06	336.18
$CD_3(4-7)_{300}$	300	1.096	451.22	453.67
$CD_1(6-7)_{100}$	100	1.130	440.57	1021.70
$CD_2(6-7)_{150}$	150	1.130	545.22	1185.65
$CD_3(6-7)_{200}$	200	1.129	635.46	1306.39
$CD_4(6-7)_{300}$	300	1.121	840.04	1620.12
$CD_5(6-28)_{100}$	100	1.117	290.48	571.43
$CD_6(6-28)_{200}$	200	1.091	454.03	762.08
$CD_7(6-28)_{300}$	300	1.078	646.29	1038.88
$CD_8(6-28)_{100}$	100	1.036	399.98	899.93
$CD_9(6-28)_{200}$	200	1.025	595.27	1185.80
$CD_{10}(6-28)_{300}$	300	1.017	766.80	1400.41

5.4.3. Recorded void ratio changes

The void ratios of the specimens at the end of each stage (from post-curing to the end of CD testing) are shown in Figure 5.15 and summarised in Table 5.4. In addition, the percent void ratio changes from end of saturation to end of consolidation and from end of consolidation to end of shearing are plotted in Figures 5.16 and 5.17 respectively. From Figures 5.15 and Table 5.4 it can be seen that, as expected, the untreated soil sample showed the highest volume change between post-curing and end of saturation conditions, as London Clay is a shrinking/swelling soil. Conversely all lime treated specimens showed less expansion than the untreated soil, indicating the favourable effect of lime in reducing the swelling potential of the natural soil. It is however observed that the lime-treated specimens are not free from expansion during saturation and that the expansion is variable between the lime-treated soil specimens. The expansion of the lime-treated specimens both after constant water curing and after saturation could be due to the effect of pozzolanic reaction products. In the presence of water during the saturation stage lasting an average of 14 days, the specimens would continue curing beyond the original constant moisture saturation period. As a result of the modification reactions and subsequently the production of cementitious compounds, the lime-treated soil can acquire a more open structure. This has been reported in the literature based on microstructural analyses (e.g. Tedesco & Russo, 2008). In time the voids can be filled by the cementitious products and the number of micropores increases (Tedesco & Russo, 2008); this could reduce the void ratio across the mixes and increase the mass of the solids. However, in the calculation presented in this thesis, the dry mass of the solids was assumed to be constant as it was difficult to quantify the exact mass of the cementitious material. Some differences in the saturation void ratios across the mixes can be noted (although the target compaction dry density of the lime treated specimens was the same); these are likely to be due to the different progress in the chemical reactions across the specimens but as there is no evidence from physicochemical testing, it is not possible to explain these differences in detail.

Figures 5.15 and 5.16 show a decrease in the void ratios of all mixes during isotropic consolidation. However, the changes in the void ratios of all lime-treated specimens are very small compared to those of the untreated soil, in particular those of the 6% lime-treated specimens. This indicates that the stiffness of the lime-treated material increased with lime percentage, as a result of the change in the soil structure after modification

and/or stabilisation reactions (the latter reactions were evidenced for the 6% lime-treated specimens during the XRD testing). On the other hand, inspecting figures 5.15 and 5.17, it can be seen that there is a considerable void ratio change (increase) between the end of consolidation and end of shearing conditions, especially for the 6% lime-treated specimens. This is consistent with the post-rupture dilation of the lime-treated specimens, as discussed earlier (see section 5.4.1)

Table 5.4: Void ratio changes from as cured initial state to end of shearing state

Specimen ID	Lime	Curing time	σ'_3	w_c	Post-curing void ratio e_0	Saturation void ratio e_s	Consolidation void ratio e_c	Peak void ratio e_p	End of shearing void ratio $e_{e/s}$
	(%)	(Days)	(kPa)	(%)	-	-	-	-	-
$CD_1(0-0)_{100}$			100		0.936	1.194	1.106	(0.988)*	0.988
$CD_2(0-0)_{200}$	0%	N/A	200	w_{opt}	0.937	1.199	1.014	(0.899)*	0.899
$CD_3(0-0)_{300}$			300		0.938	1.200	0.953	(0.840)*	0.840
$CD_1(4-7)_{100}$			100		0.949	1.166	1.153	1.122	1.141
$CD_2(4-7)_{200}$	4%	7	200	w_{opt}	0.948	1.194	1.141	1.082	1.089
$CD_3(4-7)_{300}$			300		0.944	1.207	1.128	1.059	1.051
$CD_1(6-7)_{100}$			100		0.937	1.142	1.141	1.126	1.293
$CD_2(6-7)_{150}$		7	150	w_{dry}	0.938	1.140	1.138	1.129	1.262
$CD_3(6-7)_{200}$			200		0.941	1.141	1.137	1.126	1.239
$CD_4(6-7)_{300}$			300		0.940	1.139	1.133	1.119	1.221
$CD_5(6-28)_{100}$			100		0.951	1.123	1.122	1.099	1.157
$CD_6(6-28)_{200}$	6%		200	w_{dry}	0.950	1.107	1.103	1.080	1.121
$CD_7(6-28)_{300}$			300		0.952	1.093	1.086	1.068	1.095
$CD_8(6-28)_{100}$		28	100		0.943	1.049	1.047	1.032	1.146
$CD_9(6-28)_{200}$			200	w_{wet}	0.942	1.041	1.036	1.022	1.093
$CD_{10}(6-28)_{300}$			300		0.940	1.038	1.028	1.014	1.080
(*) No peak stress observed for untreated London Clay									
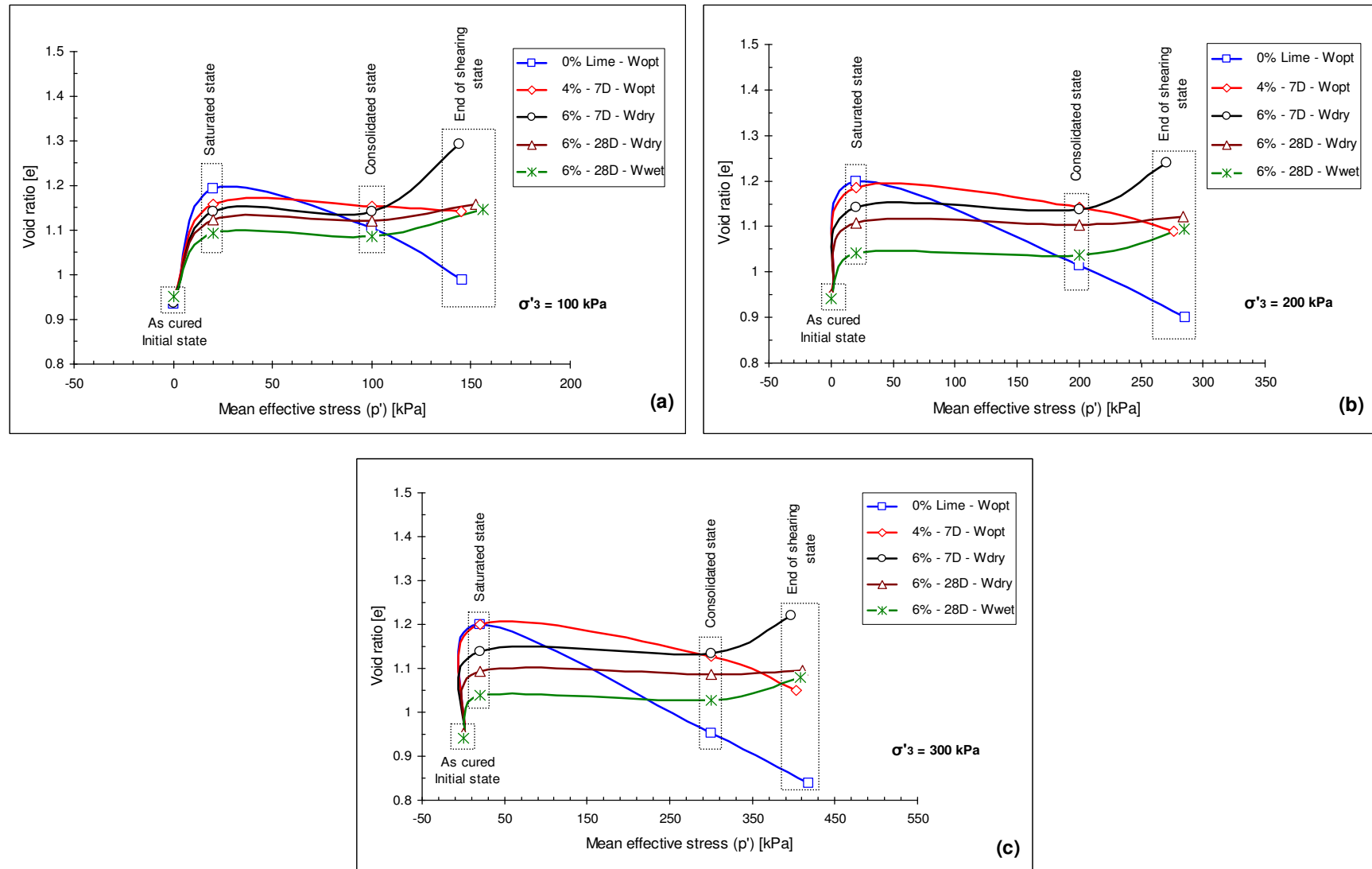
Figure 5.15: Void ratio change path from as cured initial state to end of shearing state of lime treated and untreated London Clay
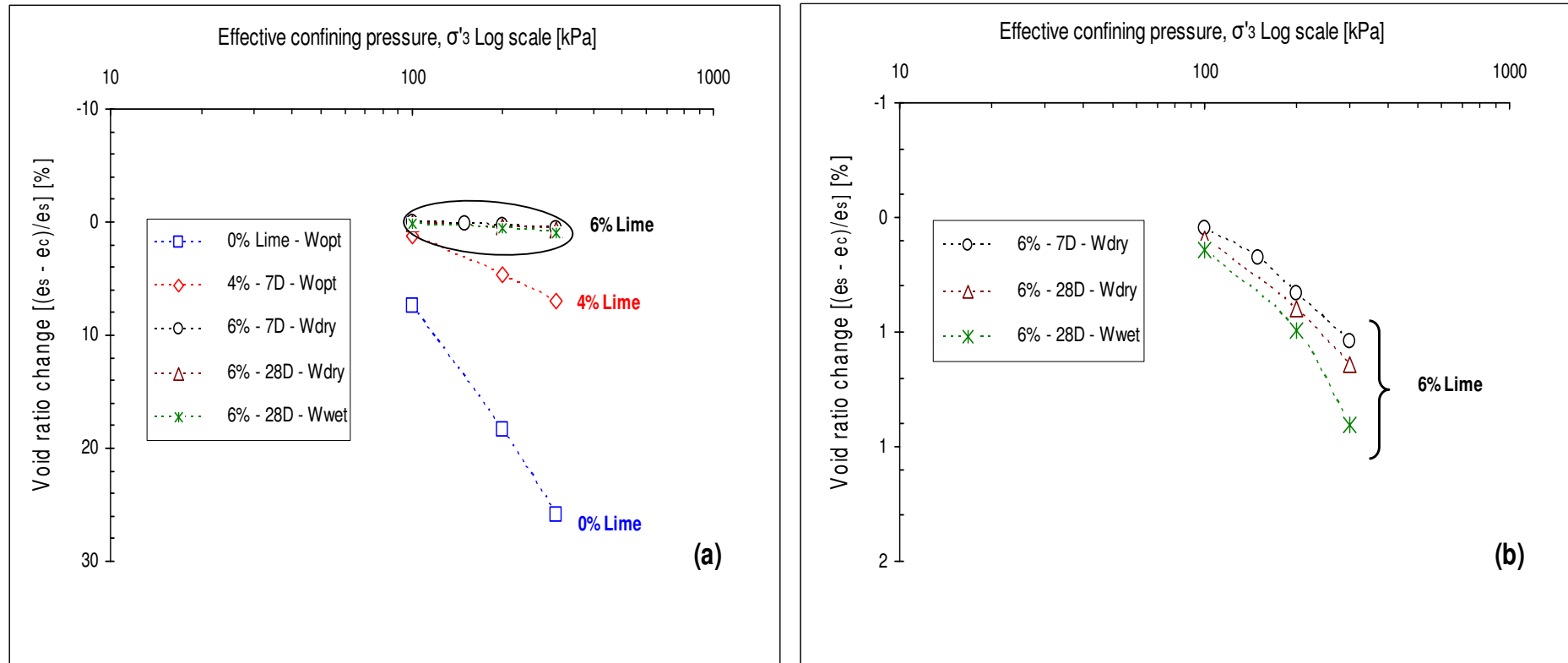
Figure 5.16: Change in void ratio (%) of lime treated and untreated London Clay from saturated state to consolidated state
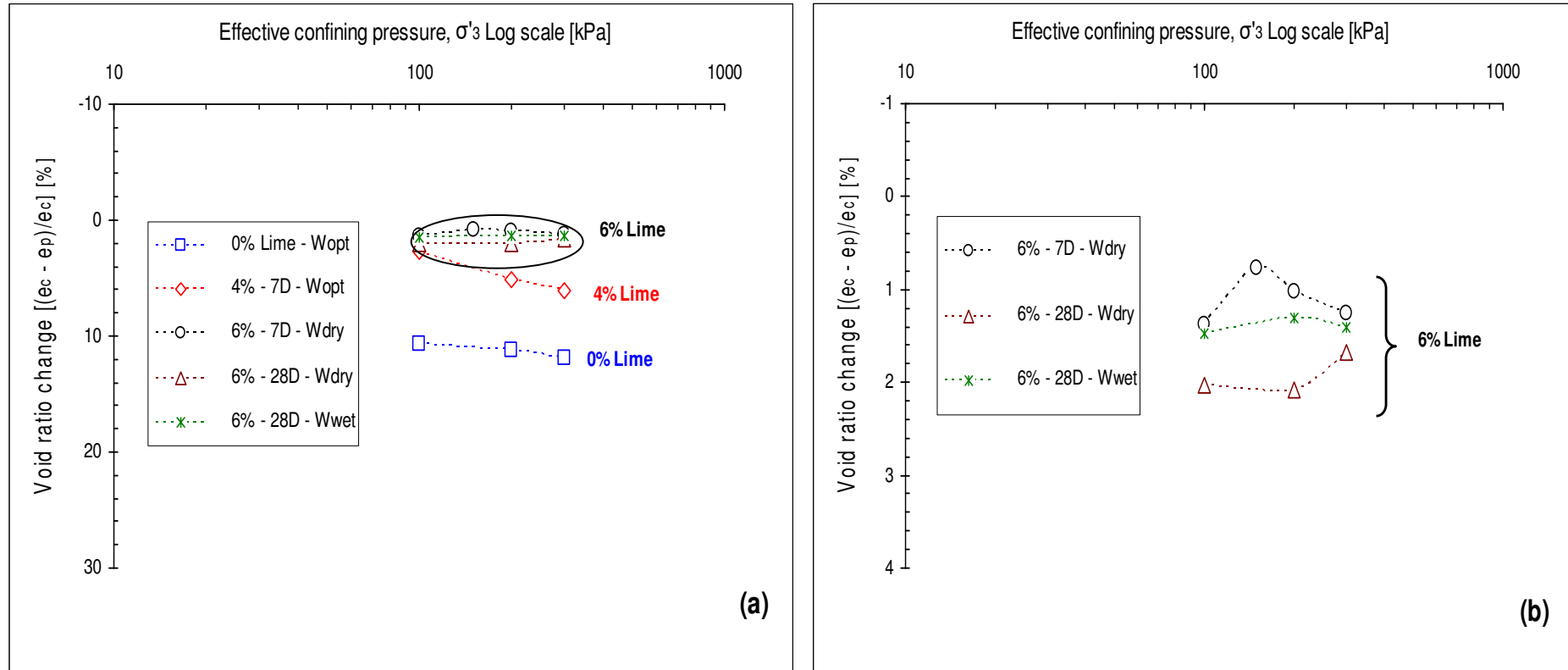
Figure 5.17: Change in void ratio (%) of lime treated and untreated London Clay from consolidated state to peak state

5.4.4. Strength indices and shear strength parameters

Lime treated materials are generally evaluated on the basis of shear strength tests performed on the material after sufficient curing times. In order to quantify the performance and development in strength of lime treated London Clay samples, two methods to evaluate the strength evolution were used:

1/ Strength index based on tested specimen peak deviator stress range (at a specific confining effective stress). The strength evaluation is associated with a set of specimens for each mixture.

2/ Strength evaluation based on individual tested specimens under CD conditions compared to UU test results.

In addition, the shear strength parameters of the Mohr-Coulomb criterion commonly used by practicing engineers are determined.

5.4.4.1. Strength index (based on set of specimens)

The strength index used will be referred to as strength index I_{sr}. It was defined as the difference between the highest and lowest obtained peak deviator stress values from each specimen type, normalised by the difference between the corresponding effective confining stresses. For the presented tests this was written as follow:

$$I_{sr} = \frac{q_{(peak/300)} - q_{(peak/100)}}{300 - 100} \tag{5.2}$$

Table 5.5 contains I_{sr} strength indices for all lime specimen types subjected to CD testing.

Table 5.5: Strength index variation for lime treated and untreated London Clay

Group	Lime (%)	Curing time (Days)	Water content w_c (%)	Strength index I_{sr} -
A	0	N/A	w_{opt}	1.09
B	4	7	w_{opt}	2.15
C	6	7	w_{dry}	3.58
D		28	w_{dry}	3.46
E		28	w_{wet}	3.24

The strength index I_{sr} results are also plotted in Figure 5.18. This illustrates the strength index evolution with lime addition and curing time. Consistently with the previously shown stress-strain results, I_{sr} increased with increasing lime content. In addition, the strength of the 7 day cured specimens was found to be slightly higher than that of the 28 days cured specimens, and so is their corresponding strength index (Group C & D). A further small decrease in I_{sr} was recorded for 28 days cured samples (Group E) prepared with 32% water content (w_{wet}) compared to those prepared at lower water contents (Group D). As would be expected, the I_{sr} of 6% lime treated specimens (Group C) is recorded to be higher than that of 4% treated specimens (Group B) when cured for 7 days.
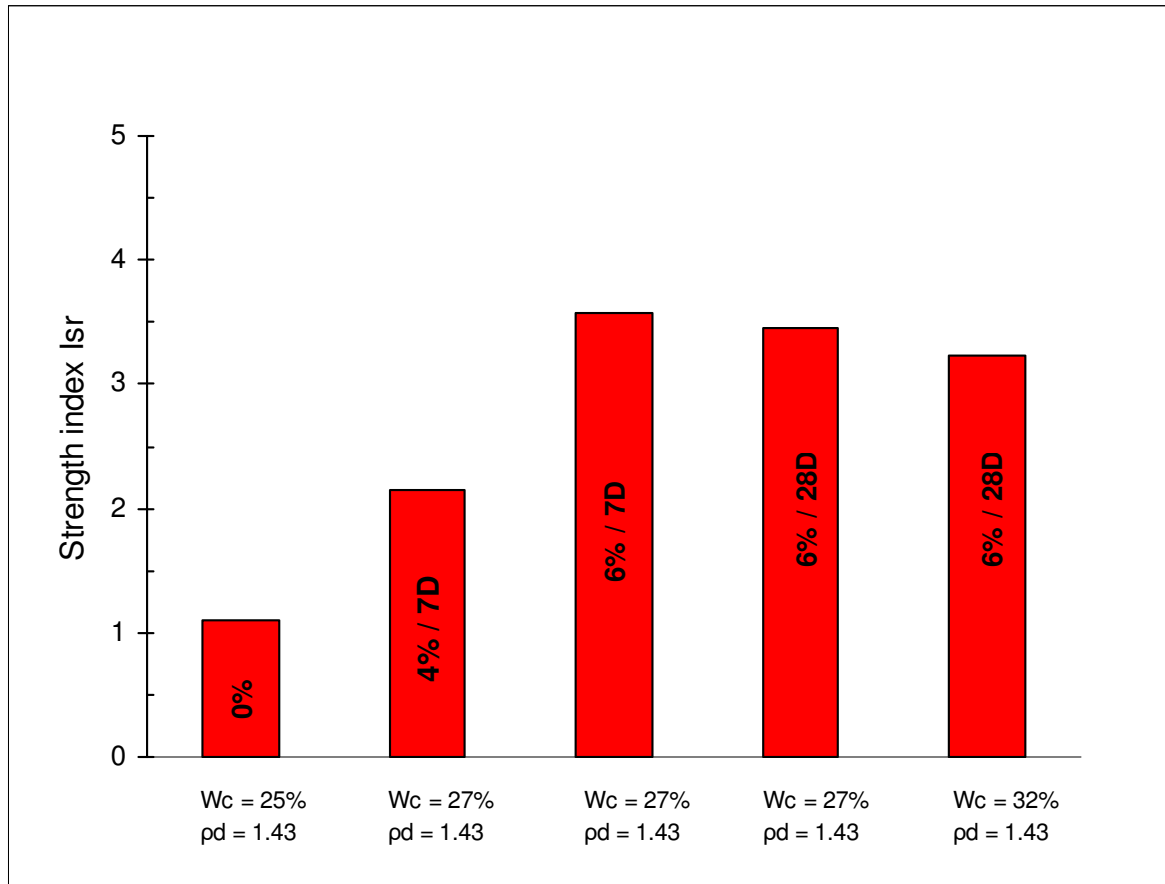
Figure 5.18: Strength index I_{sr} evolution with lime amount, curing time and compaction water content

5.4.4.2. Strength evaluation (based on individual specimen comparison)

A different approach in evaluating the strength of saturated lime treated London Clay tested under consolidated drained (CD) conditions is introduced. Individual comparison of CD tests to results obtained from UU tests performed at a confining cell pressure $\sigma_3 = 200kPa$ provides a different understanding on how strength developed during curing time due to the formation of the cementation bonds, and how these bonds degraded and others formed under saturated conditions. Note that the UU and CD tests were performed on specimens with different degrees of saturation at different rates of strain. Specimens tested under UU conditions are not subjected to any back pressure prior to testing, and typically performed faster than CD tests. For comparison, the differences in measured strength in the CD triaxial tests performed in this study are the applied back pressures, i.e. "saturated" specimens.

The artificial cementation bonds can be broken either by consolidation or shear compression in triaxial tests, but can also be weakened in the presence of high amount of water during saturation stage, while suction is reduced to almost zero. The key aspect here is the transition from dry curing condition at constant water content (CWC) to wet curing at variable water content (VWC), which exposes the lime treated samples to sufficient water during saturation for up to 14 days, and consolidation phase for up to 10 days before proceeding with shearing stage (see Fig. 5.19). The contact with water (ingress & egress) after an imposed curing time at CWC has an effect on the shearing response of the treated specimens suggesting that the presence of water plays an important role impacting on strength loss.

Lime addition to clayey soils, when cured under unsaturated conditions, produces cementation bonds to strengthen and develop a higher resistance to shear compression. However, under saturated conditions, a substantial strength reduction takes place, but remained much higher than that evaluated for untreated specimens under similar conditions. The aspect can be better visualised in Figure 5.20 showing the strength reduction of each mixture under saturated state. Results indicates that peak strength of untreated London Clay under saturated state decreases by about 52% as of the peak strength value obtained in UU test, this is attributed to a combination of bond breakage and a reduced suction to a value close to zero. Peak strength of 4% lime treated specimen cured for 7 days, obtained in UU test is observed to decrease by 61% after being subjected to CD triaxial test under saturated state, which is almost similar strength percentage drop observed in untreated sample. This is due to a combination of non existent suction under saturated state and the weakening of cementation bonds in the presence of high amount of water. A relatively smaller strength decrease was observed for 6% lime amount than 4% lime treated specimens (61% to 19% strength decrease for specimens treated respectively with 4% and 6% of lime when cured for 7 day). Similar observation was made by Le Runigo et al. (2011) when they reported the strength increase with lime addition, while saturation (by immersion) for 1 week leads to significant UCS decrease. In spite of this, their results remained much higher than that evaluated for untreated specimens. The decrease in mechanical strength due to suction decrease is common results for unsaturated soils (Cui & Delage, 1996). However, in this particular case the rate of cementation bonds degradation is believed to be the main cause for the strength reduction. These phenomena explain the loss in strength observed under CD conditions.
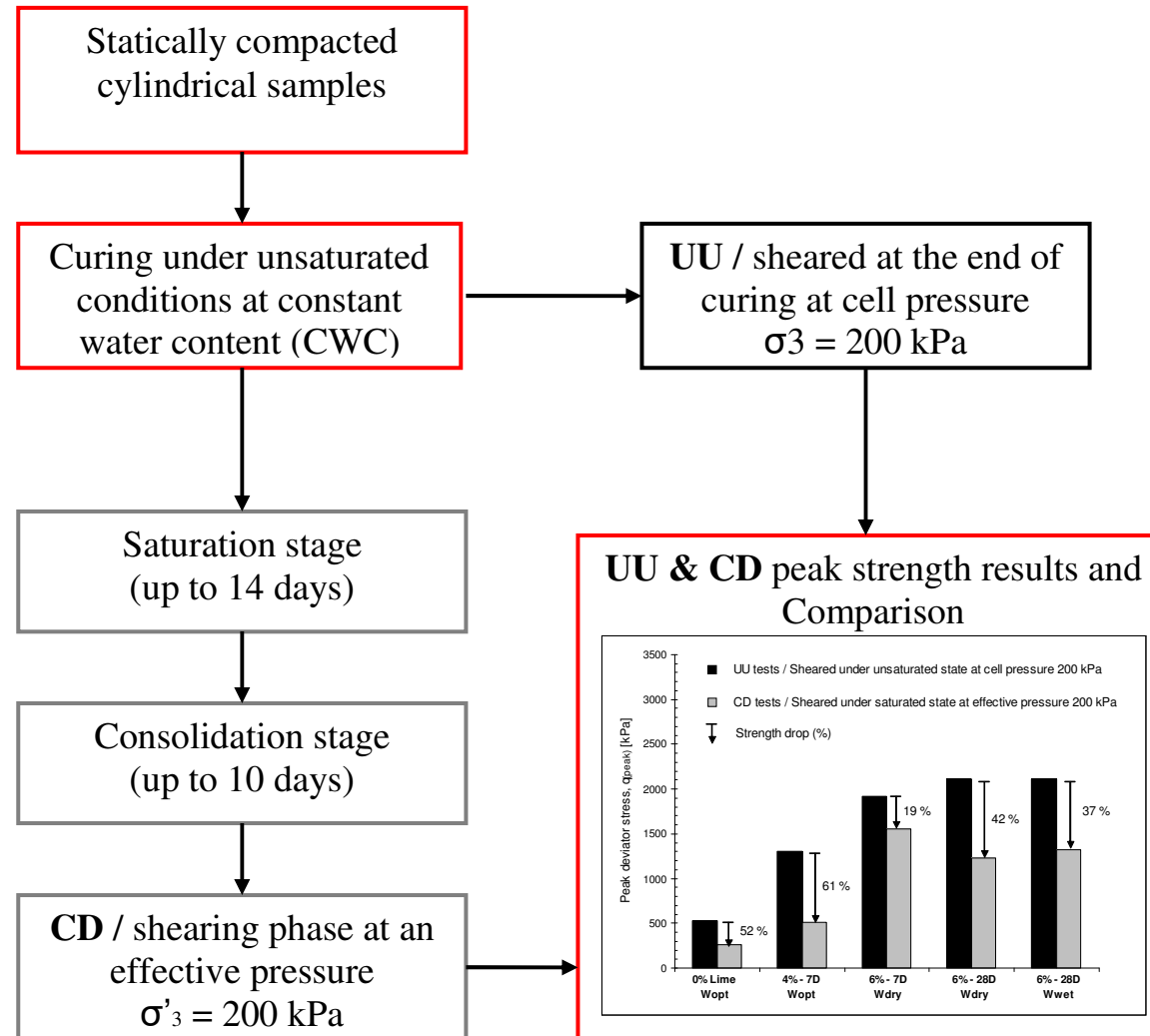
Figure 5.19: UU & CD triaxial testing stages
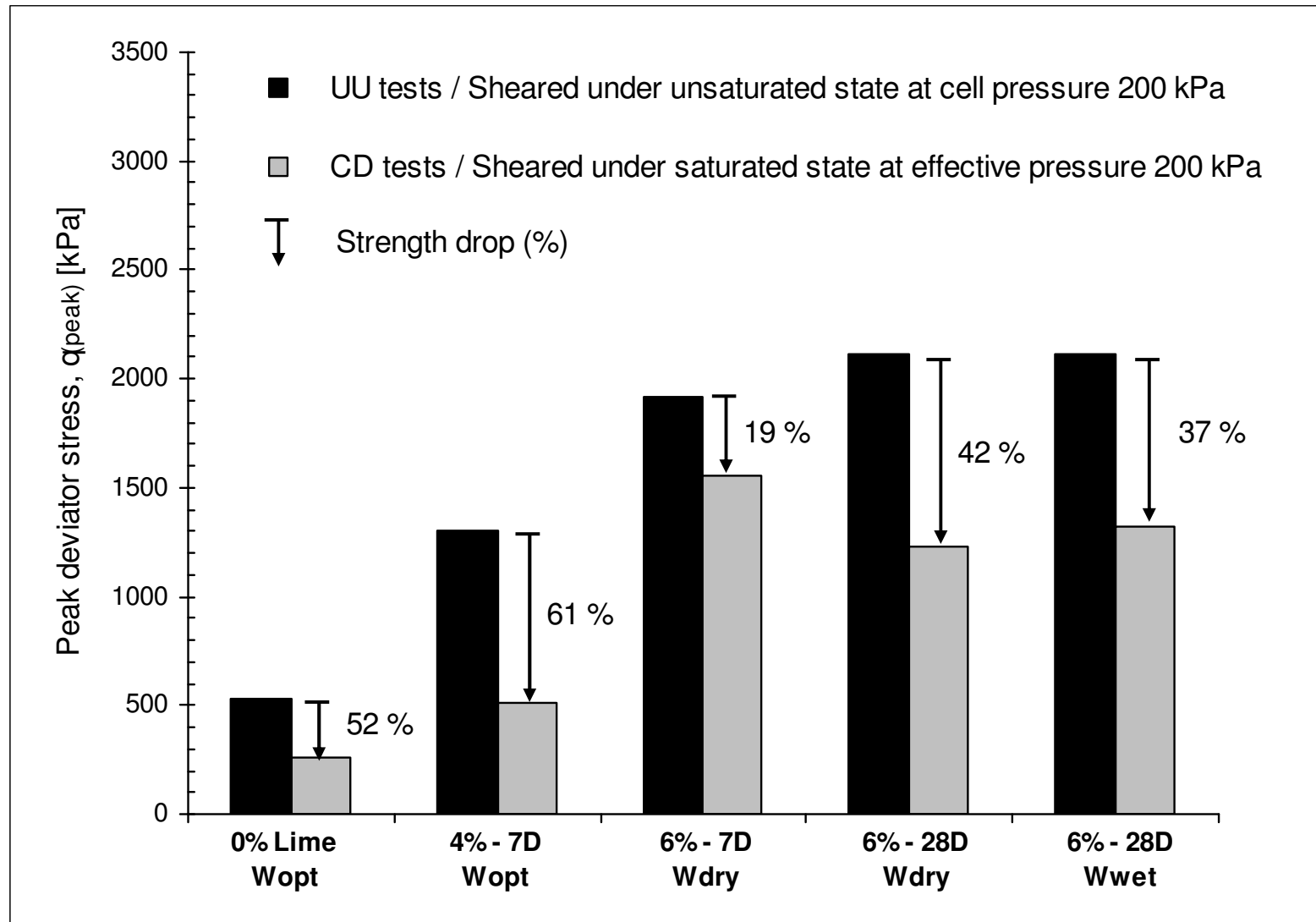
Figure 5.20: Strength evaluation in UU & CD triaxial tests / strength drop under saturated state conditions.

Moreover, UU tests results indicate that lime amount increase from 4 to 6% cured for 7 days increases the peak strength. In addition (based on the UU tests results), curing time increase from 7 to 28 days for 6% lime treated London Clay also increases the strength of the material by a further 40% as of the untreated soil, suggesting that the cementation bonds formed during the 28 days curing period at CWC are of a larger amount than the bonds formed at 7 days curing time (as evidenced by XRD analysis), thus displaying a slightly higher strength for 28 days cured specimens when tested under UU conditions (Figure 5.20). However, results from CD triaxial test performed at an effective stress $\sigma'_3 = 200kPa$ under saturated state on 6% lime treated sample shows a different response with curing time increase, surprisingly strength after 28 days curing is recorded to be slightly lower than the strength after 7 days curing, but still stands within a plateau in a similar trend seen in UU tests results and the sudden strength increase may occur after 60 days curing under CD conditions. Nevertheless, when compared to UU tests results, the peak strength after 28 days curing shows a 42% strength reduction as of the strength initially obtained in UU test, whereas only 19% strength drop for 7 days cured specimen is recorded. This indicates that the presence of high amount of water has a lesser influence in weakening the cementation bonds formed during 7 days than the bonds produced in 28 days curing at CWC. Thus, it can be concluded that specimens saturated after 28 days curing at CWC, tend to loose their pozzolanic reaction products faster, and degrade to a much lower strength than similar specimens cured for 7 days only.

In order to identify the likely cause for the strength slight reduction with curing time increase, a detailed forensic investigation was carried out; following back the steps to the earliest point possible. Note that at a later time (beyond the testing stage), it is not practically possible to physically revisit the samples to identify any anomaly which might have occurred during the preparation, nor is it possible to go back on time to identify any wrong doing in the testing procedures. However, a complete review of all the recorded measurements during the preparation for each sample was performed (i.e. soil mass, lime dosage and water content) as well as the measured dimensions of the samples from as compacted to as cured stage (i.e. diameter, length and volume). Testing procedures were performed (see Chapter 3/section 3.7.1.2) in the same way for both mixture sets as follow:

a) Saturation stage was performed for up to 14 days at $1.5kPa/hour$ for all specimens under an effective stress equal to $20kPa$ until a satisfactory B value is achieved.

b) Consolidation phase for all specimens was carried out by applying a cell pressure increase at a loading rate equal to $1.5kPa/hour$ for up to 10 days (depending on the required effective stress).

c) Shearing performed at a similar controlled shearing rate equal to $0.1\%/hour$ for all specimens.

In order to eliminate any doubt on the sample preparation and to ensure that the testing procedures were followed in a similar way as all the other specimens, a decision was taken to include in the program a fourth sample treated with 6% lime and cured for 7 days. This sample was sheared under drained conditions at $150kPa$ effective stress. This is the only additional sample in the study among all other mixtures, by following exactly the same sample preparation and tested with the same calibrated equipment using the same procedure as detailed in Chapter 3. Results from this fourth specimen showed the same response as for the first three tested samples (100, 200 and 300 kPa) and proved to be in the same strength path recorded for this set. The maximum deviator stress for the fourth tested specimen was observed to be aligned on the peak strength envelop drawn for this type of mixture (6% - 7D – w_{dry} / see Fig. 5.12). This confirms that the sample preparation, testing procedures were accurately performed. Note that Brooks et al. (1997) reported a surprising strength results of 5% lime treated London Clay when the undrained shear strength of 7 day cured sample presented higher strength than 28 day cured sample, and even higher strengths were obtained with lower lime contents. The authors attributed this latter anomaly to the compaction related effect and no explanation was given for 5% lime treated London Clay inconsistent strength results observed with curing time increase. In another separate research, Ahnberg (2007) who performed CD and CU triaxial tests on two types of soft Swedish clays (Linkoping clay and Loftabro clay), treated with lime and cement, cured for 1, 28 and 360 days. A significant exception was observed for the lime stabilised Linkoping clay, where no further strength improvement was measured between one day and one year. This lack of effect has been observed in other investigations on this type of clay (Ahnberg et al., 2003). Another exception from the general pattern of an

increase in c' with increasing time and binder quantity, is the lime stabilised Loftabro clay, which showed no difference in strength for binder quantities corresponding to 50, 100 and $200 kg/m^3$. However, the author indicated that this is common when using lime as a binder; effects of larger quantities of lime are, as a rule, observed mainly as a more accentuated long-term strength increase.

Nevertheless, in this current research, while reviewing what might have happened to the 6% lime treated specimens during the curing period, it was found that the treated samples expanded in volume due to rebound. Similar observation was made by Brooks et al. (1997) when studying lime treated London Clay and Gault Clay, reporting a radial swelling of the specimens prior to testing being in a range of 1.5 – 3.8% as of the initial measurements, they also indicated that generally marginally more swelling occurred with higher lime contents and longer curing period. For this reason the current investigation was diverted into theory to find an explanation for the obtained result.

Two main hypotheses are suggested to explain the strength reduction with curing time revealed under saturated conditions in 6% lime treated specimens. These may possibly be related to the following two observations which are believed to have had a crucial impact on the strength results.

      i)   The post-curing volume variation (expansion) observed in lime treated specimens

      ii)   The timing of the saturation stage during the CD triaxial tests.

There is a higher possibility that the result is caused by the difference in the initial void ratio at the start of the test. It is important to indicate that 6% lime treated specimens showed a higher volumetric expansion after 28 days curing period (1.8%) compared to an expansion of (0.9%) after 7 days curing (Fig. 5.21). This suggests an increase in void ratio has occurred during the dry curing period, indicating a more open structure in 28 days cured samples, consequently affecting the different testing stages (saturation, consolidation and particularly the shearing phase) due to microstructure changes. In addition, the average achieved B value during the saturation process was identified to be inferior for 7 days

(0.91) than for 28 days cured samples (0.96) (Fig. 5.21). The former specimen proved difficult to saturate, indicating a lower permeability for 7 days cured specimens due to blocked pores, the lower the permeability the better the durability (Le Runigo et al., 2011). Note that in the hope of achieving a better B value, 7 day cured specimens were left slightly longer during the saturation stage (up to 48 hours). This is probably the reason why a higher void ratio was observed at the end of saturation stage for this mixture set. In addition 7 day specimens showed higher stiffness and lower compressibility during consolidation stage. This is reflected by the smaller void ratio change recorded in percentage (saturated to consolidated state / section 5.4.3 / Fig. 5.16). Given the microstructure changes, and the differences in permeability and compressibility between specimens saturated after 7 & 28 days curing (amount of water absorbed and expelled), the stability of the pozzolanic reaction products becomes of interest. Therefore, given the amount of water that gained access into the system and remained, a potential softening and damage to the cementitious bonds can be higher in 28 days cured samples (as they showed a higher permeability) than 7 days cured samples, reflecting the reduced strength observed in 28 days cured samples under saturated state.

This seems to be the most possible reason according to Beetham et al. (2014); the authors indicated that water ingress has the potential to influence the clay mineralogy of lime treated soil in a similar manner to a natural clay soil. When lime treated specimen is in contact with abundant water of neutral pH and low Ca^{2+}, C-S-H gel will de-constitute into $Ca(OH)_2$ and silicate (Taylor, 1990). The release of these components will then effectively raise the pH and Ca^{2+} of the water, the attack on pozzolanic reaction products (already formed under unsaturated curing) can be sustained with further water supply into the specimen during the saturation stage. This is supported by McAllister & Petry (1992) who identified that where permeability is high, the leaching of Ca^{2+} from a cured lime-clay specimen is sustained at a high level for an ongoing period. Therefore, a material with a higher permeability can potentially lose strength through softening and removal of the pozzolanic reaction products (Le Runigo et al., 2009).
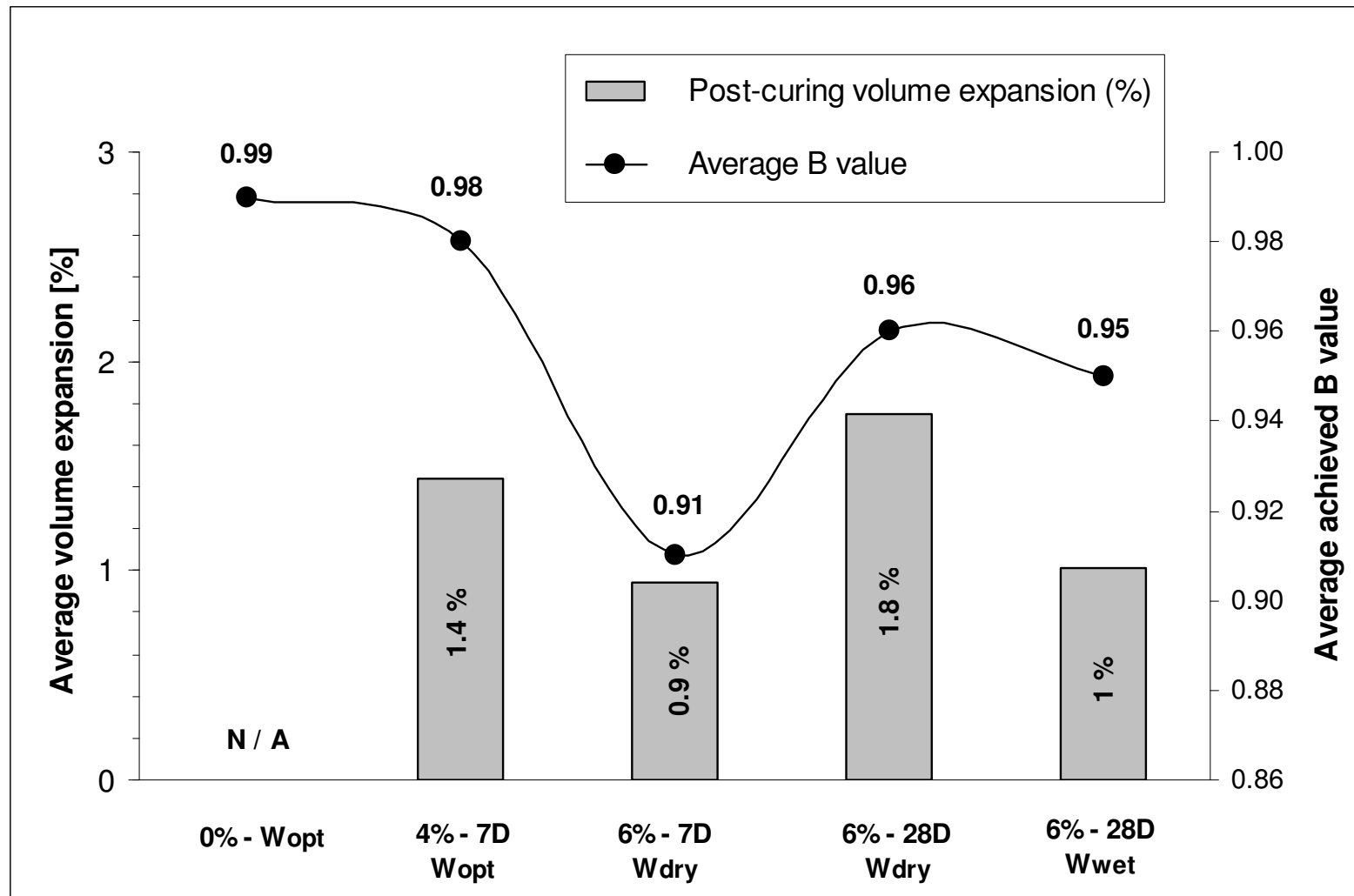
Figure 5.21: Average post-curing volume expansion and the average achieved B value for all the mixtures.

The second explanation which can be put forward is related to the timing of the saturation phase. The reaction between lime and soil continues for an extended period of time, as evidenced by the long term maintenance of high pH (>10). This reaction is maintained during the saturation process, further altering the material's structure. It is believed that early saturation (7 days after dry curing) of lime treated samples allows a uniform reaction between the remaining lime and soil minerals, while similarly prepared samples saturated at a later stage (28 days after dry curing) results in disuniformity in reaction products distribution due to the fact that a presence of sufficient amount of water is necessary for the reaction between lime and soil (note that these specimens were initially compacted to dry of optimum).

Di Sante et al. (2014) indicated that early wetting of lime treated samples developed more uniform pozzolanic products and these crystallised (which give rise to brittleness) as opposed to when they subject them to a prolonged unsaturated condition curing before saturation. In the current research, a more brittle structure was observed for specimens saturated after 7 days curing (early wetting) compared to specimens saturated after 28 days curing, which showed a gradual plastic failure due to more pronounced plastic deformation as indicated in section (5.4.1). Hence, assuming that an earlier contact with water (after 7 days curing at CWC) has allowed the formation of the crystalline reaction products under saturated conditions, it can be concluded that structural changes during saturation / consolidation stages occurred, and the formation of other cementitious bonds are possible, and the strength development in this case is more favourable after 7 day than 28 day curing.

To a lesser extent, there might be another possible reason as to why availability of water could lead to reduction in strength. There is a well known linear relationship over the full plastic range between the water content and its undrained strength and can extend to water content greater than the liquid limit condition (Koumoto & Houlsby, 2001; Sharma & Bora, 2003). Availability of water will lead to swelling and softening (i.e. a reduction in strength) of agglomerations of clay particles. Strength of cemented material is due partly to bond strength and partly due to strength of the parent material (i.e. the clay). In this case, there is a possibility for the clay to soften during saturation stage for both specimens, however, this can affect the 28 day cured sample more than the 7 day cured sample due to permeability and the amount of water absorbed.

This question is still open as not enough is known about the real causes to this result, and more tests are required for a definite conclusion. However, if the above theories are correct, this has a significant practice implication in soil stabilisation projects by mean of lime addition, at which the curing time can be reduced if an appropriate lime amount beyond ICL is used.

Finally, although it has previously been indicated in section (5.4.1), that lime treated London Clay specimens prepared at wet of optimum exhibit higher strength (under saturated state) than specimens prepared at dry of optimum, but when these are compared to UU test results to evaluate the strength loss, it shows that the pre-curing water content increases from 27 to 32% does not appear to withheld the gained strength longer in the presence of high amount of water, the strength loss during CD triaxial testing under saturated conditions is noted to be almost similar for both types of mixtures 42 and 37% drop for dry of optimum and wet of optimum respectively (Fig. 5.20).

Therefore, it can be concluded that the likely explanations for the slight strength reduction observed in 6% lime addition with curing time increase under CD conditions could have been caused by either of the three introduced possibilities or the combination of all of the following:

1. The potential loss of strength through softening and removal of pozzolanic reaction products (which have already formed during curing at CWC) due to higher amount of water ingress into the system / higher permeability, resulting in a faster degradation of the cementitious bonds in 28 days than 7 days.

2. The formation of crystalline pozzolanic products for early saturated specimens (7 days) produces stronger cementitious bonds, resulting in higher strength and exhibiting higher brittleness as indicated in section 5.4.1.

3. Swelling and softening can lead to strength reduction due to the presence of high amount of water, and this has had a higher effect on the 28 day than 7 day cured sample.

5.4.4.3. Shear strength parameters (Mohr-Coulomb criterion)

Mohr-Coulomb theory is used in geotechnical engineering as a failure criterion to identify shear strength of soils and rocks at different effective stresses. Assuming a linear relationship between the shear strength versus the effective stress, normal to the failure plane, the Mohr-Coulomb failure criterion is expressed by the following relationship.

$$\tau = c' + \sigma'_n \, \tan(\phi') \tag{5.3}$$

Where τ is the shear strength, σ'_n is the normal effective stress, c' is the intercept of the failure envelope with the τ axis named the cohesion, and ϕ' is the slope of the failure envelope called the internal friction angle.

In order to identify the peak strength parameters, Mohr Coulomb criterion can be applied at peak state for artificially cemented soils which exhibit similar behaviour as lightly and heavily over-consolidated soils.

Based on CD results, Mohr circles of effective stress at peak state are shown in Figure 5.22. From these, the shear strength parameters c' and ϕ'_{peak} were determined to assess the effect of lime dosage, curing time and compaction water content as reflected by these parameters. A summary of the values of c' and ϕ'_{peak} for the different mixtures is shown in Table 5.6. From the table, it can be seen that the friction angle as well as the cohesion increases with lime amount increase. In addition, and regardless of the initial water content, Figure 5.22 shows that 6% lime treated London Clay cured for 28 days, had a peak angle of friction $\phi'_{peak} = 39°$ and a cohesion intercept c' ranging between 145 and $181 \, kPa$. These parameters can be used on computer models to predict the material's behaviour in large scale engineering applications. The material's real behaviour can be useful for any numerical modelling and design.
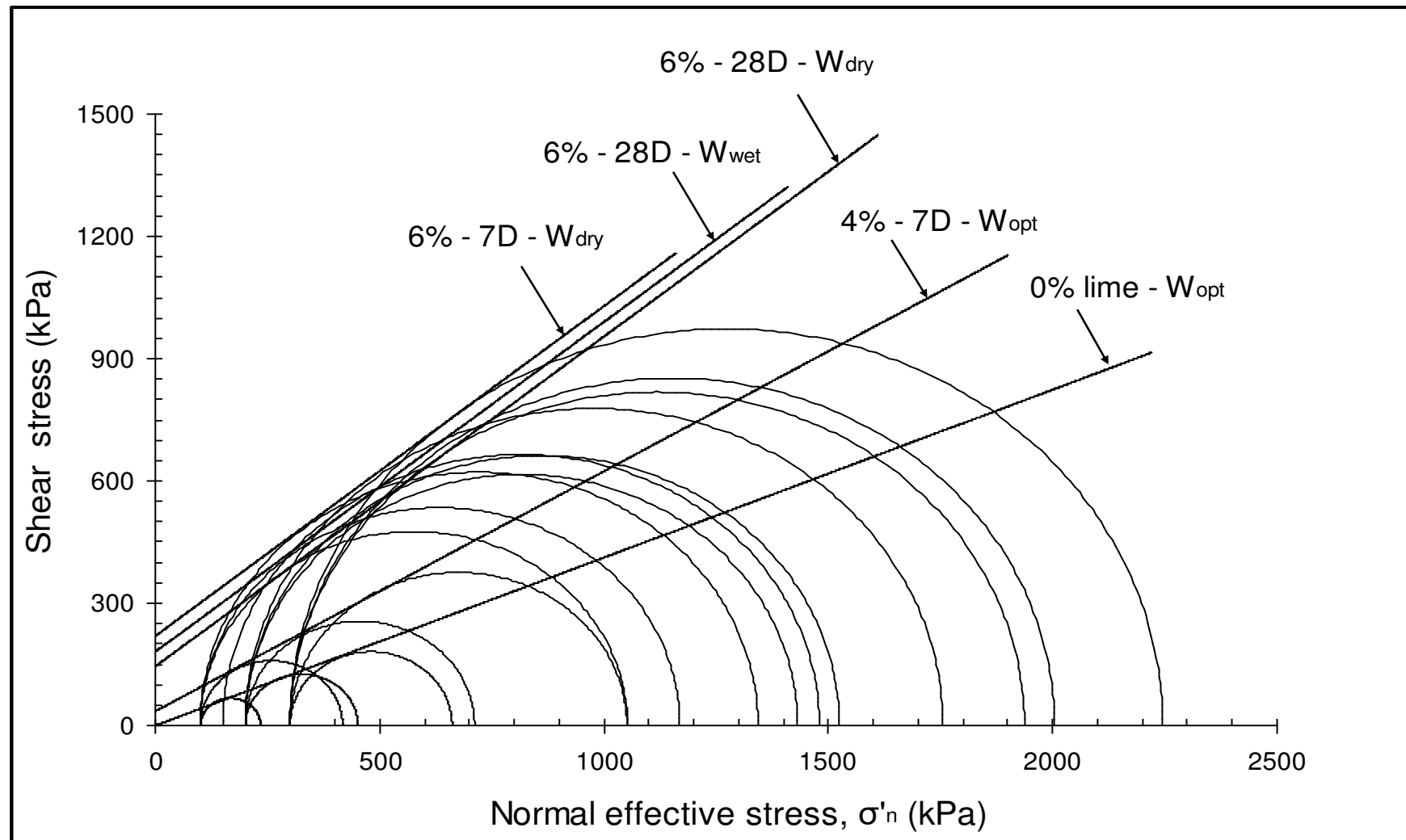
Figure 5.22: Mohr-Coulomb envelopes for lime treated & untreated London Clay

In general the results are consistent with results found in the literature, i.e. that strength parameters of lime-treated soils increase as the degree of cementation increases (e.g. Osinubi, 1998a; Le Runigo, et al., 2011). However, some researchers suggested that while there is a clear *c'* intercept reflecting the effect of cementation, the friction angle stays unchanged compared to that of the uncemented soil (Lambe, 1960; Clough et al., 1981; Cecconi & Russo, 2012). On the other hand other researchers (e.g. Consoli et al., 2000 & 2001; and Schnaid et al., 2001) found friction angles higher than values obtained for the untreated soil.

Table 5.6: Shear strength parameters at peak

Type of tests	*Lime*	*Curing time*	*Water content* (w_c)	*Cohesion* (c')	*Angle of friction* ϕ'_{peak}
	$(\%)$	$(Days)$	$(\%)$	(kPa)	(Deg)
Isotropically consolidated drained compression tests	0	N/A	w_{opt}	7	21
	4	7	w_{opt}	35	30.5
	6	7	w_{dry}	220	39
		28	w_{dry}	145	39
		28	w_{wet}	181	39

5.4.5.   Stress - Dilatancy behaviour of lime treated London Clay

The tendency of a compacted material to dilate (expand in volume) when subjected to shearing, in which there is coupling between shear and volumetric deformation, is identified as "Dilatancy". When stresses are applied to bonded materials and artificially cemented soils, they expand after rupture and exhibit volume change (dilation) under drained conditions (Cuccovillo and Coop, 1999; Asghari et al., 2003). This was the behaviour of the lime-treated specimens observed in this study (as shown in section 5.4.1). Note that an initial compression is generally observed before dilating occurs under shear. A

suitable parameter to quantify a dilatant material is the dilatancy angle (ψ) which is defined by the following expression:

$$\psi = \tan^{-1}\left(-\delta\varepsilon_v / \delta\varepsilon_s\right) \tag{5.4}$$

Where $(\delta\varepsilon_v)$ is the volumetric strain increment and $(\delta\varepsilon_s)$ is the shear strain increment; the negative sign is introduced so that the expansion (negative change in volume) will be transformed into positive dilation rate. Note that the volumetric strain was measured using the external IC volume gauge in a similar way that was used by Cuccovillo and Coop (1999).

During a constant mean effective stress shearing, at large strains, a linear relationship between the stress ratio q/p' and the rate of dilation $\delta\varepsilon_v / \delta\varepsilon_s$ exists (See Figure 5.23). This is represented by Taylor's equation as follow:

$$\frac{q}{p'} = M - a\left(\frac{\delta\varepsilon_v}{\delta\varepsilon_s}\right) \tag{5.5}$$

Where $M = \dfrac{6\sin(\phi'_{cs})}{3 - \sin(\phi'_{cs})}$ \hfill (5.6)

If ε_v is a constant, meaning that the volume change has stabilised, then:

$$\delta\varepsilon_v = 0 \rightarrow \quad \frac{\delta\varepsilon_v}{\delta\varepsilon_s} = 0 \rightarrow \quad \frac{q}{p'} = M \quad \text{indicating that the soil has reached its critical state.}$$

Figures 5.23 & 5.24 investigate the dilatancy of the specimens during the CD tiaxial tests, the results are summarised in Table 5.7. From the figures and Table 5.7, in which dilation was quantified, the effect of different factors (lime addition, curing time and compaction water content) is examined.

Table 5.7: Angle of dilation of consolidated drained (CD) testing specimens

Specimen ID	Lime	Curing time	σ'_3	Water content w_c	Post-curing void ratio e_0	Saturation void ratio e_s	Consolidation void ratio e_c	Dilatancy angle ψ_{max}
	(%)	(Days)	(kPa)	(%)	-	-	-	(Deg)
$CD_1(0-0)_{100}$			100		0.936	1.194	1.106	N/A*
$CD_2(0-0)_{200}$	0%	None	200	w_{opt}	0.937	1.199	1.014	N/A *
$CD_3(0-0)_{300}$			300		0.938	1.200	0.953	N/A *
$CD_1(4-7)_{100}$			100		0.949	1.153	1.140	7.66
$CD_2(4-7)_{200}$	4%	7	200	w_{opt}	0.948	1.176	1.124	4.2
$CD_3(4-7)_{300}$			300		0.944	1.190	1.111	2.28
$CD_1(6-7)_{100}$			100		0.937	1.142	1.141	64.84
$CD_2(6-7)_{150}$		7	150	w_{dry}	0.938	1.140	1.138	67.01
$CD_3(6-7)_{200}$			200		0.941	1.141	1.137	71.04
$CD_4(6-7)_{300}$			300		0.940	1.139	1.133	70.77
$CD_5(6-28)_{100}$	6%		100		0.951	1.123	1.122	59.39
$CD_6(6-28)_{200}$			200	w_{dry}	0.950	1.107	1.103	57.27
$CD_7(6-28)_{300}$			300		0.952	1.093	1.086	52.09
$CD_8(6-28)_{100}$		28	100		0.943	1.049	1.047	67.46
$CD_9(6-28)_{200}$			200	w_{wet}	0.942	1.041	1.036	51.61
$CD_{10}(6-28)_{300}$			300		0.940	1.038	1.028	33.20
(*) No dilation occurred								

4% Lime - 7D - W$_{opt}$

(b)

6% Lime - 7D - W$_{dry}$

Legend:
- □ 100 kPa
- ○ 150 kPa
- ◇ 200 kPa
- △ 300 kPa
- ● Maximum dilation

y-axis: Stress ratio (q/p')

x-axis: Dilatancy, D = -($\delta\varepsilon_v/\delta\varepsilon_s$)

(c)

6% Lime - 28D - W$_{dry}$
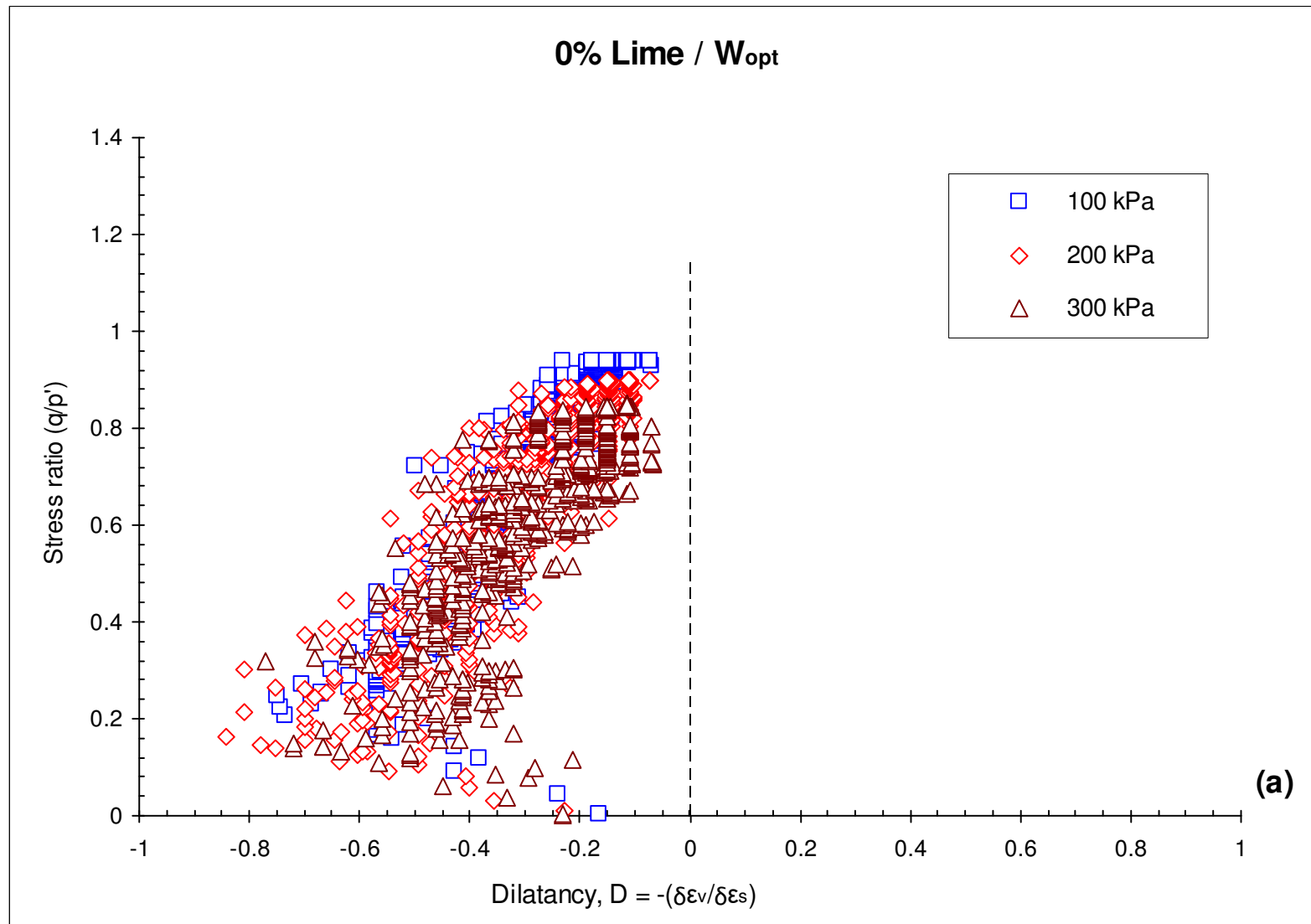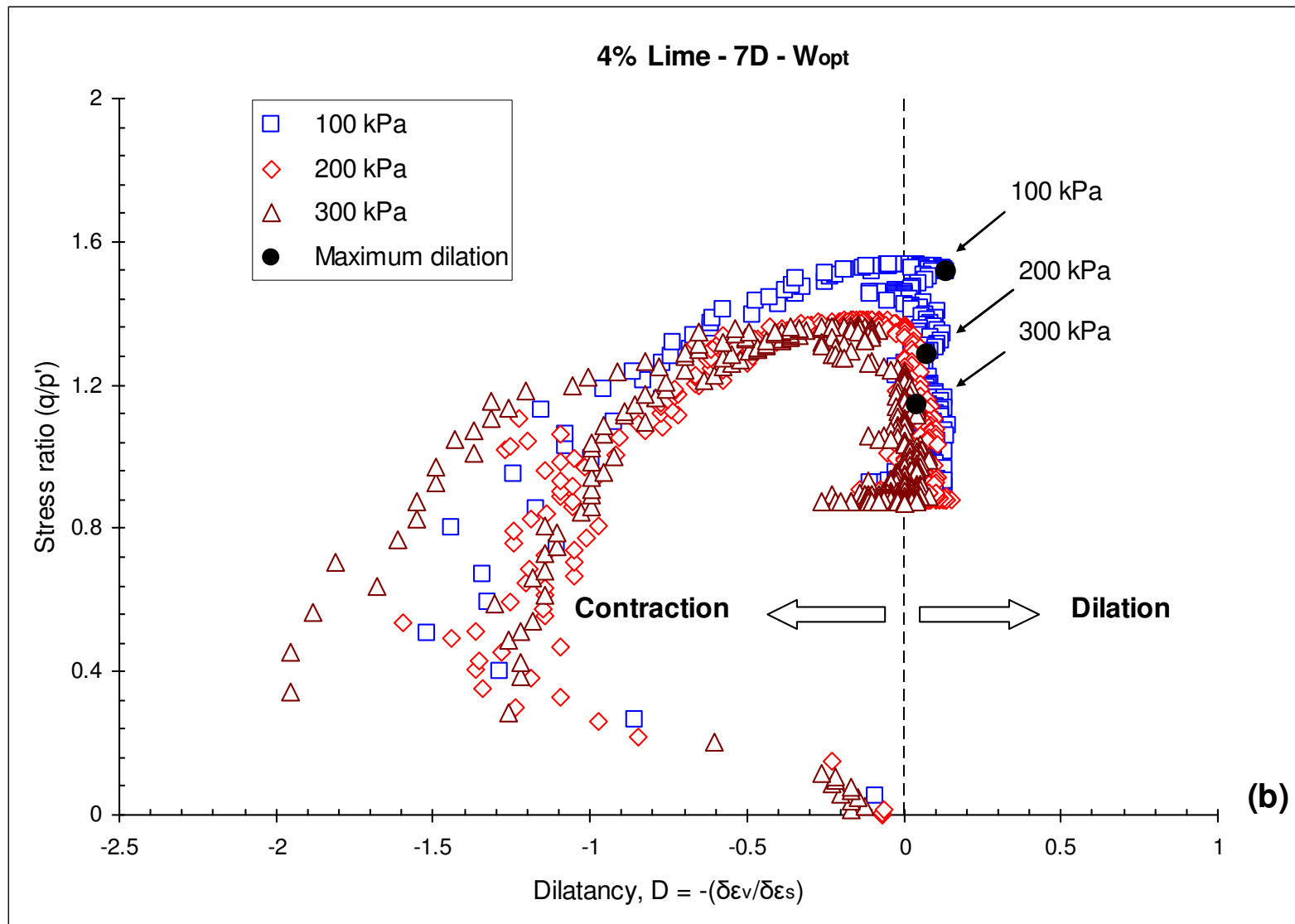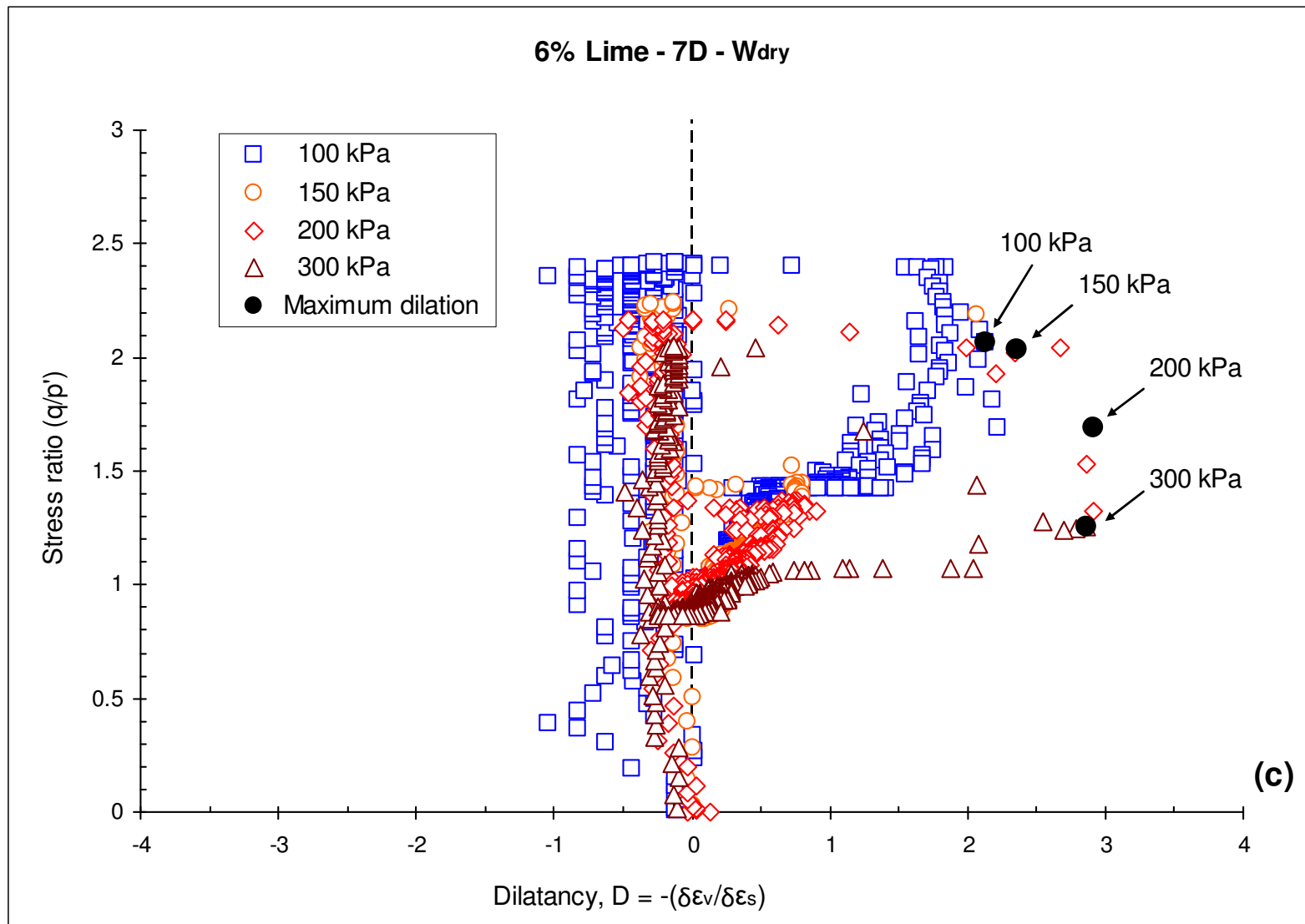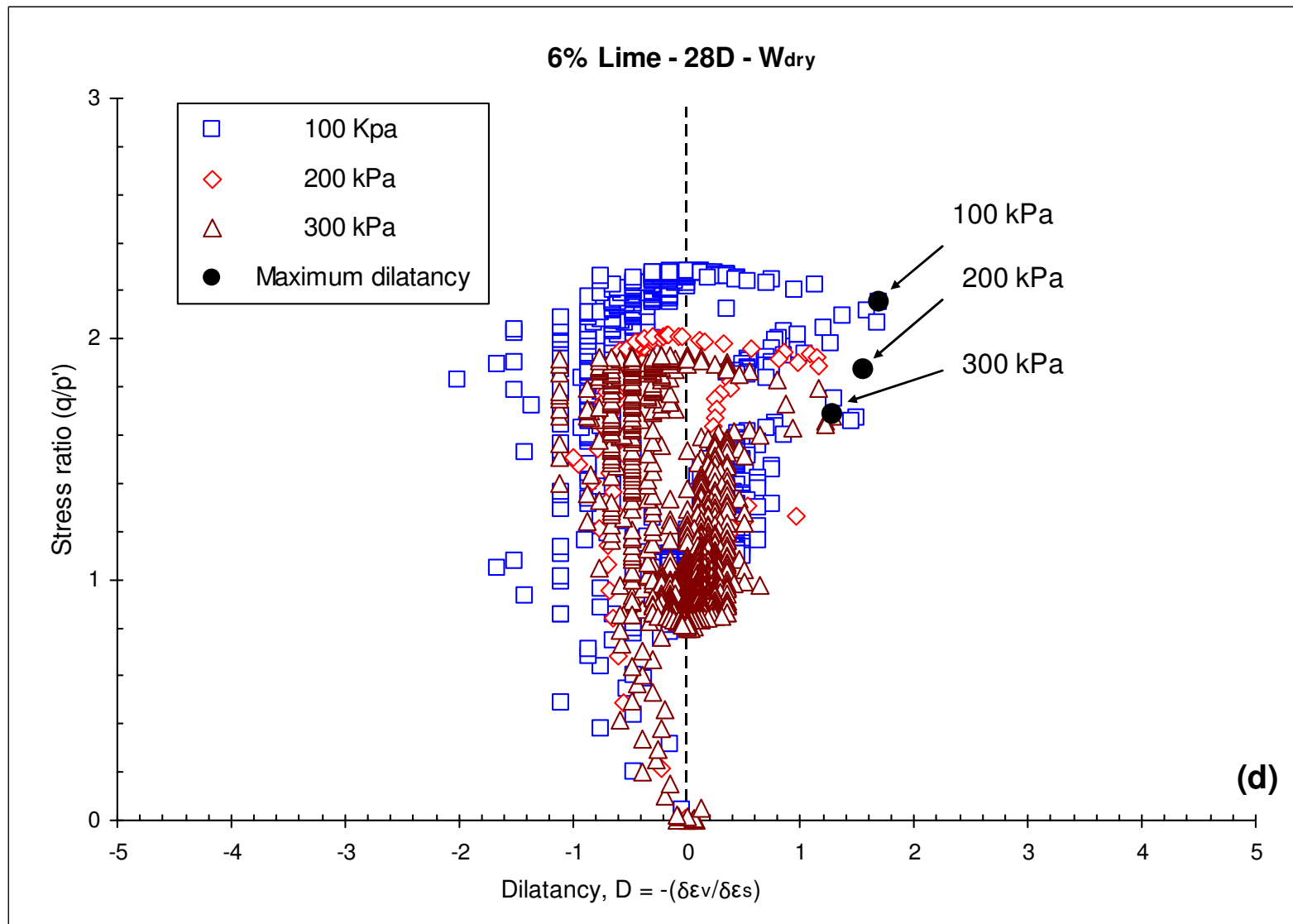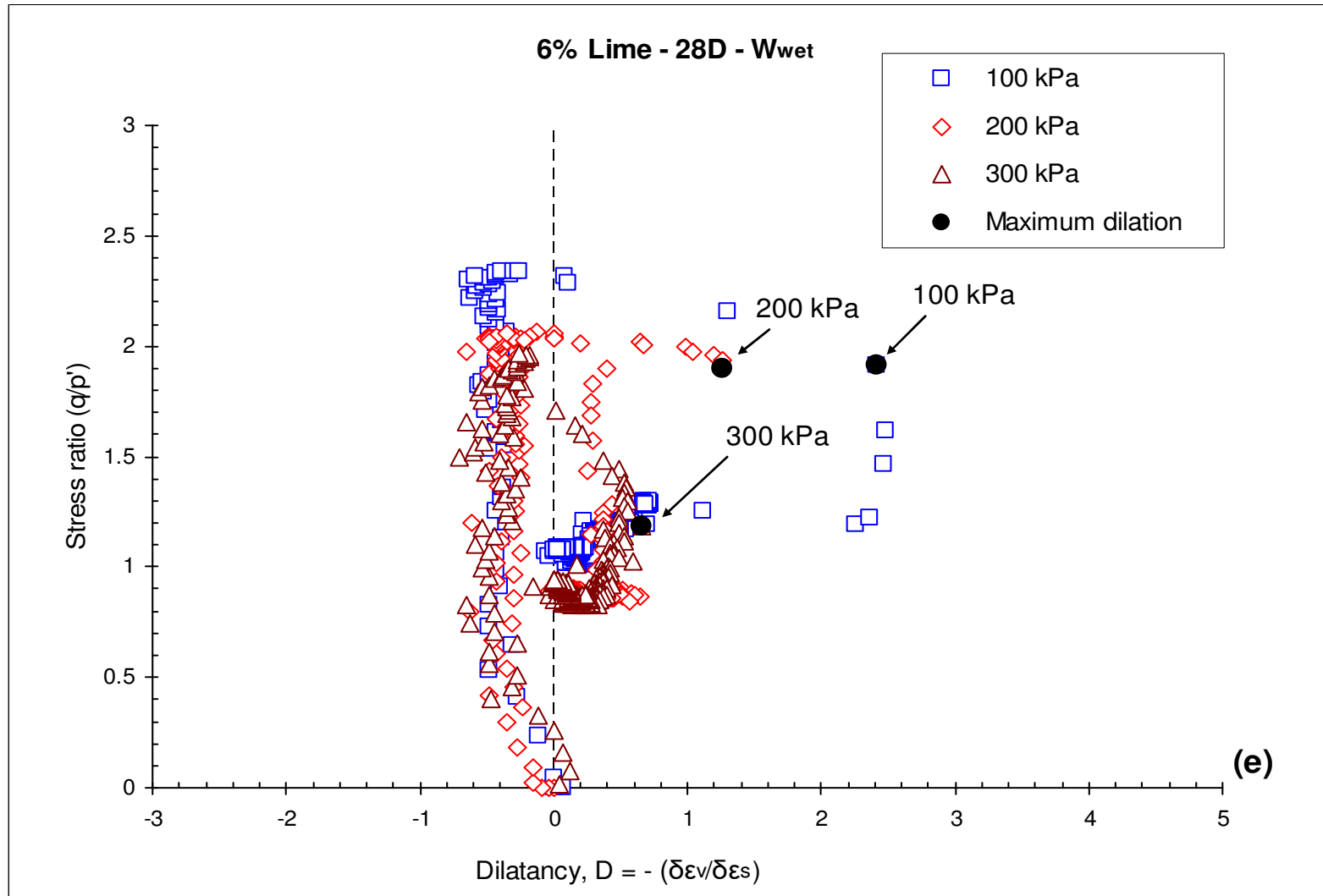
Figure 5.23: Stress-dilatancy behaviour of lime treated and untreated London Clay

0% Lime - W$_{opt}$

(a)

4% Lime - 7D - W$_{opt}$

(b)

(c)
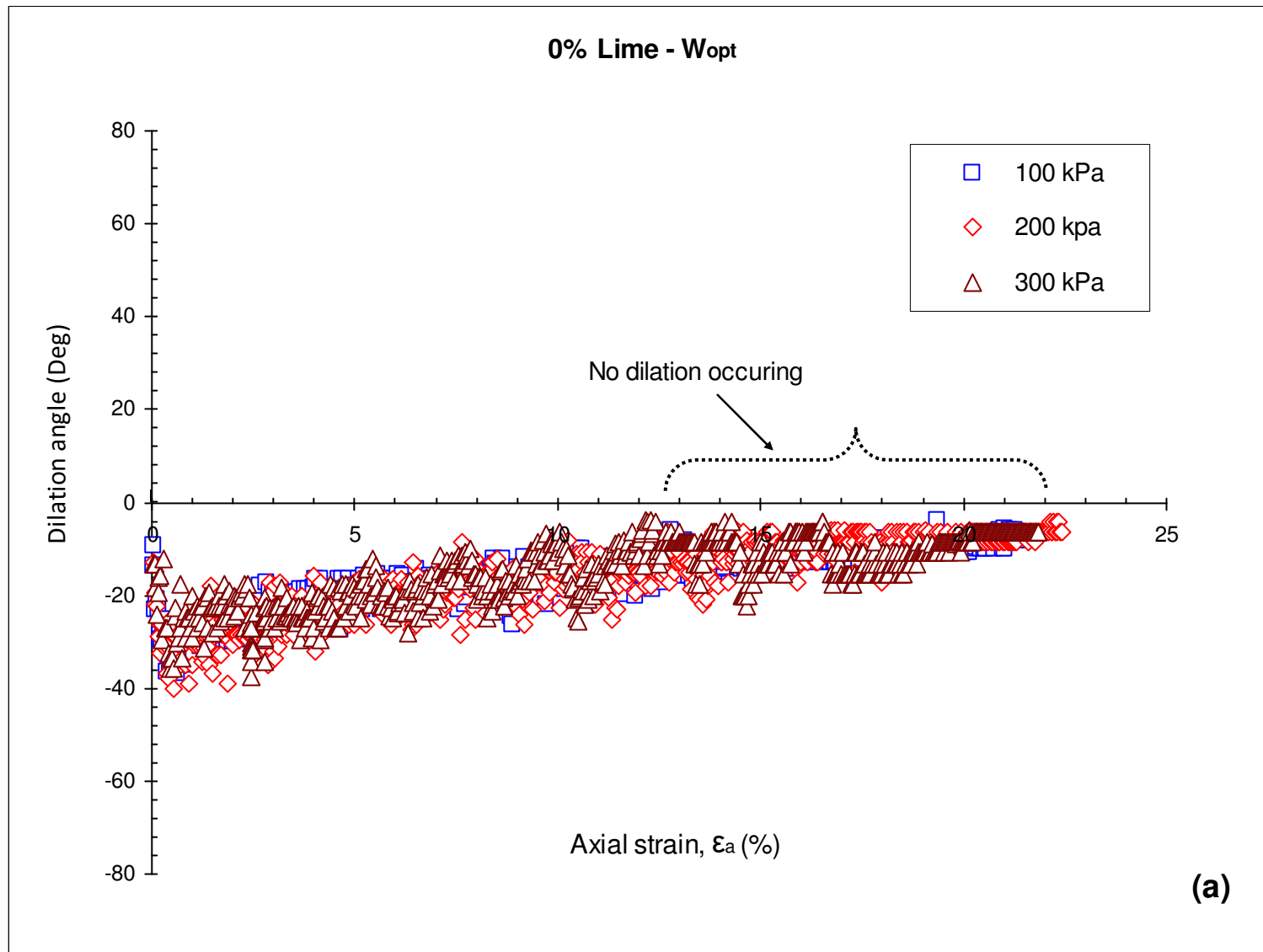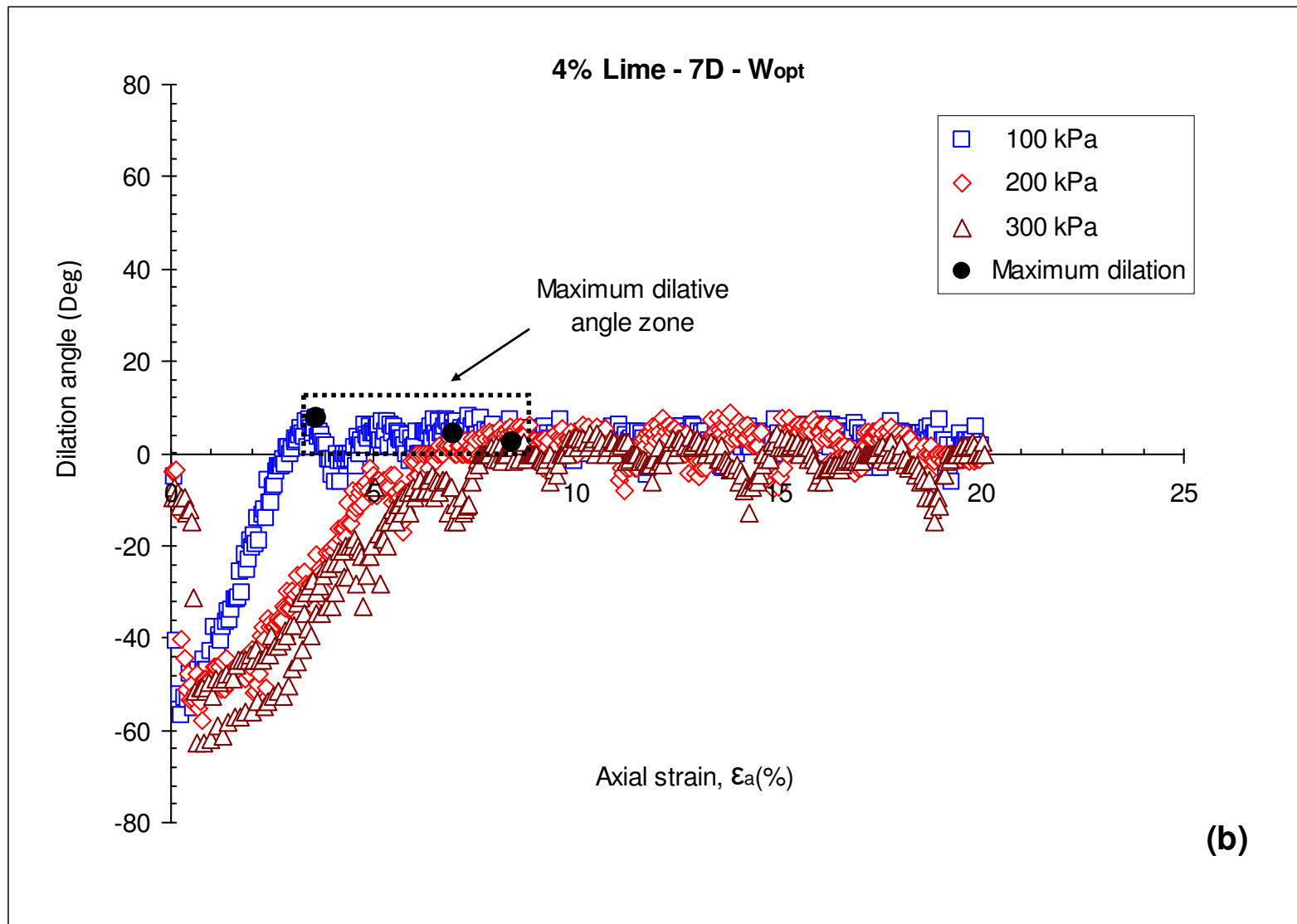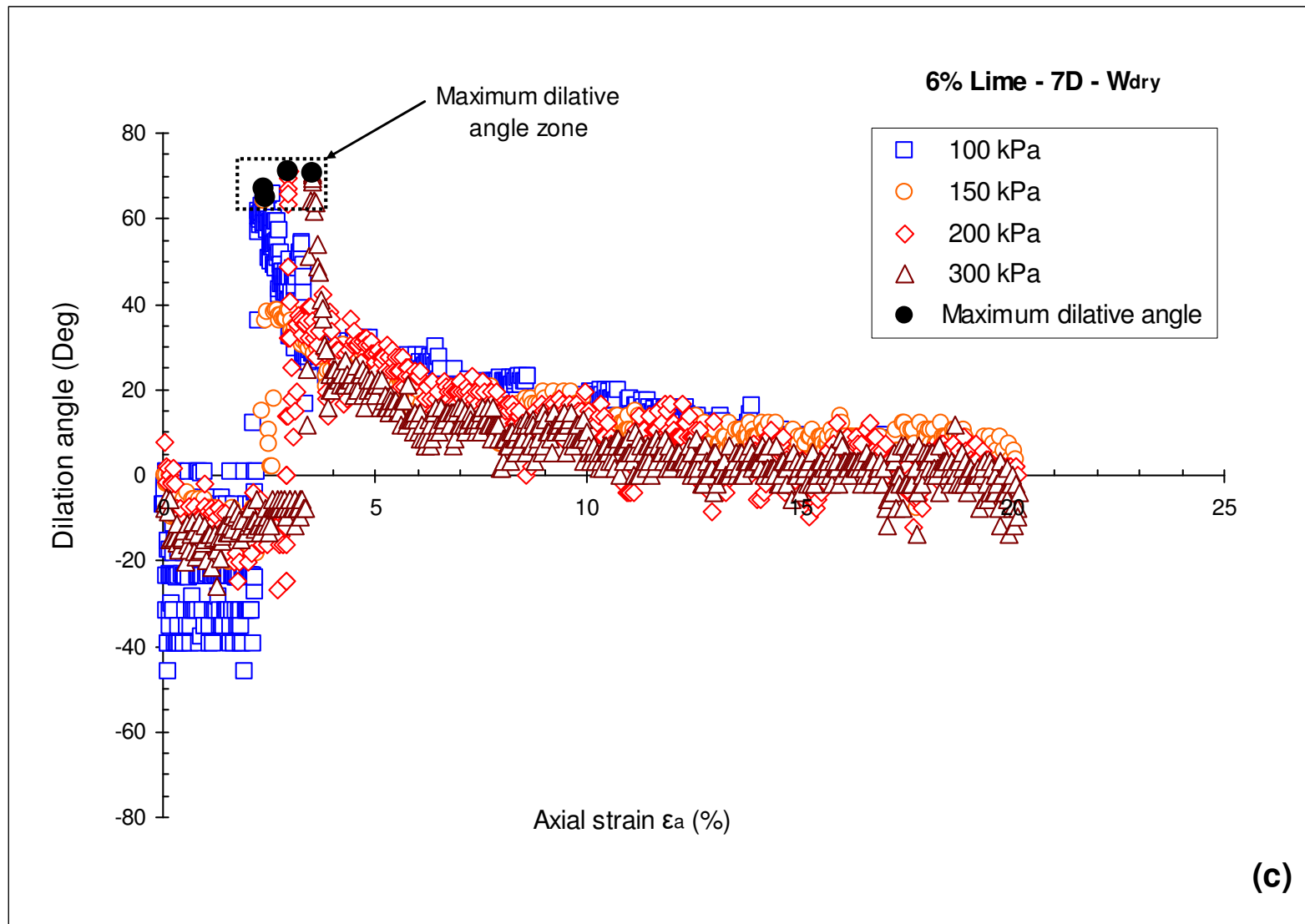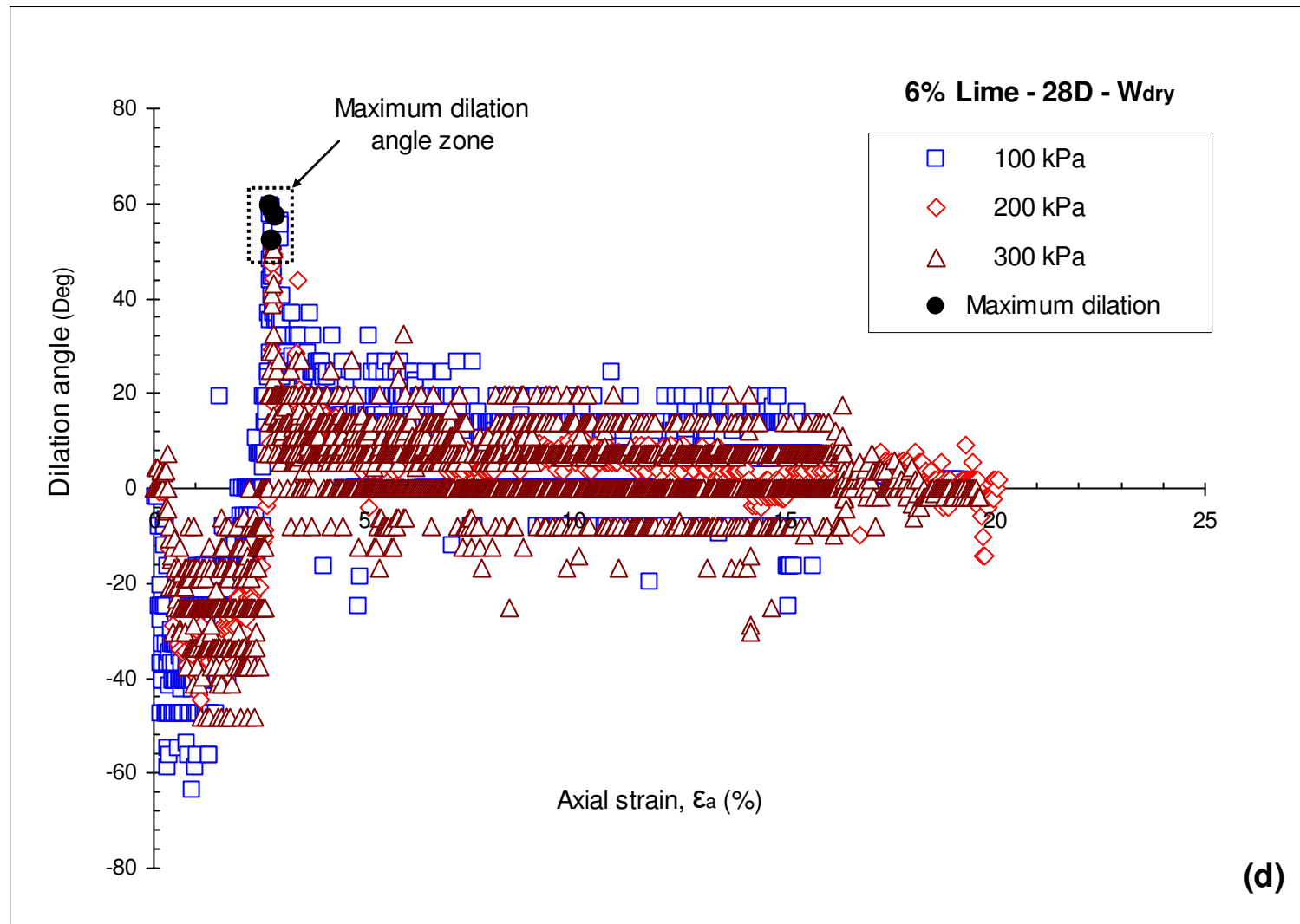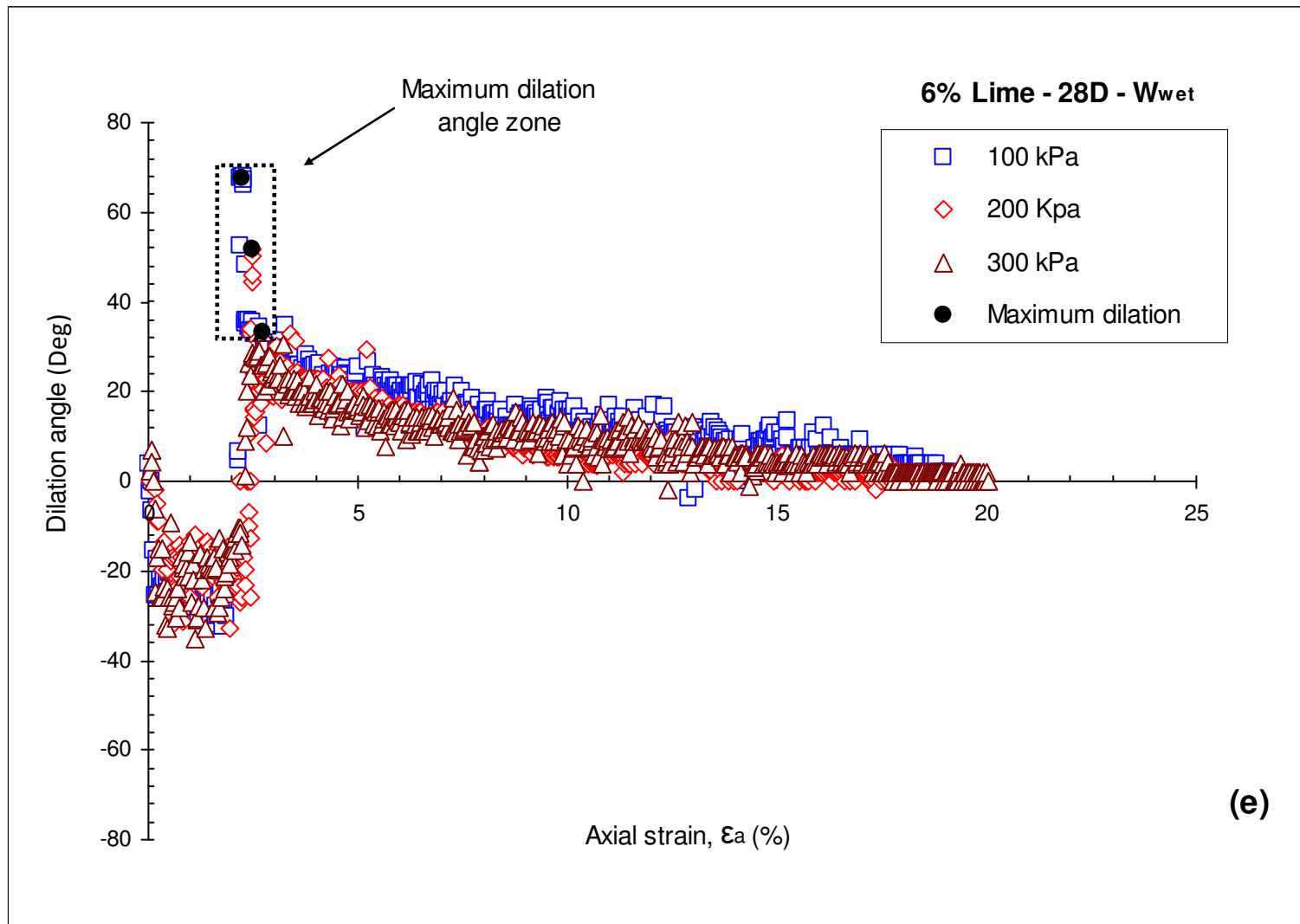
Figure 5.24: Lime treated and untreated London Clay dilation angle

For untreated London Clay, a contracting behaviour was observed for the three tested specimens at different effective confining pressures (100, 200 & 300 kPa). The initial specific volume position is on the wet side of critical state. For larger deformations, the untreated London Clay volume tends to stabilise to a constant value at a constant deviator stress. No dilation was observed for these specimens $(\psi_{max} \approx 0)$. For 4% lime treated London Clay, a higher contraction phase is observed. However, it is followed by a dilatancy phase after the peak state, which is related to destructuration. 6% lime treated London Clay specimens exhibit a limited contraction as would be expected and shown in Figure 5.23 c, d & e, until reaching the ultimate compressive state where they can not contract any further. Then failure occurs, followed by a more pronounced dilating behaviour (compared to 4% lime-treated specimens) after the peak, gradually decreasing to approach the critical state stress ratio equal to M. An inflexion is detected in the variation of the volumetric strain corresponding to an axial strain approximately between 5 and 10%. This behaviour occurs after the sample has ruptured due to the development of the shear band before the peak at a low average deviator stress, indicating a decrease in the dilating rate from this state onwards.

Overall, for all lime treated specimens, a distinct transfer from contractive to dilative response under drained conditions is observed between 2 to 3% axial strain. Volumetric response was detected to be slightly more contractive for 4% lime treated specimens (7 days curing) compared to the untreated London Clay response. Nevertheless, the lime amount increase from 4 to 6% caused an increase in the dilatancy angles, ranging between $65°$ and $70°$ which is due to cementation effects (Figure 5.24c). Such dilative behaviour if ignored can lead to significant error predicting the ultimate bearing stresses, deformation or stability of geotechnical structures.

- **Effect of lime addition on London Clay stress-dilatancy behaviour**

Lime treated London Clay dilative behaviour is considerably influenced by the amount of added lime. Figure 5.25 in which stress ratio and dilatancy behaviour obtained at constant effective confining pressure (200 kPa) are plotted. A single trend has been identified in a similar way as Coop & Wilson (2003) were able to observe for Castlegate sand.
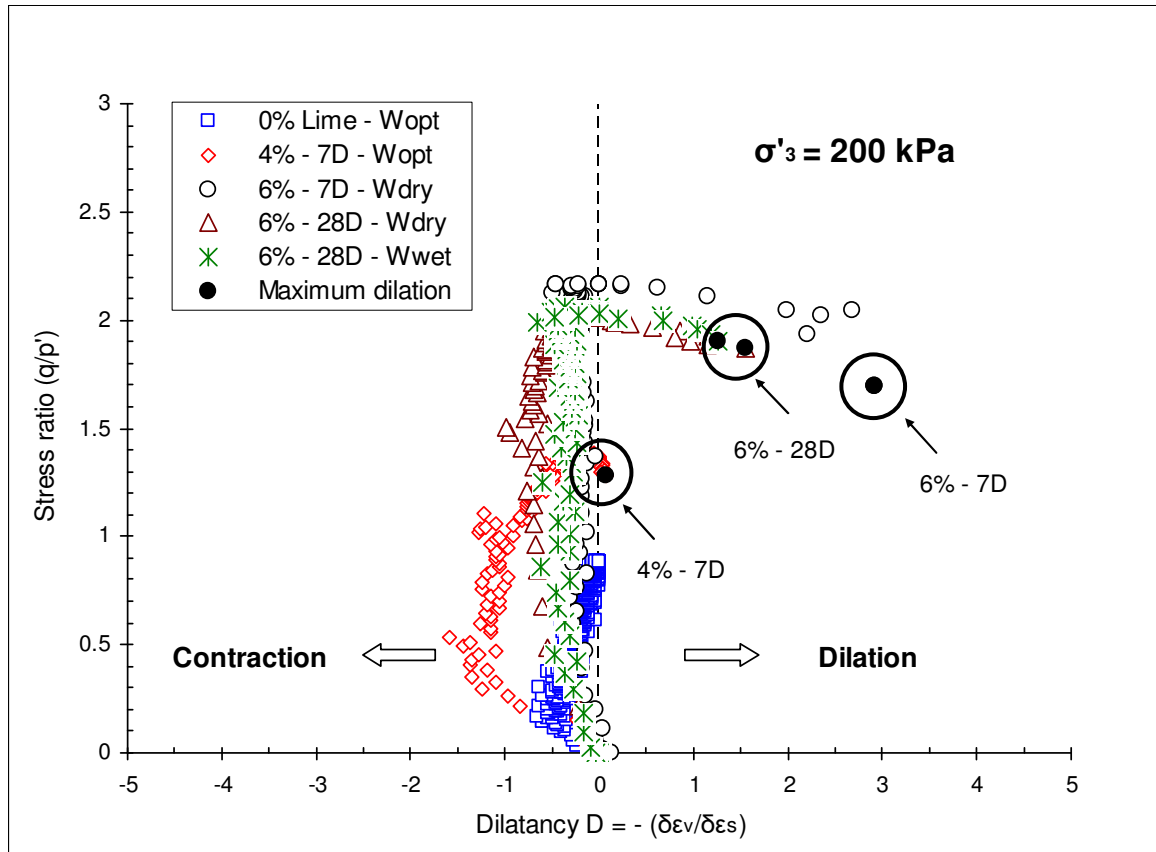
Figure 5.25: Effect of lime addition and curing time on London Clay dilatancy

The dilation behaviour seems to be more pronounced at higher lime amount (6%) where cementation bonds are stronger, which is in accordance with laboratory data of Schnaid et al. (2001) reported by Yu et al. (2007) on artificially cemented soil. In addition, Fig. 5.25 shows that lime addition increased the maximum stress ratio and dilatancy extent (for higher lime amount) occurring at a lower axial strain. However, the contraction (strain hardening) was observed to be more pronounced in 4% lime treated London Clay specimens, but has diminished with increasing lime amount from 4 to 6%. Note that the maximum dilation is not captured at the maximum stress ratio $(q/p')_{max}$, it occurs beyond the peak stress ratio. Asghari et al. (2003) indicated that in cemented samples the maximum rate of dilation take place after the maximum stress ratio which is in line with this study. Moreover, Leroueil and Vaughan (1990) showed that when dilation is due to densely packed materials, the peak and maximum dilation points coincide, but when the peak strength is controlled by cementation rather than density, the maximum rate of dilation occurs after the bonding has yielded, confirming the presence of cementation bonds in the lime treated London Clay specimens used in this study. This suggests that

cementation bond control entirely the peak shear strength of the treated samples and dilation is playing a secondary role. The most extensive dilation was observed for 6% lime treated London Clay sample cured for 7 days (Fig. 5.25), and 4% lime treated sample cured for 7 days, was found to dilate less, clearly suggesting that the higher the lime amount, the more pronounced the dilation appears to be.

- **Effect of curing time on the dilatancy of lime treated London Clay**

In order to identify the stress-dilatancy response and the behaviour mechanism of lime treated London Clay, an investigation was carried out using (q/p') - $(\delta\varepsilon_v/\delta\varepsilon_s)$ graphs. Figures 5.23 c & d show the stress dilatancy response of 6% lime treated London Clay specimens, cured for 7 and 28 days respectively. These initially displayed a compressive response (more pronounced for 28 days cured specimens), followed by dilative behaviour until reaching a maximum dilation angle. The highest maximum dilation angle was observed subsequently for the 6% treated specimens cured for 7 days (Fig. 5.25), this is due to the higher strength / brittleness exhibited by the material as indicated in section 5.4.1. The rate of dilation reduced to approach zero value at the critical state ($M = 0.87$). The sudden change in volume due to dilation suggests that bond breakage must have occurred. Similar observations were made by Lade & Overton (1989). The authors have indicated that highly interlocked particles, showed greater rates of dilation during shearing at low confining stresses.

- **Effect of effective confining pressure on lime treated London Clay dilatancy**

Based on Figures 5.23 b, c, d & e, the following observations can be made on the effect of effective confining pressure on lime treated London Clay soil. As would be expected, the stress-dilatancy curve indicates that the maximum dilatancy is obtained at a lower effective confining stress and reduces gradually with confining pressure increase. Note that dilation may be completely suppressed at high pressures (not possible to obtain with the available equipment) as reported by Asghari et al. (2003). The authors indicated that artificially cemented soils show a post-rupture dilative response in shear (brittle failure) at low confining stresses, but also showed the transition from dilative to contractive behaviour (ductile failure) at higher confining stresses.

- **Effect of the initial water content on lime treated London Clay dilatancy**

An initial water content increase from 27 to 32% produced a larger range of dilatancy angles varying between 33º and 67º (Fig. 5.24 d & e). The cohesive shear strength for all 6% lime treated specimens vanishes in the region of 2.5% strain; at the same time the frictional strength becomes dominant.

5.5. Consolidated Undrained (CU) Triaxial test

In addition to CD triaxial tests, two isotropically consolidated undrained (CU) Triaxial compression tests were performed on 6% lime treated London Clay specimens, cured for 28 days. The effective confining pressures applied to these samples were 158 and 250 kPa. Table 5.8 summarises the maximum excess pore water pressure (PWP) changes obtained during the CU tests.

The deviator stress - axial strain $(q - \varepsilon_a)$, and excess pore water pressure - axial strain $(u - \varepsilon_a)$ relationship of 6% lime treated London Clay are shown in Figures 5.27a & 5.27b. No major difference was observed in the shearing behaviour of the two specimens. However, as was expected, the peak deviator stress was found to increase with the effective confining stress increase (Figure 5.27a). The increase in effective stress caused a higher excess PWP as indicated in Figure 5.27b. It can also be observed that, at a very low strain $(\leq 2\%)$, excess PWP is shown to be of value equal or higher than effective stress. As a result, the effective stress dropped to zero, or lower in the case of $CU_1(6-28)_{158}$ specimen. This indicates rupture of the specimen by vertical splitting cracks, which is a sign of a tensile failure.

Undrained test results on 6% lime treated samples showed that the excess pore water pressure was positive at the beginning of shear (tendency for sample contraction) and changed to negative as strain increased (tendency for sample dilation). The initial state in this case is said to be on the dry side of critical. The pore pressure balances the increase in total mean stress imposed in this constant cell pressure $\delta u = \delta q / 3$ as shown in Figure 5.28b. It was seen that substantial post-peak strength reduction took place as shearing progressed (Haeri et al., 2005). No strain softening behaviour was observed, due to

breakage of cementation bonds by tensile failure, implying that 6% lime addition to London Clay after 28 days curing prevented the new material reaching the plastic state during shearing compression under undrained conditions. This explains the linear pre-peak behaviour of the specimens observed in the stress space $(q - p')$ (Figure 5.27a). Similar results were reported by Oh et al. (2008) and Muhunthan & Sariosseiri (2008).

Figure 5.28a shows the PWP changes with the stress ratio (q/p') for 6% lime treated London Clay samples cured for 28 days. Undrained tests results show higher stress ratios achieved at the maximum gradient $\left(\dfrac{q}{p'} = 3\right)$ compared to the drained tests. Also it can be seen that the maximum PWP change $(\delta\varepsilon_u / \delta\varepsilon_a)_{max}$ occurs after the maximum stress ratio, which is in line with the observations reported by Malandraki (1994) and later by Asghari et al. (2003) for other cemented materials.

Table 5.8: Isotropically consolidated undrained (CU) triaxial test data

Specimen ID	*Lime*	*Curing time*	*Initial σ'_3*	*Water content w_c*	*Post-curing void ratio e_0*	*Saturation void ratio e_s*	*Consolidation void ratio e_c*	$\left(\dfrac{\delta u}{\delta\varepsilon_a}\right)_{max}$
	$(\%)$	$(Days)$	(kPa)	$(\%)$	-	-	-	-
$CU_1(6-28)_{158}$	6%	28	158	w_{dry}	0.949	1.114	1.111	332.03
$CU_2(6-28)_{250}$			250		0.948	1.099	1.094	954.7

In the previous section, it was shown that lime treated London Clay peak stress is generally reached within a short strain range, followed by continuous post-peak deviator stress. At the end of the test, a fairly constant deviator stress was obtained at approximately 20% strains. In addition, the $\varepsilon_v - \varepsilon_a$ graphs (see Fig. 5.8 & 5.9) showed no further volume change within the same range of strains. This post-rupture state will therefore be referred to as critical state.

(a)
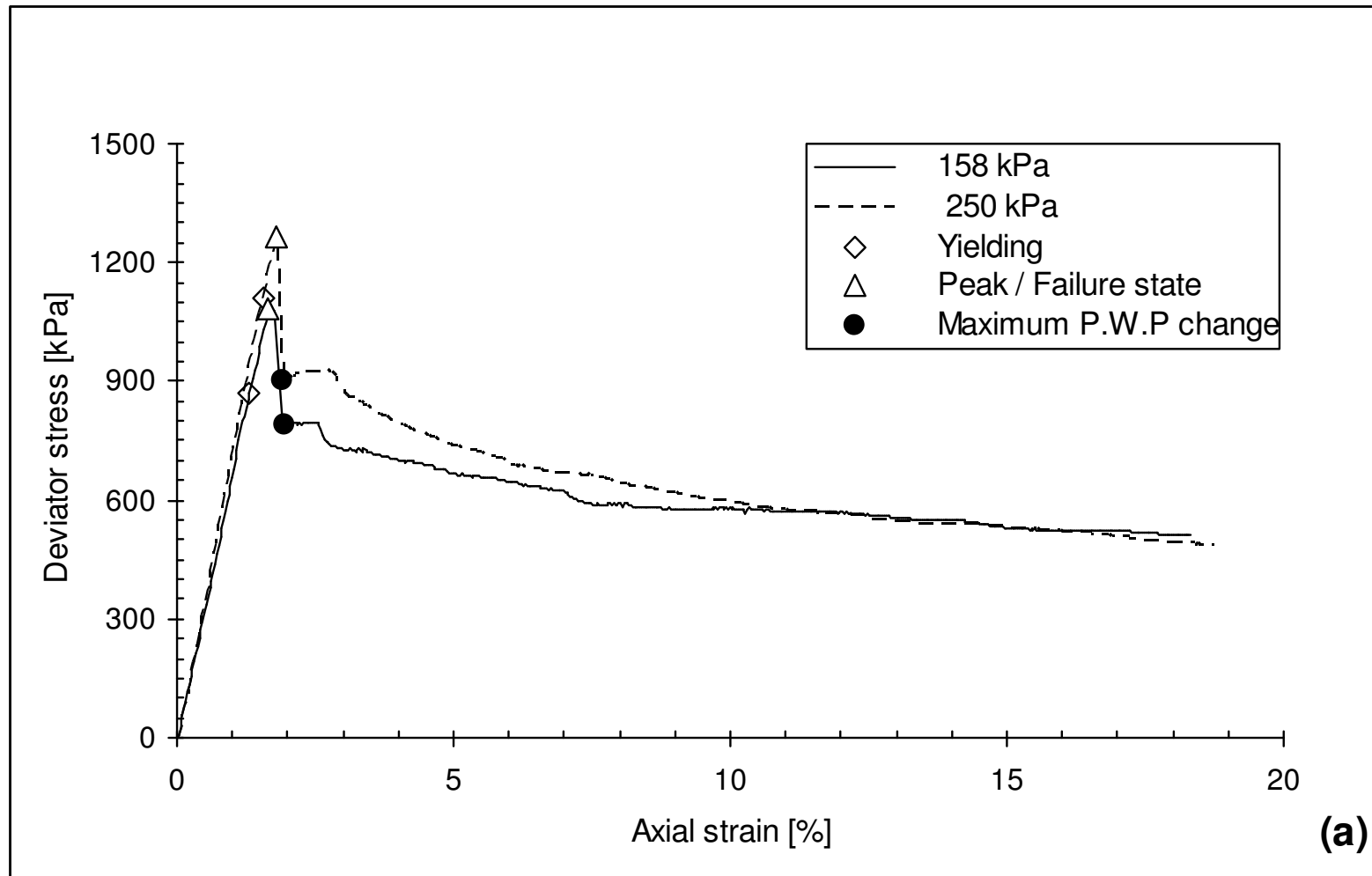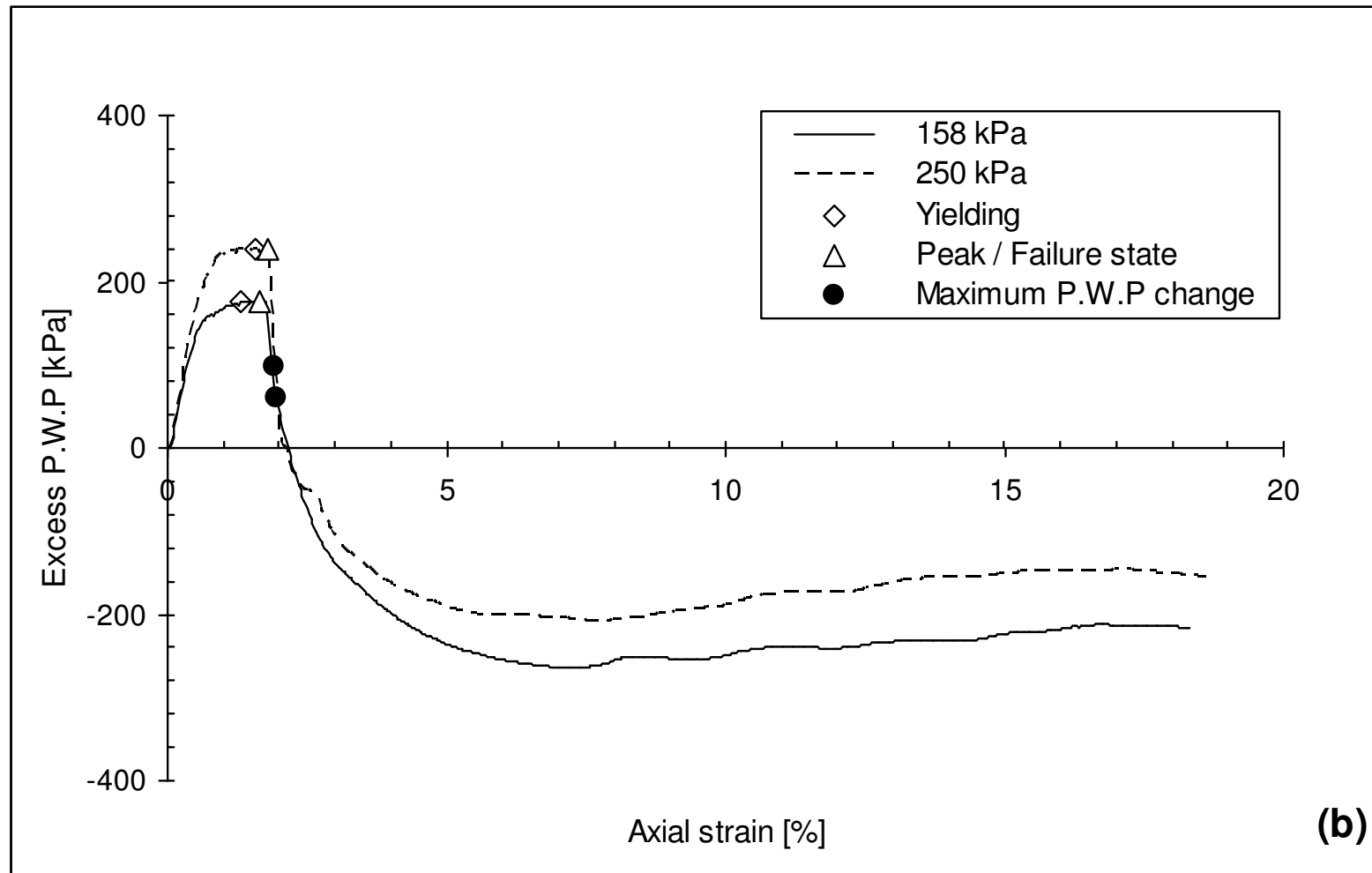
Figure 5.27: Consolidated undrained (CU) triaxial compression tests on 6% lime treated London Clay: (a) Stress-strain, (b) Excess PWP-strain

(a)
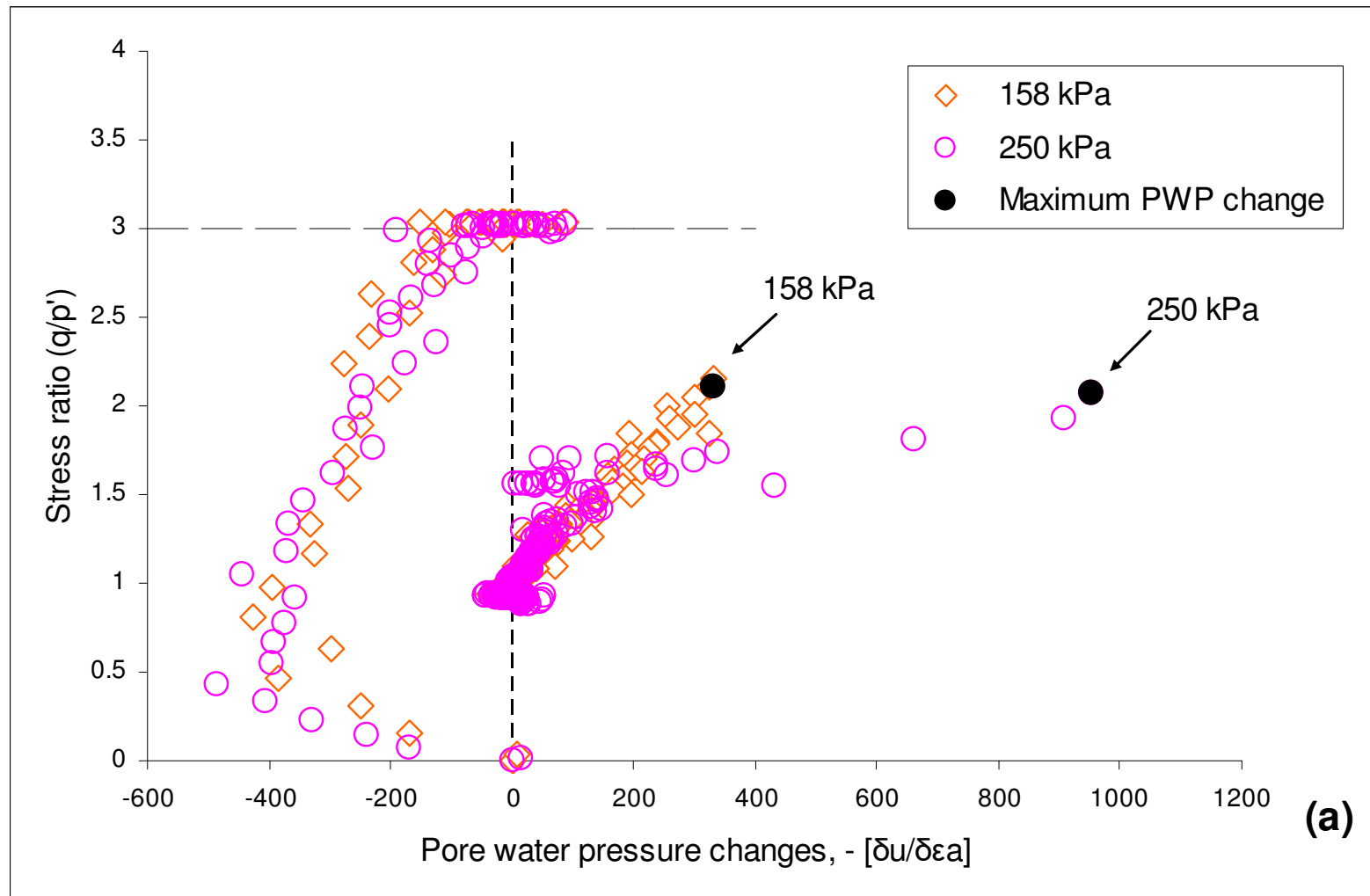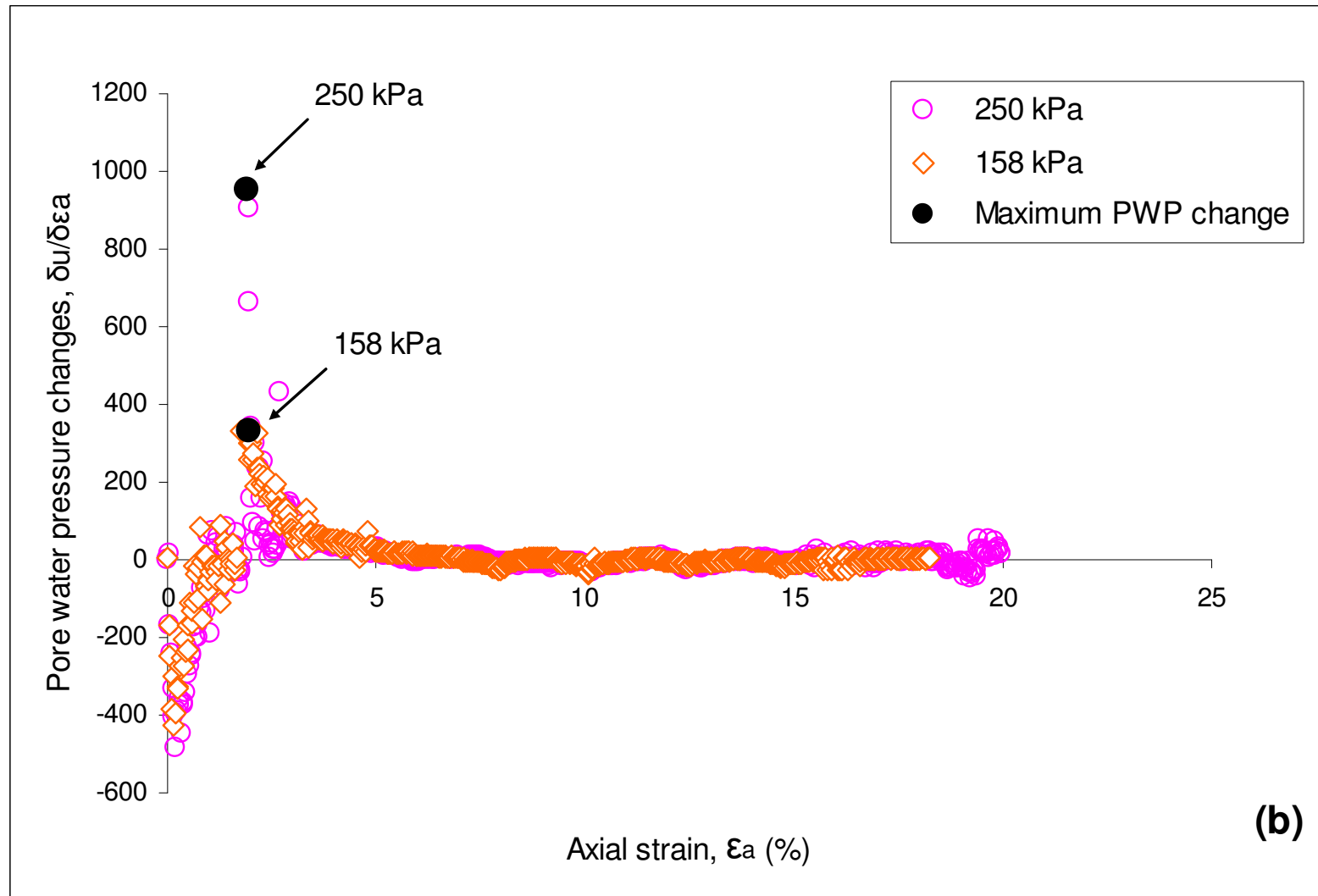
Figure 5.28: Pore water pressure change on 6% lime treated London Clay: (a) Stress ratio-PWP, (b) PWP-strain

Chapter 6

6. Interpretation of the results using CSSM framework

This chapter analyses the triaxial testing results obtained in this study using a Critical State Soil Mechanics Framework.

According to this theory, at failure there exists a unique relationships among specific volume v_{cs}, mean effective stress p_{cs}' and deviator stress q_{cs}, which can be expressed by two following equations as:

$$q_{cs} = Mp_{cs}' \tag{6.1}$$

which represents the projection of the critical state line onto $q - p'$ space, and

$$v_{cs} = \Gamma - \lambda_{cs} \ln p_{cs}' \tag{6.2}$$

which is the projection of the critical state line on $v - \ln p'$ compression plane

in the above equation q_{cs} is the deviator stress at critical state and p'_{cs} is the mean effective stress at critical state and M is the gradient of the critical state line in $q - p'$ stress space.

The critical state on the specific volume - mean effective stress (v, p') plane is thus defined by two material parameters: λ_{cs} the slope of the end of test line, and Γ, the specific volume intercept at unit pressure $(p' = 1kPa)$. The compression lines under constant stress ratios are parallel to each other (according to the theory), as shown in Figure 6.1.

In triaxial tests, the stress ratio usually approaches a constant value at the end of test state. In this study, it has proved difficult, for this type of material, to identify at a continuous shearing a constant stress ratio along with a constant volume change. This is believed to be due to the low effective stresses applied in these tests, and also to the non uniform post-peak deformation observed in lime treated London Clay samples. It is arguable if the post

rupture end of test state is a critical state (Burland, 1990). However, this is the mention given here to the end of test stresses and strains and that this state will be discussed here using the critical state of the untreated soil as a reference for comparisons.
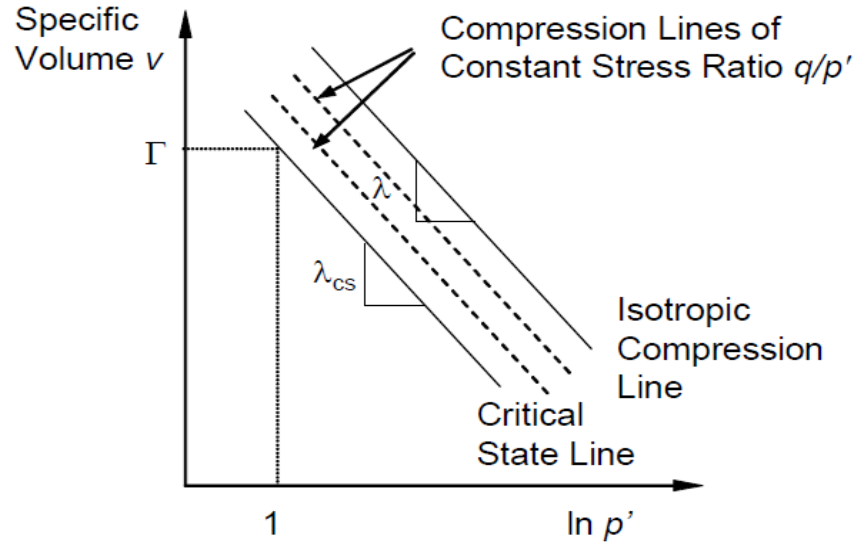
Figure 6.1: Representative critical state line & normal compression line (Mitchell & Soga, 2005)

Critical state stress ratio $(q/p')_{cs}$ values derived from the end points of the test data are presented in table 6.1. A range of critical state stress ratio variation is shown, along with a variation of critical state friction angle ϕ'_{cs} with a mean effective stress increase.

6.1. Critical state line of lime treated London Clay in stress space (q-p')

The end points were plotted in $(q-p')$ and $(v-\ln(p'))$ space graphs (Figures 6.2, 6.3 & 6.4). A best fit line believed to be close to critical state conditions was drawn through the end points in the stress plane $(q-p')$ (Figure 6.2 a, b & c). Although the theoretical treatment of non-uniform deformation development in specimens is complex (Vardoulakis, 1978 & Vermeer, 1982), the end points used in this study were found to be consistent in providing the closest state to critical state conditions.

Table 6.1: Critical state parameters of lime treated & untreated Triaxial tests

Specimen ID	σ'_3	Critical state void ratio e_{cs}	P_{cs}'	q_{cs}	$(q/p')_{cs}$	ϕ'_{cs}
	(kPa)	-	(kPa)	(kPa)	-	(Deg)
$CD_1(0-0)_{100}$	100	0.988	144.61	133.83	0.93	23.63
$CD_2(0-0)_{200}$	200	0.899	283.73	251.20	0.89	22.69
$CD_3(0-0)_{300}$	300	0.840	420.45	361.34	0.86	22.08
$CD_1(4-7)_{100}$	100	1.141	144.78	134.35	0.93	23.69
$CD_2(4-7)_{200}$	200	1.089	285.13	255.40	0.90	22.93
$CD_3(4-7)_{300}$	300	1.051	421.91	365.74	0.87	22.25
$CD_1(6-7)_{100}$	100	1.293	143.79	131.37	0.91	23.36
$CD_2(6-7)_{150}$	150	1.262	208.93	176.80	0.85	21.77
$CD_3(6-7)_{200}$	200	1.239	283.97	251.90	0.89	22.73
$CD_4(6-7)_{300}$	300	1.221	421.21	363.64	0.86	22.17
$CD_5(6-28)_{100}$	100	1.157	152.57	157.70	1.03	26.16
$CD_6(6-28)_{200}$	200	1.121	297.02	291.06	0.98	24.91
$CD_7(6-28)_{300}$	300	1.095	435.10	405.29	0.93	23.78
$CD_8(6-28)_{100}$	100	1.146	155.90	167.70	1.08	27.13
$CD_9(6-28)_{200}$	200	1.093	288.67	266.00	0.92	23.54
$CD_{10}(6-28)_{300}$	300	1.080	437.29	411.86	0.94	24.02
$CU_1(6-28)_{158}$	158	-	557.77	410.22	0.91	23.38
$CU_2(6-28)_{250}$	250	-	518.93	480.40	0.93	23.64
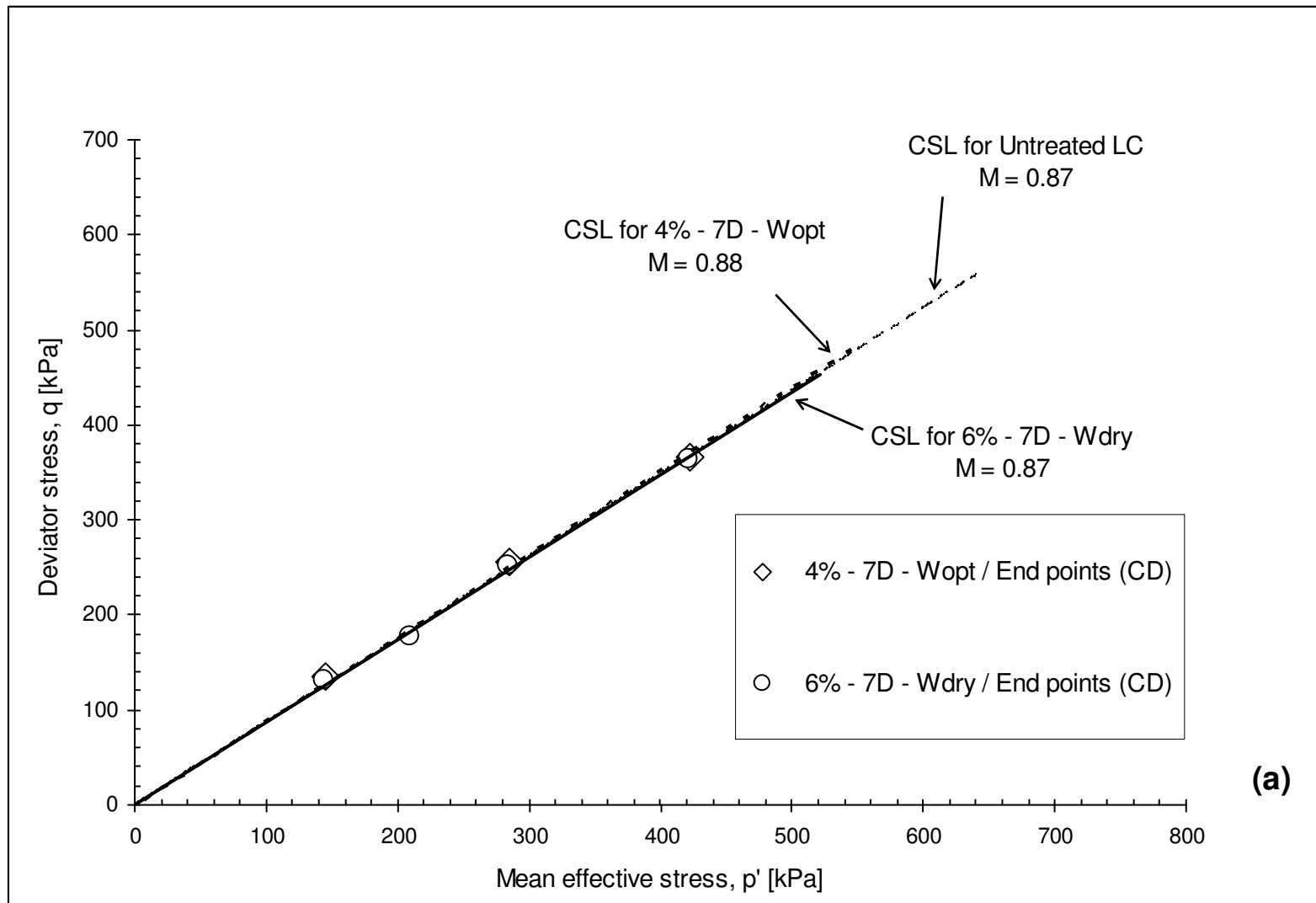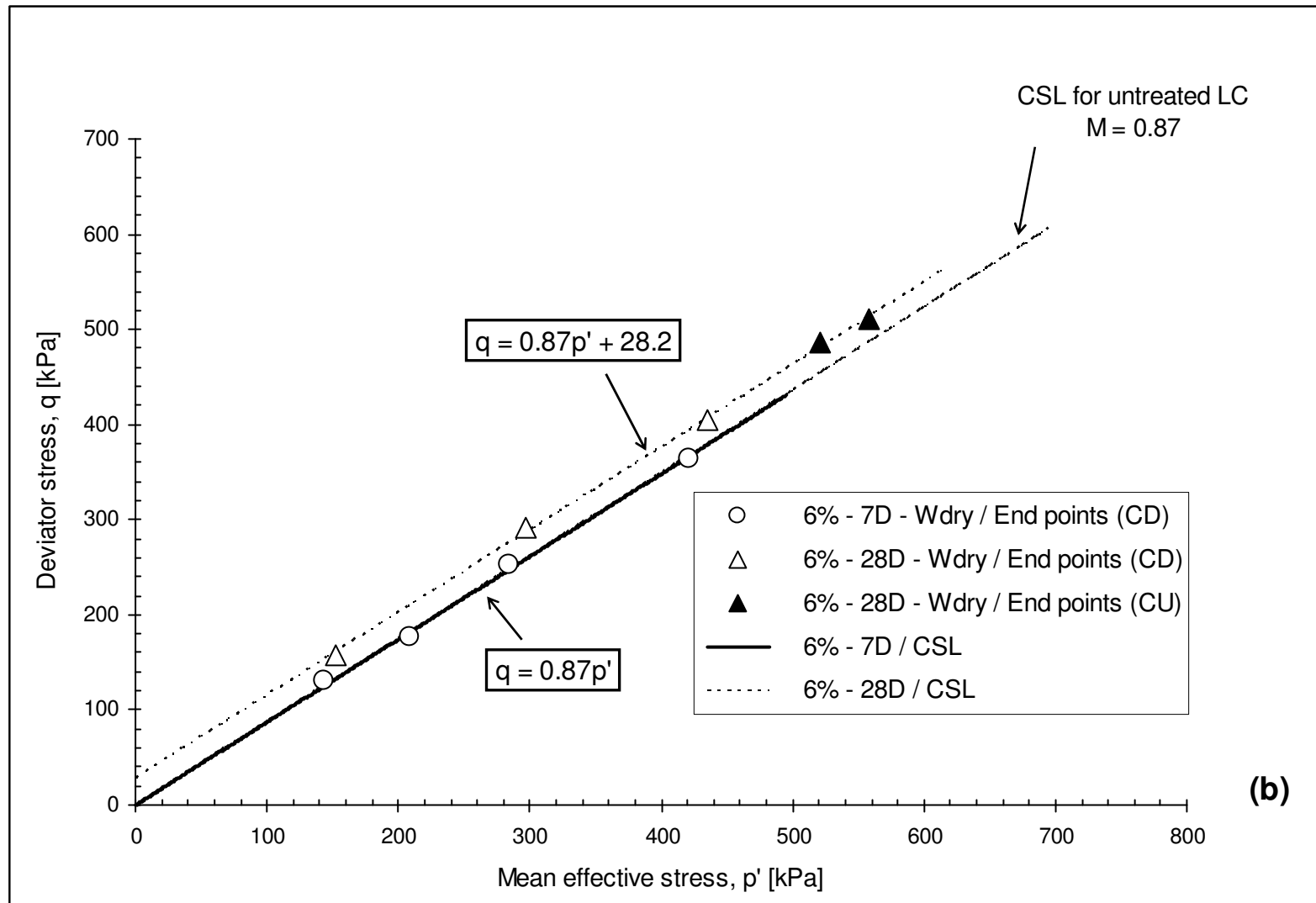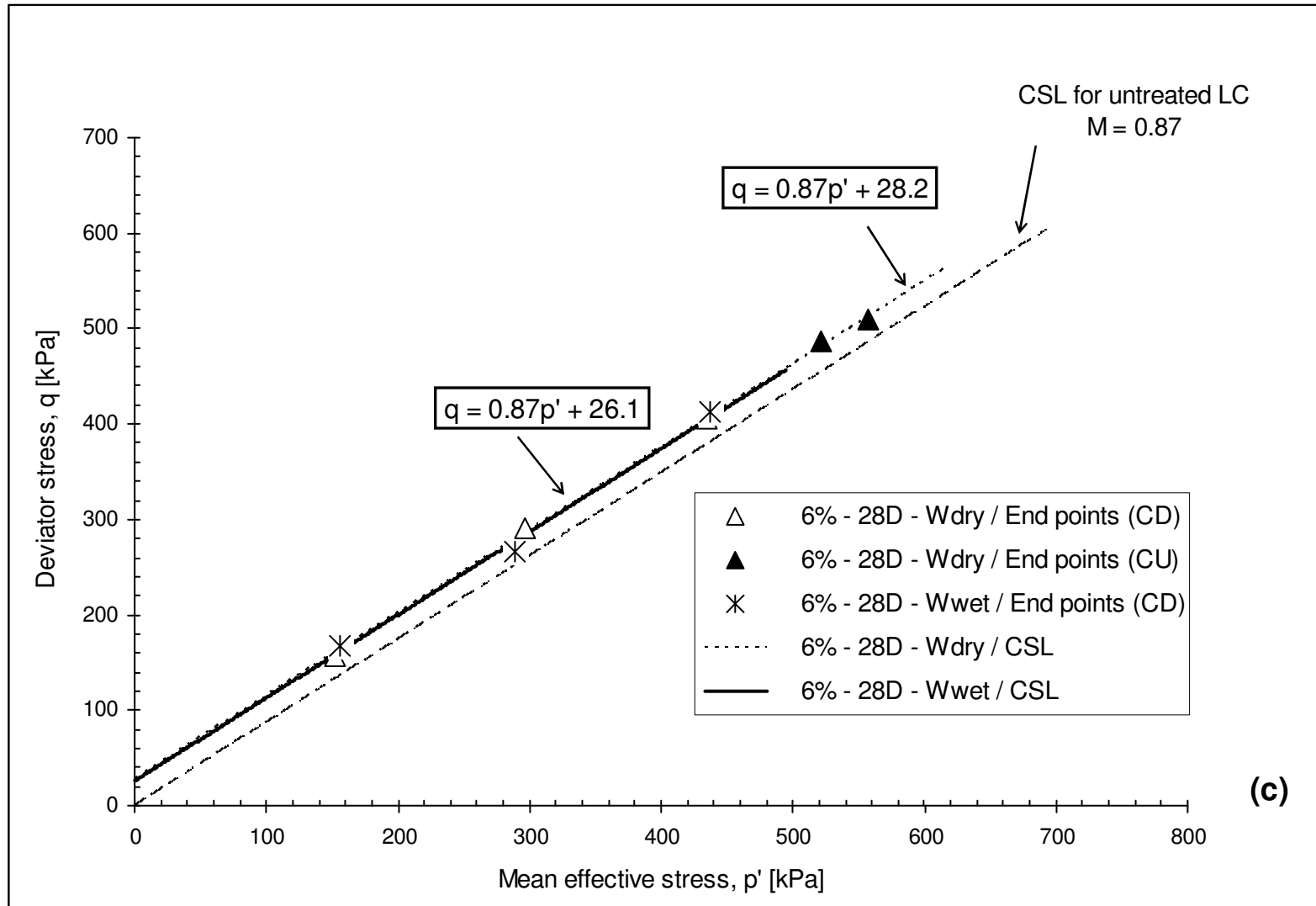
Figure 6.2: CS lines in stress plane $q - p'$ for lime treated London Clay
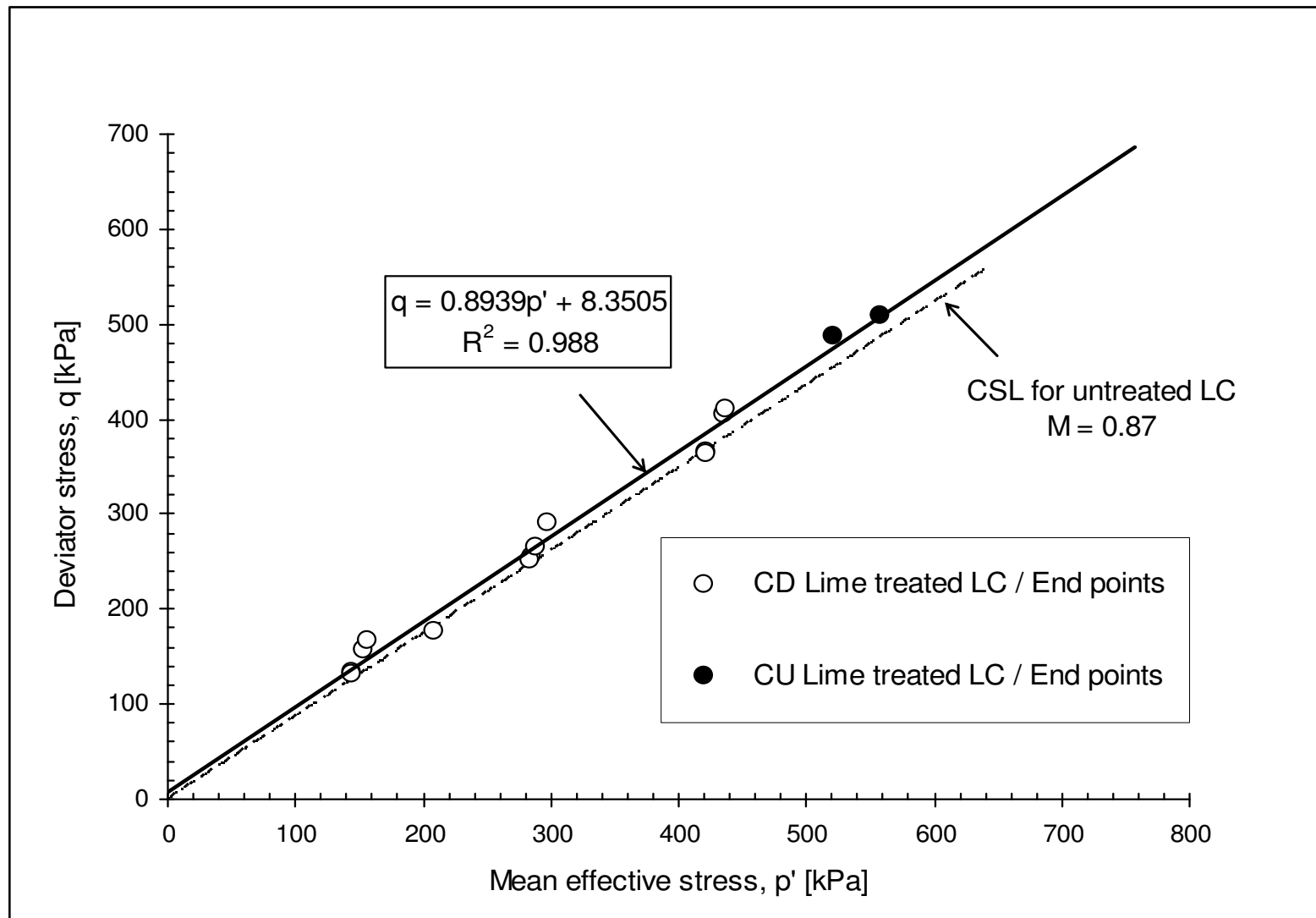
Figure 6.3: Overall CSL in stress plane $q - p'$ for all lime treated London Clay

Based on the observed results in this section, CS parameters were obtained for untreated soil and an estimate of the critical state parameters for lime treated London Clay was made. The gradient M of the critical state line (CSL) was identified from the slope of the line drawn in $(q - p')$ space by joining the end points for each set of mixture containing an average of three tested specimens, and assuming a zero intercept with the Y axis for the untreated soil.

Figure 6.2a shows the critical state lines for lime treated London Clay specimens cured for 7 days. These are found to be close to that of untreated London Clay specimens with very consistent parameter M values, namely $M_{(0\%)} = 0.87$ for untreated London Clay, $M_{(4\%)} = 0.88$ for 4% lime treated London Clay and $M_{(6\%)} = 0.87$ for 6% lime treated London Clay respectively. This indicates that lime addition (up to 6%) to London Clay did not have an effect on the CSL gradient M at early cementing times. However, when curing time increases from 7 to 28 days for similarly prepared 6% lime treated London Clay specimens, regardless of the initial water content and type of test (CD or CU), the CSL shifts slightly higher than that of the untreated London Clay with a small intercept of 26-28 kPa but remains parallel to its CSL at similar gradient M of 0.87 (Figure 6.2 b & c). Similar findings were reported by Kasama et al. (2000) when comparing cemented to uncemented clay.

The small intercept observed in 6% lime treated London Clay is probably due to changes caused by the alteration of the frictional properties of the soil. Moreover, the critical state data analysed in stress plane $q - p'$ (Figure 6.3) based on the points representing the critical state condition of all performed CD and CU triaxial tests, show that if all lime treated specimens end points are plotted together, the overall critical state line of lime treated London Clay appears to be almost parallel to untreated London Clay CSL at the same M value equal to 0.89, but lying above the untreated CSL with a cohesion intercept equal to $8kPa$. The small differences can be an artefact of the curve fitting and presumably the intercept is small enough to be ignored.

6.2. Critical state line of lime treated London Clay in compression plane (v-p')

Fig. 6.4a shows the untreated London Clay behaviour in the compression plane, which can be modelled by using the equation $v = v_\lambda - \lambda \ln p'$, where v_λ is an intercept in $(v - p')$ space varying between Γ and N. As expected, it can be seen that the CSL is approximately parallel to the isotropic compression line for 0% lime. In addition, the projection of lime treated London Clay end points onto the compression plane $(v - p')$ are drawn in Figures 6.4b, c & e, along with the CSL for the untreated London Clay. It can be observed that lime addition has an effect on the CSL which is shifted higher than that of the untreated London Clay CSL, but tilting to the left. The value of the slope parameter λ_{cs} is also reduced from 0.140 for untreated to 0.083 for 4% lime treated soil when cured for 7 days. (Note that the end of test line refers to the critical state line in the compression plane). Moreover, Figure 6.4b indicates that a lime amount increase from 4 to 6% at similar curing period of 7 days shifts the CSL even higher and a less steeper slope is observed at λ_{cs} value equal to 0.067. Thus, the CSL parameter λ_{cs} decreases with lime amount, implying the following: $\lambda_{cs(0\%)} > \lambda_{cs(4\%-7D)} > \lambda_{cs(6\%-7D)}$. A similar behaviour of cemented clay was reported by Kasama et al. (2000) in regards to the CSL shifting higher with cementation increase at an increasing λ_{cs}. However, in this study the slope parameter λ_{cs} in the compression plane $(v - p')$ was observed to be decreasing rather than increasing.

The effect of curing time increase from 7 to 28 days for the 6% lime treated London Clay soil was also investigated. End points plotted in $(v - p')$ space (see Fig. 6.4c) indicate that the CSL obtained from 6% lime treated specimens, cured for 7 days, is located higher than the CSL of specimens cured for 28 days, without a major change in the slope parameter λ_{cs} value. However, the critical state value of the specific volume Γ at $p' = 1 \, kPa$ is found to differ considerably (See Fig. 6.5 and Table 6.2). This is mainly attributed to differences in the initial volume of each set of mixture at the start of the test. As explained earlier this was caused by post-curing volume expansion as well as the volume increase during the saturation stage. On the other hand, the initial water content increase from 27 to 32% does not appear to have an effect on the CSL of the 6% lime treated London Clay. Indeed Figure 6.4d or 6.5 shows minor changes in the CSL position, with a slight difference in the slope parameter λ_{cs} of the two different soils (prepared at dry and wet of optimum respectively).

0% Lime - Wopt

Legend: □ CS points; Iso - NCL (solid line); CSL (dashed line)

$\lambda_{iso} = 0.142$

$\lambda_{cs} = 0.140$

X-axis: Mean effective stress ln(p') [kPa]

Y-axis: Specific volume V = 1+e

(a)
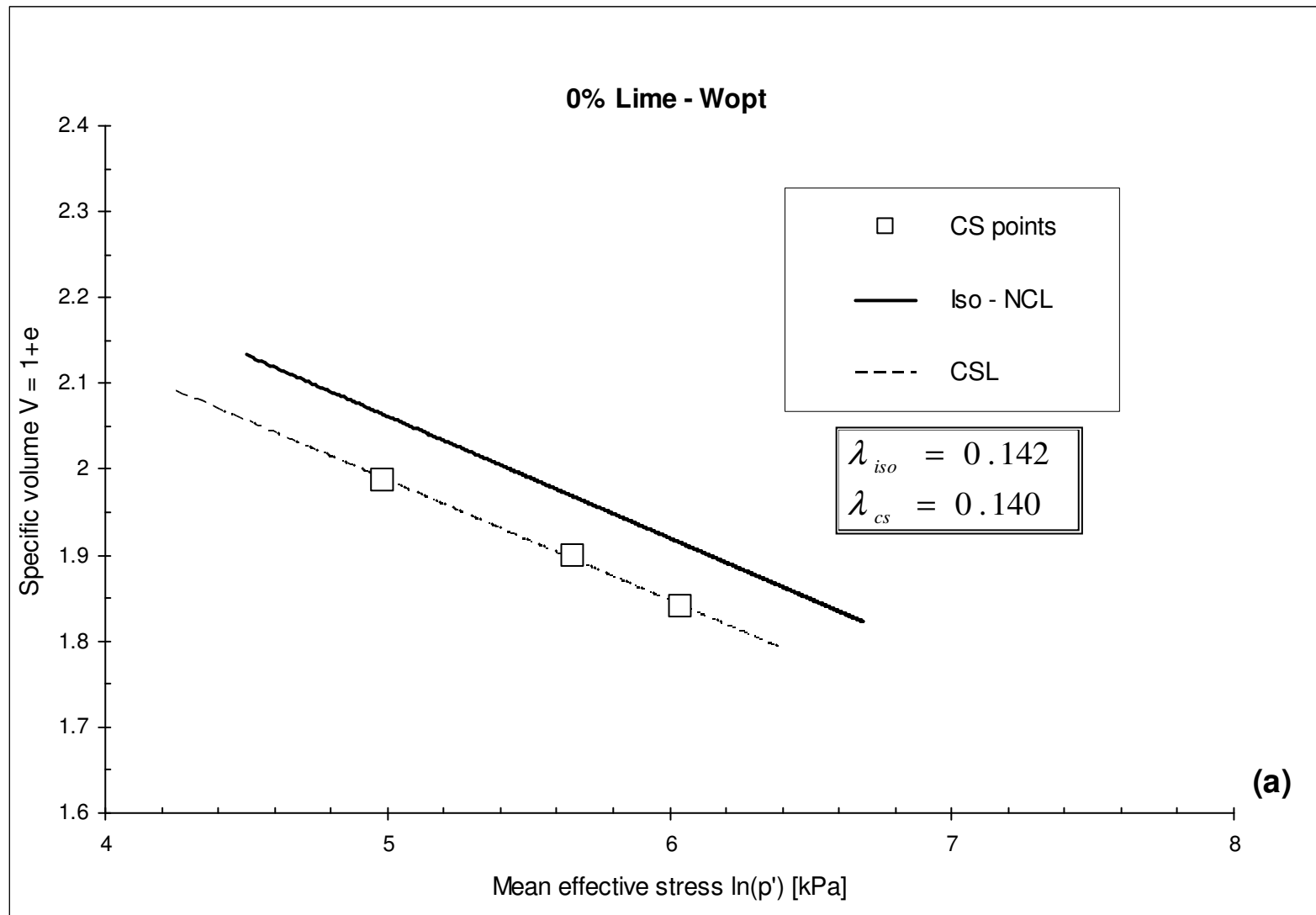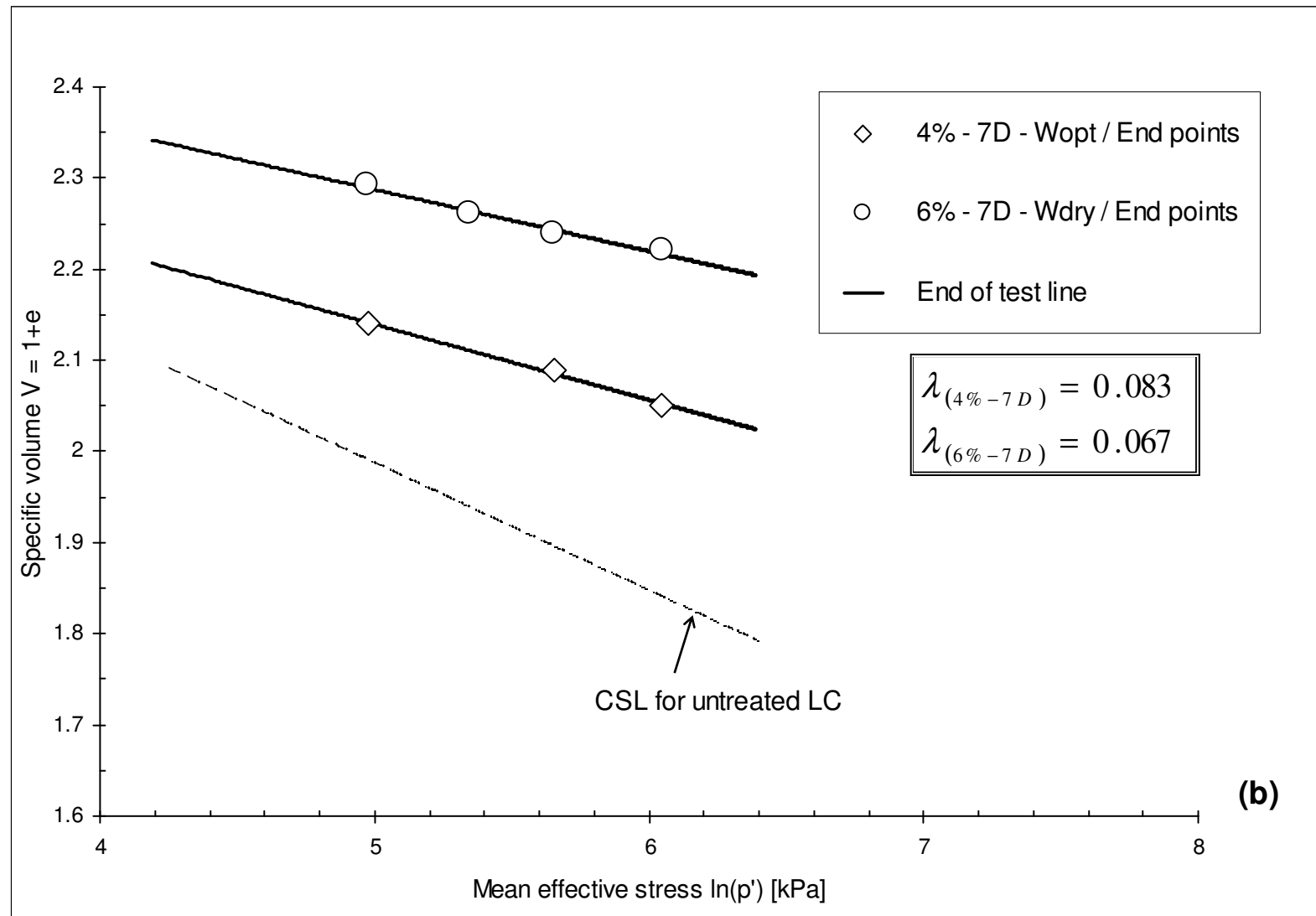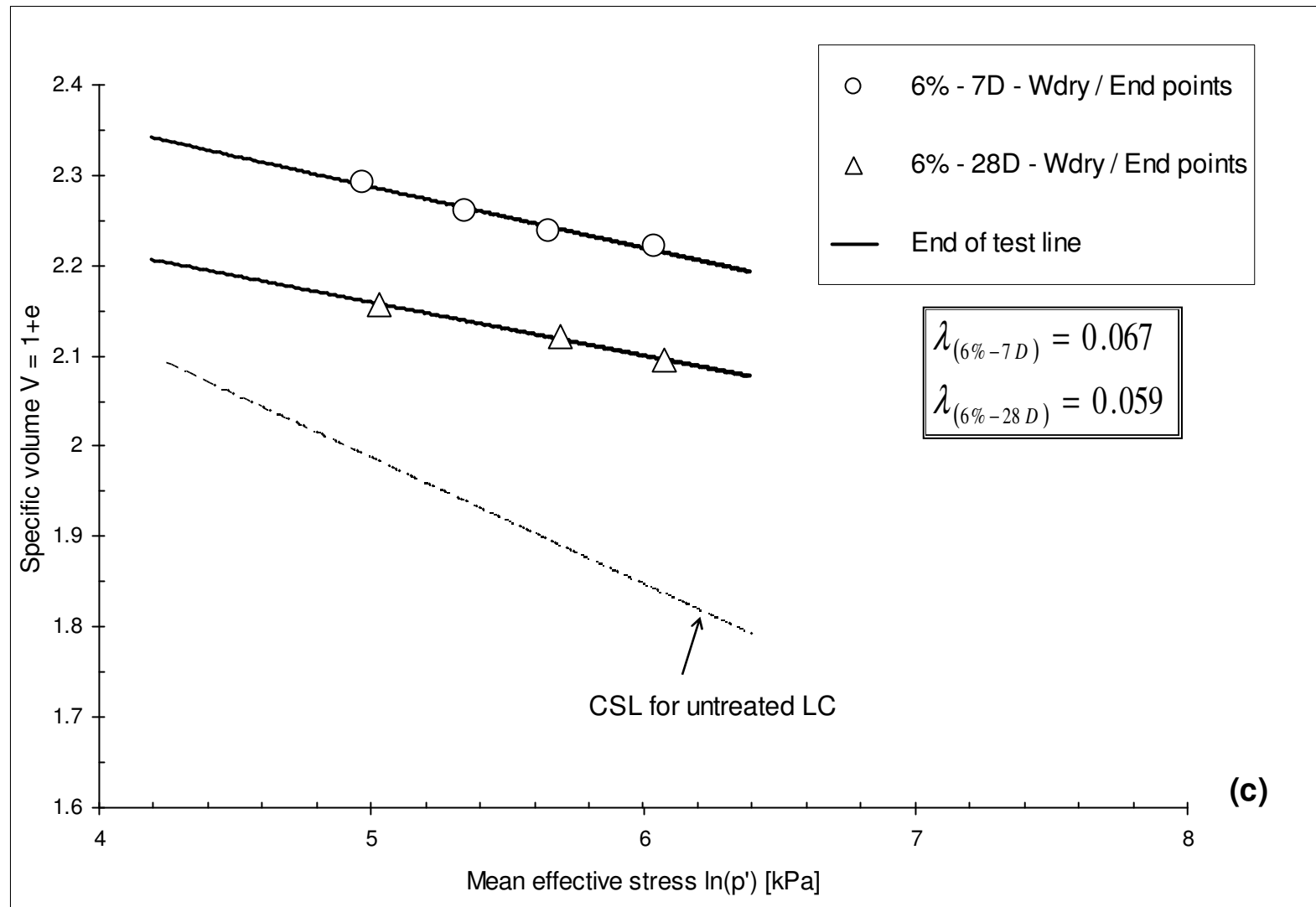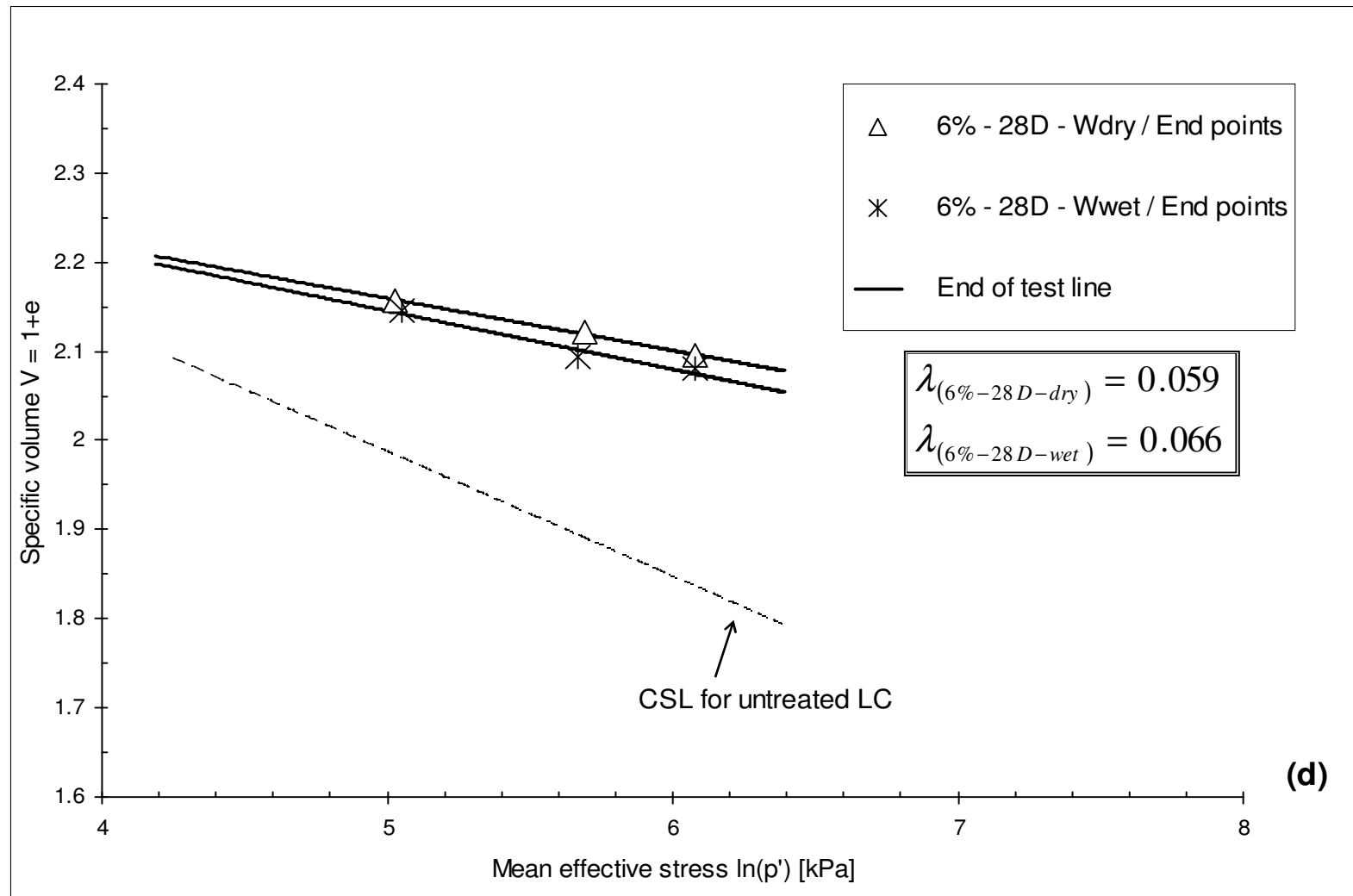
Figure 6.4: Critical state lines for lime treated London Clay mixtures in compression plane $(v - \ln(p'))$
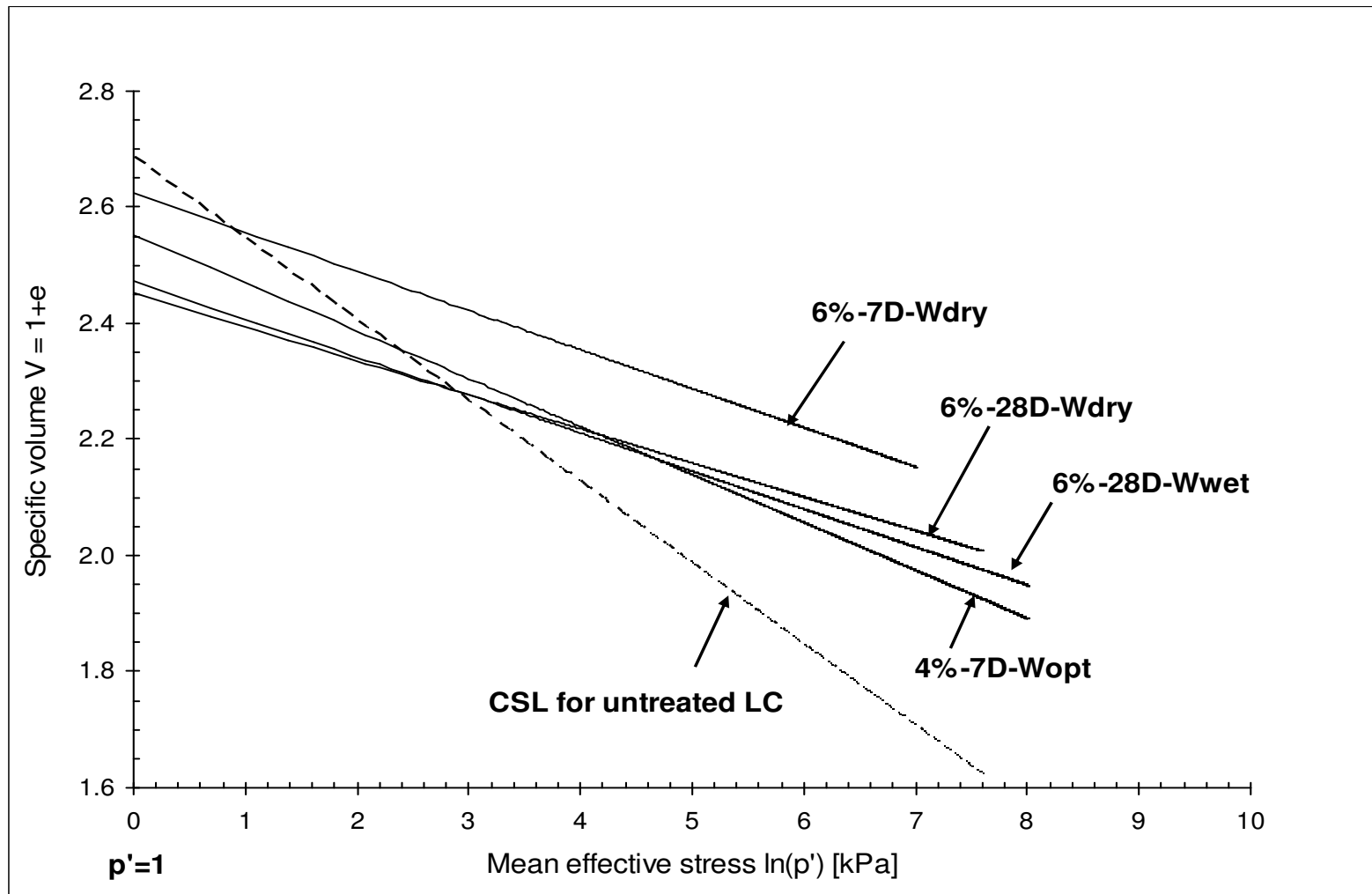
Figure 6.5: End of test lines for all lime treated London Clay in compression plane $(v - \ln(p'))$

The estimated critical state parameters λ_{cs}, Γ and M derived from the best fit lines of the results, along with the critical friction angle ϕ'_{cs} are listed in Table 6.2. It is recalled for a compression test that the angle of internal friction ϕ'_{cs} can be connected to the gradient of the critical state line M through the following equation, $\sin\phi'_{cs} = \dfrac{3M}{6+M}$ from where the Critical friction angles ϕ'_{cs} are derived.

It should be noted that parameters such as (N) (specific volume determined under isotropic consolidation) and (Γ) (specific volume determined under shearing condition) have significant practical implications in the critical state numerical modelling when effective stress analysis is required.

Table 6.2: Measured critical state parameters for lime treated and untreated London Clay

Type of test	Lime	Curing time	Water content w_c	λ_{cs}	Γ	Intercept	M	ϕ'_{cs}
	$(\%)$	$(Days)$	$(\%)$	-	-	(kPa)	-	(Deg)
CD	0	N/A	w_{opt}	0.140	2.685	0	0.87	22.33
CD	4	7	w_{opt}	0.083	2.553	0	0.88	22.56
CD	6	7	w_{dry}	0.067	2.624	0	0.87	22.33
CD	6	28	w_{dry}	0.059	2.452	28.2	0.87	22.33
CU	6	28	w_{dry}	-	-	28.2	0.87	22.33
CD	6	28	w_{wet}	0.066	2.473	26.1	0.87	22.33

6.3. Stress paths for CD & CU triaxial tests

6.3.1. Stress paths of lime treated London Clay under drained conditions

Stress paths of the consolidated drained triaxial compression tests are plotted in $(p':q)$ space as shown in Figures 6.6 a & b. The effective stress paths derived from the CD triaxial tests are straight lines, with a gradient of $\delta q / \delta p' = 3$. Regardless of lime content and the curing period, the effective stress path (ESP) of lime treated London Clay rises with clear increase of deviator stress and mean effective stress to the peak; it then falls down along the same stress path towards an ultimate state, possibly the critical state line. Conversely the untreated London Clay specimens rise steadily until reaching a more stable state where failure occurs at wet side of critical. Note that although the ESP for lime treated specimens appears to intersect the CSL in the stress plane $(p':q)$ before yielding, but in fact it is missing the CSL in (p', v, q) space, as it is better illustrated in the compression plane $(p':v)$ (see Fig. 6.8 & 6.9). After failure (post-peak), the state of the treated specimen moves back down a similar ESP to a point "C" on / or close to the CSL (Fig. 6.6 b & 6.7a, b & c).

As shown earlier (see Chapter 5, Fig. 5.8 & 5.9), untreated London Clay specimens failed by bulging, while treated London Clay specimens have ruptured due to the formation of shear surfaces (slip plane). It is interesting to note that 4% lime treated specimens cured for 7 days, which failed dry of critical, were observed to have a smoother transition from elastic to plastic behaviour, accompanied by a small post-peak drop as it can be seen in stress-strain curves, while specimens treated with 6% lime and cured for 7 days (which also failed dry of critical) showed the highest drop due to increased brittleness (see Chapter 5, section 5.4.3). This brittle failure was followed by a considerable volumetric expansion of the material.

The initial state of the material at "A", peak state at "B" and critical state / end points at "C" of each soil mixture are shown in Figures 6.6 & 6.7. The difficulties encountered in identifying clearly the critical state were discussed at the start of this section. The end points used in this work do not all lie on the drawn CSL. It was observed that the states of the material were in fact still moving towards a critical state at the end of each tested lime

treated London Clay specimen. Towards the end of the tests, some of the lime treated specimens displayed an increase in the mean effective stress p' indicating that they could fall above the critical state line. Other specimens showed a continuous decrease in mean effective stress p', suggesting that they could fall below the critical state line. A similar behaviour was observed by Smith et al., (1992) during a study on Bothkennar soil. The authors have identified that no test has truly approached a critical state conditions and only relied on the end points of different tests to plot the CS lines. However, reports in the literature indicate that high confining pressure test results in excess of 20% axial strain show that a constant stress ratio state can be obtained. On the other hand, Atkinson, (2000) and Haeri et al., (2005), indicated that the chosen critical state line might not represent the true critical sate because cemented samples showed a shear zone, therefore, it is difficult to say whether the stress conditions are representative of the sample as a whole.
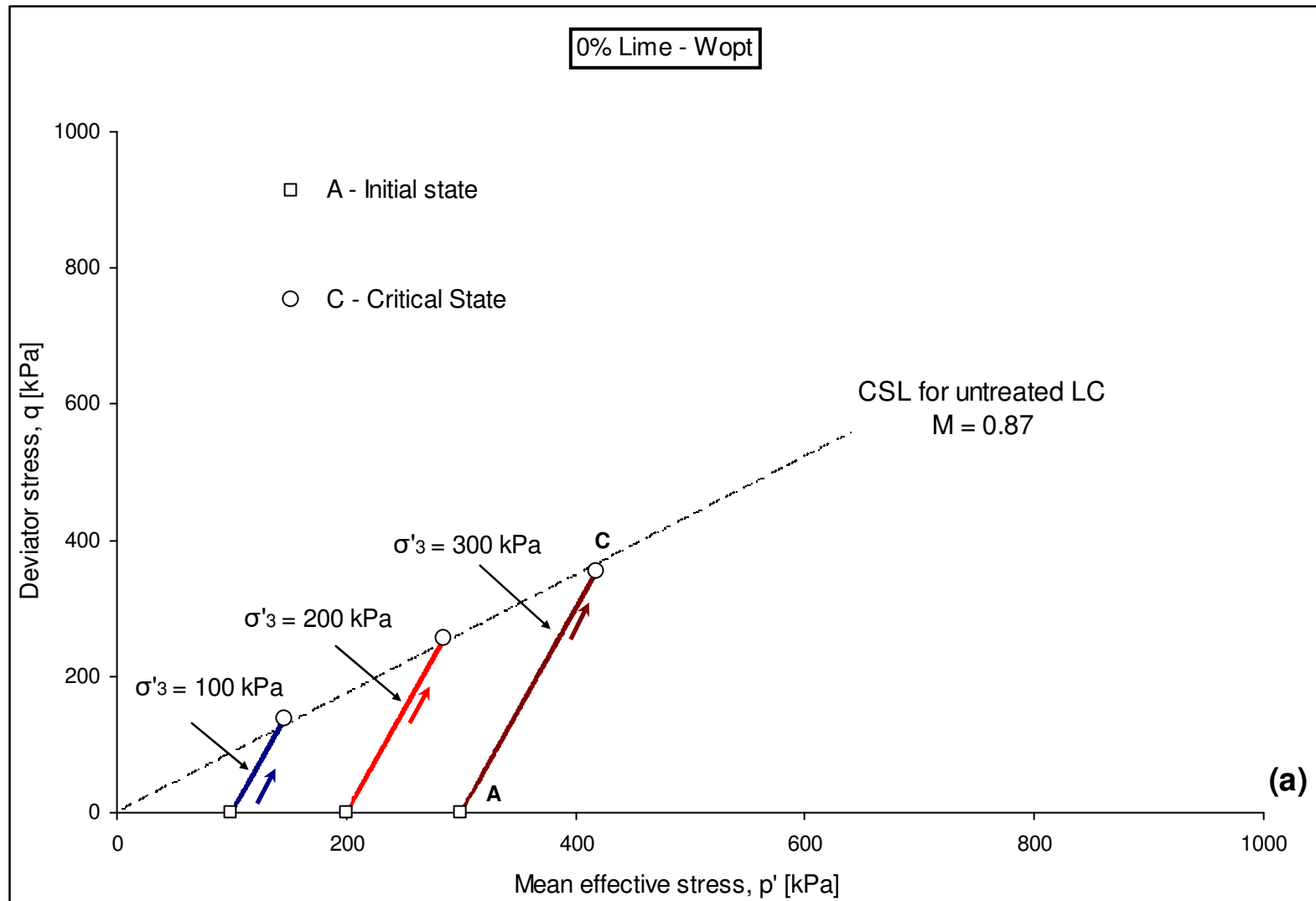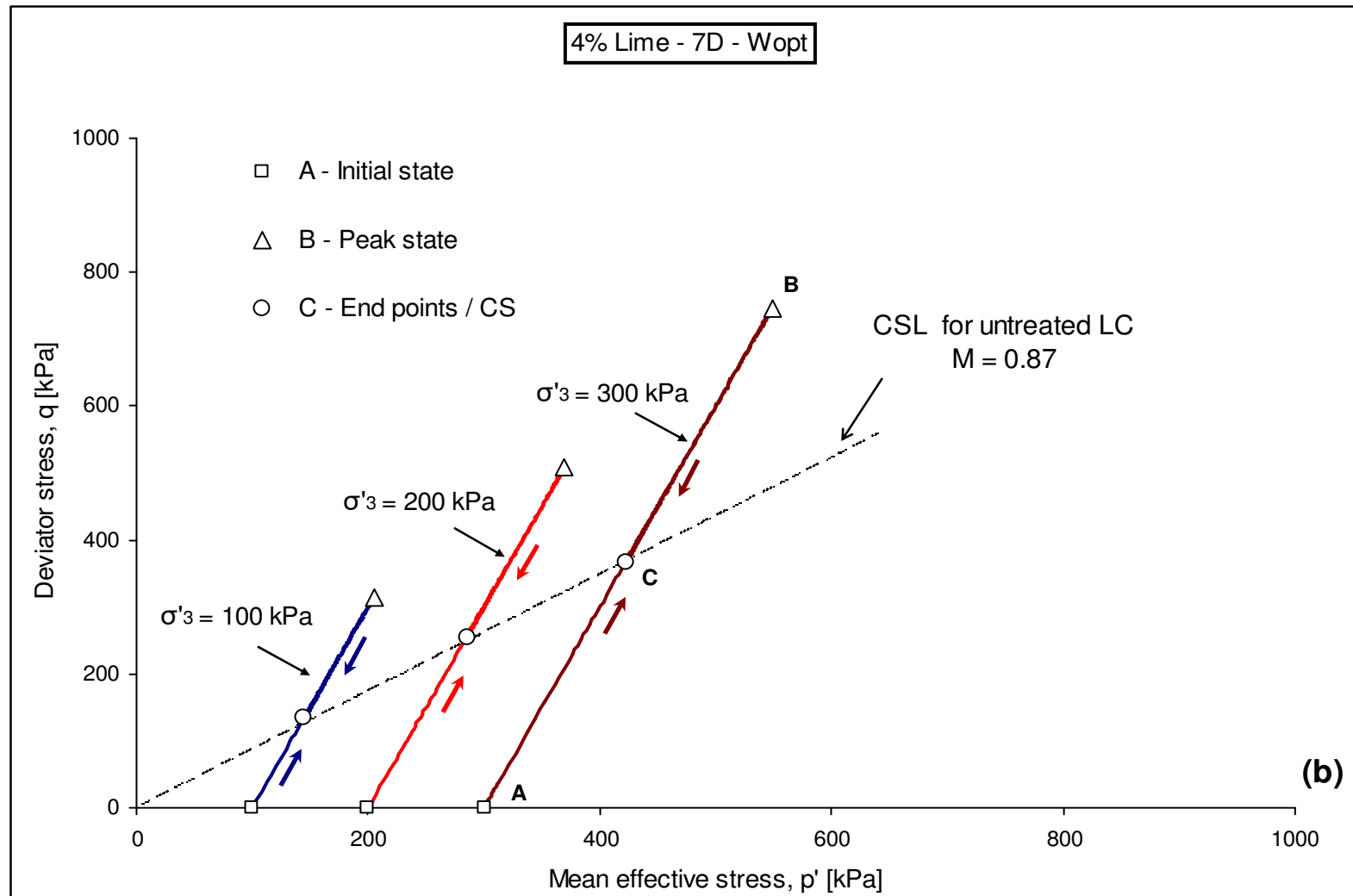
Figure 6.6: Stress paths for London Clay & 4% lime treated London Clay under drained conditions in stress plane $(q - p')$
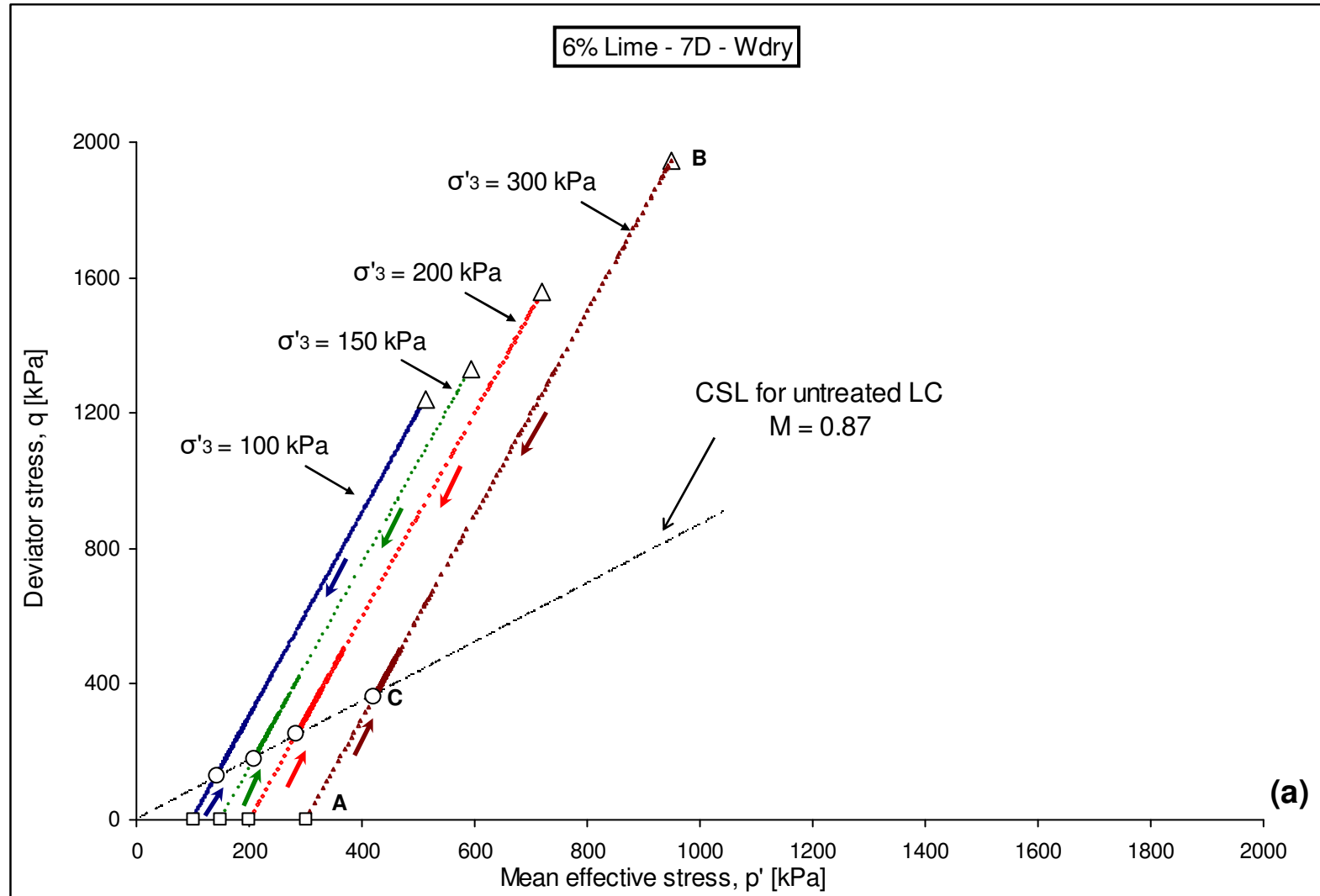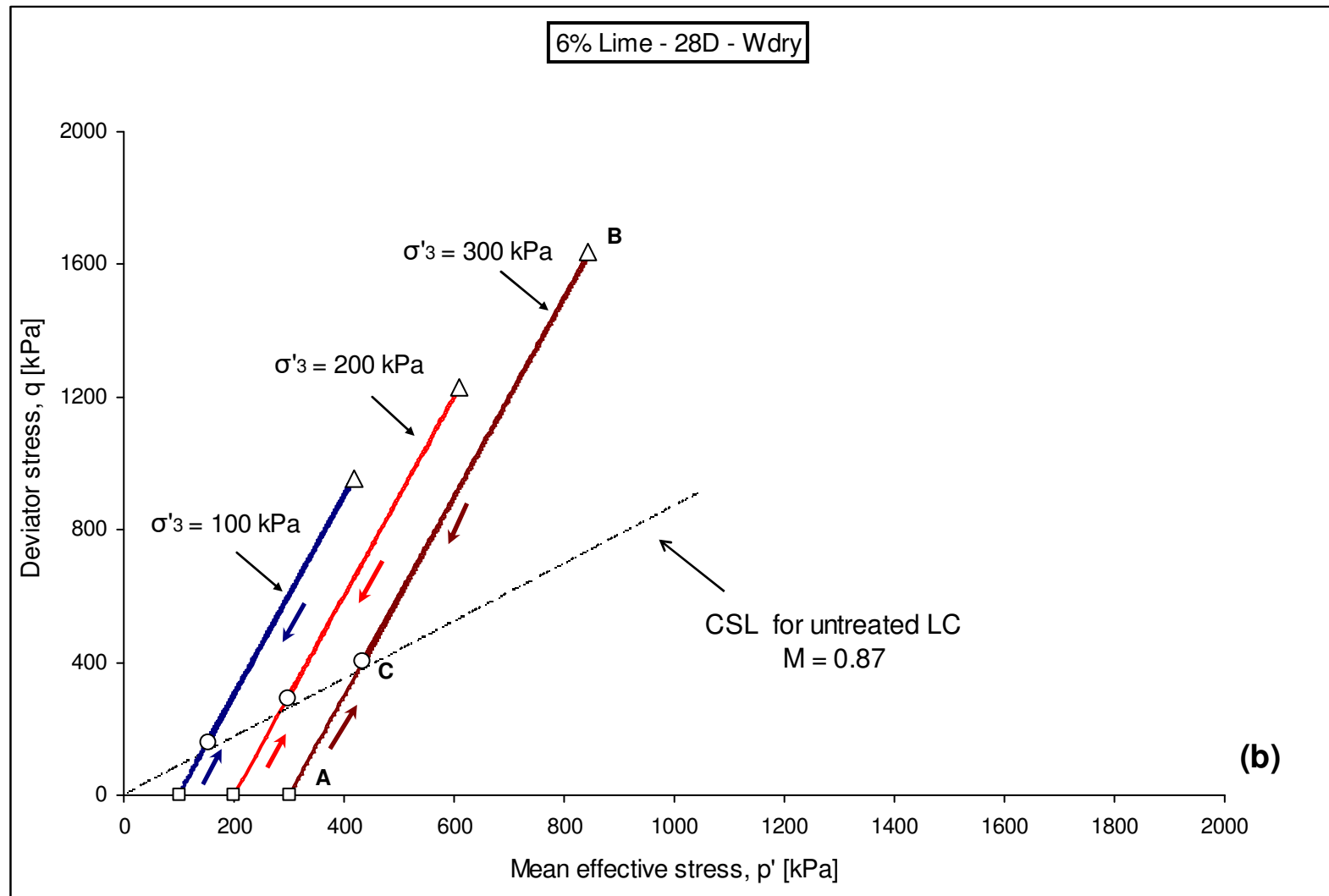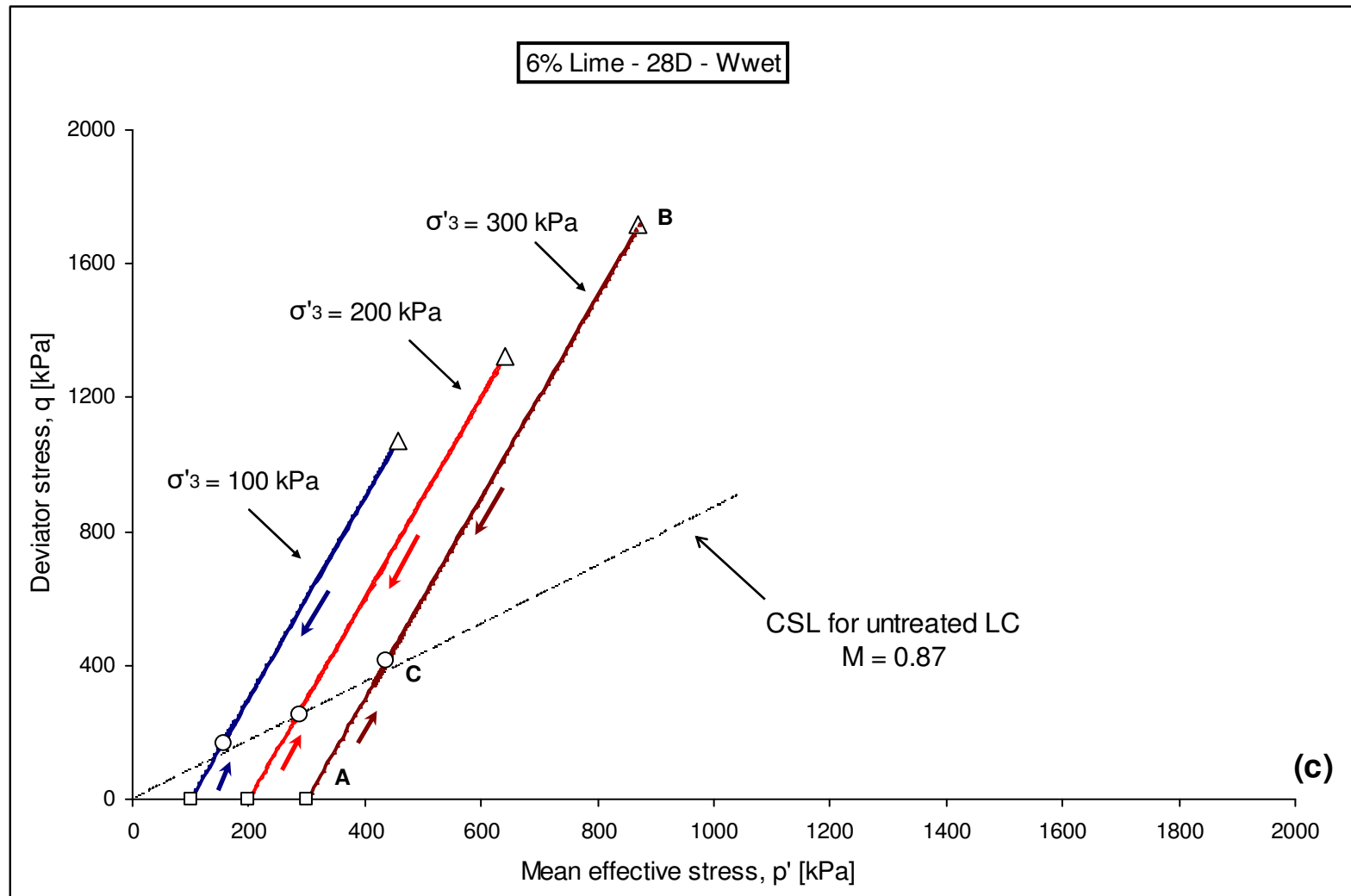
Figure 6.7: Stress paths for 6% lime treated London Clay under drained conditions in stress plane $(q - p')$

In order to observe the stress path in the compression plane of each tested mixture set, results of lime treated and untreated London Clay are plotted in $(v - \ln(p'))$ space (see Figures 6.8 & 6.9). The state of the untreated specimens initial positions were identified to be above the critical state line (wet side of CSL) at point "A", moving downward seeking the CSL during the shearing process of CD triaxial tests (Figure 6.8a). As already indicated in Chapter 5 / section (5.4.3), untreated London Clay specimens contract during shearing, until failure occurs on the wet side of critical at point "C". These specimens showed almost zero rate of volume change at the end of the test, suggesting that they are either close to, or have reached the critical state.

Similarly, 4% lime treated London Clay specimens initially showed a reduction in specific volume due to contraction. The initial state of these specimens is indicated by the point "A", moving downward during shearing compression stage (contraction). Sometime after yielding, rupture occurs at "B", where the direction route changes from contractive to dilative, accompanied by a specific volume increase with a decreasing mean effective stress. The state of the material in the compression plane $(v - \ln(p'))$ moves upward, attempting to reach the critical state at the end point "C" (Figure 6.8b), whereas 6% lime treated London Clay specimens initially positioned at point "A", move along the shearing compression path (contraction) towards the point "B" where rupture occurs. At this stage, a sudden specific volume increase is observed, resulting in an immediate direction change of the material state (dilation), following an upward path in search for the CS, and settling at the ultimate point "C" at the end of the test (Figure 6.9 a, b &c). Such specimens are described as being on the dry side of the critical.
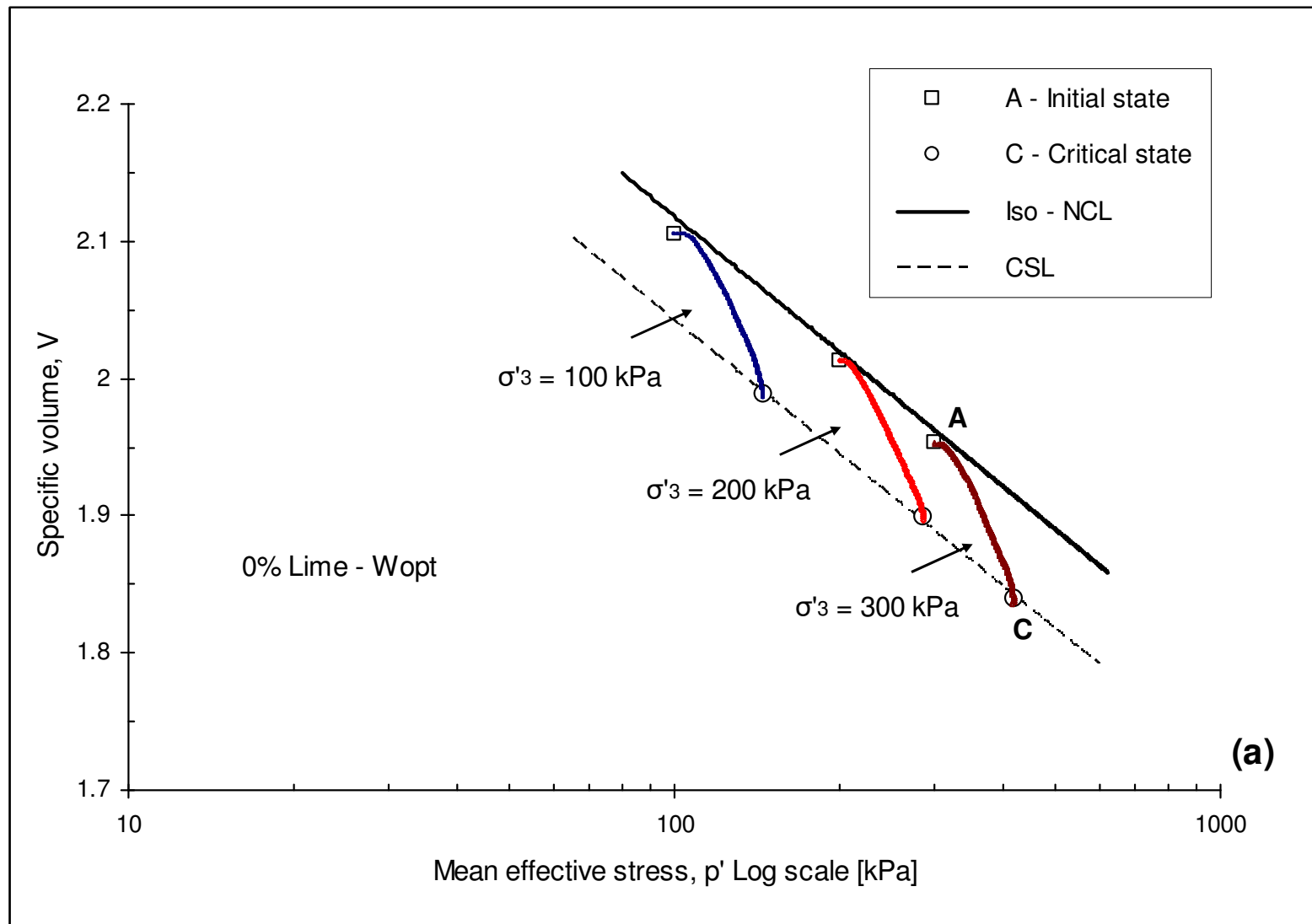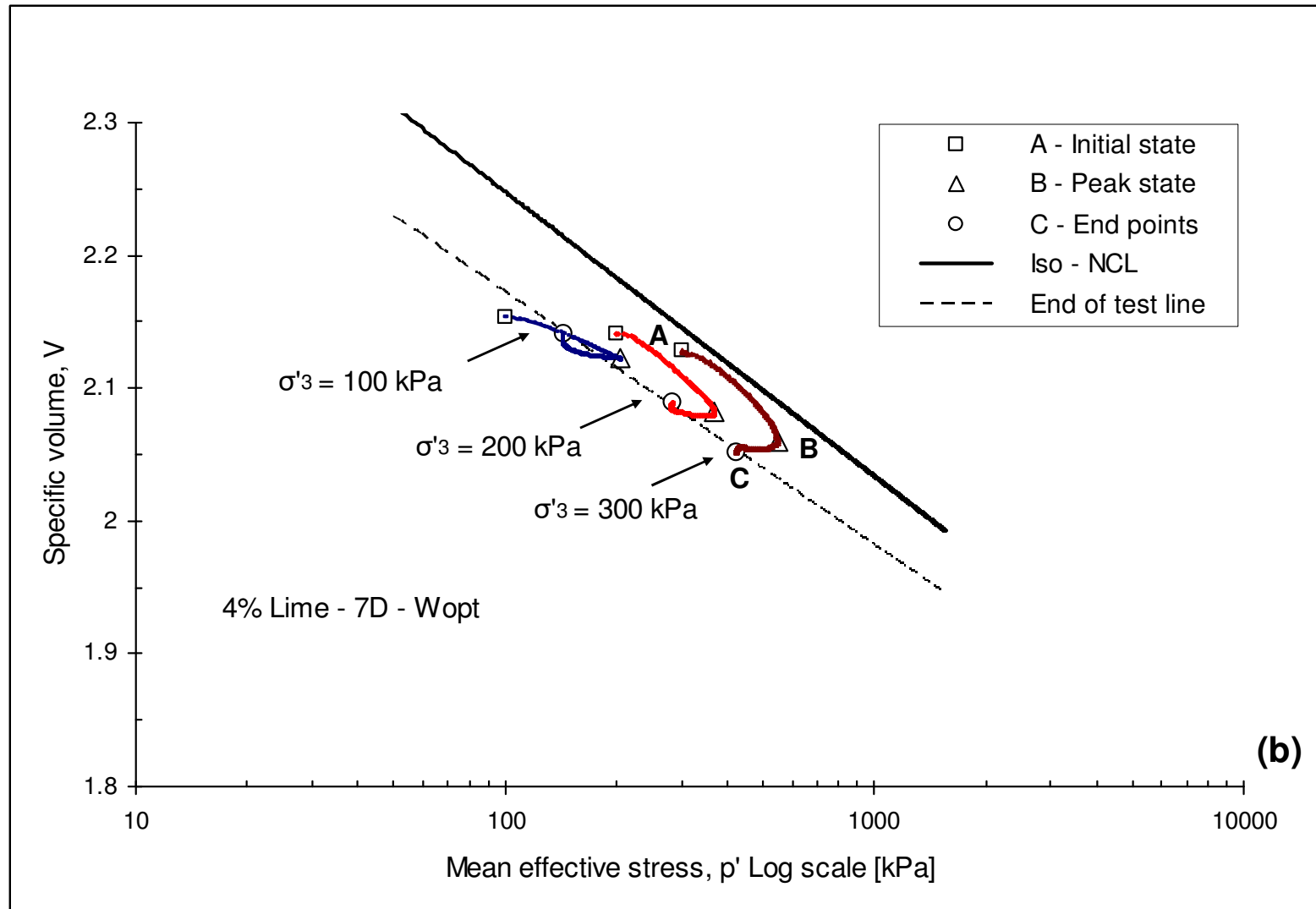
Figure 6.8: Initial side position and stress paths for London Clay & 4% lime treated London Clay in $(v - p')$ space

(a)
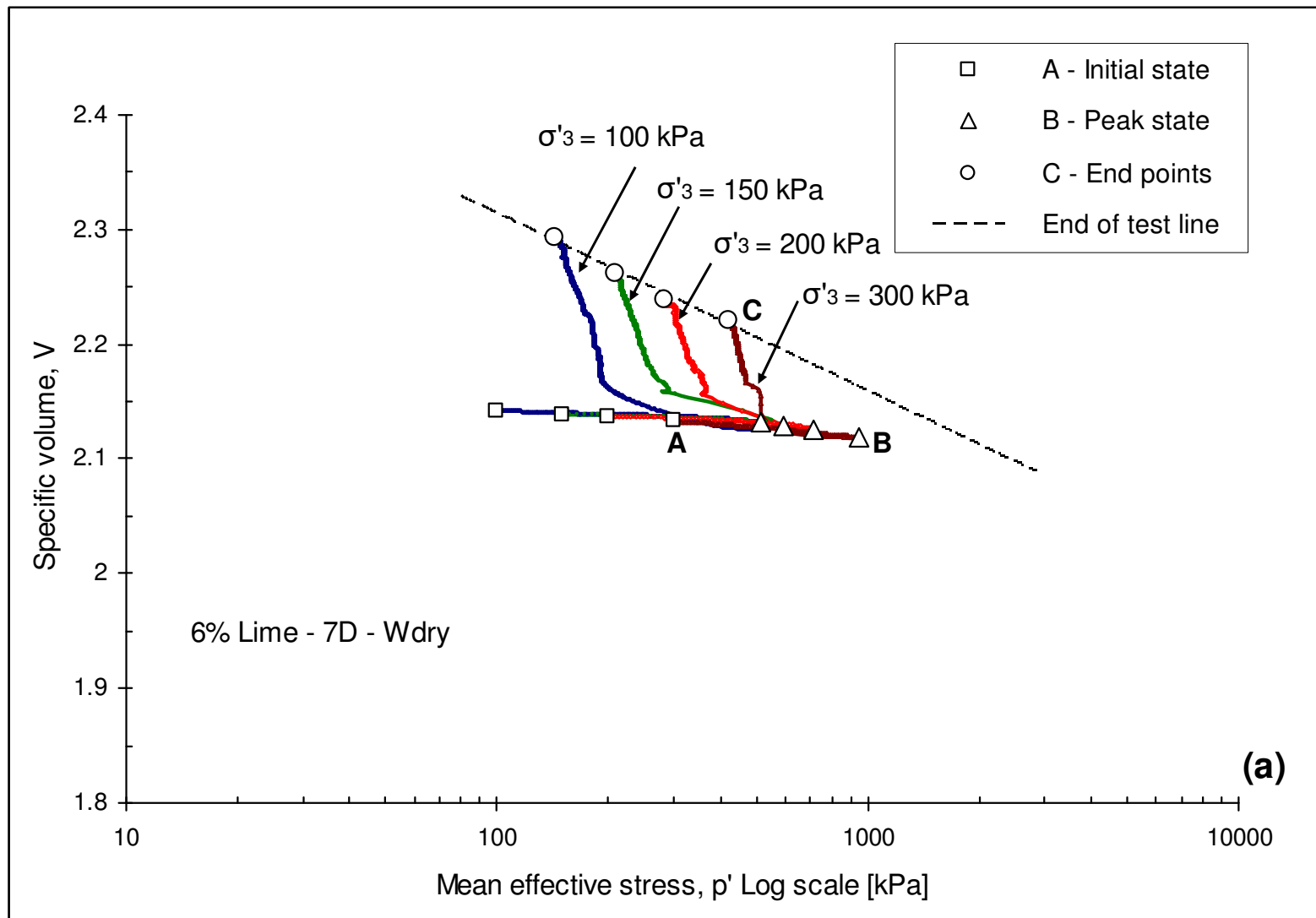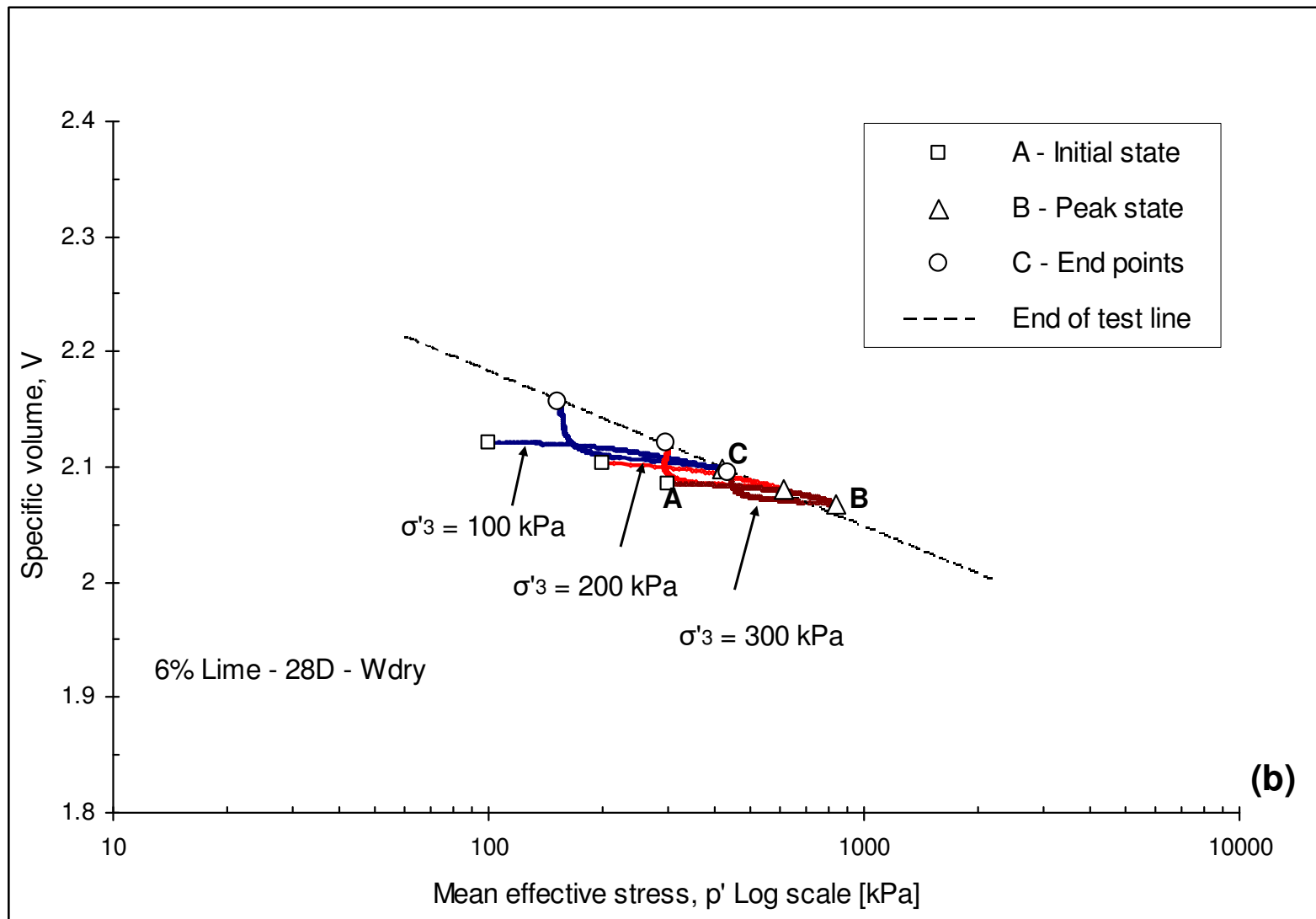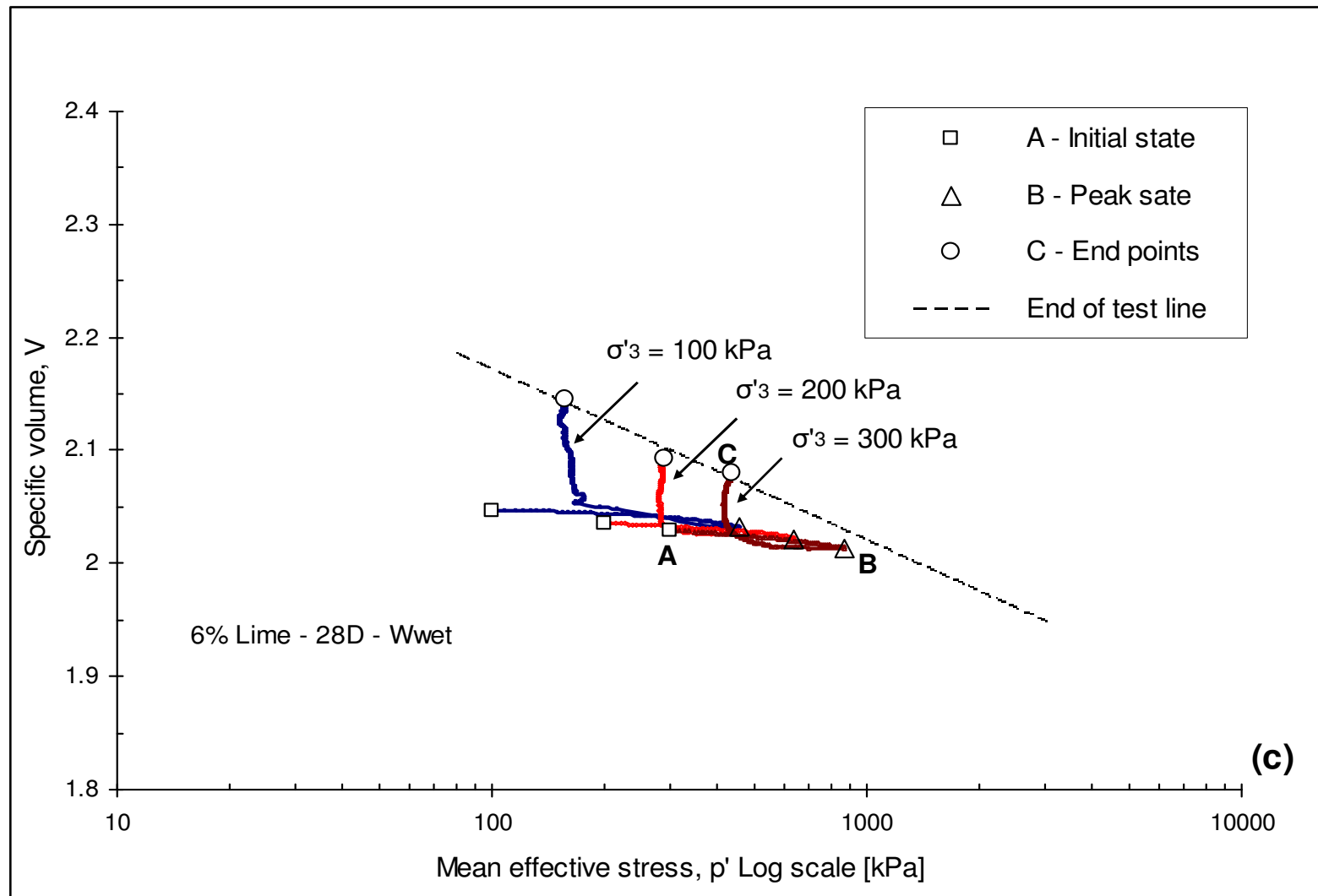
Figure 6.9: Initial side position and stress paths for 6% lime treated London Clay in $(v-p')$ space

6.3.2. Stress paths of lime treated London Clay under undrained conditions

The effective stress paths (ESP) results of two lime treated London Clay samples, sheared under undrained conditions at different effective stresses equal to 158 & 250 kPa are presented in Figure 6.10. The state of the material (for both tested specimens) is initially at point "A", rapidly rising up at a decreasing mean effective stress, crossing the CSL until reaching minimum mean effective stress value $p'_{(min)}$. At this stage each specimen's stress path shows a tendency to move from the left towards the right of its corresponding total stress as there is a reduction in the rate of increasing pore water pressure. For this type of samples, the stress path is well rounded, the state of each lime treated London Clay specimen is seen to be approaching its corresponding peak state moving upwards on the tension cut off line at a gradient equal to $\frac{1}{3}$ until rupture occurs at "B" by tensile failure due to pore pressure increase. This is followed by a sudden drop in deviator stress with a continuous mean effective stress increase, reaching the maximum $p'_{(max)}$ to curve sharply down seeking the critical state, and takes a reversing route towards the left with a decreasing mean effective stress laying on the CSL, ending at point "C". Similar stress path shape was also observed by Asghari et al. (2003) for cemented gravely sand; Haeri et al. (2005) for artificially cemented sandy gravel; Gasparre (2005) for London Clay; Xiao & Lee (2008) from isotropically consolidated undrained tests performed on cement treated marine clay and Le Runigo et al. (2011) for lime treated silty soil.

The "zero tension" or "limiting tensile strain" criteria are the most widely used among the alternative theories to quantify tensile failure (Schofield, 1980). The following simple checks can be performed to identify the cause and type of failure of the CU specimens.

$$\frac{q}{p'} = 3 \tag{6.3}$$

Where q, is the deviator stress and p', is the mean effective stress. In CSSM concept, the following apply:

$$q = \sigma_1 - \sigma_3 \tag{6.4}$$

$$p' = \frac{\sigma_1 + 2\sigma_3}{3} - u \qquad\qquad (6.5)$$

Substituting (6.4) & (6.5) in (6.3), will result in cell pressure equating the pore water pressure $\sigma_3 = u$, consequently resulting in the effective stress reaching zero $\sigma'_3 = \sigma_3 - u = 0$. For the triaxial specimen, the zero tension criteria with $\sigma'_3 = 0$ results in

$$p' = \frac{\sigma_1 - u}{3} = \frac{\sigma_1'}{3} \quad \text{or} \quad \frac{q}{p'} = 3 \quad \text{and leads to vertical split of the specimen (tensile failure)}$$

which is the case for these CU tests performed in this study. However, this tensile failure does not occur immediately after the effective stress σ'_3 reaches zero. The specimens were shown to travel up the part of the stress path (see Fig. 6.10) before complete failure occurs. This indicates that the 6% lime treated specimens have not only developed high compressive strength (as indicated in Chapter 5 / section 5.2 & 5.4) but also showed a further tensile resistance due to the development of the cementitious products.

In order to reach compressive failure for such type of material, the effective stress will have to always be positive $\sigma'_3 > 0$, implying the following:

$$\sigma_3' = \sigma_3 - u > 0 \qquad \rightarrow \sigma_3 > u$$

In this case it is recommended to perform the consolidated undrained tests at higher confining pressures, so that the pore pressure increase would not reach the applied cell pressure and the effective stress will always remain positive.

Note that the difference between the maximum and the minimum mean effective ($p'_{(max)} - p'_{(min)}$) is found to be similar for both CU tests, approximately valued to $500kPa$ (see Fig. 6.10). This indicates that the state of the material oscillates in a shearing zone within a boundary of a minimum and a maximum mean effective stress in a domain which remains constant regardless of the initial effective stress.

Overall, the 6% lime treated samples tested under undrained conditions show rigid behaviour, the strength observed is related to the cementation bonds formed during curing time, which controls the shearing stage until the bonds are broken. The role of fabric is limited to a minimum in this case.
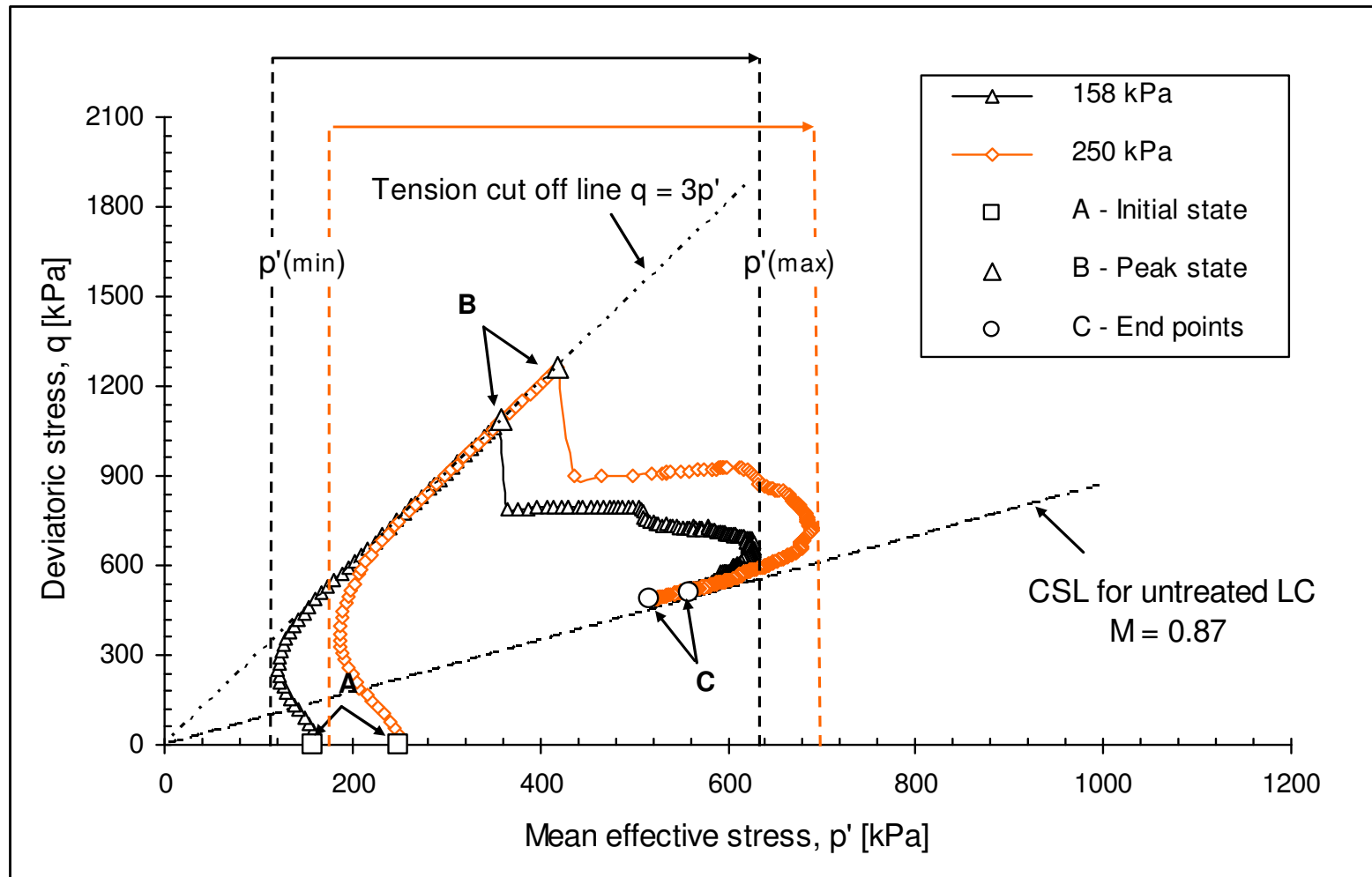
Figure 6.10: CU stress paths for 6% lime treated London Clay in stress plane $(q - p')$ (28 days curing)

Similarly, test results plotted in the compression plane $(v - \ln(p'))$ (Figure 6.11) indicates that the state of the material moves initially, at a constant volume, leftward from the starting point "A", at a decreasing mean effective stress. This stress path turns back once the minimum effective stress $p'_{(min)}$ is reached, moving towards the right, passing the CSL for 6% lime treated London Clay, to reach the peak state at "B" where rupture occurs. The path continues further to a maximum achievable effective stress $p'_{(max)}$, reversing again to follow a leftwards direction, finally ending at "C" once the test comes to an end. In addition, it was observed that the end point "C" for $CU_1(6-28)_{250}$ specimen positioned on the "End of test line" drawn in $(v - \ln(p'))$ for similar specimens tested under CD conditions. Conversely, the end point "C" for $CU_1(6-28)_{158}$ specimen was recorded not to reach the "End of test line" along the stress path (see Fig. 6.11). This is believed to be due to the test being stopped earlier than its designated target. It is noteworthy to indicate that the pore pressure was observed to be increasing at the end of the test for both specimens, implying a fall in mean effective stress.

In comparison to CU triaxial test results from similar material, CD stress path of lime treated London Clay rises up, passes the CSL to reach the material's peak state then travel's back once rupture occurs through the same route seeking the CSL which is typical of the behaviour of heavily over-consolidated and bonded materials. Conversely results from CU triaxial test show a stress path passing the CSL of untreated London Clay, moving towards its peak / failure state, to drop after rupture seeking the CSL. The end points of both types of testing lay on the same CSL, but a higher peak deviator stress is observed in samples tested under undrained conditions compared to drained tests for similarly prepared samples (Figure 6.12). This is due to volumetric straining; when volumetric strains are prevented (in undrained tests) a higher strength can be sustained before the bonds break down, until failure occurs either by tensile failure (such as in this case) or by strain softening if high enough confining pressure is applied (Malandraki and Toll, 2001). Once the treated specimen develops strain softening, the sample experiences destructuration. The OCR of these specimens is very high; these act like a material being on the dry side of the critical state. This is in line with other researchers' results on artificially cemented soils and bonded materials (e.g. Kamruzaman, 2002; Asghari et al., 2003 and Haeri et al., 2005).
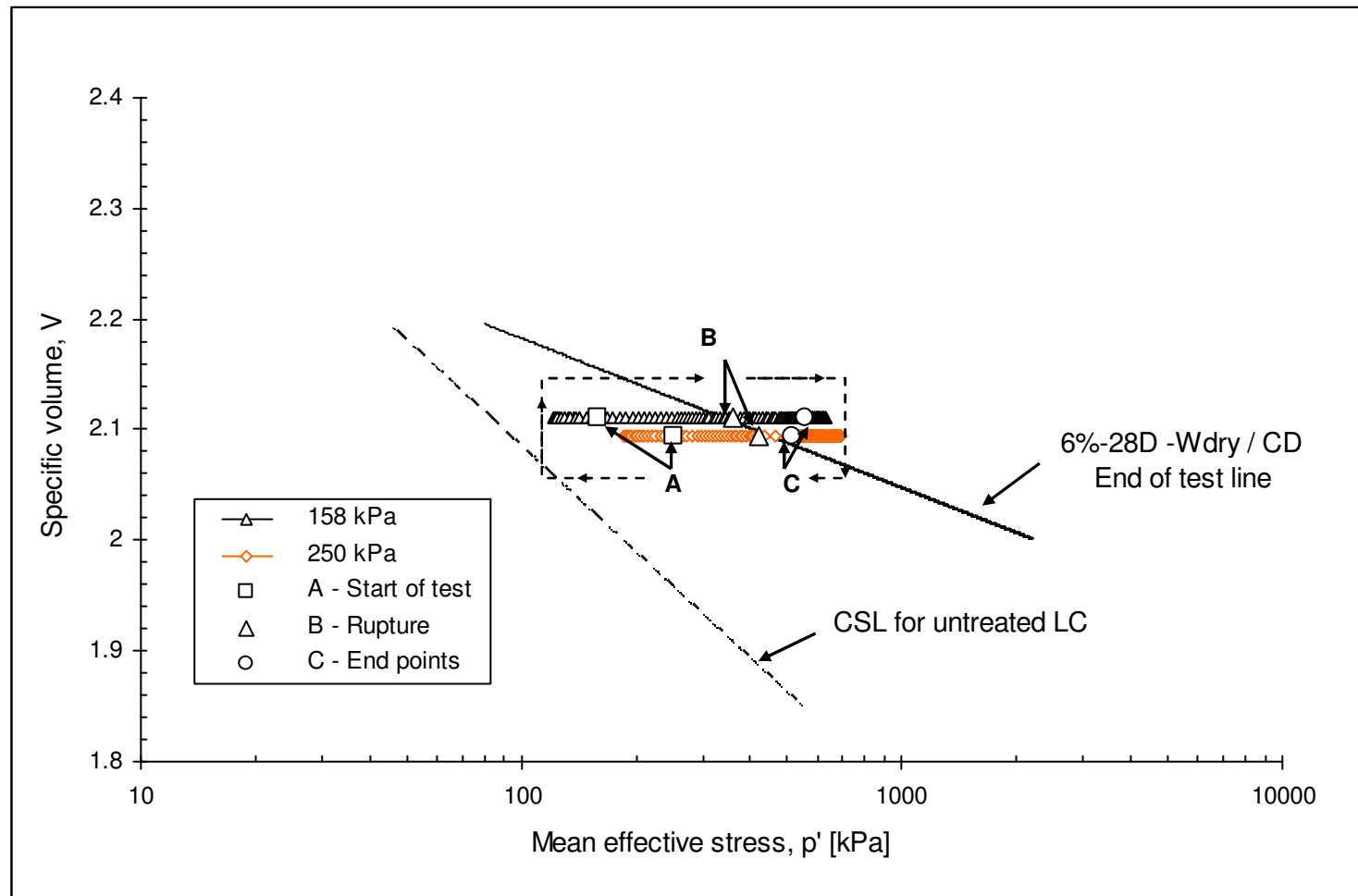
Figure 6.11: CU stress paths for 6% lime treated London Clay in compression plane $(v - p')$ (28 days curing)
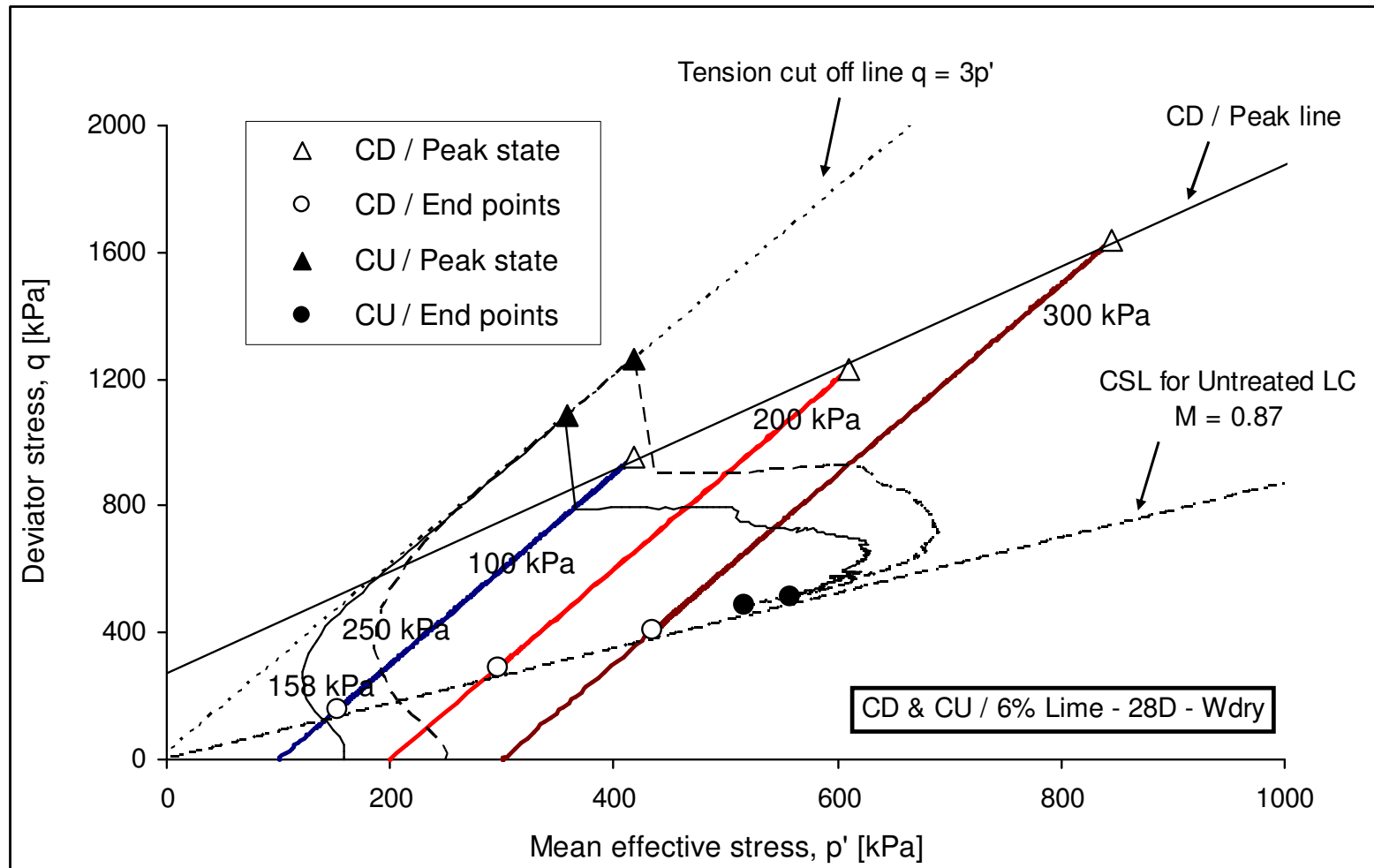
Figure 6.12: CD & CU stress paths in $(q - p')$ stress plane

6.3.3. Stress paths and the stable state boundary surface (SSBS)

One of the fundamental concepts in Critical State Soil Mechanics theory (CSSM) is that a surface exists in (p',v,q) space which defines the states of the yielding (Schofield and Wroth, 1968), this is named the Stable State Boundary Surface (SSBS) (Fig. 6.13). The state of soil sample under trixial testing is portrayed by a point in (p',v,q) space. The elastic response of the tested specimen is identified by a point lying bellow the surface, whereas the plastic yielding commences once the point reaches the surface and remains on it until failure occurs. The behaviour of bonded soils has previously been discussed by several researchers, notable contribution include Leroueil & Vaughan (1990); Burland (1990); Gens & Nova (1993); Coop & Atkinson (1993); Liu & Carter (1999); Schnaid et al. (2001); Yu et al. (2007) and Muhunthan & Sariosseiri (2008) among others. They described the effect of bonding as permitting the soil to exist in states outside the SSBS ascertained for the unbonded soil.
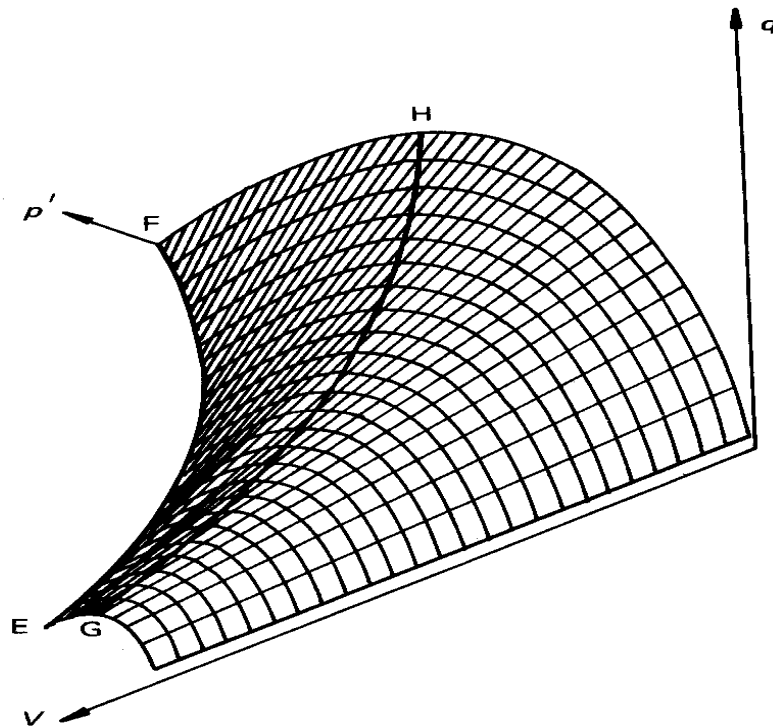
Figure 6.13: The Stable State Boundary Surface (Britto and Gunn, 1987)

In order to display information about the three quantities (p', v, q) defining the state of the soil, it is a standard practice to use a two dimensional presentation of the SSBS by normalising p' and q with respect to an equivalent consolidation pressure p'_e. This is the most useful plot to examine the effect of bonding as indicated in Fig. 6.14 which shows the normalised form of the SSBS for the modified theory. In this plot, the critical state line has become a point on the curve (yield locus) representing the SSBS.
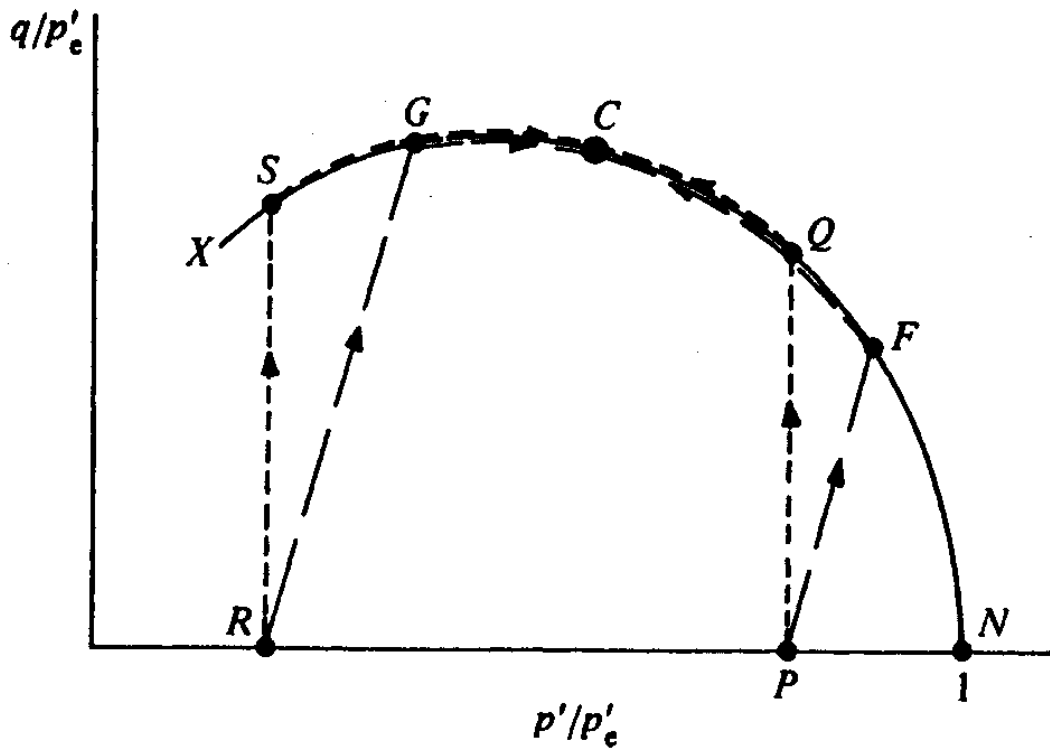
Figure 6.14: Normalised form of the Stable State Boundary Surface according to the modified theory (Muir Wood, 1990)

p'_e is defined as the mean effective stress on the isotropic compression line corresponding to specific volume at any stage of the triaxial test (e.g. Atkinson & Bransby, 1978; and Muir Wood, 1990). The isotropic normal compression line is

$$v = N - \lambda \ln p' \qquad\qquad (6.6)$$

Where N is the specific volume intercept at unit pressure $(p' = 1 kPa)$, and λ is the average experimental value found from both the isotropic compression line and critical state line in the volumetric plane.

Hence, for a particular specific volume v during a triaxial test, p'_e can be obtained by using the following expression (Muir Wood, 1990)

$$p'_e = \exp\left(\frac{N-v}{\lambda}\right) \tag{6.7}$$

The form of the SSBS according to the modified yielding theory introduced by Roscoe and Burland (1968) is presented by the following yield locus equation:

$$\frac{p'}{p'_0} = \frac{M^2}{M^2 + \eta^2} \tag{6.8}$$

Where $\eta = \dfrac{q}{p'}$

At any mean effective stress p' inside or on the current yield locus of size p'_0, the equivalent pressure p'_e can be related to p' by the following equation (Muir Wood, 1990)

$$\frac{p'}{p'_e} = \left(\frac{p'}{p'_0}\right)^{\left(\frac{\lambda-\kappa}{\lambda}\right)} \tag{6.9}$$

Hence, substituting (6.8) in (6.9)

$$\frac{p'}{p'_e} = \left(\frac{M^2}{M^2 + \eta^2}\right)^{\left(\frac{\lambda-\kappa}{\lambda}\right)} \tag{6.10}$$

The $\dfrac{q}{p'_e}$ can be determined by multiplying $\dfrac{p'}{p'_e}$ by η, resulting into the equation (6.11)

$$\frac{q}{p'_e} = \frac{\eta p'}{p'_e} = \eta\left(\frac{M^2}{M^2 + \eta^2}\right)^{\left(\frac{\lambda-\kappa}{\lambda}\right)} \tag{6.11}$$

At critical state, where $\eta = M$, both equations (6.10) & (6.11) will be simplified to:

$$\frac{q}{p'_e} = M\frac{p'}{p'_e} = M\left(\frac{M^2}{M^2 + \eta^2}\right)^{\left(\frac{\lambda - \kappa}{\lambda}\right)} \qquad (6.12)$$

A boundary surface for untreated London Clay can be drawn in a normalised space using the equations (6.10) and (6.11). For stress states on the normalised space, equation (6.12) defines a point on the yield locus (identified as critical state point on the plot / see Fig. 6.14a), corresponding to the critical state at coordinates $\left(\frac{p'}{p'_e} = 2^{-\left(\frac{\lambda - \kappa}{\lambda}\right)}; \frac{q}{p'_e} = M2^{-\left(\frac{\lambda - \kappa}{\lambda}\right)}\right)$,

whereas the point N $\left(\frac{p'}{p'_e} = 1; \frac{q}{p'_e} = 0\right)$ correspond to isotropic normal compression line.

Alternatively, plotting the surface in terms of normalised volume v_λ and stress ratio η can be used to display information about (p', v, q) values defining the state of the soil. At any values of stress ratio η characterising successive similar points on successive yield loci generates a line, which is parallel to the compression line, and has an equation of similar form as (6.6)

$$v = v_\lambda - \lambda \ln p' \qquad (6.13)$$

A yield locus is associated with an unloading reloading line in the compression plane p', v which has a general equation

$$v = v_k - \kappa \ln p' \qquad (6.14)$$

Where κ, is the slope of unloading reloading lines, and can be estimated by finding the slope of the initial elastic compression line. The expression for the specific volume at a point on unloading reloading line, corresponding to a yield locus with size p'_0 is represented by the following expression (Muir Wood, 1990)

$$v = N - \lambda \ln p'_0 + \kappa \ln \frac{p'_0}{p'} \qquad (6.15)$$

Combining (6.13) and (6.15), along with the equation of the yield locus (6.8) results in the following expression

$$v_\lambda = N - (\lambda - \kappa)\ln\frac{M^2 + \eta^2}{M^2} \tag{6.16}$$

For the modified version of the Cam Clay model N is related to other defined parameters by the following equation

$$N = \Gamma + (\lambda - \kappa)\ln 2 \tag{6.17}$$

Hence,

$$v_\lambda = \Gamma + (\lambda - \kappa)\left(\ln 2 - \ln\left(1 + \frac{\eta^2}{M^2}\right)\right) \tag{6.18}$$

The yield locus for untreated London Clay is presented in Fig. 6.15 showing a typical behaviour of a normally consolidated soil, using the general equation (6.8), the Cam Clay model (modified version) appears to fit the material's plastic response to shearing (Fig. 6.15a). From the initial state "A", stress paths for untreated London Clay specimens initially displays an elastic response with an increasing stress ratio (Fig. 6.15b) and any stress state which is on the current yield locus is shown to be close or lie on this curve. Fig. 6.15a show the soil starts yielding when the state reaches the boundary surface at "B" at stress ratio $\eta < M$, while a continued loading is associated with plastic hardening where simultaneous elastic and plastic strains are occurring. At this stage the state boundary surface is the yield surface, and the soil state is on the surface following the yield curve towards the left. A perfectly plastic critical state is reached at point "C" with $\eta \approx M$.

For lime treated London Clay specimens (see Figs. 6.16, 6.17, 6.18 & 6.19), the stress paths are shown to evolve outside the original boundary surface, implying that the yield locus in $\left(\dfrac{q}{p'_e}, \dfrac{p'}{p'_e}\right)$ space has enlarged with increasing amount of bonding in the material as compared to the original boundary. However, this expansion could not be fully drawn due to the experimental difficulties in obtaining the normal consolidation lines and the corresponding compression and critical state parameters, particularly for 6% lime treatment. The expansion of the original boundary observed in the $p'-q$ plane is due to the effect of cementation bonds.

Fig. 6.16a, representing 4% lime treated London clay specimens at 7 days curing, shows similar stress paths direction as of the untreated specimen's response which tends to seek the failure state position by following a rising path towards the peak from the initial state at a decreasing specific volume, but recorded at a much lower rate than for the untreated specimens, without a clear indication of the yielding taking place. However, based on results obtained from stress-strain behaviour (Fig. 5.9 in section 5.4.2) clearly shows that yielding occurs in (p',q) space at an axial strain varying between 1 and 3% before the specimens rupturing, which correspond to $\eta > M$. This implies that plastic strains are occurring during the progressive de-bonding, and a continued deformation is associated with plastic softening (contraction of yield locus) at a decreasing stress ratio p'/p'_e while seeking the critical state, this is typical of lightly over-consolidated specimen's behaviour.

Similarly, the 6% lime treated London Clay specimens' yielding occurs at $\eta > M$ followed by a sudden failure after rupture with a volumetric expansion to critical state, where stress ratio p'/p'_e increases.

Moreover, a lime amount increase from 4 to 6% is observed to significantly increase the domain (SSBS) where the material can subsist. However, the curing time increase from 7 to 28 days and the pre-curing water content did not have a major effect on the expanded domain. Although that yielding occurs in all 6% lime treated specimens as indicated in (p',q) space (see Chapter 5 / Figs. 5.8 & 5.9), but it is not being reflected in the normalised space $\left(q/p'_e , p'/p'_e \right)$, implying that lime treated London clay specimens have all failed in the elastic region before entering the plastic zone. This response can be explained by the presence of a higher cementation bonds developed during the curing time. The stress paths for 6% lime treated specimens (7 days cured) start from an initial state by following a direction towards the right at gradient 3, clearly showing that the original SSBS expanded much more than for specimens treated with 4% lime when cured for a similar duration, but can not be identified as yielding is skipped due to specimens rupturing before reaching the plastic zone and failing in the dry side of critical. This is typical behaviour of heavily over-consolidated soils and bonded materials, which is mainly due to the amount of cementation bonds playing an important role during the shearing stage by

initially displaying rigid type behaviour until a sudden rupture occurs due to shear band localisation.

The boundary expansion appears to be more pronounced for a higher lime amount (6%) as shown in Figs. 6.17, 6.18 & 6.19, with various amount of bonding gained (regardless of the curing time and the initial compacting conditions). This suggests that the failure surface of lime treated London Clay increases with lime amount increase, which is in agreement with the findings reported in Chapter 5 / section (5.4.4) related to the failure envelope.

Note that the MCC is the only model applied in this study, and it is only being referred to for a comparison purpose to the original SSBS. It is noted that the amount of cementation bonds will decrease with loading when bonding is gradually damaged. However, when all bonding is completely broken, lime treated London Clay specimens critical state lines, each represented by a point on $\left(q/p'_e , p'/p'_e \right)$ space have been observed to fail on / or closer to a line with a gradient value $\eta = 0.87$ as indicated in Fig. 6.20. Conversely, the boundary surface at the critical state for the lime treated specimens (assuming that the original yield locus isotropically expands and based on the drawn points) is identified to be in a higher position as of the untreated material, but also detected to be lower than their corresponding peak / failure envelope (the assumed yield locus shrinks after failure), which is also an important feature to consider in modelling and design.

Overall, it can be concluded that lime addition to London Clay allows the expansion of its existing stable state boundary surface where the untreated material subsist. The principal mechanism of bonding has the effect of shifting the state boundary surface, the enlargement is observed to be larger for a higher lime amount (6%) due to the material being stronger as shown in $\left(q/p'_e , p'/p'_e \right)$ space. Whereas, the curing time and compaction water content did not show a major effect on the treated material. The distance between the state boundary surfaces for treated and untreated soil depends principally on the strength and the amount of cementing (Atkinson, 2007).

(a)
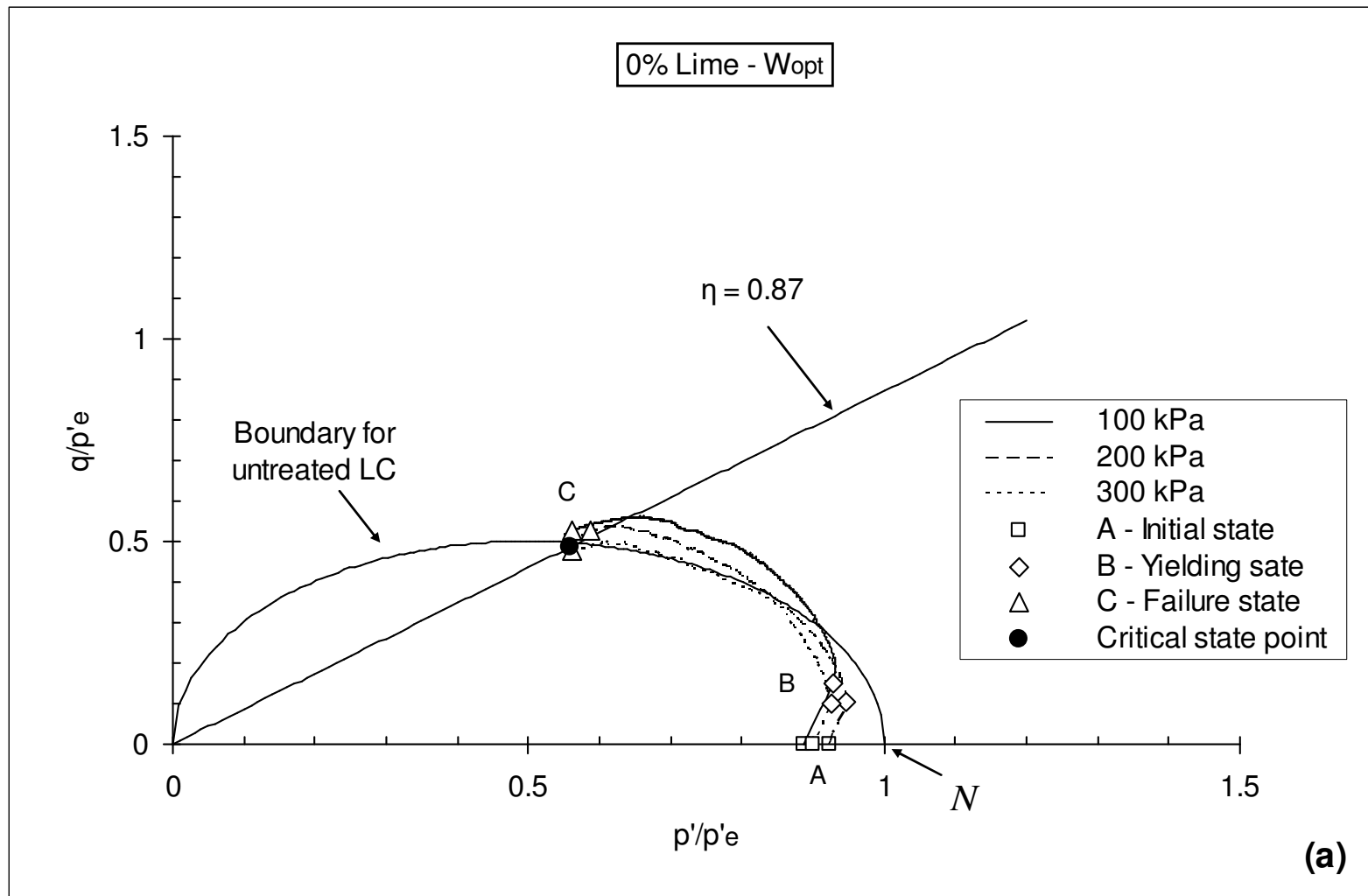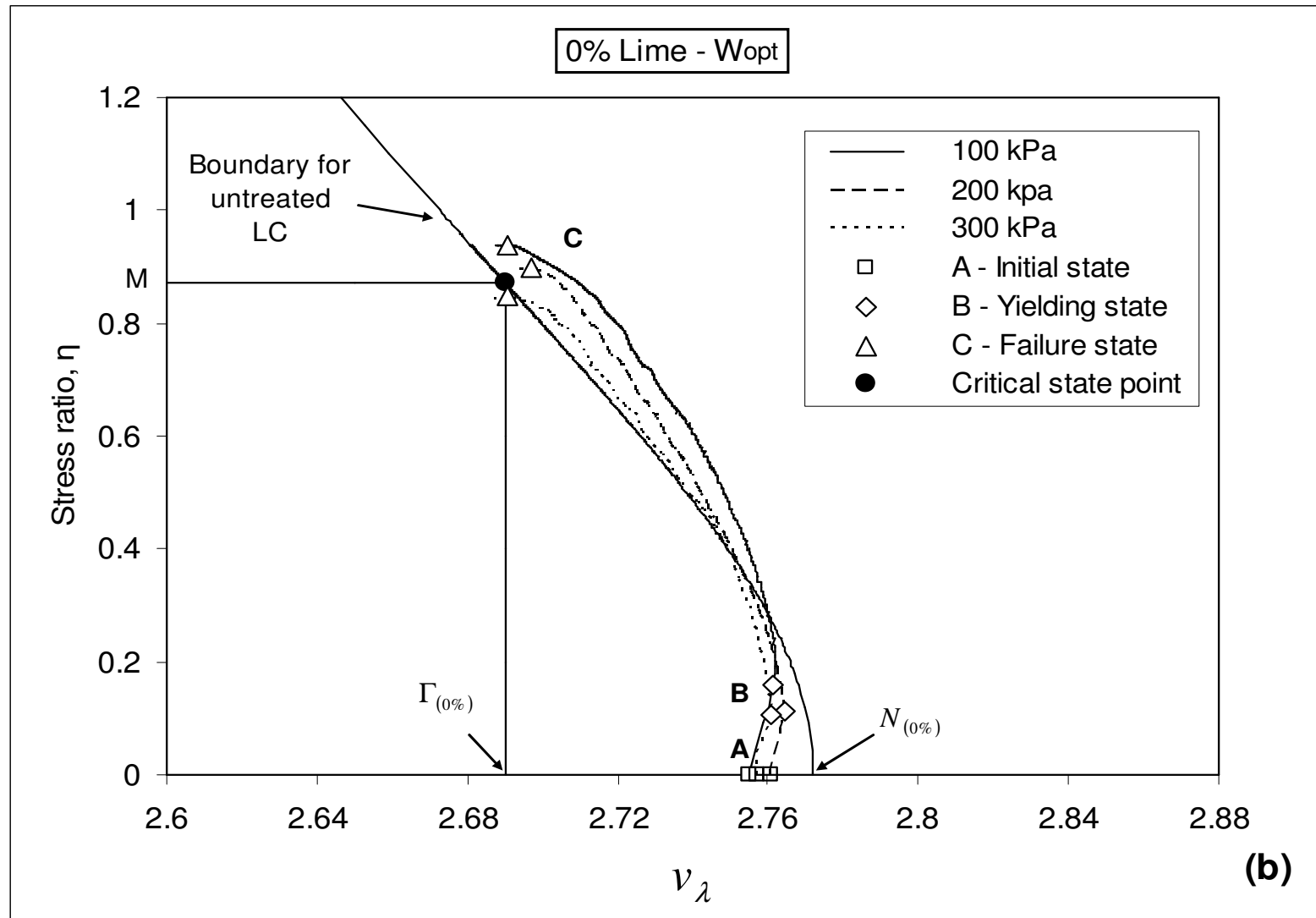
Figure 6.15: Normalised form of the stable state boundary surface for untreated London Clay (according to modified theory)
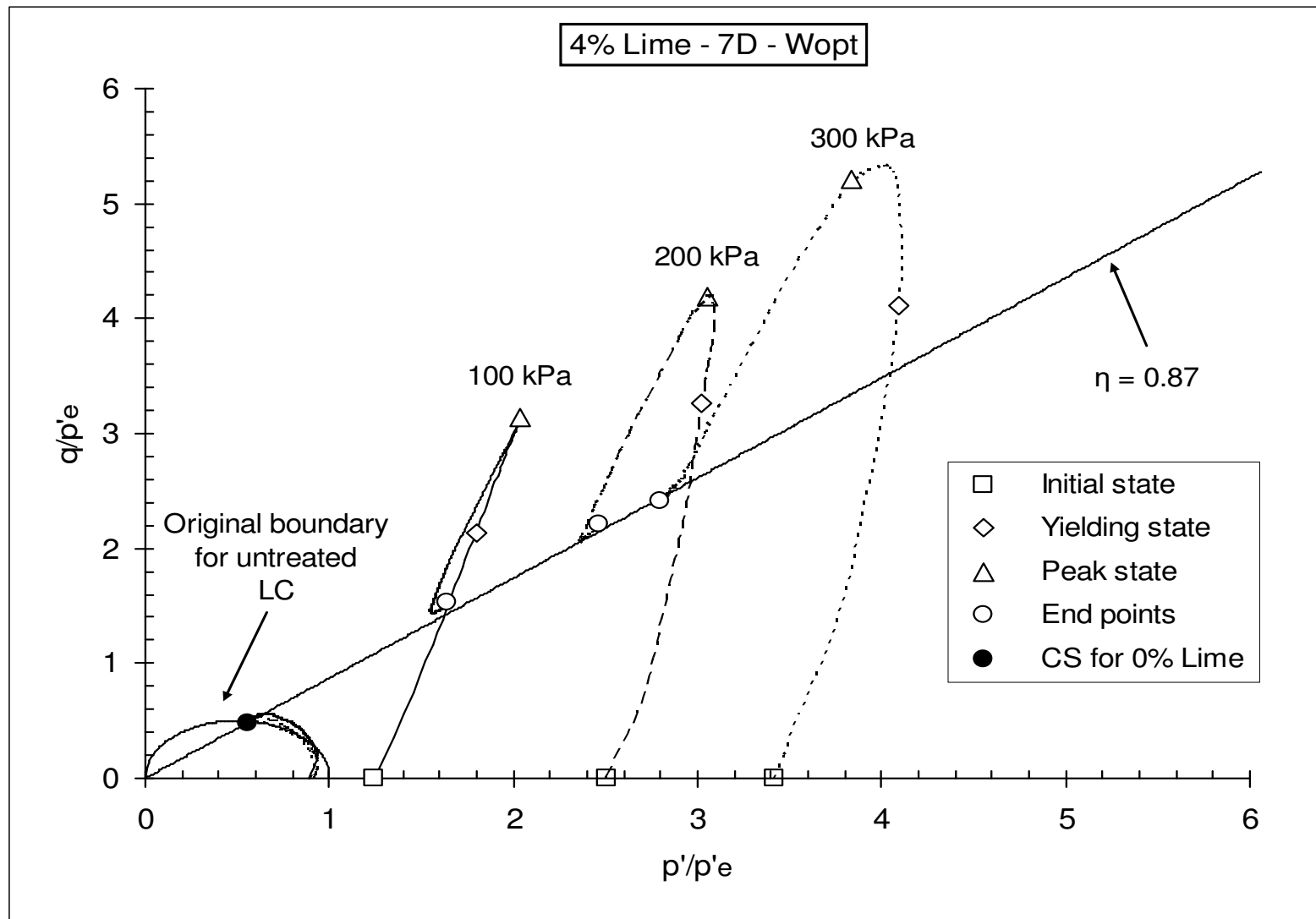
Figure 6.16: 4% lime treated London Clay stress paths compared to the original SSBS (7 days curing)
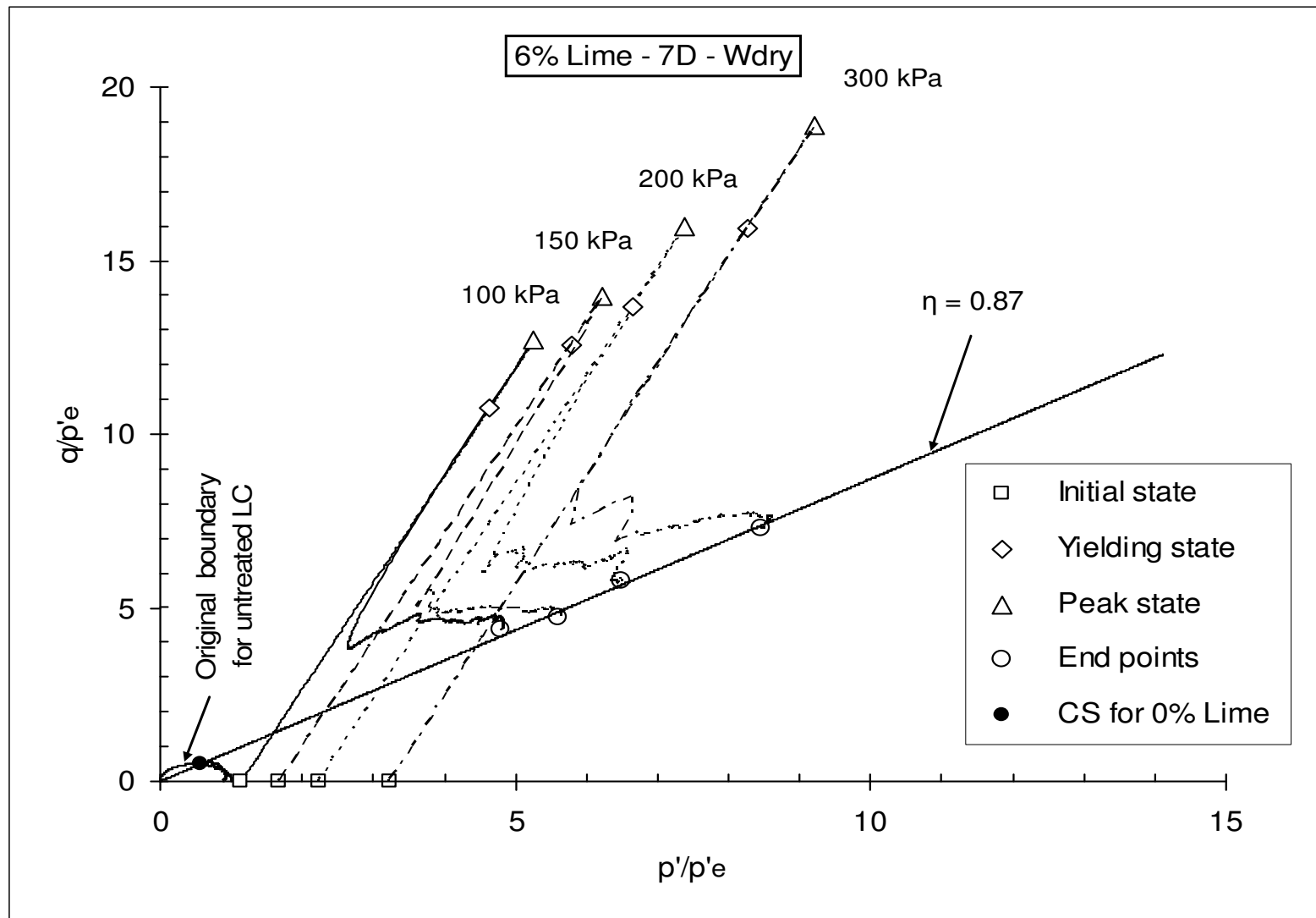
Figure 6.17: 6% lime treated London Clay stress paths compared to the original SSBS (7 days curing)
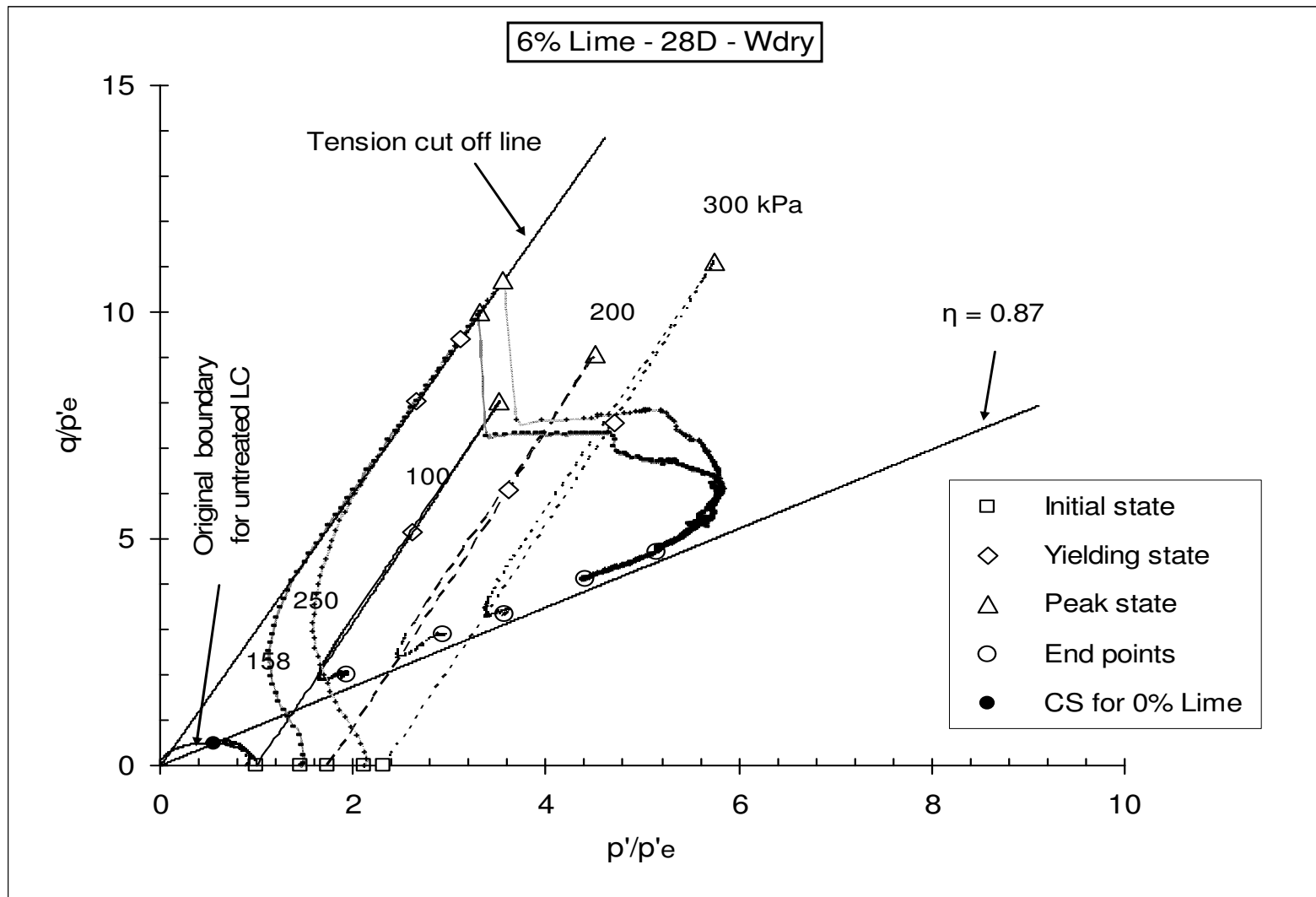
Figure 6.18: 6% lime treated London Clay stress paths compared to the original SSBS (28 days curing / w_{dry})
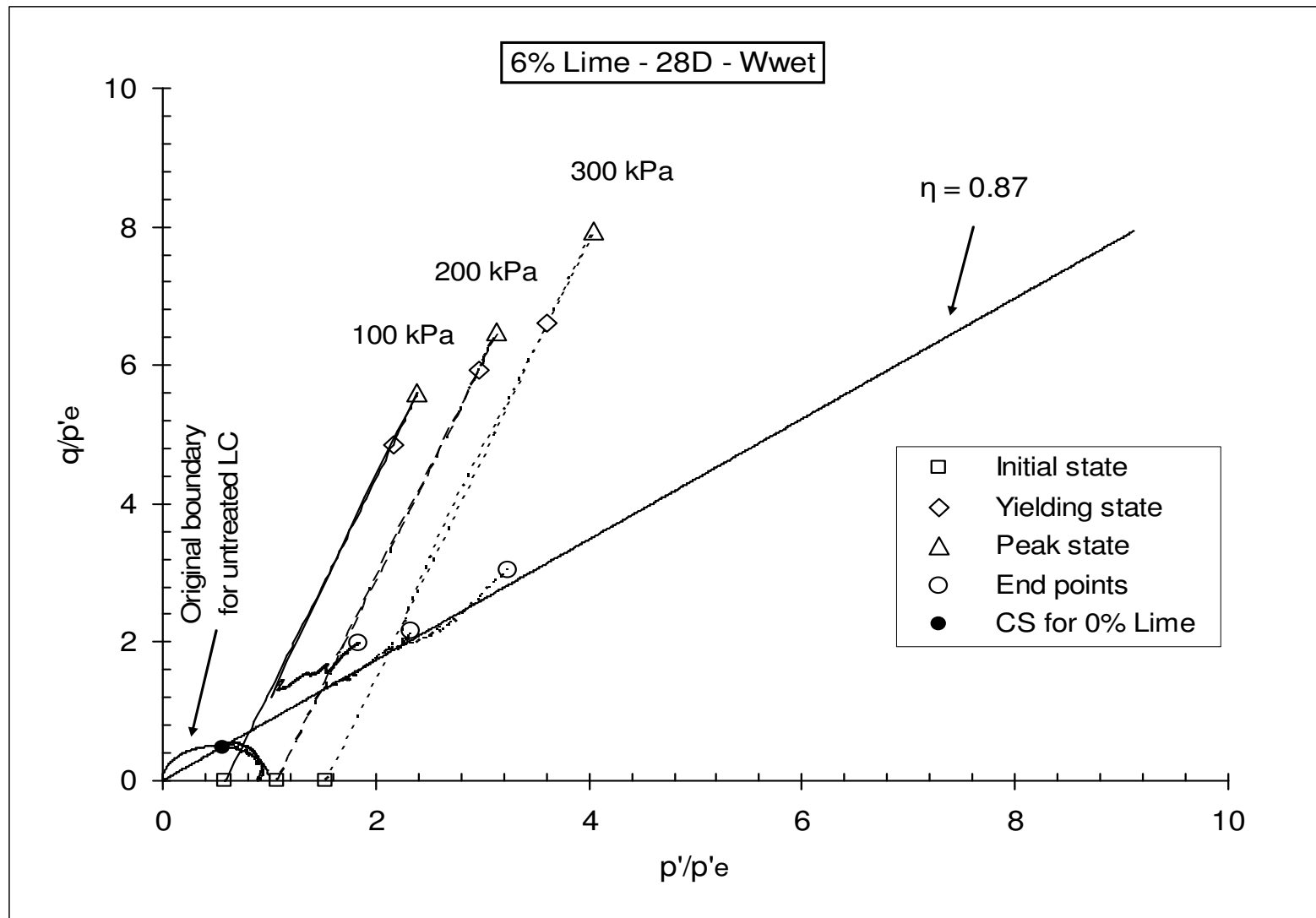
Figure 6.19: 6% lime treated London Clay stress paths compared to the original SSBS (28 days curing / w_{wet})
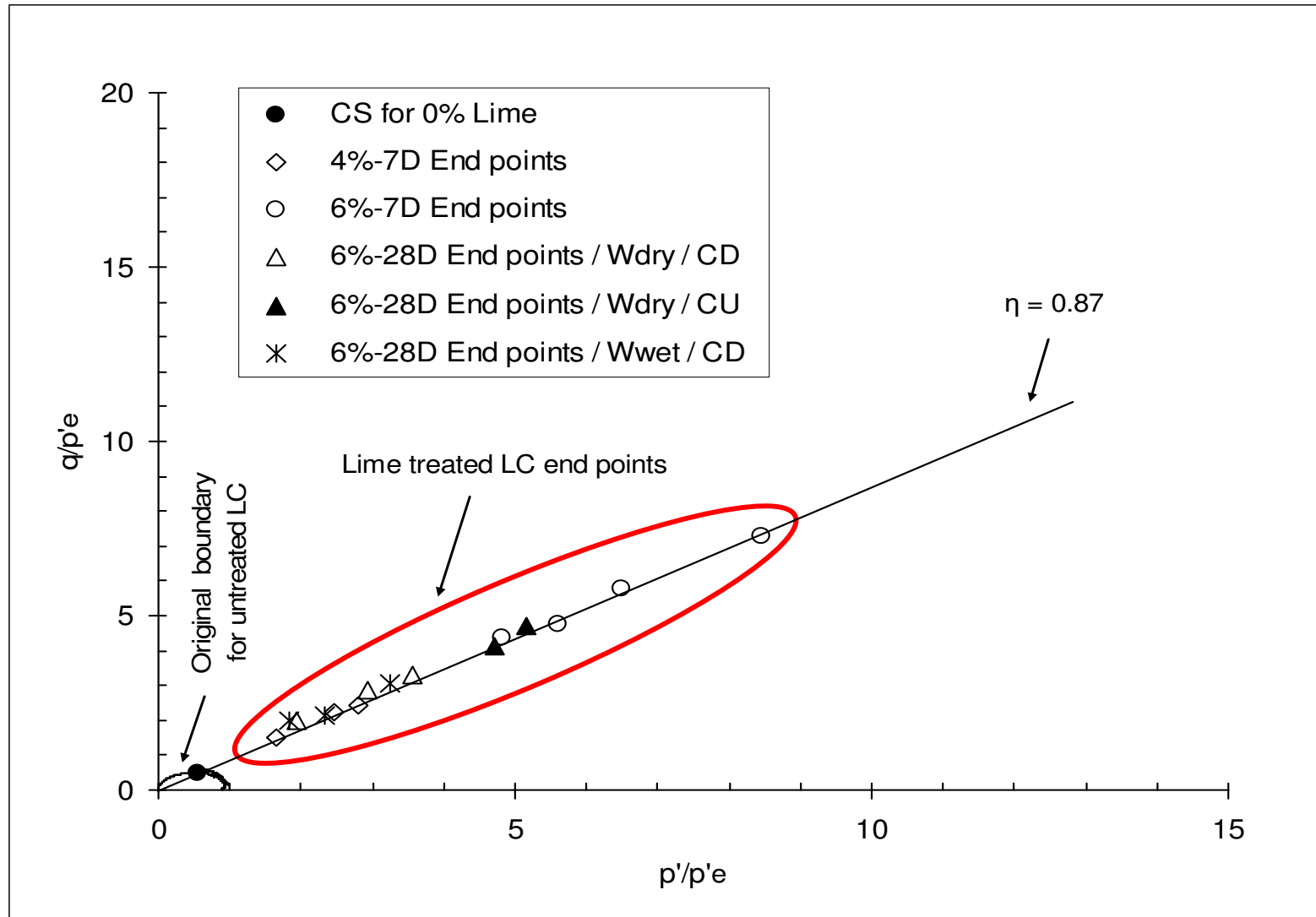
Figure 6.20: End points of lime treated London Clay in normalised stress space

6.4. Comparison of the results to other similar soils

Several studies on London Clay have been performed by other researchers to determine the geotechnical and engineering properties of the soil. Although that the geotechnical properties such as the liquid limit, plastic limit and the plasticity index of London Clay were found to vary, but generally the shear strength parameters (c' and ϕ') and the critical state parameters such as the slope parameter λ, the gradient of the critical state line M and the critical state friction angle ϕ'_{cs} were found to be almost similar. For comparison, a summary of each research results is presented in Table 6.3, indicating that the results obtained in this study are somehow within the same line as other researchers published work on London Clay. However, a limited number of studies on the same or similar soils treated with lime were found in the literature, but generally other studied clayey soils treated with different binders using the same approach are available. For instance, Brooks et al. (1997) performed a laboratory study on lime treated London Clay and Gault Clay in order to found a solution to an identified problem of the slopes on the motorway network in England and Wales that are at risk from instability. Property indices for both materials were determined by the authors and the results presented particularly for London Clay are found to be very close to the current research results (See Table 6.3).

These two clayey soils are both over-consolidated in nature and of very high plasticity. The authors used the composition of the optimum mix to make recommendations for the field trial. Cylindrical specimens were prepared (100/200), compacted to their natural water content, and treated with 5, 10 and 15% lime addition. Specimens were cured for 1, 4, 8 and 16 weeks for both treated materials. One major observation made by the authors is that radial swelling of the specimens prior to testing was in a range of 1.5 – 3.8% as of the initial measurements, they also indicated that generally marginally more swelling occurred with higher lime contents and longer curing period. Similar observation was made in this current research, by identifying a post-curing expansion of the treated specimens, depending on the lime amount and curing time.

A first set of specimens were tested in triaxial compression under undrained conditions (these were not saturated and are comparable to UU tests carried out in this research). A low confining stress of $50 kPa$ was applied during the tests to reflect or simulate the

approximate stress regime surrounding a lime stabilised soil column or lime pile used to improve slope stability at the site of potential shallow slip. The second set containing specimens cured for 16 weeks were subjected to effective stress tests, sheared under consolidated undrained conditions with pore pressure measurements. They were conducted at the confining pressures of 50, 100 and 200 kPa. To facilitate comparison to the current research, only results from the 5% lime treated soil are presented in the table. However, it is important to indicate that Brooks et al. (1997) curing procedure was carried out at variable water content using side drains straight from compaction (no dry curing performed). It is believed that his procedure results in a softening of the treated samples due to leaching. Whereas, in the current research; a dry curing method was used which consist of curing the specimens at constant water content, before being installed in the triaxial cell for the saturation and consolidation stages. This procedure results in significant strength enhancement of the treated specimens. Therefore, it can be concluded that the lower strength obtained by Brooks at al. (1997) (See table 6.4 & 6.5) is due to the different curing procedure, which may have facilitated leaching (lime loss) during moisturising and curing time, consequently affecting strength.

Nevertheless, Brooks et al. (1997) results indicated that in general strength increased with lime addition except for 5% & 10% which the authors explained that is probably due to the density effect. They also reported the effective shear strength parameters (c') and (ϕ') increase with lime amount increase (see table 6.4 & 6.5). It must be noted that, similarly to the Gault clay, a brittle failure was observed, and the strains to failure were generally small and less than one half of that of the untreated clay. Similar results as of Brooks et al., (1997) were obtained in this current study.

The other comparable research carried by Zhang (2011) on lime treated London Clay; the author mostly investigated lime treated soil response under unsaturated state. However, few UU triaxial tests were performed on as cured 4% lime treated London Clay and can be compared to the present investigation. Similar response of lime treated soil was observed in this research, and almost the same strength results were obtained with strength increasing with lime addition, except that no strength increase beyond 7 days curing (and up to 166 days) was observed in Zhang (2011) work, whereas in this research, strength was found to increase after a plateau (60 days onwards) for two different lime dosage (4% & 6%). In a recent geotechnical European conference, a keynote lecturer (Gomes Correia,

2015) using De Bel et al. (2011) study on lime treated soil has shown a sudden increase in strength with curing time after a plateau (100 days onwards), which is similar results obtained in this research related to UU triaxial tests. An explanation for this result was provided by Kinuthia (2015) as follow: "Early gains in strength are due to cation exchange effects. Cemented material is slowly formed, initially around contacts between agglomerations of clay particles and then spreads around the surface of these agglomerations. When this spreading is complete, a full matrix of cemented material exists and the higher strengths are observed (60 days onwards). At intermediate times failure takes place through the weaker element of the material (i.e. the clay particles)"

In addition, another set of 4% lime treated London Clay samples tested by Zhang (2011) under saturated state were also compared to this research, and no major differences were observed. However, a slightly higher strength was obtained in this research, which is believed to be due to the different saturation procedure performed in each study. In this research, specimen saturation was performed inside the triaxial cell straight after the dry curing period, while in Zhang (2011) study, lime treated samples were saturated for 28 days outside the triaxial cell using saturators before installing the specimens in the triaxial cell for testing. This is believed to be the main reason for the observed differences in strength values (see Table 6.4 & 6.5).

Table 6.3:. Index and Geotechnical properties of London Clay reported by other researchers

Source	Index & Geotechnical properties of LC reported by other researchers						
	w_L	w_P	I_P	G_s	λ	M	$\phi_{cs}{}'$
Skempton (1944)	77	28	49	2.71	*	*	*
Parry (1960)	78	26	52	*	0.161	0.888	22.5°
Bishop et al. (1965)	58.9 - 70.6	23.8 - 29	35.1 - 41.6	2.72 - 2.77	*	*	*
Sherwood (1993)	80	26	54	*	*	*	*
Brooks et al. (1997)	76	27	49	*	*	*	*
Sidique & Clayton (1999)	69	24	45	2.74	*	0.76	19.6°
Jardine et al. (1985)	62.3	24.3	38	2.73	0.16	0.88	22.5°
Gasparre (2005) & Gasparre et al. (2007)	59 - 74.5	21 - 32	38 - 42.5	2.65 - 2.76	*	0.85	21.3°
Pantelidou & Simpsom (2007)	*	*	*	*	*	0.86	22°
Zhang (2011)	64	26	38	2.75	0.139	0.88	22.5°
Present investigation	**73.5**	**26.1**	**47.4**	**2.76**	**0.142**	**0.87**	**22.33°**
(*): Data not available							

Table 6.4: Comparison of lime treated soil undrained strength results

Source	Lime	Undrained shear strength results & comparison					
		Sample preparation	Curing procedures	Curing time	Total stress σ_3	q_{peak}	$\tau = c_u$
	(%)	-	-	(days)	(kPa)	(kPa)	(kPa)
Brooks et al., 1997 (London Clay)	0%	Clay mixed at its natural moisture content Compacted with no adding water	After extrusion, wetting took place using side drains then wet curing	-	50	*	34
	5%			7		*	312
				28		*	246
				56		*	375
				112		*	267
Brooks et al., 1997 (Gault Clay)	0%			-	50	*	27
	5%			7		*	57
				28		*	102
				56		*	120
				112		*	123
Zhang, 2011 (London Clay)	0%	Compacted to W = 25%	N/A	-	200	600	*
	4%	Reconstituted Clay Compacted to water content W = 27%	After extrusion, dry curing at constant water content	1	200	1160	*
				7		1200	
				21		1100	
				166		1100	
Present research (London Clay)	0%	Compacted to W = 25%	N/A	-	200	529	*
	4%	Reconstituted Clay Compacted to water content W = 27%	After extrusion, dry curing at constant water content	1	200	1232.6	*
				7		1307.8	*
				28		1240.8	*
				60		1263.14	*
				120		2016.4	*
				250		2688.06	*
	6%			1	200	1448.22	*
				7		1913.39	*
				28		2117.61	*
				60		2395.67	*
				120		4510.35	*
				250		5610.77	*

Table 6.5: Comparison of lime treated soil effective stress strength results

Source	Lime	Effective stress strength results & comparison						
		Sample preparation	Curing procedure	Curing time	Effective stress σ_3'	q_{peak}	c'	ϕ'
	(%)	-	-	(days)	(kPa)	(kPa)	(kPa)	(°)
Brooks et al., 1997 (London Clay)	0%	Clay mixed at its natural moisture content Compacted with no adding water	After extrusion, wetting took place using side drains then wet curing	-	*	*	12-18	17-23
	5%			7	*	*	*	*
				28	*	*	*	*
				56	*	*	*	*
				112	50 / 100 / 200	*	65	41
Brooks et al., 1997 (Gault Clay)	0%			-	*	*	10-14	23-25
	5%			7	*	*	*	*
				28	*	*	*	*
				56	*	*	*	*
				112	50 / 100 / 200	*	30	42
Zhang, 2011 (London Clay)	0%	Compacted to W = 25%	N/A	-	50 / 100 / 200 / 400	104.3 / 173.2 / 282.6 / 477.2	19	21
	4%	Compacted to W = 27%	Dry curing at constant water content, saturated outside the cell for 28 days using saturators	7	100 / 200 / 300	278 / 431.9 / 602	38	26.5
Present research (London Clay)	0%	Compacted to W = 25%	N/A	-	100 / 200 / 300	133.83 / 256.97 / 361.34	7	21
	4%	Reconstituted Clay Compacted to water content W = 27%	Dry curing at constant water content, saturated inside the cell under an effective stress 20kPa	7	100 / 200 / 300	314.94 / 507.45 / 745.40	35	30.5
	6%			7	100 / 150 / 200 / 300	1243.02 / 1330.22 / 1558.92 / 1945.38	220	39
				28	100 / 200 / 300	952.03 / 1231.68 / 1636.96	145 - 181	39

Studies on similar soils using different approaches treated either with the same or different binder can be found in the literature. For instance, Thomas (2002), performed a study on the effect of lime addition on the various engineering properties of sulphide rich clay (lower oxford clay), which was found inadequate for lime treatment. The author included two other binders, ground granulated blast furnace slag and Portland cement to improve the strength of the material. Results showed (when compared to lime treated soil) that strength enhanced, the linear expansion reduced and durability improved. The author concluded that soil stabilisation with lime and GGBS is particularly effective for naturally occurring sulphite rich clay soils. Ahnberg (2006) carried out an extensive experimental investigation on Swedish clayey soils treated with three different binders, mainly focusing on strength properties using UCS tests and triaxial tests to study the strength behaviour under various drainage and stress conditions, resulting in an improved strength model being proposed. The author has identified that the general strength and deformation properties are the same for soils stabilised by the most common binders. However, the study did not cover the post-peak state of the treated materials, and was not extended into the critical state framework. Tedesco (2006) using lime to treat Italian clay has mainly identified the treated soil properties and the effects of lime addition as well as the curing time. Sasanian (2011) using cement to stabilise clay investigated the formation of microstructure in artificially cemented material with Portland cement, the author identified the relationships between cementitious bonding and clay mineralogy, and found that the addition of cement reduces the amount of macro-pores within the cemented material. In addition, the study was extended to investigate the yielding and stress-strain behaviour of the cemented Ottawa clay and compared to the naturally structured state in similar way carried out in this research against the reconstituted London Clay. The study was performed using the critical state framework, allowing the identification of fundamental parameters (isotropic compression and critical state parameters) to develop a constitutive model for predicting a mechanical behaviour of artificially cemented material. One important finding similar to this research is the cement addition does not have any effect on the CSL gradient M, and a new state boundary surface was identified for cemented material but an attempt to apply similar concept for naturally structured Ottawa clay was not successful. Kamruzzaman (2002) studied physico-chemical, microstructural (using SEM & XRD analysis), and the engineering properties (based on UCS) as well as the stress-strain response of cement treated Singapore marine clay based on triaxial tests. The author identified that the yield surface as well as the failure envelope shifted further upward with higher cement content

and found that yielding is associated with the breaking of cementation bonds which was confirmed by SEM images. The effective shear strength parameters (c') and (ϕ') were found to increase with the increase of cement content, which is a similar result obtained in the current study. In addition, Kamruzzaman (2002) indicated that the stiffness of the treated clay increases significantly due to cementation (similar behaviour observed in the current research), but the study was limited to the peak state only and was not taken to the critical state framework.

From this comparison, it is clear that the influence of lime addition on the geotechnical properties is unique for each soil. These compared soils are relatively inhomogeneous and have relatively different micro-structural properties due to the difference of physico-chemical nature of their components. Additionally, the chemical reactions between the soil particles and lime varied depending on the chemical and mineralogical composition of each soil treated with lime. The difference in strength is probably due to the difference in sample preparation procedure such as water content, curing conditions and most importantly the compaction related effect.

6.5.   Implications of the research for Geotechnical design

In engineering designs and safety check, engineers are only concerned about two facts of our structures: the strength and deformation of the structure. However, recent codes of practice for geotechnical design (e.g. EC7 (2004)) place an increased emphasis on carrying out explicit calculations of ground movement as opposed to carrying out ultimate limit state calculations (using ground strength) and applying large safety factors to ensure ground movements remain small. These explicit calculations of ground movements require soil stiffness and measuring these in field conditions and the laboratory has been an important area of geotechnical research during the last 30 years (Simpson, 1992; Oztoprak and Bolton, 2013)

From an economical point of view, it is becoming increasingly important to account for the properties of treated materials in the design of the geotechnical structures. In the case of lime treated clays (despite its proven efficacy) relatively little data exists on material stiffness, and there are doubts on whether designing structures on lime treated soil has to be performed to the peak state or critical state. The current research has tried to fill this gap and represent a useful starting point in the knowledge of treated clay. Laboratory tests are performed in order to improve the understanding of some of the important aspects of the strength behaviour, and assemble observations which can help researchers to develop and calibrate constitutive models of soil behaviour. These provide the link between stress increments $\delta\sigma$ and strain increments $\delta\varepsilon$ which are needed for the performance of numerical analysis of geotechnical systems (Muir Wood, 2004).

A fundamental requirement of engineering design in geotechnic is to examine the serviceability limit state and to demonstrate the movements will not exceed some limit determined by the design team. For structures such as foundations the design is controlled with serviceability limit state, the structure must not move too much. One of the methods is to apply a load factor to a collapse analysis and the question is whether the collapse analysis should be done with the peak or with the critical state strength?

Modern research on soil stiffness usually builds on the concepts of Critical State Soil Mechanics (Schofield and Wroth, 1968) according to which there is pseudo elastic behaviour (characterised by the property κ) when the soil state lies within the Stable State

Boundary Surface. When the soil is loaded it may reach the Stable State Boundary Surface and yielding commences (characterised by the property λ). Descriptions of the behaviour of bonded soils (whether bonding is due to natural or artificial causes) are based on the idea that the bonding increases the size of the Stable State Boundary Surface (see Liu & Carter, 2002 and Yu, 2007). The SSBS is not fixed in stress space, but it can expand due to plastic straining. The practical implication of this concept is that a geotechnical design using treated soil could be arrived at so that likely loadings of the ground would not result in yielding behaviour, i.e. states of the soil would continue to lie beneath the Stable State Boundary Surface and thus excessive deformations of the ground would be avoided. For instance, the failure of slopes made by cutting through soil mass is very common. When a cut slope is made, removal of soil from one side causes the release of horizontal stress and the soil on the other side is under decreasing effective stress. The failure of soil mass in this scenario is at low stress state. Most of the slope stability analysis methods assume that failure surface is either inclined planar or circular and uses the shear strength parameters (c' and ϕ') obtained from triaxial compression tests for the analysis. In case of cut slopes in cemented soils, failure occurs by detachment of bonds (brittle failure) and hence the failure surface may not be circular. For lime treated soils, they exhibit high cohesion due to the artificial bonding of the cementing agent and therefore cannot be easily lost on removal of stress. Based on the triaxial tests results analysed using Mohr-coulomb failure criterion, lime addition to London Clay is assumed to increase the shear strength parameters (at peak state) from values of $c' = 7kPa$ and $\phi' = 21°$ to a maximum achievable of $220kPa$ and $39°$ with 6% lime addition.

For structures such as slopes in rural locations, where relatively movements do no damage, the design is controlled by the ultimate limit state with an applied factor of safety. For soils, it has to be decided between the peak or critical state (Atkinson, 2007). Slope stability can be investigated using the slip circle to identify the factor of safety (FOS). One of the methods which can be used to determine the factor of safety, based on the effective stress analysis, is Bishop's conventional method. This is given by the following expression:

$$F_s = \frac{1}{\sum W \sin \alpha} \sum \left[c'l + W(\cos \alpha - r_u \sec \alpha) \tan \phi' \right] \qquad (6.19)$$

Where,

W : The weight of the slice

α : The angle between the total normal force (acting on base of the slice) and the vertical

c' and ϕ' : Effective stress parameters (cohesion and friction angle respectively)

l : The length of slice base (taken as straight line)

$r_u = \dfrac{u}{\gamma_{sat} Z}$: The pore pressure ratio for a steady seepage, with $(u = u_0 + \Delta u)$ being the pore

pressure at any point and Z is the vertical depth of the slope.

The first step in the analysis is to conveniently divide the sliding sector of the slope into suitable number of equal vertical slices. The flow net must be established so that the equipotentials through the centre points of each slice can be inserted, and then determine the pore pressure ratio r_u at the mid point of the base of each slice. To determine the area of a particular slide its mid-height is multiplied by its breadth (b), the weight of the slice is then obtained $(W = \gamma_{sat} \times Area)$, and then set of as a vector below it. When working by hand the final analysis of forces acting on a vertical slice is best carried out by tabulating the calculations. However, in most design offices, slope stability problems are now computerised (Smith, 2006).

To facilitate the evaluation of the FOS of slope treated with lime, variables are separated from constants in the expression (6.19). Assuming that the saturated unit weigh γ_{sat} is constant for all mixtures, the only variable parameters in the expression (6.19) are c' and ϕ'. All other parameters are constants and will carry the same values for all the mixtures. Therefore the constant parts in the expression (6.19) can be presented in the following form:

$$A = \frac{l}{\sum W \sin \alpha} \tag{6.20}$$

$$B = \frac{\sum W (\cos \alpha - r_u \sec \alpha)}{\sum W \sin \alpha} \tag{6.21}$$

238

Where A and B are constants, the Bishop's conventional expression (6.19) can be rewritten as:

$$F_s = c'A + B\tan\phi' \qquad\qquad (6.22)$$

Designing to the peak state, the effective stress parameters c'_p and ϕ'_{peak} values are needed. Table 6.6 presents values of the peak and critical state determined in this research.

Table 6.6: Peak state and critical state strength parameters of lime treated London Clay

Soil + Lime		0%	4%	6%		
Curing time		N/A	7 D	7 D	28 D / dry	28 D / wet
Peak state strength parameters	c'_p (kPa)	7	35	220	145	181
	ϕ'_{peak} $(°)$	21	30.5	39	39	39
Critical state strength parameters	c'_{cs} (kPa)	0	0	0	26.1	28.2
	ϕ'_{cs} $(°)$	22.33	22.56	22.33	22.33	22.33

The factor of safety value for each mixture can be estimated from the expression (6.22) as follow:

$$F_{s(0\%)} = 7A + 0.41B$$

$$F_{s(4\%)} = 35A + 0.59B$$

$$F_{s(6\%)} = (145\xleftrightarrow{to}220)A + 0.8B$$

The above equations clearly indicate that the FOS increases with lime amount. In order to evaluate the increase of the factor of safety, the values of constants A and B have to be determined, which in turn are related to the weigh (W), the angle (α) and the pore pressure ratio (r_u) for each slice, the increase as of the FOS of the untreated soil can then be evaluated.

It can be concluded that lime addition increases the factor of safety for slope stability $F_{s(0\%)} < F_{s(4\%)} < F_{s(6\%)}$, this can successfully be applied for re-instatement of slopes and embankments slips (which are a major problem on many highways and canals cuttings in the UK) by using lime as a binder (ICI, 1990). Lime addition to soil, which enhances the FOS of the slope when designed to the peak state strength, is also beneficial in conditioning the fill and so aiding compaction during construction.

For most purposes, the critical state strength is the worst that need to be considered in design. Depending on the problem faced, if there are pre-existing slip surfaces or if large displacements are expected, then the critical state strength should be considered in design. In the other hand, there are cases in which the critical state strength should be used in geotechnical design. For instance, in a slope, the shear stress on the potential slip surface is governed by the critical state, because even in a stable slope, there will probably be strains in the ground larger than 1% (Atkinson, 2007). For this reason, design using the critical state strength is used, and factors of safety values (as a function of the constants A & B) are also determined here. Note that these factors of safety values are the same as of the untreated soil (see Table 6.7).

Table 6.7: Factors of safety for lime treated & untreated London Clay

Soil + Lime	0%	4%	6%		
Curing time	N/A	7 D	7D	28D - dry	28D - wet
Factor of safety at peak state	$7A + 0.41B$	$35A + 0.59B$	$220A + 0.8B$	$145A + 0.8B$	$181A + 0.8B$
Factor of safety at critical state	$0.41B$	$0.42B$	$0.41B$	$26.1A + 0.41B$	$28.2A + 0.41B$

One important result from the current research is the observation of the experimental evidences never pointed out before; the ultimate angle of friction of the treated soil (i.e. after strain softening from peak) is just the same as that of the untreated soil. Schofield and Wroth (1968) proposed that geotechnical design should be carried out using ultimate (i.e. critical state) strengths, an idea that is consistent with the requirement of material ductility

for plastic design. This approach has significantly influenced current geotechnical design practice in the UK (although much design is still carried out using peak strengths).

For instance, to determine the bearing capacity of a foundation, several analytical methods can be used in design (Smith, 2006). The general form of the bearing capacity equation for $\bar{q}$ is proposed by Meyerhof (1963).

$$\bar{q} = c' N_c s_c i_c d_c + \gamma Z N_q s_q i_q d_q + 0.5 \gamma B N_\gamma s_\gamma i_\gamma d_\gamma \qquad (6.23)$$

Where

c' is the cohesion, γ is the unit weight of the soil, Z is the depth and B is the least dimension or diameter of the footing

s_c, s_q and s_γ are shape factors

i_c, i_q and i_γ are inclination factors

d_c, d_q and d_γ are depth factors

The coefficients N_c, N_q and N_γ depend upon the soil's angle of shearing resistance ϕ' and can be obtained from Meyerhof's equation as they are recognised as being the most satisfactory in geotechnical design according to Atkinson (2007).

$$N_c = (N_q - 1)\cot\phi' \qquad (6.24)$$

$$N_q = \tan^2\left(45° + \frac{\phi'}{2}\right)e^{\pi\tan\phi'} \qquad (6.25)$$

For the remaining factor N_γ, an equation proposed by Vesic (1973) is the mostly used in geotechnics

$$N_\gamma = 2(N_q + 1)\tan\phi' \qquad (6.26)$$

The shape factors are intended to allow for the shape of the foundation on its bearing capacity. The factors have largely been evaluated from laboratory tests and the values in present use are those proposed by De Beer (1970)

$$s_c = 1 + \frac{B}{L} \cdot \frac{N_q}{N_c} \qquad (6.27)$$

$$s_q = 1 + \frac{B}{L} \tan \phi' \qquad (6.28)$$

$$s_\gamma = 1 - 0.4 \frac{B}{L} \qquad (6.29)$$

The inclination factors are estimated from Mayerhof's expressions as follow: (Smith, 2006)

$$i_c = i_q = (1 - \alpha / 90°)^2 \qquad (6.30)$$

$$i_\gamma = (1 - \alpha / \phi)^2 \qquad (6.31)$$

Where, α is the eccentric load inclination to the vertical. The depth factors are intended to allow for the shear strength of the soil above the foundation. Hansen (1970) proposed the following (see table 8):

Table 6.8: depth factors for geotechnical design

Depth factors	$Z/B \leq 1.0$	$Z/B > 1.0$
d_c	$1 + 0.4(Z/B)$	$1 + 0.4 \arctan(Z/B)$
d_q	$1 + 2 \tan \phi'(1 - \sin \phi')^2 (Z/B)$	$1 + 2 \tan \phi'(1 - \sin \phi')^2 \arctan(Z/B)$
d_γ	1.0	1.0
(arctan) values are expressed in radians		

The bearing capacity of a foundation can be determined immediately after a construction. In current geotechnical practices, both the peak and ultimate (critical state) strengths are used in design, depending on the country and the problem faced. However, CSSM argued the use of the ultimate / critical state strength (Schofield & Wroth, 1968).

The choice of soil parameters for bearing capacity equation can be used with either the undrained or the drained soil parameters. The general procedure is to work with undrained parameters (c_u' and ϕ_u') (with ϕ_u' taken equal to zero). However, in this study, the relevant effective stress parameters c' and ϕ' for drained test are used from Table 6.6, with c' generally taken as equal to zero according to Smith (2006).

For simplicity, we assume that the structure is a rectangular shallow foundation ($Z/B \leq 1.0$), and only a vertical load is acting on the foundation, $\alpha = 0$, implying that $i_c = i_q = i_\gamma = 1$

In this research, parameters were determined under saturated state conditions, therefore it is appropriate to use the saturated unit weight $\gamma_{sat} = \dfrac{(G_s + e_{sat})}{1 + e_{sat}} . \gamma_w$ which is calculated based on the average value from the set of performed tests in this study for each mixture, γ_w is the unit weight of water equal to $9.81 kN/m^3$. The average values are presented on Table 6.9.

Table 6.9: Average values of saturated unit weigh for each mixture

Soil + Lime		0%	4%	6%		
Curing time		N/A	7 D	7 D	28 D / dry	28 D / wet
Saturated unit weight	$\gamma_{sat}(kN/m^3)$	17.68 17.66 17.66	17.69 17.59 17.54	17.78 17.79 18.09 17.79	17.85 17.91 17.96	18.14 18.17 18.19
	Average γ_{Av}	**17.67**	**17.61**	**17.86**	**17.91**	**18.17**

The N_q value for peak state in each mixture can be separately determined.

$$N_q(0\%) = \tan^2\left(45° + \frac{21}{2}\right).e^{\pi\tan(21)} = 7.07$$

$$N_q(4\%) = \tan^2\left(45° + \frac{30.5}{2}\right).e^{\pi\tan(30.5)} = 19.48$$

$$N_q(6\%) = \tan^2\left(45° + \frac{39}{2}\right).e^{\pi\tan(39)} = 55.96$$

As recommended in design practice, in drained test, c' is taken equal to zero, and the value of ϕ' (either at peak or at critical state) is used in the expression (6.23). The bearing capacity can be determined as follow:

$$\overline{q} = \gamma_{sat}Z.N_q\left(1+\frac{B}{L}\tan\phi'\right)\times1\times\left[1+2\tan\phi'(1-\sin\phi')\left(\frac{Z}{B}\right)\right]+0.5\gamma_{sat}B\left[2(N_q+1)\tan\phi'\right]\times\left[1-0.4\frac{B}{L}\right]\times1\times1$$

When working at the peak state, N_c, N_q and N_γ increase with lime amount increase (due to ϕ'_{peak} increase). Replacing γ_{sat}, N_q as well as the peak friction angle $\phi'_{(peak)}$ values in the bearing capacity expression for each mixture, the following is obtained:

$$\overline{q}(0\%) = Z(124.93)\left[1+\frac{B}{L}\times0.38\right]\left[1+0.49\times\frac{Z}{B}\right]+0.5B(109.48)\left[1-0.4\times\frac{B}{L}\right]$$

$$\overline{q}(4\%) = Z(343.04)\left[1+\frac{B}{L}\times0.59\right]\left[1+0.58\times\frac{Z}{B}\right]+0.5B(424.93)\left[1-0.4\times\frac{B}{L}\right]$$

$$\overline{q}(6\%)_{7D-dry} = Z(1001.12)\left[1+\frac{B}{L}\times0.8\right]\left[1+0.6\times\frac{Z}{B}\right]+0.5B(1650.35)\left[1-0.4\times\frac{B}{L}\right]$$

$$\overline{q}(6\%)_{28D-dry} = Z(1002.24)\left[1+\frac{B}{L}\times0.8\right]\left[1+0.6\times\frac{Z}{B}\right]+0.5B(1652.2)\left[1-0.4\times\frac{B}{L}\right]$$

$$\overline{q}(6\%)_{28D-wet} = Z(1016.79)\left[1+\frac{B}{L}\times0.8\right]\left[1+0.6\times\frac{Z}{B}\right]+0.5B(1676.18)\left[1-0.4\times\frac{B}{L}\right]$$

In order to evaluate the effect of the lime addition on the bearing capacity of the foundation, some arbitrary dimension values for the foundation are given ($B = 2m$, $Z = 1m$, and $L = 4m$), therefore, the bearing capacity values for each mixture can be evaluated (see Table 6.10)

Table 6.10 present the bearing capacity of lime treated and untreated London Clay for both states (peak state) indicating the increase due to lime addition and the (critical state) where the bearing capacity is the same for all soil mixtures. Analysing the results (based on the arbitrary dimensions given), It can be concluded that adding lime to London Clay, under saturated state conditions, the bearing capacity at peak state increases by 3 times as much for 4% lime addition, and by 11 times as much for 6% lime, resulting in the following: $\overline{q}(0\%) < \overline{q}(4\%) < \overline{q}(6\%)$, which is an advantage to take in consideration in design practice, but high factors of safety are required to avoid excessive soil deformations.

Table 6.10: Bearing capacity of a foundation laid on of lime treated London Clay

Soil + Lime	0%	4%	6%		
Curing time	N/A	7 D	7D	28D - dry	28D - wet
Bearing capacity at peak state $\overline{q}_{peak}(kPa)$	272.67	913	3137.06	3145.84	3191.5
Bearing capacity at critical state $\overline{q}_{cs}(kPa)$	321.71	330.07	325.18	326.09	330.83

An old concept for calculating settlements (e.g. construction fill) is used to ensure stress changes due to construction of the fill do not reach yield, thus avoiding excessive settlements and ensures the design stays within the yielding surface. This concept consist of performing either oedometer tests or isotropic compression triaxial tests on natural samples from different depth, the effective stress values at yield for each sample (which increases with depth Z) are used as the limit to ensure that the construction of (e.g. the fill) does not cause stresses changes beyond the elastic deformation. In critical state concept, the modelling approach is to work within the yield surface which is similar to the above concept used for settlement calculations. The stable state boundary surface (SSBS) was identified to expand with lime addition (See section 6.3.3), bounded by the tensile strength

envelope as the upper limit and the critical state line as the lower limit. This larger domain, expressible as a function of p and q, is the boundary to all permissible states of stress that the new material can sustain without yielding. The SSBS could not be fully drawn due to lack of further triaxial testing in different stress path direction as well as the pre-consolidation pressure which is needed to identify the size of the yield surface. Nevertheless, by assuming that the yield surface increased shape is isotropic, it can be drawn based on MCC model as shown in Figures 6.21.
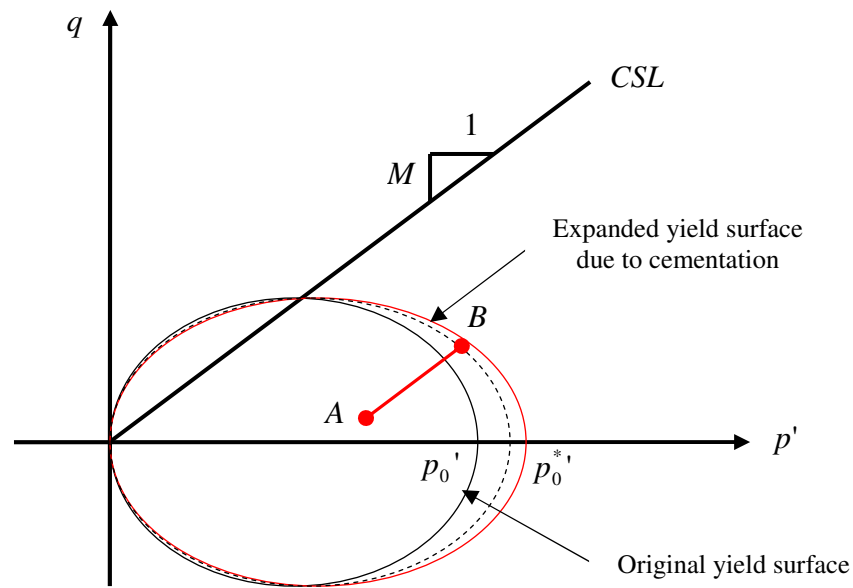
Figure 6.21: Yield surface likely increase due to cementation

Where p'_0 and $p_0^{*}{}'$ are the pre-consolidation pressures for untreated and lime treated soil respectively.

When a treated soil is loaded from an initial state $A(p_a':q_a)$ to final state $B(p_b':q_b)$ (as shown in Fig. 6.21), the state of the material (stress path) travels beyond the original boundary surface of the untreated soil (as indicated in section 6.3), but the stresses still be oscillating within the elastic deformation zone of the newly expanded surface. The gained advantage here is that the expansion of the yield surface allows for a safe design by avoiding the yielding limit state which is also known to increase with depth.

This gained knowledge that is applied to useful practical outcomes with the aid of appropriate theoretical analysis, is of a significant interest to geotechnical engineers, and provides an understanding mechanism picture for modelling purposes of the critical state behaviour of lime treated soil. Applying the concept on lime treated soil under load (e.g. foundations, which are generally more rigid than flexible and tend to impose a uniform settlement), an approximate mean value of settlement under the foundation can be determined by using the elastic parameters obtained from the CD triaxial tests performed on each mixture. This also means that in the critical state concept, soil deformations are occurring inside the yield surface and do not go beyond the SSBS (which has enlarged due to cementation).

For a rectangular foundation, the mean value of the immediate settlement is given by:

$$\rho_i = \frac{pB(1-v^2)F_i}{E} \tag{6.32}$$

Where,

ρ_i : The immediate settlement under the foundation

B : The width of the foundation

p_i : The uniform contact pressure (arbitrary values given in table 6.12)

$E = E_{Av}$: Average Young's modulus of elasticity for the soil (see table 6.11)

$v = v_{Av}$: Average Poisson's ratio of the soil determined using the expression $v = -\dfrac{\Delta\varepsilon_r^e}{\Delta\varepsilon_a^e}$

where $\varepsilon_r^e = \dfrac{\varepsilon_v^e - \varepsilon_a^e}{2}$ (see Table 6.11)

F_i : Influence factor depending upon the diminutions of the foundation.

Table 6.11: Elastic parameters of lime treated and untreated London Clay

Soil + Lime		0%	4%	6%		
Curing time		N/A	7 D	7D	28D - dry	28D - wet
Poison's ratio	v	0.34 0.31 0.36	0.31 0.33 0.35	0.34 0.41 0.41 0.39	0.29 0.29 0.36	0.33 0.36 0.33
	Average v_{Av}	0.34	0.33	0.39	0.31	0.34
Secant Elastic Modulus	$E_{sec}(kPa)$	8986.7 10648.1 15061.4	17301.4 14736.3 21151.6	58311.4 60956.4 57287.7 60264.3	52881.5 55314 75183.2	54275.8 61257.6 80384.3
	Average E_{Av}	11565.4	17729.77	59204.95	61126.23	65305.9

A reinforced concrete foundation used previously to determine the ultimate bearing capacity, with the same dimensions, is also used here ($B = 2m$, $L = 4m$), and based on these dimensions (i.e. $L/B = 2$), F_i will take the value of 1, as per Skempton (1951) recommended values. An immediate settlement under the foundation can be determined in this case. The mean value of settlement for a rectangular foundation on the surface of semi-elastic medium can be written from the expression (6.32) as follow:

$$\rho_i = \frac{p_i \times 2(1 - v_{Av}^2) \times 1}{E_{Av}}$$

To evaluate the settlement reduction due to lime addition, arbitrary pressure values are suggested. Immediate settlement values for each suggested pressure are presented in the Table 6.12.

Table 6.12: Immediate settlement under a foundation constructed on lime treated soil

Soil + Lime			0%	4%	6%		
Curing time			N/A	7 D	7D	28D - dry	28D - wet
Possible pressure	50kPa	**Immediate Settlement** $\rho_i(mm)$	7.6	5.0	1.4	1.5	1.4
	100kPa		15.3	10.1	2.9	3.0	2.7
	200kPa		30.6	20.1	5.7	5.9	5.4

The results in Table 6.12 clearly indicate (regardless of the pressure p_i) that 4% lime addition reduces immediate settlement by almost 35%, while 6% lime addition further reduces the settlement by as much as 80% as of the settlement determined for the untreated soil, benefiting the construction industry. Lime addition not only increases the shear strength, but reduces settlement. In the case of deep excavation projects, the soil improvement work (by lime addition) is generally carried out before the start of an excavation that provides an improved soil layer and helps in limiting the movement of soil below the final excavation level. In this application the stiffness behaviour of treated clay layer is more critical than its shear strength.

From the above, it can be concluded that designing a foundation on lime treated soil indicates that:

a) Bearing capacity either

- is increased by designing to peak strength
- Stays the same by designing to critical state strength

b) Much increased scope for elastic deformation allows for the design to be within the increased boundary surface (due to cementation), which is an advantage to take in consideration.

The British standards (BS 8004:2015) gives further details on how foundations should be designed according to limit state principles and provides information missing from Eurocode 7 but of importance to UK practice. The standards give a list of safe bearing capacity $(\overline{q}_s)$ and allowable bearing pressure $(\overline{q}_a)$ values. Slopes, foundations and walls designed to these values will normally have an adequate factor of safety (F_s) against the ultimate bearing capacity $(\overline{q}_u)$, and a load factor (L_f) against the peak strength $(\overline{q}_{peak})$. For treated soil, safe bearing capacity, allowable bearing pressure, and the ultimate bearing capacity are designated by $(\overline{q}_s^*)$, $(\overline{q}_a^*)$ and $(\overline{q}_u^*)$ respectively (see Fig. 6.22).

$$\overline{q}_s = \frac{1}{F_s}\overline{q}_u$$

$$\overline{q}_a = L_f \overline{q}_{peak}$$

These factors are intended to move the design away from a collapse state into a safer state, where movements are acceptably small. A factor of safety is applied to soil strength and its purpose is to ensure that the structure does not approach its ultimate limit state. A load factor is applied to a load and its purpose is to ensure that the deformations remain within a small strain range to restrict the ground movements (Atkinson, 2007). This is better illustrated in the Figure 6.22, where lime treated soil response to shearing, which was shown in section 6.3 (stress paths) to go beyond the critical state line of the untreated soil, comes back after reaching its peak to the same ultimate state (critical state). Hence, designing to the peak state (where the soil fails) means going beyond the ultimate state and approaches the collapse state where it requires a much higher factor of safety for the bearing capacity. In order to avoid the danger of collapse, one could conclude from the current research that a sensible way forward for design of structures on lime treated soils would be to use the ultimate strengths for limit state design, but take advantage of the enhancement of stiffness that soil treatment delivers.
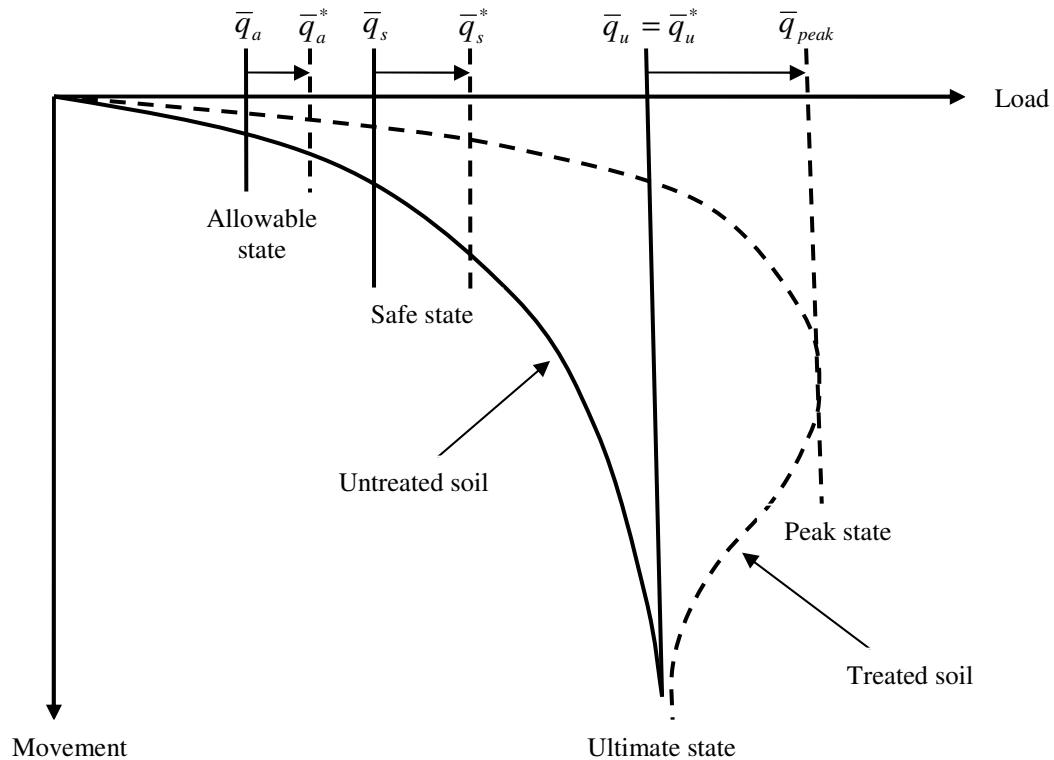
Figure 6.22: Treated and untreated soil response under load

6.6.   Research findings link to existing models and modelling

Research studies of stress-strain are expected to lead to useful design calculations. When the constants of lime treated soil are obtained by interpretation of test data the question that immediately arises is of their use in design calculation. Parameters such as cohesion (c'), angle of friction (ϕ'), dilatancy angle (ψ) and the void ratio (e) obtained through subsequent tests data in a laboratory investigation, as well as other experimental findings, are fundamental for the development of suitable constitutive models to predict the material's behaviour in large scale engineering applications. The material's real behaviour can be useful for any numerical modelling and design. Such a framework would assist engineers in preliminary design studies and minimise the number of trials needed to determine the required lime amount and the curing period.

Geotechnical engineers only need to know soil strength parameters for use in limiting-stress design calculations. Schofield & Wroth (1968) indicated that only critical state data of the soil is fundamental to the choice of soil strength parameters. For this reason, the state of the material was explored beyond the peak and analysed using the CSSM framework. The critical state framework is examined here to highlight its feasibility to quantify the behaviour of lime treated soil. Based on the theoretical considerations within the critical state framework, several basic concepts for the development of a constitutive model or an expansion of existing models for cemented soils are presented.

In this research, the SSBS at the critical state was identified to expand with lime addition, but could not be fully drawn as further triaxial testings are needed in order to determine the shape and the size of the new boundary. However, based on the results obtained in this research, such as the slope parameter λ decreasing with lime amount in the compression plane $(v - p')$, and the unchanged gradient M of the critical state line in the stress plane $(q - p')$ with a negligible intercept, the likely expansion of the SSBS could be guessed as drawn in Fig. 6.23, showing its shifted position and the change in size. The CSL projection onto the stress plane $(q - p')$ and the compression plane $(v - p')$ are also plotted in Figs. 6.24a & 6.24b. Using the MCC yield function, the yield locus of the untreated material is drawn in the stress plane as shown in Fig. 6.24a.

From Fig. 6.24a, it can be observed that the yield surface of the treated material in the stress plane $(q - p')$ slightly reduces in size from the origin $p' = 0$ to $p' = p_i'$, and increases from $p' = p_i'$ to $p' = p_0^{*'}$. The projection of the state material from the space $(v - q - p')$ to the compression plane $(v - p')$ reflects that the critical state lines of both the treated and untreated soil intersect at mean effective stress p_i' (see Fig. 6.24b) and its value can be determined as follow:

The critical state line in the compression plane can be modelled using the following equation (Muir Wood, 1990).

$$v = \Gamma - \lambda \ln p' \tag{6.33}$$

At the intersection point I (see Fig. 6.24b), the treated and untreated soil's specific volume v_i is the same, implying the following:

$$v_i = v_{(untreated)} = v_{(treated)}$$

From (6.33) the following can be written

$$\Gamma - \lambda \ln p' = \Gamma^* - \lambda^* \ln p' \tag{6.34}$$

Therefore the mean effective stress p_i' at the intersection point I can be written as follow:

$$p' = p_i' = e^{\frac{\Gamma - \Gamma^*}{\lambda - \lambda^*}} \tag{6.35}$$
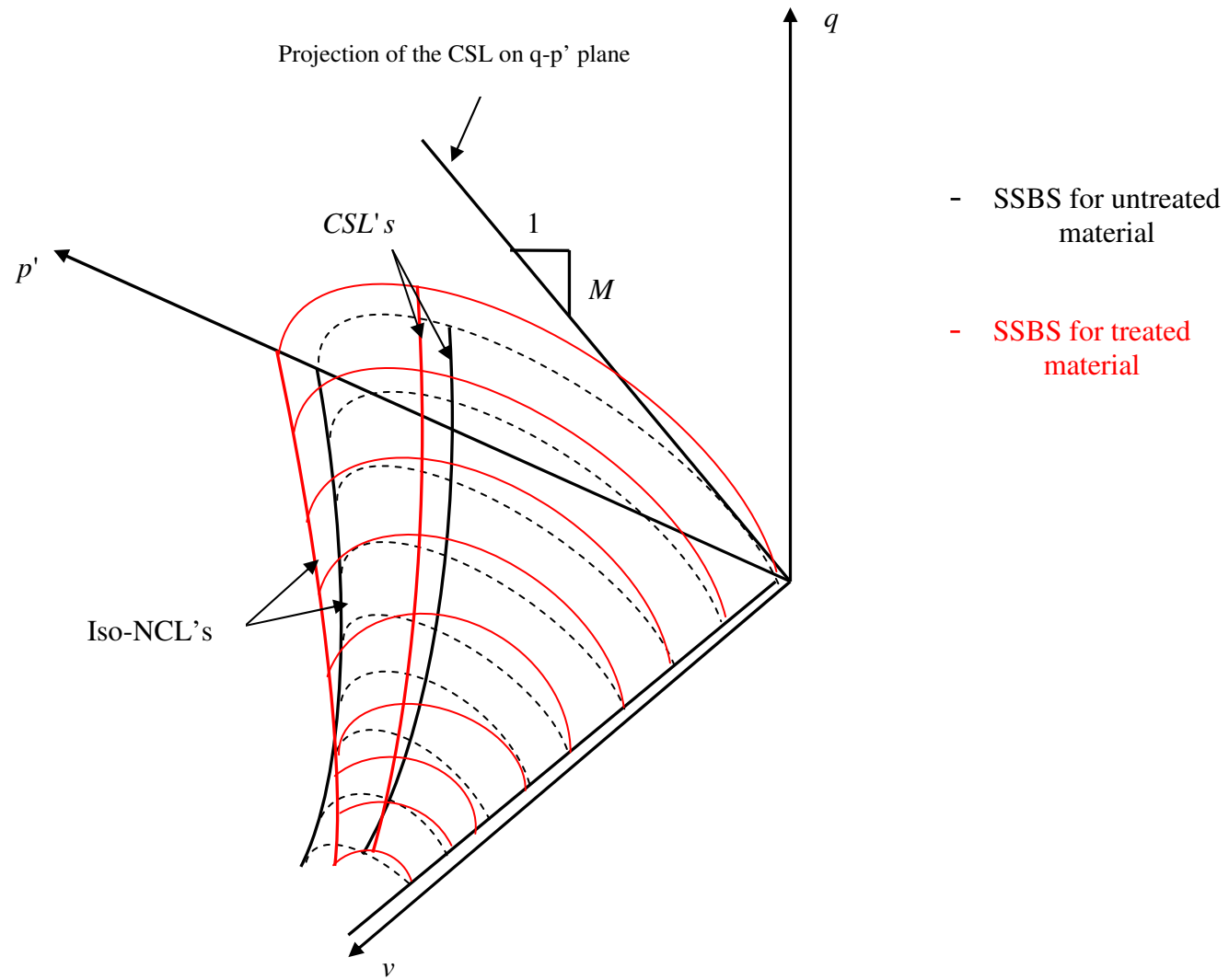
Figure 6.23: SSBS expansion of lime treated material in $v - q - p'$ space
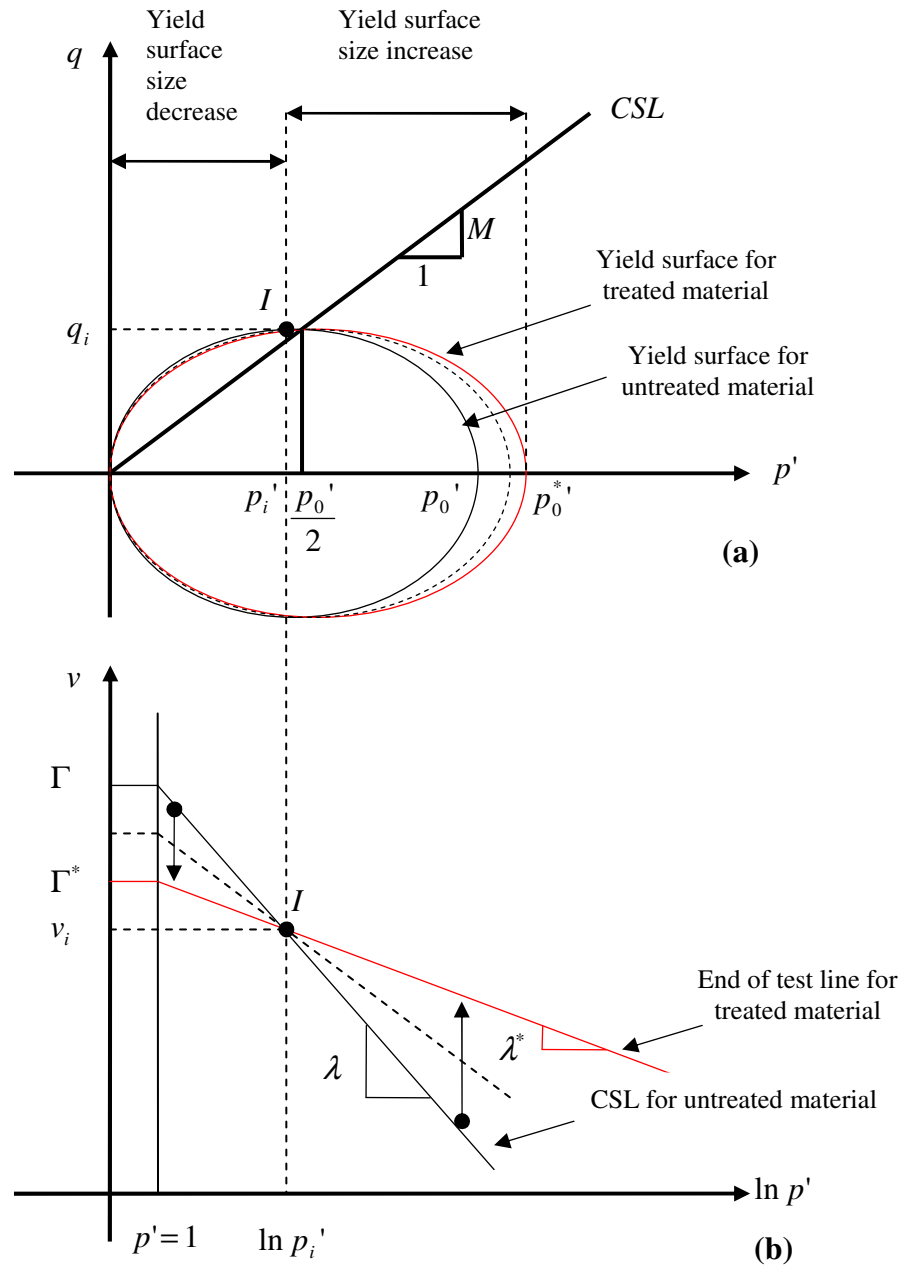
Figure 6.24: Size and shape change of the yield surface after lime treatment

Also, the projection of the state material from $(v - q - p')$ space to the stress plane $(q - p')$ (see Fig. 6.24a) at the critical state is mirrored as follow:

Using the yield function derived from the MCC model for the untreated material,

$$q = M \sqrt{p'(p_0' - p')} \qquad (6.36a)$$

If p_i is known, then q_i can be determined from (6.36a) as follow:

$$q_i = M \sqrt{p_i'\left(p_0' - p_i'\right)} \qquad\qquad (6.36b)$$

The point I $(q_i : p_i')$ can be drawn in the stress plane. In addition, the yield surface of the treated material in the stress plane starts from the original point $(0:0)$ as of the untreated material. From this point onwards, the size of surface is below the original yield surface and gradually increases until the two yield surfaces coincide at the point I $(q_i : p_i')$ (see Fig. 6.24a). From this intersection point and beyond, the treated yield surface surpasses the untreated yield surface by increasing to its maximum size, controlled by the tip pressure $p_0^{*'}$. The yield surface enlargement to the right side due to bonding (horizontal increase) is measured by the difference between the treated and untreated isotropic pre-consolidation pressures and its value is equal to $(p_0^{*'} - p_0')$.

From the above analysis, it can be concluded that the shape of the yield surface changes with lime addition and the increase in size is anisotropic. Providing further triaxial testing are performed on different directions for lime treated soil, the new SSBS can be drawn based on the observed changes of λ^*, κ^* and Γ^* using the equation (6.18), this can be written as follow:

$$v_\lambda = \Gamma^* + \left(\lambda^* - \kappa^*\right)\left[\ln 2 - \ln\left(1 + \frac{q^2}{M^2 p^{2'}}\right)\right] \qquad\qquad (6.37)$$

To achieve a better agreement between predicted and observed cemented soil behaviour, a large number of modifications to the standard and modified Cam Clay models have been proposed over the last two decades. In order to relate the important findings of this research, such as the critical state angle of friction ϕ'_{cs} being the same as for the comparable untreated material, and the slope parameter λ decreasing with cementation. $(\lambda > \lambda^*)$, to models and modelling. Two suitable models which have the potential to be extended using the findings of the current research are introduced here. The authors of these two models having both assumed that the CSL in the stress plane shifting higher at a

constant gradient M which is similar to the current research findings, but a different assumption on the changes of the slope parameter λ in the compression plane with cementation was put forward for each suggested model. A brief description of the models is made in this section, and a comparison of their yield surfaces increase to the likely yield surface increase derived from this study is also presented. Note that no existing model associated with cementation with a decreasing λ is available in the literature.

Kasama et al. (2000) proposed a constitutive model for cemented soils incorporating cementation using an extended critical state concept. The authors claim that this model can be used for all artificially cemented clay.

Failure state conditions with cementation in $q - p'$ and $e - \ln(p')$ space were given by:

$$q = Mp'$$
$$e = \Gamma - \lambda \ln p'$$

Γ : is the void ratio (e) for the critical state at $p' = 1kPa$

λ : is the slope of the critical state line and/or normally consolidated line

M : is the Cam Clay parameter describing the stress ratio at the critical state

Two assumptions were made by the authors in order to introduce the cementation effect in the failure state (taken here as the critical state).

1. The failure state line (which in fact is the final state and is the CSL) in $q - p'$ space is parallel to that of an uncemented clay with an intercept p'_r characterising the cementation. Similar results were obtained in this study but the failure state is not the final ultimate state.

2. the failure state line of cemented clay in the compression plane $e - \ln(p' + p'_r)$ is steeper than that of the uncemented material with the slope parameter λ increasing with the cementation $(\lambda^* > \lambda)$, while in the current study, the CSL of the treated soil

in the equivalent compression space ($v - \ln p'$) also shift higher but at a decreasing

value of the equivalent slope parameter ($\lambda^* < \lambda$) (see Fig. 6.25a)

The failure state line in $q - p'$ and $e - \ln(p' + p'_r)$ was extended by the authors as follow:

$$q = M(p' + p'_r)$$

$$e = \Gamma^* - \lambda^* \ln(p' + p'_r)$$

Where p'_r is the cementation defined as a value of p' at $q = 0$ and Γ^* is the void ratio for

the failure state (CS) at which p=1kPa in the $e - \ln(p' + p'_r)$ space. M is the CSL gradient

in $q - p'$ and given by a modified stress ratio η^* at failure state in which

$$\eta^* = \frac{q}{p'^*} = \frac{q}{p' + p'_r}$$

where $p'^* = p' + p'_r$ is the modified stress.

When the cementation effect is introduced, the yield function takes the following general

form:

For $c = 1$, $\quad f = q^2 + 2(Mp'^*)^2 \ln\left(\frac{p'^*}{p'^*_0}\right) = 0$

For $c \neq 1$, $\quad f = p'^{*2} - p'^{*2}\left(\frac{p'^*_0}{p'^*}\right)^{2(c-1)/c} + \frac{c-1}{M^2}q^2 = 0$

$p'^*_0 = p'_0 + p'_r$, where p'_0 is the hardening parameter.

The shape of the yield curve changes elliptically with the increasing parameter c, and with

variation of p'_r, indicating the extension of the yield curve with both parameters. This

theoretically explains the existence of tensile strength in cemented clay. The proposed

model by Kasama et al. (2000) may be suitable to describe the experimental data obtained

in this research. However, the slope parameter λ of the CSL in the compression plane

does not increase as assumed by the author, but will have to be taken at different decreasing values for each lime amount.

In another interesting model proposed by Tamagnini et al. (2011), which is an extension of MCC model, the authors used the principal of thermodynamics and the classic theory of plasticity to account for cementation bonds. The new model using an associative flow rule was developed to simulate the behaviour of saturated cemented soils, it describes the process of bonding and debonding based on exchange of mass (m) between the granular skeleton and the bonding material. The extended MCC model contains the same number of parameters as the MCC model $(M, \lambda, \kappa, \Gamma, p_0'$ and $\omega)$, the newly introduced parameter ω accounts for controlling the hardening (due to changes in the mass of the cementing material).

The authors assumed that the yield locus derived from the MCC model yield function, expands at a constant shape $(\lambda = \lambda^*)$ (see Fig. 6.25b) and is represented by the following equation:

$$f = q^2 + M^2 p'(p' - p'_0) = 0 \tag{6.38}$$

Where,

q : The deviator stress

p' : The mean effective stress

M : The slope of the critical state line in $q - p'$ plane

p'_0 : The pre-consolidation pressure which controls the size of the elliptical yield locus

In elastic plastic model such as the MCC model, the incremental stress-strain relations are defined by the following equations:

$d\varepsilon_v = d\varepsilon_v^e + d\varepsilon_v^p$ Is the volumetric increment

$d\varepsilon_s = d\varepsilon_s^e + d\varepsilon_s^p$ Is the deviatoric increment

The elastic volumetric strain increment $(d\varepsilon_v^e)$ and plastic volumetric strains increment $(d\varepsilon_v^p)$ can be written as follow:

$$d\varepsilon_v^e = \kappa \frac{dp'}{p'} \tag{6.39}$$

$$d\varepsilon_v^p = (\lambda - \kappa)\frac{dp'_0}{vp'_0} \tag{6.40}$$

Where,

κ : The slope of the unloading re-loading line (k-line)

λ : The slope of the normal compression line in the compression plane $v - p'$

$d\varepsilon_v^e$: The elastic volumetric strain increment

$d\varepsilon_v^p$: The plastic volumetric strain increment

The condition for (6.39) and (6.40) to cancel out

$$d\varepsilon_v^e + d\varepsilon_v^p = 0 \qquad \text{or} \qquad \kappa\frac{dp'}{p'} = -(\lambda - \kappa)\frac{dp'_0}{p'_0} \tag{6.41}$$

The change in p'_0, and relatively in the yield function, are controlled by the plastic volumetric strain ε_v^p. Equation (6.41) provides a link between changes in mean effective stress p' and changes in the size of the yield locus controlled by p'_0. The authors indicated that in the new extended MCC model, the change in p'_0 also accounts for effects of bonding / debonding in the following form:

$dp'_0 = dp'_{0(MCC)} + dp'_{0(Bond)}$, the last term according to thermodynamics can be written as:

$dp'_{0(Bond)} = \omega p'_0\, dm$, this term describes the evolution of the yield surface produced by changes in bonding mass (m), where (ω) controls the rate of change in p'_0 caused by change in bonding mass.

Also, in this proposed model, the authors assumed that the material obeys the normality conditions, implying that the vector of plastic strain increments $(d\varepsilon_v^p)$ are in the direction of the outwards, normal to the yield locus.

In CSSM yielding states of a material is represented by a surface in (p', v, q), called a SSBS. States below the SSBS represent elastic states, whereas states above the SSBS are impossible. The CSL and NCL all lie on the SSBS, the usual path followed by cemented material when sheared to failure contains an initial elastic phase within the SSBS followed by yielding where the state of the material is on the SSBS seeking the CSL until reaching the end of the test (end point).

During the cementation process, the authors assumed that the void ratio is constant and does not change, while in this research it was found that the specimen volume changes with curing time, implying that the void ratio increases which it should be taken in consideration. The pre-consolidation pressure, which reflects the start of the yielding of the material, is assumed to increase with cementation, which is the results observed in the isotropic compression test on lime treated and untreated London Clay. The authors have presented this as follow:

$$p'_0 = p'_{0(MCC)} * e^{(\omega m)}$$

In terms of the compression plane $(v - p')$, this means that a point on the initial NCL moves to the iso-NCL of the cemented soil in the unloading re-loading line, and the horizontal move was deduced to be equal to (ωm). This point lies inside the SSBS for the cemented material. The authors assumed that the slope parameter λ of the CSL and iso-NCL is constant $(\lambda = \lambda*)$. However in this research, results indicated that while the parameter M in the stress plane $(q - p')$ is unchanged, the value of the parameter λ in the compression plane $(v - p')$ was found to decrease with lime addition $(\lambda^* < \lambda)$, consequently affecting the value of (Γ). In addition, the elastic parameter κ, which is the slope of the unloading re-loading line, is also assumed to be constant for the proposed model, while in this research it was found to decrease with cementation $(\kappa^* < \kappa)$. It is

therefore recommended for the new SSBS equation to consider (λ) and (κ) as decreasing parameters with cementation and (Γ) as a variable.

In addition, the upward displacement of the CSL in the $(v - p')$ caused by the cementation was evaluated by the authors to be equal to $(\lambda - \kappa)\omega m$, while in this current research, the observed changes in the parameter λ (which decreases with lime addition) does not reflect a vertical displacement of the CSL in the compression plane as assumed by the authors, but shows a change in its position by rotating around the intersection point I in the compression plane, its right side moves upwards and the left side moves downwards (see Fig. 6.24b). This indicates that the SSBS changes in size and shape, implying that the increase is anisotropic.

In addition, since λ is found to decrease with cementation in this study, $\omega = \dfrac{1}{(\lambda - \kappa)}$ can not be assumed a constant as suggested by the authors but is a variable parameter depending on cementation and can be Witten as follow: $\omega^* = \dfrac{1}{(\lambda^* - \kappa^*)}$

Despite having the same unchanged value of the CSL gradient M in the stress plane $(q - p')$, differences in yield surface increase due to cementation are observed between the two proposed models and the current study. This is better illustrated in Fig. 6.25, where the yield surfaces show their unique increase in size and path depending on the slope parameter λ^* in the compression plane $(v - p')$, either increasing as suggested by Kasama et al. (2000), constant as for Tamagnini et al. (2011) model or decreasing as in the current research findings.
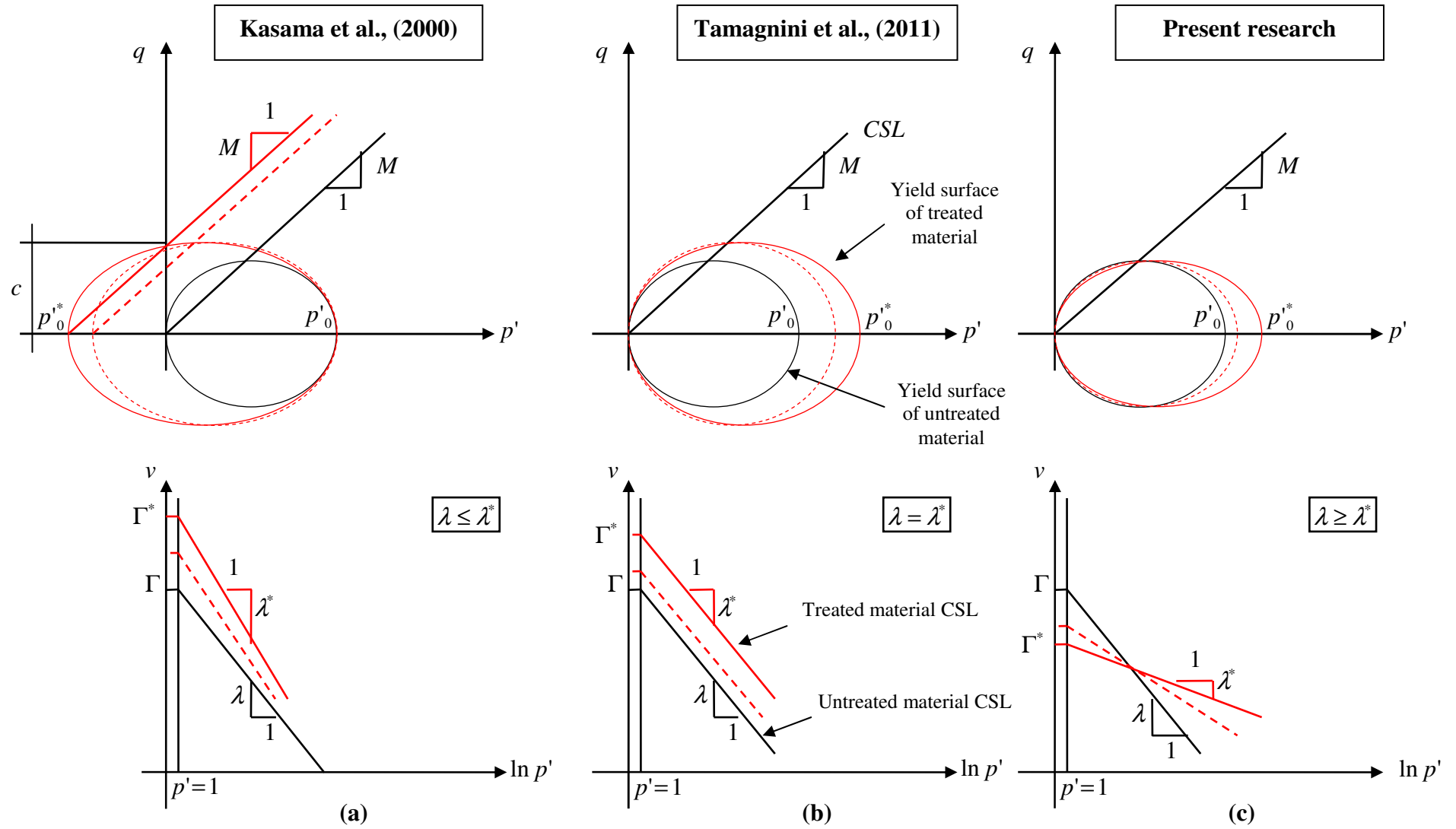
Figure 6.25: Yield surface comparison of the current results with available models for treated soil

Chapter 7

7. Conclusions and recommendations

7.1. Summary and conclusions

This thesis investigated the influence of lime dosage, curing period and the compaction water content on the mechanical response of London Clay. The study was carried out in order to identify the important parameters governing the mechanical behaviour of lime-treated London Clay. Laboratory results from UU, CD & CU triaxial tests on several types of lime treated London Clay specimens were examined, and theoretical analysis were conducted. The main focus was on observing the changes in the mechanical properties and behaviour of the treated soil, and on interpreting these based on physicochemical and XRD testing. Valuable information on the shear strength behaviour is provided, the reported data may be found useful for the development of constitutive models and further study

In the following, the main findings and conclusions based on the testing results are presented. The conclusions formulated along this thesis lead to suggestions which can allow the continuation of the study.

1. XRD results indicated that higher curing time leads to the formation of increasing amount of cementitious compounds (CSH, CAH and CSAH hydrates) which would cause the increase of the strength of the soil. Lime content higher than the ICL causes more cementitious compounds to form, confirming the importance of determining an adequate lime amount for the treatment of a particular soil. Overall, the pozzolanic reactions due to lime addition are responsible for the formation of the cementitious bonds during the curing time at constant water content, resulting in enhanced strength. The pH level for treated samples, cured between 1 and 250 days was observed to decrease, suggesting that long term strength gain for 6% lime treated London Clay specimens is due to pozzolanic activity leading to the formation of cementitious products.

2. These newly formed phases CSH, CAH & CSAH observed in the XRD analysis are consistent with the considerable strength gain and the increase in stiffness of the treated soil. At higher lime amount (6%) the pozzolanic reaction activity progresses faster. This accelerates the hydrate products formation, and increases their quantity, leading to a significant shear strength gain (exhibited in both UU and CD triaxial test). The explanation for a lesser quantity of hydrates produced in 4% lime treatment is associated with the limited pozzolanic reaction development due to lower lime amount available. Results clearly show structural changes are possible and are expected as lime substantially improves the soil physical properties in the large majority of applications. In line with this, the triaxial tests (both UU and CD) showed that strength improvement is more pronounced for specimens with higher lime amount at similar curing period rather than higher curing period and a similar lime amount. This suggests that the impact of curing period prior to saturation was less significant than the lime content effect.

3. Although, based on CD tests, the strength increased with lime percentage as of UU triaxial tests results, there are differences between CD and UU test regarding the effect of curing time. Once the treated specimen is in contact with external water, a slightly higher strength is gained for specimens initially cured for 7 days as opposed to 28 days curing when tested under saturated state. Hence, it is likely that treated specimens cured for 7 days are in more favourable conditions, due to their earlier contact with water, facilitating the pozzolanic reactions with the available lime, thus resulting in higher strength gain. This indicates that the prevailing parameter in terms of strength development may not be the length of the initial curing time but rather the timing of the saturation stage in which the specimen was in contact with water. This is consistent with concrete behaviour where curing usually takes place in the presence of water. In line with this, the specimens compacted wet of optimum showed slightly higher strength increase.

4. It was also observed that the strain associated with the peak deviator stress decreases with an increase in lime amount. The addition of lime content resulted in brittle behaviour causing the peak/failure to occur at smaller strain levels, the brittleness increased with a higher lime content. These treated specimens failed "dry" of critical state line, displaying an approximately linear elastic pre-yield

response followed by an abrupt failure. The sudden strength decrease observed after the peak can be attributed to rapid breakage of strong bonds which have developed in particular for 6% lime treated specimens during the curing time as it has been evidenced by the XRD analysis. Specimens that exhibited an elasto-plastic gradual yielding (ductile response) are said to have failed "wet" of CSL. It is important that this sudden strength reduction be carefully modelled to better understand the lime treated ground behaviour beyond the peak conditions under large strains.

5. Lime addition increased the initial yield stress. In addition, the peak / failure envelops of lime treated soil is shown to shift higher with lime amount increase and becomes steeper due to cementation effect. The envelops appear to form straight lines in this study, but are not parallel to the untreated soil failure line. The addition of lime increased the shearing resistance angle (ϕ'_{peak}). The ϕ'_{peak} increased to 30.5° with 4% lime addition and to 39° for 6% lime amount. The cohesion (c') in London Clay soil was also observed to increase with lime amount, but not consistently with the curing period increase. 4% lime addition increased the cohesion to 35 kPa, whereas 6% lime at 7 days curing resulted in 220 kPa. The curing time increase from 7 to 28 days for 6% lime addition has resulted in a lower cohesion (145 kPa), while no effect on the effective peak angle of friction was observed. This implies that the peak state behaviour of lime treated London Clay is predominantly dependent on cementation bonds rather than friction. These parameters are fundamental for the development of suitable constitutive models to predict the material's behaviour which can be useful for any numerical modelling and design.

6. The behaviour of lime treated London Clay presents the same features as over-consolidated clay and bonded materials, namely a contractive-dilatant response. For instance, at an effective stress $\sigma_3' = 200 kPa$ the dilatancy angle of 4% lime treated London Clay was 4.2°. An increase in lime content from 4 to 6% also increased the dilatancy angle from 4.2° to 71.04° at 7 days curing and to 57.27° at 28 days curing. The compaction water content increase did not show a significant effect on the maximum dilation angle value which is another important factor to not ignore

in geotechnical design and modelling. As expected, the dilation angle of lime treated samples decreased with the effective stress increase, suggesting that dilatancy may disappear at a high effective stress. It was also observed that the maximum rate of dilation in drained tests and the maximum rate of excess pore water pressure in undrained tests did not occur at the same strain level as the maximum stress ratio in lime treated specimens. This is the expected behaviour of cemented geomaterials.

7. Lime addition to London Clay does not have an affect on the ultimate strength or the gradient M of the CSL. However, when curing time increased from 7 to 28 days for similarly prepared 6% lime treated London Clay specimens, irrespective of the compaction water content, the CSL shifted higher indicating the presence of an intercept in $(q - p')$ space, but remained parallel to the CSL of the untreated soil at a very similar gradient M determined to be between 0.87 and 0.88. In addition, regardless of the lime amount, curing time and the compaction water content, an overall CSL was drawn and found to be almost at the same gradient M value equal to 0.89, lying above the original CSL with a negligible intercept 8 kPa. This indicates that no changes are required in critical state design of lime treated soil.

8. Moreover, the parameter λ_{cs} which represent the slope of the CSL in $(v - p')$ space, decreases with lime addition: $\lambda_{cs(0\%)} > \lambda_{cs(4\%-7D)} > \lambda_{cs(6\%-7D)}$. On the other hand, for a curing time increase from 7 to 28 days for 6% lime treatment, the CSL shifted to a lower position in $(v - p')$ space, without any major change in the slope parameter λ_{cs} value. However, the intercept $v_\lambda = \Gamma$ which locates the CSL in the compression plane was found to vary. This variation is believed to be related to the initial specific volume of the specimens. Note that these parameters are usually used in critical state numerical modelling.

9. Lime addition to London Clay allowed the expansion of the stable state boundary surface where the untreated material subsists. The larger area is bounded by the tensile strength envelope as the upper limit and the critical state line as the lower limit. No single SSBS was identified for lime treated soil but the stress paths in the

normalised space $\left(q/p'_e , p'/p'_e \right)$ showed the soil to be stronger due to the increasing amount of bonding in the material as compared to the original boundary. The expansion of the original boundary observed in the normalised space is due to the effect of cementation bonds. The CSL (represented by a point for each mixture) was noted to increase with the lime amount. Conversely, the curing time and compaction water content did not show a major effect on the SSBS for similar material treated with the same amount of lime. More importantly, after the SSBS expansion (post-rupture), it was observed that all lime treated soil end points fail on or close to the same line at a stress ratio η equal to 0.87. However, the corresponding critical state lines of lime treated specimens were located at a higher position than the CSL of the untreated soil. Thus, it is essential to note that these points are not on the same boundary surface.

7.2. Practical implications

In the last few decades, there has been an increasing demand in road transportation and construction projects as a result of fast growing economy, obliging governments to build more roads, highways and construction projects. It would be ideal to find a satisfactory soil as it exists in nature; unfortunately such a thing is of a rare occurrence, and building structures on unsuitable soil is highly risky, while replacing it with a better material will be costly and environmentally damaging. An alternative approach to improve the geotechnical parameters of a problematic soil is to use one of several ground improvement methods developed in the construction industry. Lime stabilisation is one of the most effective ground improvement methods in civil engineering industry, due to its cost effectiveness, easy adaptability and its instant beneficial effect on mechanical behaviour of the soil. The lime stabilisation technique is routinely applied in a variety of applications, such as road foundation, railways, retaining walls reinforcement and bearing capacity soil improvement in similar construction projects. It is essential to highlight that the present work was limited to a low range of effective stresses, making it attractive to a large variety of problems such as shallow foundations assented on improved layers and pavement structures.

In order to obtain realistic predictions, the use of appropriate soil models that can satisfactorily describe the soil behaviour is necessary. Parameters such as cohesion (c'), angle of friction (ϕ'), the dilatancy angle (ψ) and the void ratio (e) obtained through subsequent tests data in a laboratory investigation, as well as other experimental findings, are fundamental for the development of suitable constitutive models to predict the material's behaviour in large scale engineering applications. The material's real behaviour can be useful for any numerical modelling and design. Such a framework would assist engineers in preliminary design studies and minimise the number of trials needed to determine the required lime amount and the curing period.

One important result from the research is the ultimate angle of friction of the treated soil is just the same as that of the untreated soil. The SSBS is not fixed in stress space, but it can expand due to plastic straining. The practical implication of this concept is that a geotechnical design using treated soil could be arrived at so that likely loadings of the ground would not result in yielding behaviour, i.e. states of the soil would continue to lie beneath the Stable State Boundary Surface and thus excessive deformations of the ground would be avoided. One could conclude from the current research that a sensible way forward for design of structures on lime treated soils would be to use the ultimate strengths for limit state design, but take advantage of the enhancement of stiffness that soil treatment delivers.

7.3. Recommendations for further research

The present work provides a conceptual basis and useful sets of data for the development of suitable constitutive models describing the features observed for the behaviour of lime treated London Clay. In addition, several recommendations can be made based on this work in regard to both research and practical applications. In particular, a number of points which deserve further investigation were identified:

1. The study on behaviour of lime treated London Clay under drained and undrained conditions was performed on isotropically consolidated samples, sheared under a constant effective stress (σ_3'). Further investigation should consider a clockwise change of stress path directions in order to identify the complete state boundary

surface. For instance, strain controlled triaxial tests at a constant vertical effective stress (σ_1') and a constant mean effective stress (p') would be of interest to research. Also, it is recommended to carry out tests at higher confining pressures in order to determine the complete compression parameters needed for constitutive modelling.

2. In the laboratory, as a parametric study, it would be interesting to follow the investigation by varying the dry density and a wider range of water contents (dry and wet of the optimum for each mixture). In addition, tests under saturated conditions on lime treated samples cured for 60 days and beyond are needed to identify the strength evolution path with time and compare to UU tests results.

3. In addition, tests at microscopic level (SEM) are fundamental to better comprehend the complex reactions occurring in lime treated soils and their geotechnical properties development. Examining the influences of lime on the molecular structure of treated soil through infrared spectroscopy tests can also be useful.

4. It is highly recommended to cure specimens while in the compacting mould to eliminate the volume expansion due to rebound and avoid changes in the initial void ratio before the start of the triaxial test. Moreover, in order to accurately perform data processing, determination of the true post-curing void ratio for lime treated specimen is of high importance, therefore more tests such as porosity and pore size distribution are a must for tracking the changes that take place in lime treated soil.

5. A deeper understanding of the changes occurring in the mineralogy of lime treated soil is essential for better interpretation of the modifications in the geotechnical properties. Therefore, more XRD tests should be performed on lime treated London Clay samples cured beyond 60 days. In addition, XRD tests on lime treated samples should be performed under saturated state to identify the newly formed phases and the possibility of these phases disappearing during the saturation stage. These investigations would be useful to assess the strength evolution and generalise the validity of the conclusions derived from the present work.

6. The durability of the treated soil is another unknown. For in-situ ground treatment, it is necessary to study the behaviour of the lime treated material in the long run. The concern over long-term performance stems from questions about whether the change in soil structure due to cementation bonding process may be fully or partially reversed, and whether some of the engineering properties gained through cementation would be lost.

References

Advanced Geotechnical soil stabilisation website (2014) *Detailed AGSS-ICS Mechanism.*

Åhnberg, H. (1996) Stress dependent parameters of cement and lime stabilised soils. Grouting and Deep Mixing, Procedings of IS-Tokyo'96, *The Second International Conference and Ground Improvement Geosystems,* Tokyo, May 14-17 pp. 387-392

Åhnberg, H., Johansson, S. E., Pihl, H., & Carlsson, T. (2003) Stabilising effects of different binders in some Swedish soils. *Ground Improvement*, 7 (1), 9–23.

Åhnberg, H., & Johansson, S. E. (2005) Increase in strength with time in soils stabilised with different types of binder in relation to the type and amount of reaction products. *Swedish Deep Stabilization Research Centre, from Proceedings of the International Conference on Deep Mixing*, Stockholm, Swenden, Vol. 1.1.

Åhnberg, H. (2006) *Strength of stabilised soils-A laboratory study on clays and organic soils stabilised with different types of binders.* PhD thesis, Swedish geotechnical institute, Sweden.

Åhnberg, H. (2006) Effects of consolidation stresses on the strength of some stabilised Swedish soils. *Ground improvement*, 10(1), pp. 1-13.

Åhnberg, H. (2007) On yield stresses and the influence of curing stresses on stress paths and strength measured in triaxial testing of stabilised soils. *Canadian Geotechnical Journal*. 44(1), pp. 54-66

Al-Kiki, I. M., Al-Zubaydi, A. H., & Al-Attala, M. A. (2012) Compressive and Tensile Strength of Fibrous Clayey Soil Stabilized with Lime. *Al-Rafidain Engineering*, 20(2), p. 66

Al-Mukhtar, M., Lasledj, A. & Alcover, J. F. (2010) Behaviour and mineralogy changes in lime-treated expansive soil at 20 °C. *Applied Clay Science*, 50(2), pp. 191-198

Al-Rawas, A. A., Hagoa, A. W. & Al-Sarmib, H. (2005) Effect of lime, cement and Sarooj (artificial pozzolan) on the swelling potential of an expansive soil from Oman. *Building and Environment*, 40(5), pp 681-687

Arabani M, Nashaei M. A. L., & Veis Karami M. (2005) A study on lime stabilised clayey sands. Part 1: Geomechanical properties based on a simple nonlinear elastic model. *6th international conference on GIT, 2005*

Arabi, M. & Wild, S. (1986) Microstructural Development in Cured Soil-Lime Composites, *Journal of Materials Science*, 21(2), pp. 497-503.

Arabi, M, & Wild S. (1989) Property changes induced in clay soils when using lime stabilization. *Transportation Research Board, Municipal Engineer*, 6(2), pp. 85–99.

Arroyo, M., Ciantia, M., Castellanza, R. & Gens, A. (2011) A soft-rock model for cement-improved clays. *Proceedings of the 15th European Conference on Soil Mechanics and Geotechnical Engineering*, 12-15 September, 1, pp 501 - 506

Asghari, E., Toll, D. G., & Haeri, S. M. (2003) Triaxial behaviour of a cemented gravely sand, Tehran alluvium. *Geotechnical and Geological Engineering*, 21(1), pp. 1-28.

Atkinson, J. H. (2000) Non-linear soil stiffness in routine design. *Geotechnique*, 50(5), pp. 487-508.

Atkinson, J. H. & Bransby, P. L. (1978) The Mechanics of soils. McGraw Hill, London.

Atkinson, J. H. (2007) The mechanics of soils and foundations. Taylor & Francis, London.

Barker, J. E. (2002) *Ion migration associated with lime piles*. PhD thesis, University of Birmingham. UK.

Barksdale, R.D. & Blight, G.E. (1997) Compressibility and settlement of residual soils. *In: Mechanics of residual soils. Geotechnical Engineering,* Blight Ed. Rotterdam: A.A. Balkema, pp. 95-154.

Basma, A. & Tuncer, E. R. (1991) Effect of lime on volume change and compressibility of expansive clays. *Transportation Research Board,* Transportation research Record 1295, pp. 52-61

Baudet, B. & Stallebrass, S. A. (2004) Constitutive model for structured clays. *Geotechnique*, 54(4), pp. 269-278.

Beetham, P., Dijkstra, T., Dixon, N., Fleming, P., Hutchinson, R. & Bateman, J. (2014) Lime stabilisation for earth works: A UK perspective. *Proceedings of the ICE – Ground improvement*, 168(2), pp. 81-95

Bell, F. G. (1988) Stabilization and treatment of clay soils with lime, part 1—basic principles. *Transportation Research Board , Ground Engineering,* 21(1), pp. 10-15.

Bell, F. G, (1989) Lime stabilisation of clay soils. *Bulletin of international Association of engineering geology* N 39 Paris.

Bell, F. G. (1996) Lime stabilisation of clay minerals and soils. *Engineering Geology*, Elsevier, 42(4), pp. 223-237.

Bhattacharja, S., Bhatty, J. I. and Todres, H. A. (2003) *Stabilization of Clay Soils by Portland Cement or Lime - A Critical Review of Literature*, PCA R&D Serial No. 2066, Portland Cement Association, Skokie, Illinois USA, 60 pages.

Bishop, A. W., Webb, D. L. & Lewin, P. I. (1965) Undisturbed samples of London Clay from the Ashford Common Shaft: Strength-effective stress relationships, *Geotechnique,* 15(1), pp. 1-31

Bishop, A. W. (1971). The influence of progressive failure on the choice of stability analysis. *Geotechnique*, 21(2), pp. 168-172.

Bishop, A. W. & Wesley, L. D. (1975) A hydraulic triaxial apparatus for controlled stress path testing. *Géotechnique*, 25(4), pp. 657-670.

Boardman, D.I., Glendinning, S. & Rogers, D. (2001) Development of stabilization and solidification in lime-clay mixes. *Geotechnique* 50 (6), pp. 533–543.

Booth, A. R. (1975) The factors influencing collapse settlement in compacted soils. *Proceedings of 4th International conference on Expansive Soil.* Colorado, pp. 117-134.

Borja, R., Tamagnini, C & Amorosi, A. (1997) Coupling plasticity and energy-conserving elasticity models for clays. *Journal of Geotechnical and Geoenvironmental Engineering* 123(10), pp. 948–957

Boynton, R. (1980) *Chemistry and technology of lime and limestone*. John Wiley & Sons Inc.

Brandl, H. (1981) Alteration of soil parameters by stabilization with lime. *Proc. Xth International Conference on Soil Mechanics and Foundation Engineering.* Stockholm, Vol. 3, pp. 587-594.

Bressani, L. A. (1990) *Experimental properties of bonded soils*. PhD thesis, Imperial College, London.

British Standards Institution (2015) *BS. 8004: 2015: Code of practice for foundations.* London BSI

British Standards Institution (1990) *BS.1924 – 1 & 2: 1990 Stabilized materials for Civil Engineering Purposes.* London: BSI

British Standards Institution (1990) *BS 1377 – 2,3,4 & 8: 1990 Soils for Civil Engineering Purposes.* London: BSI

Britto, A.M. & Gunn, M.J.(1987) *Critical State Soil Mechanics via Finite Elements.* Chichester: Ellis Horwood Ltd.

Brooks, A. H., West, G. Carder, D. R. (1997) Laboratory trial mixes for lime stabilised soil columns and lime piles. TRL report 306, UK Highways agency.

Burland, J. B. (1990) On the compressibility and strength of natural clays. *Géotechnique* 40(1), pp. 329-378.

Cabarkapa, Z. (2001) *Mechanical behaviour and modelling of unsaturated soil*. PhD. thesis, South Bank University, London.

Cabane, N. (2004) *Sols traités à la chaux et aux liants hydrauliques: contribution à l'identification et à l'analyse des éléments perturbateurs de la stabilisation.* PhD thèse, Ecole National Supérieure des Mines de St–Etienne, France.

Cabrera, J. G. & Nwakanma, C. A. (1979) Pozzolanic Activity and Mechanics of Reaction of Red Tropical Soil-Lime System, *Transportation Research Record, No. 702*, National Research Council, Washington D. C. pp. 199-207.

Callisto, L. & Calabresi, G. (1998) Mechanical behaviour of a natural soft clay. *Geotechnique,* 48(4), pp. 495–513.

Cardoso, R. & Maranha das Neves, E. (2012) Hydro-mechanical characterization of lime-treated and untreated marls used in a motorway embankment. *Engineering Geology,* 133–134, pp. 76–84

Cecconi, M., Viggiani, G., & Rampello, S. (1998) An experimental investigation of the mechanical behaviour of a pyroclastic soft rock. *Geotechnics of Hard Soils-Soft Rocks*, (eds. Evangelista & Picarelli), vol. 1, pp. 473-480

Cecconi, M. & Russo, G. (2012) Geotechnical properties of lime stabilised pyroclastic soils. *Electronic Journal of Geotechnical Engineering (EJGE)*, 17(S), pp. 2581-2597

Chandler, R. J. (1966) The Measurement of Residual Strength in Triaxial Compression. *Geotechnique*, 16(3), pp. 181-186.

Chen, W. F. & Mizuno, E. (1990) Nonlinear Analysis in Soil Mechanics, (Theory and Implementation). *Developments in geotechnical engineering*, Vol. 53, pp. 1-672, Elsevier Science, Amsterdam, Netherland.

Choquette, M., Bérubéa, M. A. & Locat, J. (1987) Mineralogical and microtextural changes associated with lime stabilization of marine clays from eastern Canada. *Applied Clay Science*, 2(3), pp. 215–232.

Clara, H. & Handy R. L. (1963) Characteristics of lime retention by montmorillonitic clays. *Highway Research Record 29*: pp. 55–69

Clarke, A. J. (2007) *Compressibility and permeability of lime-stabilised London Clay*, BEng final year project dissertation, London South Bank University. UK

Clough, G. W., Sitar, N., Bachus, R. C. & Rad, N. S. (1981) Cemented sands under static loading. *Journal of Geotechnical Engineering*, ASCE, 107(6), pp. 799–817.

Collins, I. F. & Kelly, P. A. (2002) A thermomechanical analysis of a family of soil models. *Geotechnique*, 52 (7), pp. 507-518.

Consoli, N., Prietto, P., & Ulbrich, L. (1998) Influence of fibre and cement addition on behaviour of sandy soil. *Journal of Geotechnical and Geoenvironmental Engineering,* 124(12)**, pp.** 1211-1214.

Consoli, N. C., Rotta, G. V., & Prietto, P. D. M. (2000) Influence of curing under stress on the triaxial response of cemented soils. *Geotechnique*, 50(1), pp. 99-105

Consoli, N. C., Prietto, P. D. M., Carraro, J. A. H. & Heineck, K. S. (2001) Behaviour of Compacted Soil-Fly Ash-Carbide Lime Mixtures. *Journal of Geotechnical and Geoenvironmental Engineering*, 127(9), pp. 774-782.

Consoli, N., Montardo, J., Donato, M. & Prietto, P. (2004). Effect of material properties on the behaviour of sand–cement–fibre composites. *Ground Improvement,* 8 (2)**,** 77-90.

Consoli, N. C., da Silva Lopes, Jr. L., Foppa, D. & Heineck, K. S. (2009) Key parameters dictating strength of lime / cement-treated soils. *Procedings of the ICE – Geotechnical Engineering*, 162(2), pp. 111-118

Coop, M. R., & Atkinson, J. H. (1993) The mechanics of cemented carbonate sands. *Géotechnique*, 43(1), pp. 53-67.

Coop, M. R. (1999) The influence of particle breakage and the state behaviour of sand. *International workshop on soil crushability*, IWSC, Japan.

Coop, M. R. & Willson, S.M. (2003) Behavior of Hydrocarbon Reservoir Sands and Sandstones. *Journal of Geotechnical and Geoenvironmental Engineering*, ASCE, 129(11), pp. 1010-1019.

Cotecchia, F. & Chandler, R. J. (1997) The influence of structure on the pre-failure behaviour of a natural clay. *Géotechnique, 47(3), pp.523-544.*

Cotecchia, F. & Chandler, R. J. (2000) A general framework for the mechanical behaviour of clays. *Geotechnique,* 50(4), pp. 431–447.

Cuccovillo, T. & Coop M. R. (1993) The influence of bond strength on the mechanics of carbonate soft rocks. *Proc. Int. Symp. Geotechnical Eng.* Hard soils-Soft Rocks, Athens, Balkema, Rotterdam, pp. 447-455

Cuccovillo, T. & Coop M. R. (1997) Yielding and pre-failure deformation of structured sands. *Geotechnique* ,47(1), pp. 69-72.

Cuccovillo, T. & Coop, M. R. (1999) On the mechanics of structured sands. *Géotechnique*, 49(6), pp. 741–60.

Cui Y. J. & Delage P. (1996) Yielding and plastic behaviour of an unsaturated compacted silt. *Géotechnique*, 46 (2), pp. 291-311.

Dahale, P. P., Nagarnaik P. B & Gajbhive A. R. (2012) Utilization of Solid Waste for Soil Stabilization: A Review. *Electronic Journal of Geotechnical Engineering*, Vol. 17(Q), pp. 2443-2461

Dash, K. S. & Hussain, M. (2012) Lime Stabilization of Soils: Reappraisal. *Journal of Materials in Civil Engineering*, ASCE, 24 (6), pp. 707-714

De Beer, E. E, (1970) Experimental determination of the shape factor and the bearing capacity factors for sands. *Geotechnique*. 20, (4), pp. 387-411

de Brito Galvao, T. C., Elsharief, A. & Simoes, G. F. (2004) Effects of lime on permeability and compressibility of two tropical residual soils. *Journal of Environment Engineering, ASCE,* 130(8), pp. 881-885

Delage, P., Audiguier, M., Cui, Y.-J., & Howat, M. D. (1996) Microstructure of a compacted silt. *Canadian Geotechnical Journal*, 33(1), pp. 150-158.

di Prisco, C., Mattioti, R. & Nova, R. (1992) A mathematical model of grouted sand allowing for strength degradation. Procedings, NUMOG 4, Prande and Pietruszczack (eds.), Swansea, pp 25-35

Diamond, S. & Kinter, E. B. (1965) Mechanisms of Soil-Lime Stabilization - An Interpretative Review. *Highway Research Board*, Washington, DC, Highway Research Record 92, pp. 83-102.

Dineen, K. (1997) *The influence of soil suction on compressibility and swelling*. PhD thesis, Imperial College London, London, UK.

Di Sante, M., Fratalocchi, E., Mazzieri, F. and Pasqualini, E. (2014) time of reactions in a lime treated clayey soil and influence of curing conditions on its microstructure and behaviour. *Applied clay science*, 99, pp. 100-109

Dumbleton, M.J. (1962) *Investigations to assess the potentialities of lime stabilization in the United Kingdom.* Road Research Technical Paper No. 64. Road Research Laboratory, Crowthorne, Berks.

Eades, J. L, & Grim, R. E. (1960) Reaction of Hydrated Lime with Pure Clay Minerals in Soil Stabilization. *Highway Research Board, Highway Research Board Bulletin 262,* pp. 51-63.

Eades, J. L., & Grim, R. E. (1966) A Quick Test to Determine Lime Requirements for Soil Stabilization. *Highway Research Board*, *Highway Research Record* 139, pp. 61-72

EC7 (2004), Eurocode 7: Geotechnical Design - Part 1: General rules, BS EN 1997-1:2004, British Standards Institution, London.

Eisazadeh, A., Kassim, K. A. & Nur, H. (2012) Cation exchange capacity of phosphoric acid and lime stabilised Montmorillonite and Kaolinitic soils. *Geotechnical and Geological Engineering,* 30(6), pp. 1435-1440.

Gasparre, A. (2005) *Advanced* laboratory characterisation of London Clay. PhD thesis, Imperial College London, London, UK.

Gasparre, A., Nishimura, S., Coop, M. R. & Jardine, R. J. (2007) The influence of structure on the behaviour of London clay. *Geotechnique,* 57(1), pp. 19-31

Gens, A. & Nova, R. (1993) Conceptual bases for a constitutive model for bonded soils and weak rocks, *Proc., Int. Symp. on Geotech. Eng. of Hard Soils- Soft Rocks*, Vol. 1, Balkema, Rotterdam, The Netherlands, pp. 485–494.

Glenn, G. R. & Handy, R. L. (1963) Lime-clay mineral reaction products. *Transportation research board, Highway Research record 29, pp. 70-80.*

Goldberg, I. & Klein, A. (1952) Some effects of treating expansive clays with calcium hydroxide. *American Society for Testing and Materials*, Spec. Tech. Publ. 142, pp. 53-71.

Gomes Correia, A. (2015) Geotechnical engineering for sustainable transportation infrastructure. *XVI European conference on Soil Mechanics & Geotechnical Engineering, "Geotechnical engineering for infrastructure and development"* 13-17 Sep. 2015, Edinburgh, Scotland, UK.

Greaves, H. M. (1996) An introduction to lime stabilization. *Proceedings, Seminar on Lime Stabilization*, Loughborough University, Thomas Telford, London, pp. 5–12.

Haeri, S. M., Hosseini, S. M., Toll, D. G., Yasrebi, S. S. (2005). The behaviour of an artificially cemented sandy gravel. *Geotechnical and Geological Engineering*, 23(5), pp. 537-560

Hansen, J. B, (1970) A revised and extended formulae for bearing capacity. *Danish Geotech*. Inst., Bulletin 28, Copenhagen.

Harris, P. and Scullion, T. (2009) Stabilizer Diffusion in Swelling Soils. *Proc. Of Contemporary Topics in Ground Modification, Problem Soils, and Geo-Support: ASCE*, (eds: Iskander M., Laefer, D. F. & Hussein, M. H.) pp. 566-573.

Hausmann, M. R. (1990) *Engineering principles of Ground modifications*. McGraw-Hill Ryerson, Limited – Technology & Engineering – p. 632

Head, K. H. (1986) *Manual of soil laboratory testing, effective stress tests*: Volume 3, London, Pentech Press limited.

Head, K. H. (1992) *Manual of soil laboratory testing, permeability, shear strength and compressibility:* Volume 2, New York, second edition, John, Wiley & Sons, Inc.

Head, K. H. (2006) *Manual of soil laboratory testing, soil classification and compaction tests:* Volume 1, New York, third edition, John, Wiley & Sons, Inc.

Hight, D. W. & Jardine, R. J. (1993) Small-strain stiffness and strength characteristics of hard London Tertiary clays. *Proc. Int. Symp. on Hard Soils-Soft Rocks*, Athens,Vol1, pp.533-552.

Hight, D. W., Gasparre, A., Nishimura, S., Minh, N. A., Jardine, R. J. & Coop, M. R. (2007) Characteristics of the London Clay from the Terminal 5 site at Heathrow Airport. *Geotechnique* 57(1), pp. 3-18.

Hilf, J. W. (1956) An investigation of pore water pressure in compacted cohesive soils. *Transportation research board.* Technical memorandum 654, bureau of reclamation. Denver, US – p. 109

Hilt, G. H. & Davidson, D. T. (1960) Lime fixation in clayey soils. *Highway Research Board Bull*, 262: pp. 20-32

Holt, C.C. & Freer-Hewish, R. J. (1996) Lime treatment of capping layers in accordance with the current specification for highway works. *Proceedings, Seminar on Lime Stabilization,* Loughborough University, Thomas Telford, pp 51-61

Holtz, W. G. (1969) Volume change in expansive soils and control by lime treatment. *Proceedings 2nd International Conference on Expansive Soils,* Texas, pp 157-174

Hong, Z. S., Zeng, L. L., Cui, Y. J., Cai, Y. Q. & Lin, C. (2012) Compression Behaviour of Natural and Reconstituted Clays. *Géotechnique,* 62(4), pp. 291-301.

Horpibulsuk, S., Miura, N., & Bergado, D. T. (2004). Undrained shear behaviour of cement admixed clay at high water content. *Journal of Geotechnical and Geoenvironmental Engineering*, ASCE ;130(10), pp.1096-105.

Horpibulsuk, S., Liu M. D., Liyanapathirana, D. S., & Suebsuk, J. (2010) Behaviour of cemented clay simulated via the theoretical framework of Structured Cam Clay model. *Comput. Geotech.*; 37(1–2), pp. 1-9.

Huang, J. T. & Airey, D. W. (1993) Effect of cement and density on an artificially cemented sand. *Geotechnical Engineering of hard soil-soft rocks:* Rotterdam, Balkema, pp. 553-560.

Huang, J. T. & Airey, D. W. (1998) Properties of artificially cemented carbonate sand. *Journal of Geotech. Geoenviron. Eng.*,124(6), pp. 492-499.

Imperial Chemicals Industry (ICI). (1990) Lime Stabilisation Manual. Second edition. UK.

Ingles, O. G. & Metcalf, J. B. (1972) *Soil stabilization*. Butterworths Pty. Ltd, Australia.

Ismail, M. A., Joer, H. A., Randolph, M. F., & Sin, W. H. (2002) Effect of cement type on shear behaviour of cemented calcareous soil. *Journal of Geotechnical Engineering,* ASCE; 128(6), pp. 520-529.

Jardine, R. J., Fourie, A. B., Maswoswe, J. & Burland, J. B. (1985) Field and laboratory measurements of soil stiffness. *Proc. 11th Int. Conference on Soil Mechanics and Foundation Engineering*, San Francisco 2, 511–514.

Jotisankasa, A. (2005) *Collapse behaviour of a compacted silty clay*. PhD thesis, Imperial College London, London, UK.

Kamruzzaman, A. H. M. (2002) *Physico-chemical and engineering behaviour of cement treated Singapore marine clay*. PhD thesis, National University of Singapore.

Kamruzzaman, A. H. M., Chew, S. H., & Lee, F. H. (2009) Structuration and Destructuration Behavior of Cement-Treated Singapore Marine Clay. *Journal of Geotechnical and Geoenvironmental Engineering*, 135(4), pp. 573–589.

Karaoulanis, F. E. & Chatzigogos, Th. (2011) Elasto-viscoplastic modelling of soft rock time dependent behaviour. *Proc. of the 15th European Conference, Soil Mechanics and Geotechnical Engineering*. Athens, Greece. pp. 551-556

Kasama, K., Ochiai, H., & Yasufuku, N. (2000) On the stress-strain behaviour of lightly cemented clay based on an extended critical state concept. *Soils and foundations*, *Japanese Geotechnical Society,* 40(5), pp. 37-47.

Khattab, S. A. A. (2002) *Etude Multi-echelles d'un sol plastique traite a la chaux*. Ph.D Thesis, University of Orleans, France.

King, C. (1981) The stratigraphy of the London Clay and associated deposits. Tertiary Research Special Paper 6, pp. 1-158.

Kinuthia, J. (2015) Personal communication.

Koliji, A., Vulliet, L., & Laloui, L. (2010) Structural characterization of unsaturated aggregated soil. *Canadian Geotechnical Journal*, 47(3), pp. 297–311.

Koumoto, T. & Houlsby, G. T. (2001) Theory and practice of the fall cone test. *Geotechnique* 51(8): 701–712.

Kuwano, R. (1999) *The stiffness and yielding anisotropy of sand*. PhD thesis, Imperial College London, London, UK.

Lade, P. V., & Overton, D. D. (1989) Cementation effects in frictional materials. *Journal of Geotechnical Engineering,* 115(10), pp. 1373–1387

Lagioia, R. & Nova, R. (1995) An experimental and theoretical study of the behaviour of a calcarenite in triaxial compression. *Géotechnique*; 45(4), pp. 633–648.

Lagioia, R., Purzin, A. M. & Potts, D. M. (1996) A new versatile expression for yield and plastic potential surfaces. *Computers & Géotechnics*; 19(3), pp. 171–191.

Lambe, T. W. & Whitman, R. V. (1959) The role of effective stress in the behaviour of expansive soils. *Prec. 1st Annual Colorado Soil Mechanics Conference*, pp. 33-66.

Lambe, T. W. (1960) A mechanistic picture of shear strength in clay. Res. Conf. On shear strength of cohesive soils. ASCE, pp. 555-580

Larson, R. (1977) Basic behaviour of Scandinavian soft clays. Swedish *Geotechnical Institute,* Report No. 4, Linkoping.

Lasledj, A. (2009) *Traitement des sols argileux à la chaux : processus physico-chimique et propriétés géotechniques*. PhD thesis, Orleans University, Orleans. France.

Le Runigo B., Cuisinier O., Cui Y.J., Ferber V., Deneele D. (2009) Impact of the initial state on fabric and permeability of a lime treated silt under long term leaching. *Canadian Geotechnical Journal*, 46 (11), pp. 1243-1257.

Le Runigo, B., Verber, V., Cui, Y. J., Cuisinier, O., & Deneele, D. (2011) Performance of lime-treated silty soil under long-term hydraulic conditions. *Engineering Geology*, Elsevier, 118(1-2), pp. 20-28

Leroueil, S. & Vaughan, P. R. (1990) The general and congruent effects of structure in natural soils and weak rocks. *Géotechnique*, 40(3), pp. 67–488.

Leroueil, S. & Barbosa, A. (2000) Combined effect of fabric, bonding and partial saturation on yielding of soils. *Proc. Asian Conf. On Unsaturated Soils*, pp. 527-532.

Little, D. N., Nair, S., & Herbert, B. (2010) Addressing sulphate-induced heave in lime treated soils. *Journal of Geotechnical and Geoenvironmental Engineering*, 136(1), pp. 110-118.

Liu, M. D. & Carter, J. P. (1999) Virgin compression of structured soils. *Géotechnique,* 49(1), pp. 43-57.

Liu, M. D. & Carter, J. P. (2002) A Structured Cam Clay model. *Canadian Geotechnical Journal,* 39(6), pp. 1313-1332.

Liu, M. D., Pemberton, S. & Indraratna, B. A., (2010) study of the strength of lime treated soft clays. *International Symposium and Exhibition on Geotechnical and Geosynthetics Engineering: Challenges and Opportunities on Climate Change*, December 7-8, Bangkok, Thailand, pp. 245-251.

Locat, J., Bérubé, M. A., & Choquete, M. (1990) Laboratory investigations on the lime stabilization of sensitive clays: shear strength development. *Canadian Geotechnical Journal*, 27(3), pp. 294-304.

Locat, J., Trumblay, H. & Leroueil, S. (1996) Mechanical and hydraulic behaviour of soft organic clay treated with lime. *Canadian Geotechnical Journal*, 33(4), pp. 654-669.

Maccarini, M. (1987) *Laboratory studies of a weakly bonded artificial soil*. PhD thesis, University of London.

Malandraki, V. (1994) *The engineering behaviour of a wealthy bonded artificial soil*. PhD thesis, University of Durham, UK.

Malandraki, V. & Toll, D. G. (2001) Triaxial tests on a weakly bonded soil with changes in stress path. *Journal of Geotechnical and Geoenvironmental Engineering*, 127(2), pp. 282-291.

Maubec, N. (2010) *Approche multi-echelle des traitements des sols a la chaux: Etude des interatcions avec les argiles*. PhD thesis, Nantes University, Nantes.

McCallister, L.D. and Petry, T.M. (1992) Leach tests on lime-treated clays. *Geotechnical testing journal*, 15(2), pp. 106-114.

Metelkova, Z., Bohac, J., Prikryl, R. & Sedlarova, I. (2012) Maturation of loess treated with variable lime admixture: Pore space textural evolution and related phase changes. *Applied clay science,* 61: pp. 37-43

Meyerhof, G. G, (1963) Some recent research on the bearing capacity of foundations. *Canadian Geotechnical journal.* 1 (1), pp. 16-23

Mitchell, J. K. (1976) *Fundamentals of soil behaviour*, John Wiley & Sons, Inc.

Mitchell, J. K. (1986) Practical problems from surprising soil behaviour. *Journal of Geotechnical Engineering ASCE*, 112(3), pp. 259–289.

Mitchell, J. K. & Dermatas, D. (1992) Clay soil heave caused by lime sulphate reactions: *Innovations and uses of lime*. ASTM Spec. Tech. Publ. 1135, pp. 41-64

Mitchell, J. K. & Soga, K. (2005) *Fundamentals of soil behaviour*. Third edition, John Wiley & Sons, Inc.

Molenkam, F., & Luger, H. G. (1981) Modelling and minimization of membrane penetration effects in tests on granular soils. *Geotechnique*, ICE, 31(4), pp. 471-486

Muhunthan, B. & Sariosseiri, F. (2008) Interpretation of geotechnical properties of cement treated soils. Research Report, Washington (State). *Department of Transportation. Office of research & Library services*, p. 155

Muir Wood, D. (2004). *Geotechnical modelling*. Spon Press, Taylor & Francis Group, UK.

Muir Wood, D. (1990). *Soil behaviour and critical state soil mechanics*. Cambridge University Press, Cambridge, UK.

Nalbantoglu, Z. & Tuncer, E. R. (2001) Compressibility and hydraulic conductivity of chemically treated expansive clay. *Canadian Geotechnical journal*, 38(1), pp. 154-160.

Narasimha Rao, S., & Rajasekaran G. (1996) Reaction products formed in lime-stabilized marine clays. *Journal of Geotechnical Engineering,* 122(5): 329–336.

Ninjgarav, E., Chung, S. G., Jang, W. Y., & Ryu, C. K. (2007) Pore Size Distribution of Pusan Clay Measured by Mercury Intrusion Porosimetry. *Journal of Civil Engineering, KSCE*, 11(3), pp. 133–139.

Nishimura, S. (2005) *Laboratory study on anisotropy of natural London Clay.* Ph.D. thesis, Imperial college, London. UK

Noble, D. F. & Plaster, R.W. (1970) Reactions in Portland cement – clay mixtures. *Final report, Virginia Highway Research Council*, Charlottesville.

Nova, R., Castellanza, R. & Tamagnini, C. (2003) A constitutive model for bonded geomaterials subject to mechanical and/or chemical degradation. *Int. Journal for Numerical and Analytical Methods in Geomechanics,* 27(9), pp. 705–732

Oh, E. Y. N., Bolton, M. W., & Balasubramaniam, A. S. (2008) Undrained behaviour of lime treated soft clays. *Proceedings of the Eighteenth International Offshore and Polar Engineering Conference,* Vancouver, BC, Canada, July 6-11.

Oka, F., Kimoto, S. & Kato, R. (2011) Seepage-deformation coupled numerical analysis of Unsaturated river embankment using an elasto-plastic model. *In: First International Conference on Geotechnique, Construction Material and Environment,* Mie, Japan, pp.15-22.

Okyay, U. S. & Dias, D. (2010) Use of lime and cement treated soils as pile supported load transfer platform. *Engineering Geology,* 114(1-2), pp. 34–44. Elsevier.

Ola, S. A. (1978) Geotechnical properties and behaviour of some stabilized Nigerian lateritic soils, *Quarterly Journal of Engineering Geology*, 11(2), pp. 145-160.

Ormsby, W. C., & Kinter, E. B. (1973) Strength Development and Reaction Products in Lime-Montmorillonite-Water Systems. *Public Roads,* 37(4), pp. 136-148.

Osinubi, K. J. (1998a) Influence of Compactive Efforts and Compaction Delays on Lime-Treated Soil. *Journal of Transportation Engineering*, ASCE, 124(2), pp. 149-155.

Osinubi, K. J. (1998b) Permeability of lime treated lateritic soil. *Journal of Transportation Engineering*, ASCE, 124(5), pp. 465-469

Osula, D. O. A. (1991) Lime modification of problem laterite. *Engineering Geology,* 30(2), pp. 141-154.

Osula, D. O. A. (1996) A comparative evaluation of cement and lime modification of laterite. *Engineering Geology*, 42(1), pp. 71–81.

Oztoprak, S. and Bolton, M.D. (2013), Stiffness of sands through a laboratory test database, Geotechnique, 63, No. 1, 54-70.

Pantelidou, H. & Simpson, B. (2007) Geotechnical variation of London Clay across central London. *Géotechnique,* 57(1), pp. 101 –112

Parry, R. H. G. (1960) Triaxial compression and extension tests on remoulded saturated clay. *Geotechnique.* 10 (4), pp. l66-180.

Petry, T. M. & Little, D. N. (2002) Review of stabilization of clays and expansive soils in pavement and lightly loaded structures – History, practice and future. *Journal of Materials in Civil Engineering*, ASCE, 14 (6), pp. 447-460.

Porbaha, A. Shibuya, S. & Kishida, T. (2000) State of the art in deep mixing technology. Part III: geomaterial characterization. *Proceedings of the ICE- ground Improvements*, Volume 4, Issue 3, 1 January 2000, pp 91-110.

Puppala A. J. Intharasombat N. Vempati R. K. (2005) Experimental studies on ettringite-induced heaving in soils. *Journal of Geotechnical and Geoenvironmental Engineering.* ASCE,131(3), pp. 325-337

Rajasekharan, G. & Narasimha Rao, S. (1997) Lime stabilization technique for the improvement of marine clay. *Soils and Foundations*, 37(2), pp. 97–104

Rajasekaran, G., & Narasimha Rao, S. (2002) Permeability characteristics of lime treated marine clay. *Ocean Engineering*, 29(2), pp. 113-127.

Rampello, S. & Silvestri, F. (1993) The stress-strain behaviour of natural and reconstituted samples of two over-consolidated clays. *In: Geotechnical Engineering of Hard Soils-Soft Rocks,* (Eds: Anagnostopoulos, A., Schlosser, F., Kalteziotis, N. & Frank R.) Balkema, Rotterdam.

Rao, S. M., Reddy, B. V. V., & Muttharam, M. (2001) The impact of cyclic wetting and drying on the swelling behaviour of stabilised expansive soils, *Engineering Geology*, 60(1-4), pp. 223-233.

Rao, S. M. & Thyagaraj, T. (2003) Lime slurry stabilisation of an expansive soil *Proceedings of the Institution of Civil Engineers Geotechnical Engineering*, 156(3), pp. 139-146.

Rao, S. M. & Shivananda, P. (2005a) Compressibility behaviour of lime-stabilized clay. *Geotechnical and Geological Engineering,* 23 (3), pp. 309–319.

Rao, S. M. & Shivananda, P. (2005b) Role of curing temperature in progress of lime-soil reactions. *Geotechnical and Geological Engineering*, Springer, 23(1), pp. 79–85

Richardson, D. (1988) *Investigations of threshold effects in soil deformation.* PhD thesis, City University, UK.

Rogers, C. D. F. & Glendinning, S. (1996) Modification of clay soils using lime. *Proceedings, Seminar on Lime Stabilization,* Loughborough University, Civil and Building Engineering Department, London, pp 99–114

Rogers, C. D. F., Glendinning, S. & Roff, T. E. J. (1997) Lime modification of clay soils for construction expediency. P*roceedings of the ICE - Geotechnical Engineering*, 125(4), pp. 242-249

Rogers, C. D. F. & Glendinning, S. (2000) Lime requirement for stabilization. *In: Journal of transportation research board,* Volume 1721, Geomaterials 2000, pp. 9-18

Rotta, G.V. Consoli, N.C., Prietto, P.D.M., Coop, M.R. & Graham. J. (2003) Isotropic yielding in an artificially cemented soil cured under stress. *Géotechnique*, 53(5), pp. 493-501.

Rouainia, M. & Muir Wood, D. (2000) A kinematic hardening constitutive model for natural clays with loss of structure. *Geotechnique,* 50(2), pp. 153–64.

Russo, G. (2005) Water retention curves of lime stabilised soils. In Tarantino, A., Romero, E. & Cui, Y. J. (eds); Advanced Experimental Unsaturated Soil Mechanics: 391-396; *Proc. Of the Int. Workshop an Advanced Experimental Unsaturated Soil Mechanics, Experus 2005,* Trento (1), pp. 27-29 Rotterdam, Balkema.

Sangrey, D. A. (1972) Naturally cemented sensitive soils. *Geotechnique*, 22(1), pp. 139–152.

Sariosseiri, F. & Muhunthan, B. (2009) Effect of cement treatment on geotechnical properties of some Washington State soils. *Engineering Geology*, 104 (2), p. 119-125.

Sasanian, S. (2011) *The behaviour of cement stabilised clay at high water contents*. PhD thesis, University of Western Ontario, London, Ontario, Canada.

Saxena, S. K., & Lastrico, R. M. (1978) Static properties of lightly cemented sand. *Journal of Geotechnical Engineering,* 104(12), pp. 1449–1464.

Schmitz, R. M. (2006) Can the diffuse double layer theory describe changes in hydraulic conductivity of compacted clay? *Geotechnical and Geological Engineering* 24(6), pp. 1834-1845.

Schnaid, F., Prietto, P. D. M. & Consoli, N. C. (2001) characterisation of cemented sand in triaxial compression. *Journal of Geotechnical and Geoenvironmental Engineering*, 127(10), pp. 857-868

Schofield, A. N. & Wroth, P. (1968) *Critical State Soil Mechanics.* McGraw Hill, London.

Schofield, A. N. (1980) Cambridge geotechnical centrifuge operations. *Geotechnique*, 30(3), 227-268.

Sharma, B. & Bora, P. K. (2003) Plastic limit, liquid limit and undrained shear strength of soil: Reappraisal. *Geotechnical and Geoenvironmental Engineering.* 129(8): 774–777.

Sherwood, P. T. (1993) *Soil stabilization with cement and lime: State of Art Review*. HMSO, London.

Siddique, A. & Clayton, C. R. I. (1999) Mechanical properties of reconstituted soft London Clay. *Journal of civil engineering, the institutions of civil engineers*, 27 (1) Bangladesh.

Simpson, B. (1992), Retaining Structures: displacement and design, Geotechnique, 42, No. 4, 541-576.

Singh, J., Kumar, A., Ritesh Jain, R., Khullar, N. K. (2008). Effect of Lime on Properties of Soil. *Proceedings of the 12th International Conference of international association for computer methods and advances in geomechanics (IACMAG).* Goa, India, October 6-11.

Sivakumar, V. (1993) *A critical sate framework for unsaturated soil*, PhD thesis, University of Sheffield, Sheffield, UK.

Sivapullaiah, P. V., Sridharan, A. & Bhaskar Raju, K. V. (2000) Role of amount and type of clay in the lime stabilization of soils. *Proceedings of the ICE, Ground Improvement*, 4(1), pp. 37-45.

Skempton, A. W. (1944). Notes on the compressibility of clays. *Quaterly Journal of Geological Society.* Vol c (100), pp. 119-135.

Skempton, A. W., Schuster, R. L. & Petley, D. J. (1969) Joints and fissures in the London clay at Wraysbury and Edgware. *Géotechnique*, 19(2), pp 205-217

Smith, A. (2006) Smith's Elements of Soil Mechanics, 8th edition. Blackwell publishing, Oxford, UK.

Smith, P. R., Jardine, R. J., and Hight, D. W. (1992) The yielding of Bothkennar clay. *Geotechnique*, 42(2), pp. 257–274.

Sorensen, K. K., Baudet, B. A. & Simpson, B. (2007) Influence of structure on the time-dependent behaviour of a stiff sedimentary clay. *Geotechnique,* 57(1), pp. 113-124.

Standing, J. R. & Burland, J. B. (2006) Unexpected tunnelling volume losses in the Westminster area, London, *Geotechnique*, 56(1), pp. 11-26

Tabani, P. (1999) *Transfert hydrique dans des sols déformables*. PhD thesis, Institut Nationale Polytechnique de Lorraine, Nancy. France.

Tamagnini, R., Mavroulidou, M. & Gunn, M. J. (2010) Numerical integration and analysis of equilibrium in unsaturated multiphase media. *Numerical Methods in Geotechnical Engineering*. Benz, Th. & Nordal, S. (eds), Taylor & Francis Group, London, pp 337-342.

Tamagnini, R., Mavroulidou, M. & Gunn, M. J. (2011) Cemented soil modelling based on the principles of thermodynamics and the critical state theory; In: Anagnostopoulos, A., Pachakis,M., Tsatsanifos, C. (Eds.), *Proc. of the XV European Conference on Soil Mechanics and Geotechnical Engineering, Geotechnics of Hard Soils and Weak Rocks*, Athens 12–15 September 2011. IOS Press, Amsterdam, pp. 1013-1018.

Taylor, H. F. W. (1990) *Cement chemistry*. Academic press, London, UK.

Tedesco, D. V. (2006) *Hydro-mechanical behaviour of lime stabilised soils*. PhD thesis, Cassino university, Italy.

Tedesco, D. V. & Russo, G. (2008) Time dependency of water retention properties of lime stabilised compacted soil; In: Toll et al., (Eds), *Proc of the 1st European Conference on Unsaturated Soils: Advances in Geo-engineering.* Durham 2-4 July 2008. Taylor and Francis Group, London, pp. 277-282.

Tembo, K. (2005) *Influence of lime stabilisation on volume changes, compressibility and hydraulic conductivity of London Clay.* MSc dissertation, London South Bank University.

Thomas, B. I. (2002) *Stabilisation of sulphide rich soil: Problems and solutions*. PhD thesis, Glamorgan university, UK.

Toll, D. G. (2002) Triax 4.3 User Manual. *Geotechnical System Research.*

Tremblay, H., Leroueil, S., & Locat, J. (2001) Mechanical improvement and vertical yield stress prediction of clayey soils from eastern Canada treated with lime or cement. *Canadian Geotechnical Journal.* 38(3), pp. 567–579.

Uddin, K., Balasubramaniam, A. S., & Bergado, D. T. (1997). "Engineering behavior of cement-treated Bangkok soft clay." *Geotechnical Engineering Journal*, 28(1), 89–119.

Vatsala, A., Nova, R. & Srinivasa Murthy, B. R. (2001) Elastoplastic model for cemented soils. *Journal of Geotechnical & Geoenvironmental Eng.,* 127(8), pp. 679–87.

Vardoulakis, I. (1978) Equilibrium bifurcation of granular earth bodies. *In Advances in analysis of geotechnical instabilities.* SM study 13, paper 3. University of Waterloo Press, Waterloo, Ont. pp. 65–119.

Vaughan, P. R. (1988) Keynote lecture: Characterising the mechanical properties of residual soil. *Proc. 2nd Int. Conf. Tropical soils*. Singapore, 2, pp. 469-87.

Venkatarama Reddy, B. V. & Jagadish, K. S. (1993) The static compaction of soils. *Geotechnique*, 43 (2), pp. 337 – 341.

Vermeer, P. A. (1982) Five-constant model unifying well-established concepts. *International Workshop on Constitutive Behaviour of Soils*, Grenoble, Balkema, pp. 175-197.

Vesic, A. S, (1973) Analysis of ultimate loads of shallow foundations. *Journal of soil mechanics and foundations.* ASCE, 99 (SMI), pp. 45-73.

Ward, W. H., Samuels, S. G. & Butler, M. E. (1959) Further studies of the properties of London Clay. *Geotechnique*, 9(2), pp. 33-58.

Ward, W. H., Marsland, A. & Samuels, S. G. (1965) Properties of the London clay at the Ashford Common shaft: In-situ and undrained strength tests. *Geotechnique*, 15(4), pp.321-344.

Webb, D. L. (1964) *The mechanical properties of undisturbed samples of London Clay*. PhD Thesis, Imperial College, University of London.

Wild, S., Arabi, M., & Leng-Ward, G. (1986) Soil-Lime reaction and microstructural development at elevated temperatures. *Clay Minerals,* 21(3), pp. 279-292.

Whitman, R.V., Roberts, J. E., Mao, S. W. (1960) The Response of Soils to Dynamic Loadings. Report 4. One Dimensional Compression and Wave Velocity Tests. MIT Soil Eng. Div. Report to Waterways Experiment Station, Corps of Engineers, U.S. Army, on Contract DA-22-079-eng-224, August.

Wroth, C. P. (1972) General theories of earth pressure and deformation. *In: Proc. 5ᵗʰ European Conf. on Soil Mechs. and Foundation Eng.*, Madrid, 2, pp. 33-52.

Xiao, H. W. & Lee, F. H. (2008) Curing Time Effect on Behavior of Cement Treated Marine Clay. *Proc. Of World Academy of Science, Engineering and Technology*, Singapore, 43, pp. 71-78.

Yan, W. M. & Li, X. S. (2011) A model for natural soil with bonds. *Géotechnique,* 61(2), pp. 95-106.

Yong, R. N., Ouhadi, V. R., (2007) Experimental study on instability of bases on natural and lime/cement-stabilised clayey soils. *Applied clay science*, 35(3-4), pp. 238-249.

Yu, H. S, (2007), *Plasticity and Geotechnics*, Springer.

Yu, H. S., Tan, S. M. & Schnaid, F. (2007) A critical state framework for modelling bonded geomaterials. *Geomechanics and Geoengineering*, 2(1), pp. 61-74.

Zhang, X. (2011) *Hydro-mechanical properties of lime-stabilised London Clay*. PhD Thesis, London South Bank University, UK.

Appendix A

A1.

Table A1.1: Indicative data calibration for back pressure transducer of the IC system

Readings	Actual values	calculated values	Error	Percent error
µV	N	N	N	%
-463.89	0.0	-0.942	0.942	0.13
4568.62	100.0	100.373	-0.373	0.05
7057.31	150.0	150.475	-0.475	0.07
9522.56	200.0	200.105	-0.105	0.01
12004.92	250.0	250.08	-0.08	0.01
14489.18	300.0	300.092	-0.092	0.01
16972.8	350.0	350.092	-0.092	0.01
19453.88	400.0	400.041	-0.041	0.01
21934.98	450.0	449.991	0.009	0.00
24421.73	500.0	500.054	-0.054	0.01
26905.99	550.0	550.067	-0.067	0.01
29380.12	600.0	599.876	0.124	0.02

A2. Determination of the initial air content

The air void is calculated based on the measurements taken at the initial state (as cured), but corrected at the end of the test once the dry density and the water content are both identified.

Below are the details on how to determine the initial air void for each specimen, by following the steps indicated in table A2.1, from initial measurement (as compacted) to the final step at the end of the test when the sample is removed and its final water content and dry density determined.

Table A2.1: Indicative procedure for 6% lime treated LC specimen measurements during each stage

Target Measurement values			
Length	L_0	*mm*	76
Diameter	d_0	*mm*	38
Water masse	$M_{water(0)}$	*g*	33.28
Dry soil masse	$M_{soil(0)}$	*g*	123.25
Masse of used wet soil	$M_0 = M_{water(0)} + M_{soil(0)}$	*g*	156.53
Water content	w_0	*%*	27
Volume	$V_0 = \left[\pi \times d_0^{\;2} \times L_0\right]/4$	cm^3	86.19
Area	$A_0 = \left[\pi \times d_0^{\;2}\right]/4$	mm^2	1134.11
Bulk density	$\rho_{b(0)} = \left[M_{water(0)} + M_{soil(0)}\right]/V_0$	g/cm^3	1.816
Dry density	$\rho_{d(0)} = M_{soil(0)}/V_0$	g/cm^3	1.43

Measurements after compaction			
Measured length (average)	L_1	mm	76.46
Measured diameter (average)	d_1	mm	38.05
Measured volume	$V_1 = \left[\pi \times d_1^{\,2} \times L_1\right]/4$	cm^3	86.94
Measured area	$A_1 = \left[\pi \times d_1^{\,2}\right]/4$	mm^2	1136.52
Compacted sample masse	M_1	g	156.39
Masse loss (%)	$100 - \left[\left(M_1/M_0\right) \times 100\right]$	$\%$	0.09
Corrected water masse	$M_{water(1)} = \left[M_{water(0)} \times \left(100 - loss_{(\%)}\right)/100\right]$	g	33.25
Corrected soil masse	$M_{soil(1)} = \left[M_{soil(0)} \times \left(100 - loss_{(\%)}\right)/100\right]$	g	123.14
Corrected dry density	$\rho_{d(1)} = M_{soil(1)}/V_1$	g/cm^3	1.42
Corrected bulk density	$\rho_{b(1)} = M_1/V_1$	g/cm^3	1.80
Corrected water content	$w_1 = \left[M_{water(1)}/M_{soil(1)}\right] \times 100$	$\%$	27.00
Soil specific gravity	$G_{S(soil)}$	-	2.76
Soil-Lime specific gravity	$G_{S(soil+\lim e)}$	-	2.74

Measurements after curing (28 days)			
Measured length (average)	L_2	mm	77.14
Measured diameter (average)	d_2	mm	38.28
Corrected volume	V_2	cm^3	88.78
Corrected area	A_2	mm^2	1150.89
Masse after curing	M_2	g	156.39
Corrected water masse	$M_{water(2)} = M_{water(1)} - [M_1 - M_2]$	g	33.25
Corrected soil masse	$M_{soil(2)} = M_{soil(1)}$	g	123.14
Corrected dry density	$\rho_{d(2)} = M_{soil(2)} / V_2$	g/cm^3	1.39
Corrected bulk density	$\rho_{b(2)} = M_2 / V_2$	g/cm^3	1.76
Corrected water content	$w_2 = [(M_2 - M_{soil(2)}) / M_{soil(2)}] \times 100$	$\%$	27.00

Quantified initial values			
Degree of saturation	$S_{r(0)} = \left[(\rho_b \times w_2 \times G_{s+l})/(\rho_w \times G_{s+l} \times (1+w_2) - \rho_b)\right]$	-	0.76
Void ratio	$e_0 = \left[(w_2 \times G_{s+l})/S_{r(0)}\right]$	-	0.98
	$e_0 = \left[G_{s+l}/\rho_{d(2)}\right] - 1$	-	0.98
	$e_0 = \left[G_{s+l} \times V_2/M_{soil(2)}\right] - 1$	-	0.98
	$e_{sat} = e_0 - \left((1+e_0) \times (V_{expansion}/V_2)\right)$	-	1.07
Air volume	$V_{air} = \left[e_0 \times V_{soil}\right] - V_{water}$	cm^3	10.59
	$V_{water} = M_{water(2)}$	cm^3	33.25
	$V_{soil} = V_2 - V_{air} - V_{water}$	cm^3	44.94
	$V_{air} = \left[(e_0 \times V_2) - (1+e_0) \times V_{water}\right]/\left[1+e_0\right]$	cm^3	10.59
Water volume used for saturation	$V_{gauge(sat)}$	cm^3	14.85
Sample volume expansion	$V_{expansion} = V_{gauge(sat)} - V_{air}$	cm^3	4.27
Final saturated sample volume	$V_{final} = V_2 + V_{expansion}$	cm^3	93.05
Consolidated values			
Water volume used for consolidation	$V_{gauge(con)}$	cm^3	14.66
Volume change	$\Delta V_c = V_{gauge(sat)} - V_{gauge(con)}$	cm^3	0.2
Consolidated sample's volume	$V_c = V_{final} - \Delta V_c$	cm^3	92.85
Consolidated void ratio	$e_c = \left[(G_{s+l} \times V_c)/M_{soil(2)}\right] - 1$	-	1.07
	$e_c = e_{sat} - \left((1+e_{sat}) \times (\Delta V_c/V_{final})\right)$	-	1.07

After Shearing process			
Sample masse	Wet masse after removal M_3	g	170.48
	Dry sample masse M_4	g	123.56
Final water content	$w_f = [(M_3 - M_4)/M_4] \times 100$	$\%$	37.97
Initial water content	$w_i = [(M_2 - M_4)/M_4] \times 100$	$\%$	26.57
Initial water volume	$V_{i(water)} = M_{i(water)} = [M_2 - M_4]$	cm^3	32.83
Initial bulk density	$\rho_{b(i)} = [M_{i(water)} + M_4]/V_2$	g/cm^3	1.76
final bulk density	$\rho_{b(f)} = M_3/V_c$	g/cm^3	1.84
Initial dry density	$\rho_{d(i)} = M_4/V_2$	g/cm^3	1.39
Corrected values / Used for data processing			
Initial degree of saturation	$S_{r(i)} = [(\rho_{b(i)} \times w_i \times G_{s+l})/(\rho_w \times G_{s+l} \times (1+w_i) - \rho_{b(i)})]$	-	0.75
Final degree of saturation	$S_{r(f)} = [(\rho_{b(f)} \times w_f \times G_{s+l})/(\rho_w \times G_{s+l} \times (1+w_f) - \rho_{b(f)})]$	-	0.98
Initial void ratio	$e_{(i)} = [(w_i \times G_{s+l})/S_{r(i)}]$	-	0.97
Initial air volume	$V_{air(R)} = [(e_{(i)} \times V_2) - (1+e_{(i)}) \times V_{i(water)}]/[1+e_{(i)}]$	cm^3	**10.86**
Real expanded volume	$V_{expansion} = V_{gauge(sat)} - V_{air(R)}$	cm^3	4.00
Saturated volume	$V_{sat(R)} = V_2 + V_{gauge(sat)} - V_{air(R)}$	cm^3	92.78
Saturated void ratio	$e_{sat(R)} = e_{(i)} - ((1+e_{(i)}) \times (-V_{expansion}/V_2))$	-	1.06
Consolidated volume	$V_{c(R)} = V_{sat(R)} - \Delta V_c$	cm^3	92.58
Consolidated void ratio	$e_{c(R)} = [(G_{s+l} \times V_{c(R)})/M_4] - 1$	-	1.05
	$e_{c(R)} = e_{sat(R)} - ((1+e_{sat(R)}) \times (\Delta V_c/V_{sat(R)}))$	-	1.05

Appendix B

B1. Applied corrections to triaxial data

- **Water content and dry density corrections**

Due to post curing mass change and volume expansion of lime treated London Clay samples, a method was developed in order to quantify the pre-curing water content and dry density, as well as the post-curing water content and its related dry density, which results in identifying the void ratio of lime treated specimen prior to subjecting the specimen to triaxial testing. (See form A2.1/ Appendix A)

- **Length and diameter correction**

l_c is the consolidated length obtained from the post-curing samples' length l_0 and the average axial displacement change $l_{x(c)}$ measured by the two internal axial strain transducers at the end of the consolidation stage.

$$l_c = l_0 \pm l_{x(c)}$$

Similarly, the length at the start of the split line l_{split} is determined by using the internal axial instrumentation as follow.

$$l_{split} = l_0 \pm l_{x(split)}$$

d_c Is the diameter of the specimen at the end of the consolidation stage, it is identified from the initial samples' diameter d_0 and the radial displacement measured by the internal radial strain transducer $d_{x(c)}$ from the start of the test to the end of the consolidation stage.

$$d_c = d_0 \pm d_{x(c)}$$

Similarly, the diameter at the start of the split line d_{split} is determined by using the internal axial instrumentation as follow.

$$d_{split} = d_0 \pm d_{x(split)}$$

Where $d_{x(split)}$ is the radial displacement measured by the internal radial strain transducer from the start of the test to the start of slip line.

- **Volume change corrections**

Providing that there is no leakage in the system and the back pressure line is allowed to expand overnight prior to Triaxial testing, no other correction should be necessary. However, the amount of water moving into the sample during the saturation process does not necessarily correspond to the total volume change of the specimen. The air bubbles contained initially in the samples are absorbed into the flowing water during saturation, occupying the air voids space while the back pressure is gradually raised to form one solid block. Hence, the movement of water into or out of specimen from the back pressure system is not a true measure of the volume change of the specimen.

The volume change can be determined using measurements of axial and radial strain instrumentation mounted directly on the specimen, this technique should give more or less an accurate value of sample volume change during saturation / consolidation as indicated by Cabarkapa, (2001). However, it has proved difficult in this study to rely on this technique during the shearing process of lime treated London Clay, due to the internal instruments dislocating from their position or reaching the maximum set limit long before achieving the 20% axial strain target. Experience has shown that it generally happens after the peak (failure surface), particularly for highly brittle specimens, which is found to oscillate between 5 and 10% axial strain. Therefore, the most reliable instrument for volume change measurement in this study was found to be the Imperial college volume gauge. A methodical procedure was developed, and consistently applied during this work in order to determine, prior to the test, the approximate amount of initial air void V_{air} contained in each specimen. This in turn is taken in consideration during the volume change correction (See table A2.1 / Appendix A).

- **Area correction**

Two types of failures were observed on the tested specimens during the shearing process, namely ductile failure for statically compacted London Clay samples (Barrelling) and brittle failure for artificially cemented London Clay samples (failure surface). The area corrections proposed by Head (1986) were adopted for the two failure modes.

The correction to apply for the deviator stress value due to the increasing area caused by the barrelling at an increasing axial strain is:

$$q = (\sigma_1 - \sigma_3) = \frac{P}{A_c} \left(\frac{100 - \varepsilon_a(\%)}{100 - \varepsilon_v(\%)} \right)$$

p : Applied shearing load (kPa)

A_c : Sample's consolidated area (mm^2) = $\dfrac{V_c}{l_c}$, where V_c is the consolidated volume

ε_a : Axial strain $(\%)$

ε_v : Volumetric strain $(\%)$

If failure occurs by single slipping along the sheared surface, the effective plan area decreases during shearing process as indicated by Head, (1986) (See figure B1.1)
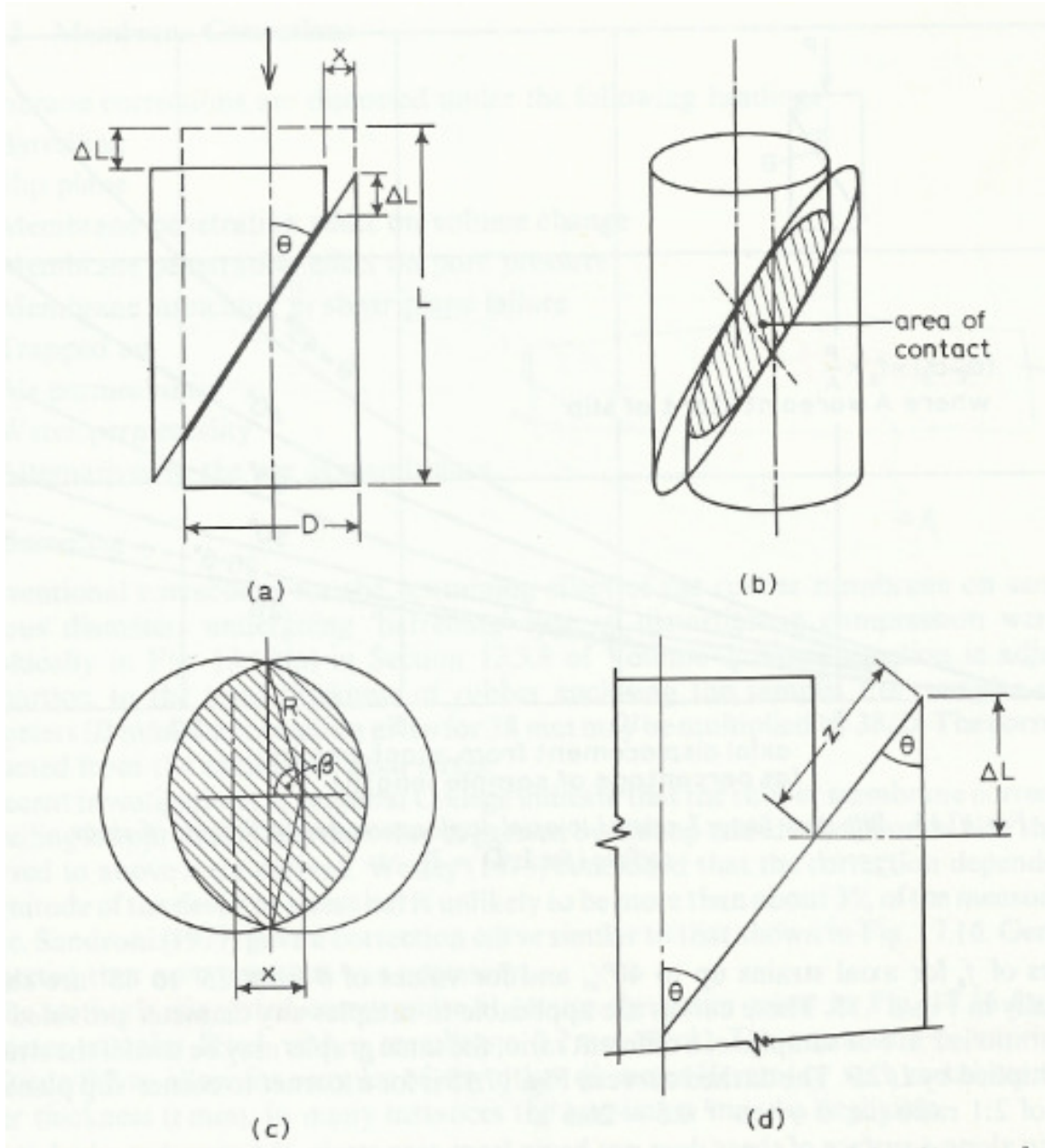
Figure B1.1: Area correction due to single-plane slip: **(a)** mechanism of the slip, **(b)** area of
contact between the two portions of the sample, **(c)** projected area of contact,
(d) displacement along slip surface related to vertical deformation (after Head, 1986)

This can be calculated using the expression given by Chandler, (1966) namely:

$$\frac{A_{slip(x)}}{A_{slip(0)}} = \frac{2}{\pi}(\beta - \sin\beta\cos\beta)$$

Where:

$A_{slip(0)}$: Area of the sheared sample at the start of the slip line

$A_{slip(x)}$: contact area at any axial displacement during the slip

$$\cos \beta = \frac{l_{slip}}{d_{slip}} \, \varepsilon_{a(slip)} \, \tan \theta$$

(θ) Is the inclinaison of the slip surface relative to the sample axis, $(\varepsilon_{a(slip)})$ is the axial strain measured from the start of the slip, (l_{slip}) is the length of sample at the start of slip, and (d_{slip}) is the diameter at the start of the slip. Note that the internal axial and radial instrumentation were used to identify the approximate length and diameter of the specimens at / or close to the start of the slip line.

- **Membrane correction**

Chandler, (1968) investigated the effect of membrane stretching in shear plane failure and concluded that soils such as stiff clays and artificially cemented soils, which exhibit a high strength, shows a considerable drop in strength when slip plane develops. These materials are not likely to be influenced by the membrane restraint effect, this was found to be insignificant, therefore it was neglected in data analysis. Moreover, as recommended by Molenkam & Luger (1981) and due to the observed smoothness on all lime treated specimen's external surfaces, the effect of penetration membrane into the voids between particles at the interface in volume change is negligible.

B2. Main formulae used

For compacted sample, the post-curing void ratio (e_0) was determined based on the following formulae

$$e_0 = \frac{G_s * (1 + w_0)}{\rho_{b0}} - 1$$

Where:

w_0 is the post-curing water content, determined through the method previously described in section B1 and referred to as w_2 in table A2.1.

$\rho_{b0} = \dfrac{M_0}{V_0}$ is the post-curing bulk density determined through the ratio of the post-curing mass M_0 over the post-curing total volume V_0 of the sample (Note that M_0 and V_0 are referred to as M_2 and V_2 in table A2.1)

The saturated void ratio (e_s) was determined using the following formulae

$$e_s = e_0 - (1 + e_0) * \left(\frac{\Delta V_{sat}}{V_0} \right)$$

ΔV_{sat}, is the measured volume change at the end of saturation stage based on the recorded IC volume change gauge $V_{gauge(sat)}$, less the initial air volume of the sample V_{air}. It is worth noting that the pressure applied to the triaxial cell has a negligible effect on the volume cell expansion due to the low pressure applied during this experimental work. Thus, it was considered to be constant during the whole test. In addition, the system is pressurised for several hours overnight prior to the specimen being installed. Therefore, the specimen volume expansion during saturation stage is calculated based only on the measured IC volume change and the initial air void.

$$\Delta V_{sat} = V_{gauge(sat)} - V_{air}$$

The consolidated void ratio (e_c) was also calculated using the equation below

$$e_c = e_0 - (1 + e_0) * \left(\frac{\Delta V_{con}}{V_0} \right)$$

ΔV_{con} is the measured volume change at the end of the consolidation stage, equal to the recorded IC volume change gauge $V_{gauge(con)}$, less the initial air volume of the sample V_{air}.

$$\Delta V_{con} = V_{gauge(con)} - V_{air}$$

Axial strain (ε_a) calculation during shearing stage is directly related to the ratio of the axial length change (Δl) measured from the external axial displacement, over the pre-shearing length of the sample, which in this case is the consolidated length (l_c), presented by the following formulae.

$$\varepsilon_a = \frac{\Delta l}{l_c}$$

The volumetric strain (ε_v) during shearing stage is determined using the IC volume change gauge, and based on the ratio of the measured volume change ΔV over the specimen's total volume at the end of the consolidation stage V_c.

$$\varepsilon_v = \frac{\Delta V}{V_c}$$

V_c is calculated by adding the recorded water volume from the IC volume gauge at the end of consolidation stage $V_{gauge(con)}$, to the initial volume V_0, less the sample's post-curing air volume V_{air}.

$$V_c = V_0 + V_{gauge(con)} - V_{air}$$

The shear strain of lime treated / untreated London Clay sample (ε_s) was identified based on the following formulae.

$$\varepsilon_s = \varepsilon_a - \frac{\varepsilon_v}{3}$$